



**University of
Nottingham**

UK | CHINA | MALAYSIA

Gold-Catalysed Nucleophilic Allylation of Azinium Ions

A thesis submitted to The University of Nottingham for the
degree of Doctor of Philosophy

By

Luke O'Brien

September 2022

Declaration

I hereby declare that, except for where specific reference is made to other sources, the work contained within this thesis is the original work of my own research and any collaboration is clearly indicated. This thesis has been composed by myself and has not been submitted, in whole or part, for any other degree, diploma or other qualification. I confirm that the work submitted is my own, except work which has formed part of jointly-authored publications. The contributions of myself and other authors to this work have been specifically indicated where relevant. I confirm that appropriate credit has been given with the thesis where references has been made to the work of others.

The following thesis contains results reported in the following publication:

“Gold(I)-Catalyzed Nucleophilic Allylation of Azinium Ions with Allylboronates”

O'Brien, L; Argent, S. P.; Ermanis, K.; Lam, H. W. *Angew. Chem. Int. Ed.* **2022**, *61*, e202202305.

Table of Contents

Acknowledgements	iv
Abstract	v
Abbreviations	vi
1.0 Introduction	1
1.1 Transition Metal-Catalysed Allylation Reactions	1
1.2 Gold-Catalysed Allylations	3
1.2.1 Redox Neutral Gold-Catalysed Allylations.....	4
1.2.1.1 Addition of Nucleophiles to Electrophilic Allylating Agents	4
1.2.1.2 Rearrangement Cascades.....	17
1.2.1.3 Addition of Nucleophilic Allylating Agents to Electrophiles	38
1.2.1.4 Miscellaneous Additions of Allyl Fragments.....	45
1.2.2 Redox Active Gold-Catalysed Allylations	48
1.3 Nucleophilic Dearomatisation of Azinium Salts <i>via</i> Allyl Reagents	53
1.3.1 Addition of Allylstannanes.....	54
1.3.2 Addition of Allylsilanes	58
1.3.3 Addition of Allyl Halides	59
1.3.4 Addition of Miscellaneous Allyl Reagents	61
1.4 Summary	63
2.0 Results and Discussion	64
2.1 Aims and Objectives.....	64
2.2 Reaction Optimisation	64
2.3 Reaction Scope	76
2.4 Product Manipulations	86
2.5 Mechanistic Studies	86
2.6 Extension to Other Nucleophiles.....	101
2.7 Development Towards an Enantioselective Variant.....	105
2.8 Conclusions and Future Work.....	117
3.0 Experimental	120

3.1 General Information.....	120
3.2 Preparation of Pinacolboronates.....	121
3.3 Preparation of Azinium Salts	131
3.4 Gold-Catalysed Nucleophilic Allylation of Azinium Ions	146
3.5 Product Manipulations.....	172
3.6 Allylation using Enantiopure Allyl Pinacolboronate 453	176
3.7 Deuterium Labelling Studies.....	178
3.8 TEMPO Studies.....	179
3.9 ¹ H NMR and ¹¹ B NMR Studies.....	180
3.10 Uncatalysed Nucleophilic Allylation of Azinium Ions.....	180
3.11 Other Gold-Catalysed Nucleophilic Additions to Azinium Ions	182
3.12 Synthesis of Gold Complexes	185
4.0 References.....	200
5.0 Appendix: Publication.....	209

Acknowledgements

First, I would like to thank my supervisor Prof. Hon Wai Lam for his supervision throughout my PhD studies. Choosing you as my supervisor was one of the best decisions I could've made. You have taught me so many things over the years that I will be forever grateful for. There are many qualities that I appreciate about you, one of which is your sense of humour. I have enjoyed my time as a member of the Lam group.

A huge thank you to the CDT for giving me the opportunity to conduct research at the University of Nottingham, with a special mention given to Prof. Peter Licence and Perislava Williams, who manage the centre so flawlessly. I would also like to thank all of my fellow CDT students for their much-needed support and morale boosts.

I would like to mention the people who I have had the pleasure to work so closely with over my studies. First, Dr. Alistair Groves who thought me so many fundamental techniques, your patience and guidance must have been tested with me, but you stuck through it, and for that I will be forever grateful. Second, Dr. Somnath Karad, your support and guidance will always be appreciated and you are one of the most hard-working people I've ever met.

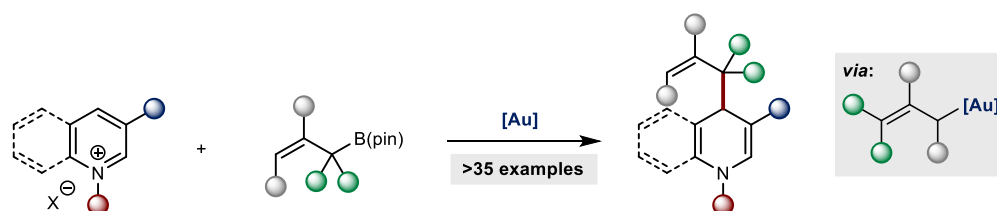
My time at Nottingham wouldn't have been as enjoyable had I not been surrounded by such wonderful and quirky lab members. I want to thank all the members of the Lam group (past and present), in particular Simone, Harley, Dmitry and Jack for all the fantastically absurd conversations and jokes. Jack, your dress sense still confuses me to this day! But, in all seriousness, their help and advice, especially when unforeseen chemistry related problems arose was extremely appreciated.

A special mention goes out to Dr. Johnny Moore and Dr. Kieran Jones for proofreading this body of work. I know it must not have been easy but your feedback was greatly appreciated. To my housemates Aoife and Tom, for all the great memories over the last few years. You guys were a welcomed distraction from chemistry.

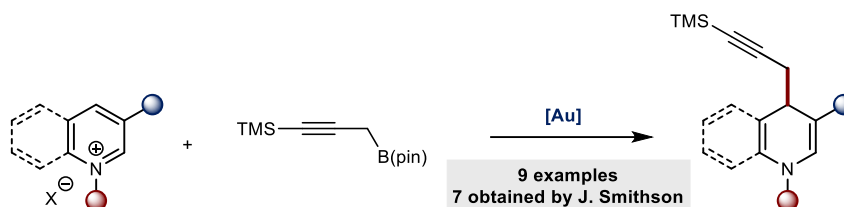
Last but not least, I would like to thank my family. Although I rarely show it, I have always appreciated everything you have done for me. You were always so kind and supportive. This wild journey wouldn't have been possible without your unconditional confidence in me.

Abstract

Herein is described the gold(I)-catalysed nucleophilic allylation of azinium ions utilising allyl pinacolboronates. The reaction is regioselective for the 4-position of the azinium ion, generating functionalised 1,4-dihydropyridines and 1,4-dihydroquinolines in excellent yields. In-depth mechanistic studies confirm σ -allylgold(I) species as the reactive intermediates, generated *via* S_E2' transmetalation from the corresponding allyl pinacolboronate. These reactions represent the first example of accessing allylgold(I) intermediates from allylboron reagents. Attempts to develop an enantioselective variant of this reaction are also described.



Furthermore, this mode of reactivity has been extended to include other nucleophilic coupling partners. In particular, the gold(I)-catalysed regioselective nucleophilic addition of propargyl pinacolboronates has been established.



Abbreviations

9-BBN	9-borabicyclo[3.3.1]nonane
Å	Angstrom
Ac	Acetyl
Ad	Adamantyl
aq.	Aqueous
B ₂ (pin) ₂	bis(pinacolato)diboron
B(pin)	4,4,5,5-tetramethyl-1,3,2-dioxaborolane
BArF	tetrakis(3,5-bis(trifluoromethyl)phenyl)borate
BINAP	(1,1'-binaphthalene-2,2'-diyl)bis(diphenylphosphine)
BIPHEP	2,2'-bis(diphenylphosphino)biphenyl
Bn	benzyl
Boc	<i>tert</i> -butyloxycarbonyl
bpy	2,2'-bipyridine
br	broad
CFL	compact fluorescent light bulb
cod	cyclooctadiene
cy	Cyclohexyl
d.r.	diastereomeric ratio
dba	dibenzylideneacetone
DCC	<i>N,N'</i> -dicyclohexylcarbodiimide
DCE	1,2-dichloroethane
DFT	density functional theory
DIPEA	<i>N,N</i> -diisopropylethylamine
DIPT	diisopropyl-tartrate
DMAP	4-dimethylaminopyridine
DME	dimethyl ether
DMSO	dimethyl sulfoxide
<i>ee</i>	enantiomeric excess
EWG	electron-withdrawing group
Fmoc	9-fluorenylmethyloxycarbonyl
HFIP	1,1,1,3,3,3-hexafluoro-2-propanol

HMBC	heteronuclear multiple-bond correlation
HPLC	high performance liquid chromatography
HRMS	high-resolution mass spectrometry
<i>i</i> -	<i>iso</i> -
IPr	1,3-bis(2,6-diisopropylphenyl)imidazol-2-ylidene
LA	Lewis acid
M.S.	molecular sieves
MTBE	methyl <i>tert</i> -butyl ether
NAPDH	nicotinamide adenine dinucleotide phosphate
NBS	<i>N</i> -bromosuccinimide
NMR	nuclear magnetic resonance
NR	no reaction
Nu	nucleophile
PBE0	Perdew-Burke-Ernzerhof-0
Piv	pivaloyl
Py	pyridine
QUINAP	1-(2-diphenylphosphino-1-naphthyl)isoquinoline
r.r.	regioisomeric ratio
<i>rac</i>	racemate
RT	room temperature
SMD	solvation model density
<i>t</i> -	<i>tert</i> -
TBAF	tetra- <i>n</i> -butylammonium fluoride
TBDPS	<i>tert</i> -butyldiphenylsilyl ether
Tc	thiophene-2-carboxylate
TEMPO	2,2,6,6-tetramethylpiperidin-1-yl)oxyl
Tf	triflyl
TFE	2,2,2-trifluoroethanol
THF	tetrahydrofuran
TIPS	triisopropylsilyl ether
Tle	<i>tert</i> -leucine
TMP	2,2,6,6-tetramethylpiperidine
TMS	trimethylsilyl ether

Troc	trichloroethoxycarbonyl
Ts	tosyl
TZVP	triple zeta valence plus polarization

Throughout this work, “wedges” have been used to indicate stereochemistry at quaternary centres and “blocks” have been used to indicate stereochemistry at tertiary centres.

1.0 Introduction

1.1 Transition Metal-Catalysed Allylation Reactions

Carbon-carbon (C-C) bonds form the ‘backbone’ of the majority of organic compounds. Therefore, forming C-C bonds will always be one of the most valuable and essential reactions in the development of synthetic organic chemistry.¹ The transition metal-catalysed allylation reaction has been an important transformation in forming C-C bonds in recent years. This reaction can be categorised *via* the reactivity of the allyl moiety, exhibiting either an electrophilic or nucleophilic profile. Transition metal-catalysed allylation reactions involving allylic radicals are another powerful technique to form C-C bonds. Generating π -allyl intermediates *via* a radical addition can proceed with high selectivity, building unparalleled complexity in a single step.²

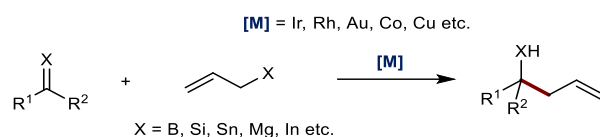
The transition metal-catalysed electrophilic allylation reaction (Scheme 1) typically involves the oxidative addition of metals into allylic fragments producing allylmetal species that are susceptible to nucleophilic attack.³ Stabilised nucleophiles attack at the carbon chain of the *in-situ* formed π -allyl complex, whilst unstabilised nucleophiles directly react with the metal centre, typically *via* transmetalation, followed by subsequent reductive elimination leading to C-C bond formation.⁴



Scheme 1: Typical metal-catalysed electrophilic allylation reaction.

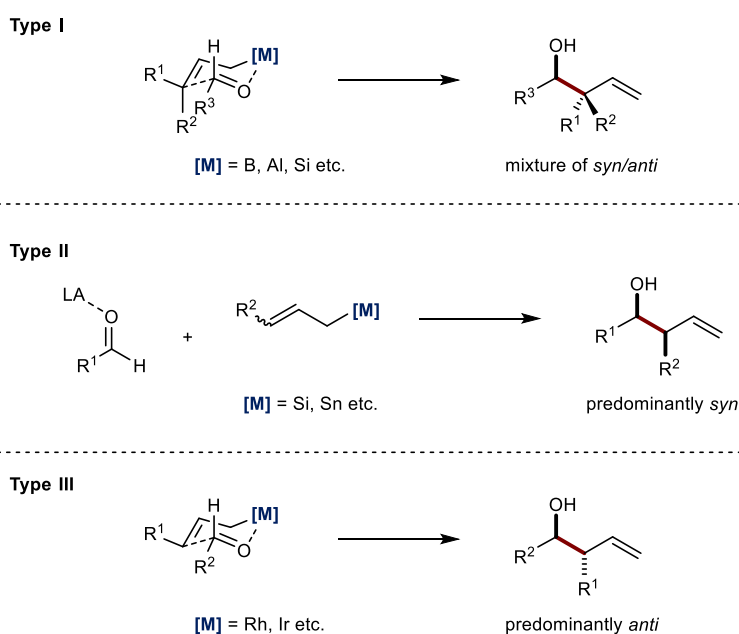
The transition metal-catalysed nucleophilic allylation reaction (Scheme 2) characteristically involves the addition of an allylmetal species, formed *via* transmetalation, to a π -electrophile. This allows for the installation of two versatile functional groups within close proximity to one another.⁵ This reaction allows for the direct synthesis of functionalised homoallylic alcohols and amines which are key chemical precursors for the synthesis of complex natural products.⁶ Homoallylic alcohols and amines often contain multiple functional handles, which facilitates further modification, increasing molecular complexity. Allylmetal species can be generated from

a variety of allylic precursors *via* transmetalation. The most commonly utilised allylic precursors are allylic silanes,⁷ allylic stannanes,⁸ allylic Grignards,⁹ and allylic boronates.¹⁰



Scheme 2: Typical metal-catalysed nucleophilic allylation reaction.

In 1983 Denmark and co-workers classified the nucleophilic addition of allylmetal species to π -electrophiles. (Scheme 3).¹¹ This classification is supported by previous findings, including Hoffman's model.^{12,13} Type I additions involve the activation of the electrophile to form a closed six-membered chair-like transition state. This typically generates the γ -allylated product, retaining the geometry of the allylic metal species. Due to the organised transition state, type I reactions typically exhibit superior diastereocontrol in comparison to type II. Type II additions require a Lewis acid to activate the electrophile and proceed through an open transition state with *antiperiplanar* or *synclinal* orientation, predominately forming the *syn*-adduct. Finally, type III reactions proceed *via* a closed transition state similar to type I, predominately forming the *anti*-adduct, as rapid equilibration of (*E*)- vs. (*Z*)-allylmetal intermediates forms the thermodynamically favourable (*E*)-isomer.

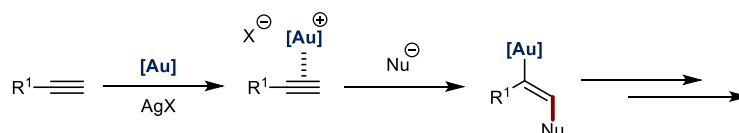


Scheme 3: Modes of addition for different allylmetal reagents.

Allylic precursors have been utilised extensively in combination with various transition metals to generate synthetically valuable products. Palladium is the most commonly reported metal to perform such transformations;¹⁴ however, other metals have been shown to participate in similar reactivity such as rhodium,¹⁵ cobalt,¹⁶ copper,¹⁷ and gold.¹⁸

1.2 Gold-Catalysed Allylations

Homogeneous gold catalysis has been shown to catalyse a myriad of synthetic organic transformations.^{19–21} Acting as strong carbophilic Lewis acids which are both air- and moisture tolerant,²² gold-catalysed transformations predominately involve the addition of nucleophiles to unsaturated C-C bonds under mild reaction conditions (Scheme 4). This alkenyl gold intermediate can undergo further reactivity to form complex molecular scaffolds through unique reaction pathways. These transformations exhibit excellent chemoselectivities and good overall functional group tolerance, which has led to its widespread utility towards the synthesis of complex biologically relevant targets.²³



Scheme 4: Gold reactivity with alkynes.

In a significant proportion of gold-catalysed transformations, a silver additive is required to enable reactivity. This forms a more active cationic gold complex with a bound counterion, generating AgCl as a by-product. The exact role of this counterion formed *via* this process is currently unknown; however, some general trends have been documented by Bandini and co-workers.²⁴ Weakly coordinating anions such as SbF₆[−] and BF₄[−] will generate a more electrophilic gold centre, facilitating reactivity. Strongly coordinating anions can affect the catalyst resting state or promote protodeauration. Furthermore, basic anions such as tosylates and acetates can exert a ‘folding effect’ forcing reactive partners into a favourable geometry, controlling chemo-, regio- and enantioselectivity.

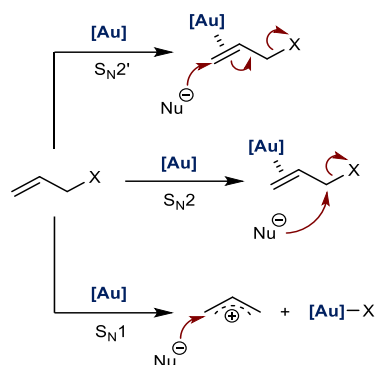
Gold catalysis has been applied to allylation chemistry, expanding its applicability towards the synthesis of densely functionalised compounds.¹⁸ The unique capability of gold catalysis to promote site-selective rearrangements allows for the incorporation of allyl moieties, generating greater molecular complexity.¹⁸ This literature review will categorise each gold-catalysed allylation based on the absence/presence of an oxidation change within the gold complex, further sub-divided based on the reactivity profile of the allylating agent. Furthermore, gold-catalysed hydrofunctionalisation of allenes followed by nucleophilic addition to alkynes and alkenes is another approach towards installing allyl fragments. However, these transformations will not be discussed within this literature review.^{25,26}

1.2.1 Redox Neutral Gold-Catalysed Allylations

The vast majority of gold-catalysed allylations typically maintain either a +1 or +3 oxidation state with respect to the catalyst utilised. Gold was considered one of the most inert metals, having a high redox potential ($\text{Au}^{\text{I}}/\text{Au}^{\text{III}}$), preventing undesired reaction pathways.²⁷⁻²⁹ However recently, two electron redox cycles involving gold ($\text{Au}^{\text{I}}/\text{Au}^{\text{III}}$) have been achieved, requiring harsh stoichiometric oxidants to enable reactivity.³⁰⁻³³ This alternative two electron redox cycle is characteristic of late transition metals and has emerged as an alternative approach to install allyl fragments.

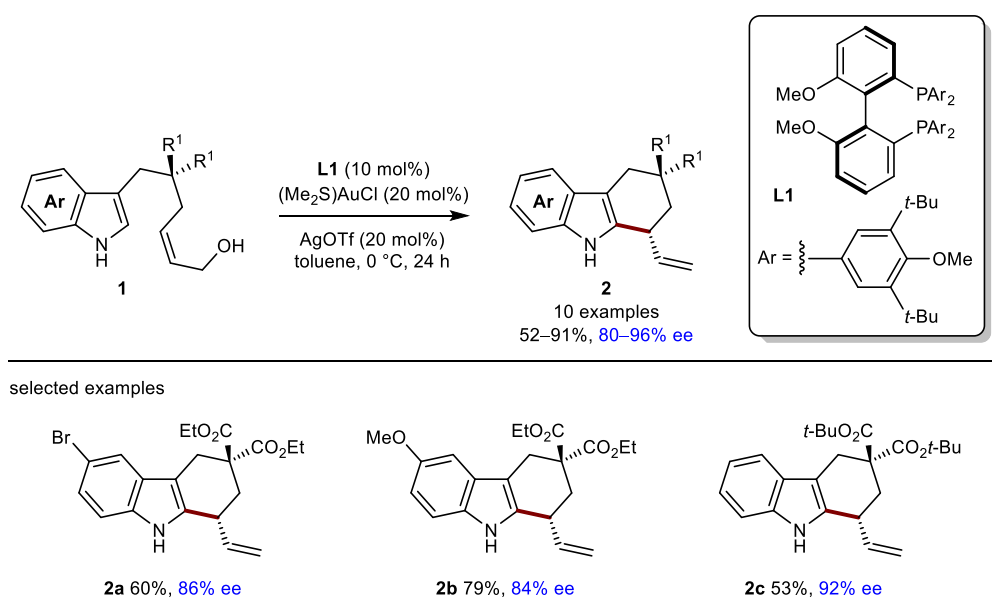
1.2.1.1 Addition of Nucleophiles to Electrophilic Allylating Agents

The addition of nucleophiles to electrophilic allylating agents is a common technique to install allyl fragments within complex molecular structures. The structure of the allylic precursor and gold catalyst determines whether the reaction belongs to a formal $\text{S}_{\text{N}}1$, $\text{S}_{\text{N}}2$ or $\text{S}_{\text{N}}2'$ reaction profile (Scheme 5).



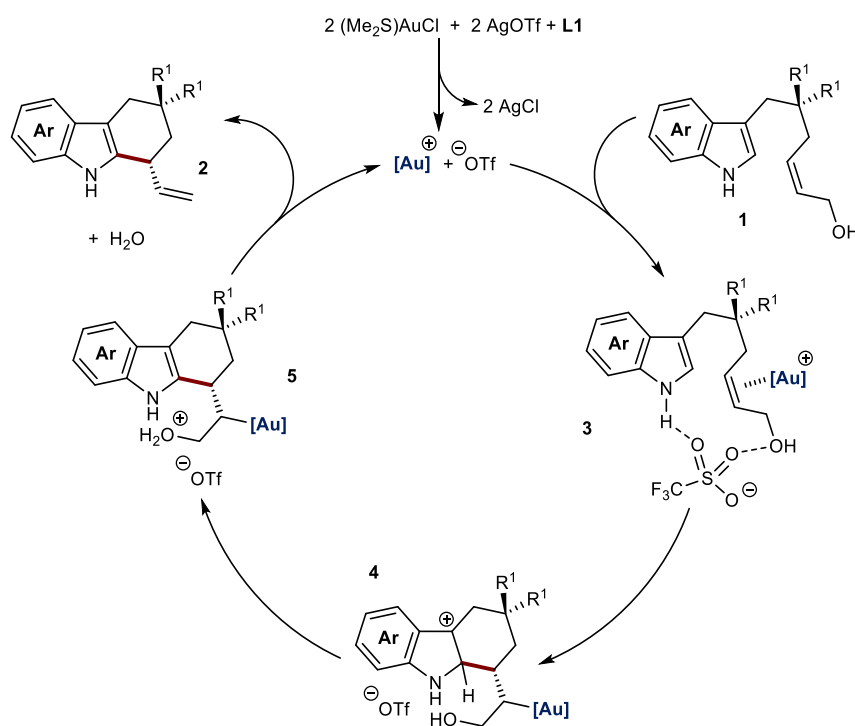
Scheme 5: Modes of activation for gold-catalysed addition of nucleophiles to allylic precursors.

In 2009, Bandini and co-workers reported the intramolecular enantioselective allylation of malonate substituted indoles, generating the desired products in high yields and enantioselectivities (Scheme 6).³⁴ The counterion of the silver additive proved crucial for enabling reactivity, increasing both the reaction rate and stereoselection. The functional group tolerance was modest, with both electron-withdrawing (**2a**) and electron-donating substituents (**2b**) on the indole fragment, producing the desired products with good enantiocontrol. Variation of the malonate moiety was limited to alkyl groups (**2c**). Subjecting (*E*)-allylic alcohols to the reaction conditions, gave the desired product in reduced yields and enantioselectivity. The formation of water as the only by-product underlines the sustainability of this reaction.



Scheme 6: Enantioselective gold-catalysed allylation of indoles.

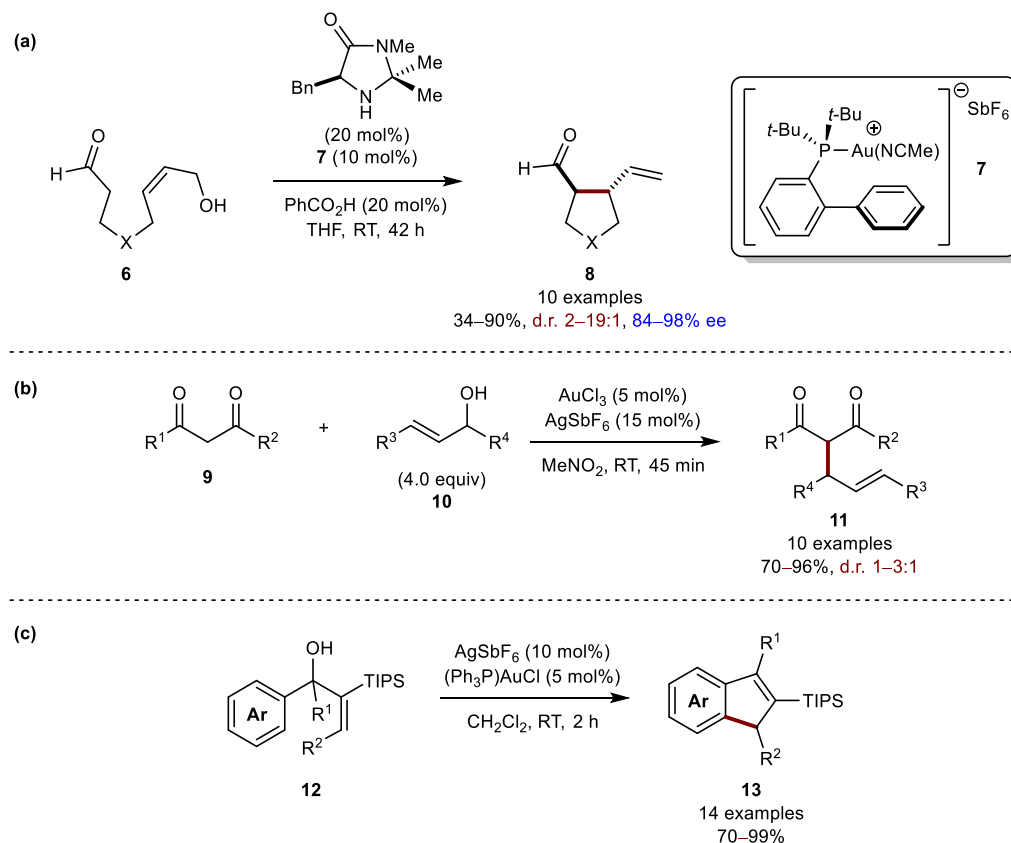
The proposed mechanism is initiated by the co-ordination of the active gold catalyst with the allylic moiety of indole **1**, affording species **3** (Scheme 7). Supported by DFT calculations,³⁵ the authors propose the triflate counterion exerts a ‘folding effect’ forcing both reactive partners into a favourable geometry. A formal S_N2' *anti*-auroindolation of the alkene occurs, forming intermediate **4**. Nucleophilic attack of the C3 indole carbon is disfavoured with respect to nucleophilic attack by the C2 carbon. Rearomatization of the indole *via* proton transfer occurs, assisted by the triflate counterion, generating species **5**. Subsequent *anti*-elimination follows, liberating the desired product **2** and regenerating the active gold catalyst.



Scheme 7: Proposed mechanism for the formation of **2**.

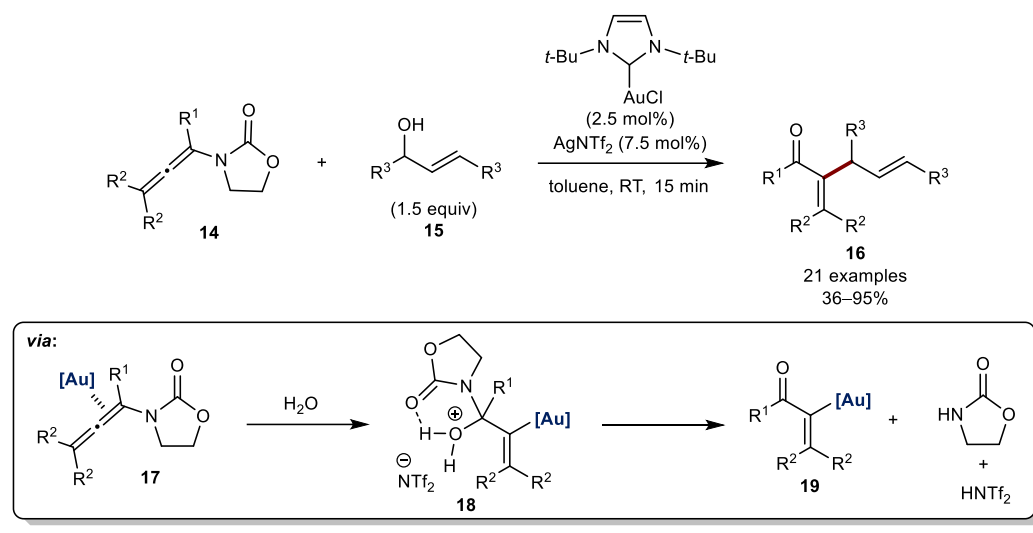
Bandini and co-workers extended this concept to include enamine catalysis, reporting the intramolecular enantioselective allylation of aldehydes with allylic alcohols (Scheme 8a).³⁶ The reaction generated the desired products in good yields and excellent enantioselectivities. Of note to reactivity was the utilisation of electrophilic gold catalyst **7**, which gave superior yields in comparison to other known catalysts. In 2009, Chan and co-workers reported the gold(III)-catalysed allylation of 1,3-dicarbonyls with allylic alcohols, generating the desired products (**11**) in good yields under mild reaction conditions (Scheme 8b).³⁷ However, densely substituted allylic alcohols gave poor regiocontrol. In 2012, Yamamoto published a synthetic route towards 2-indanones *via* a

gold(I) annulation pathway (Scheme 8c).³⁸ The reaction was tolerant to a wide array of functional groups, accessing the desired products in excellent yields. The reaction was extended to access substituted cyclopentadienes through an analogous pathway.

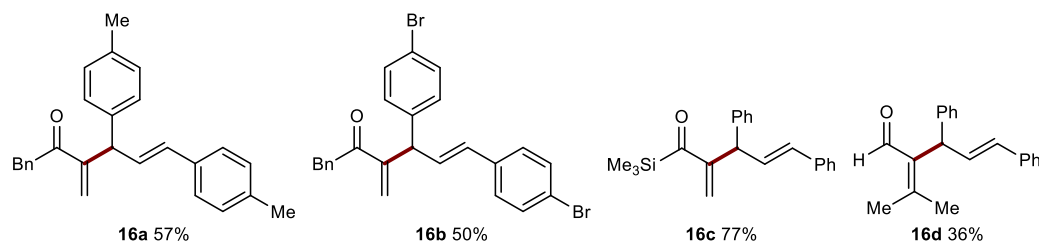


Scheme 8: Gold-catalysed allylations via dehydration.

The generation of α -gold(I) enals was investigated by Bandini and co-workers. (Scheme 9).³⁹ The electrophilic activation of allenamide **14**, followed by nucleophilic attack by water and elimination gave the reactive α -gold(I) enal **19**. This species would further react with an allylic alcohol furnishing the desired allylated product **16** as seen previously (see Scheme 7). The authors had to increase the electrophilicity of the gold catalyst, which in turn generated a more nucleophilic α -gold(I) enal, producing the desired product in increased yield. The substrate scope was good, with various electron-donating (**16a**) and electron-withdrawing substituents (**16b**) being tolerated in the reaction without any significant loss in yield. Moreover, the methodology could be extended to furnish acyl silanes (**16c**) and aldehydes (**16d**). Experimental evidence in conjunction with DFT calculations conducted by the authors suggest the active reaction pathway occurs through a S_N1 mechanism.

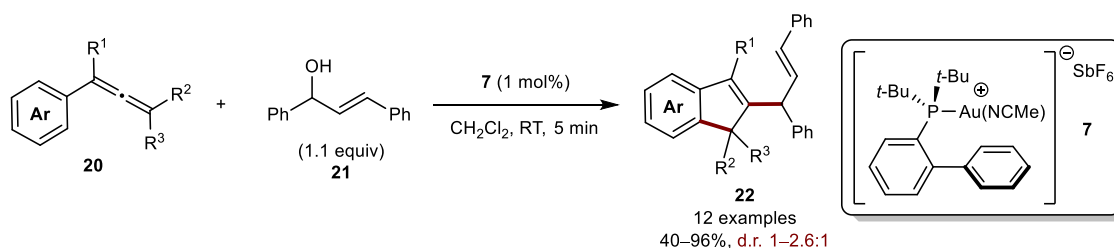


selected examples



Scheme 9: Gold-catalysed allylation of allenes.

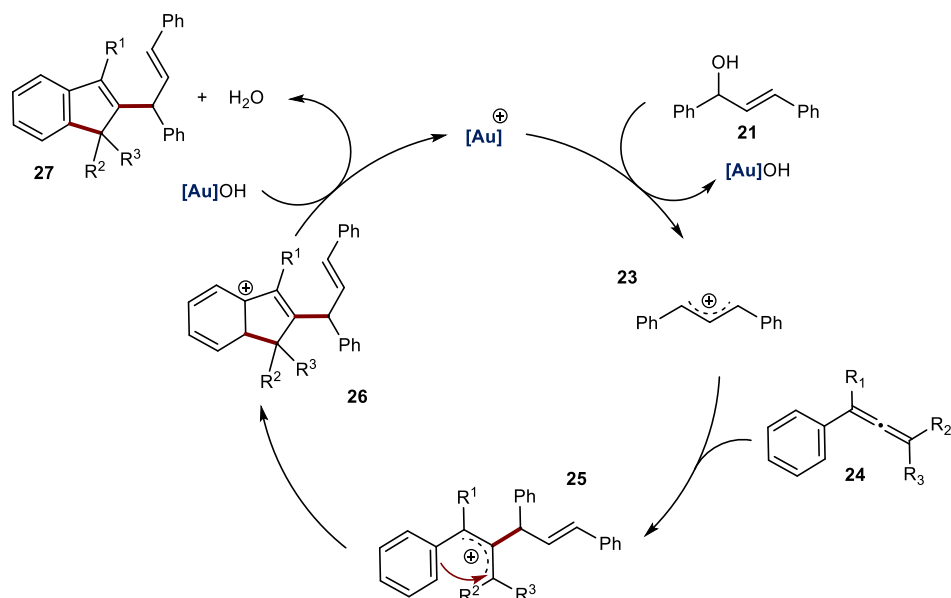
In 2016, Maulide and co-workers extended the work of Bandini towards the synthesis of substituted indenenes *via* the coupling of allenes and allylic alcohols (Scheme 10).⁴⁰ The corresponding indenenes were generated in good yields; however, poor diastereocontrol was observed. As stated by Bandini, a highly electrophilic gold catalyst (**7**) was required to promote reactivity.



Scheme 10: Gold-catalysed coupling of alcohols and allenes.

The proposed mechanism (Scheme 11) is initiated by activation of the allylic alcohol by the cationic gold complex, forming carbocation **23**. The formation of a carbocation *via* a S_N1 pathway is supported by mechanistic experiments whereby the product formation is governed *via* the highest stabilising benzylic carbocation. Carbocation **23** is intercepted by allene **24** forming intermediate **25**. A Friedel-Crafts type cyclisation,

followed by rearomatisation affords the desired indene (**27**), liberating water as a by-product and regenerating the desired active catalyst.

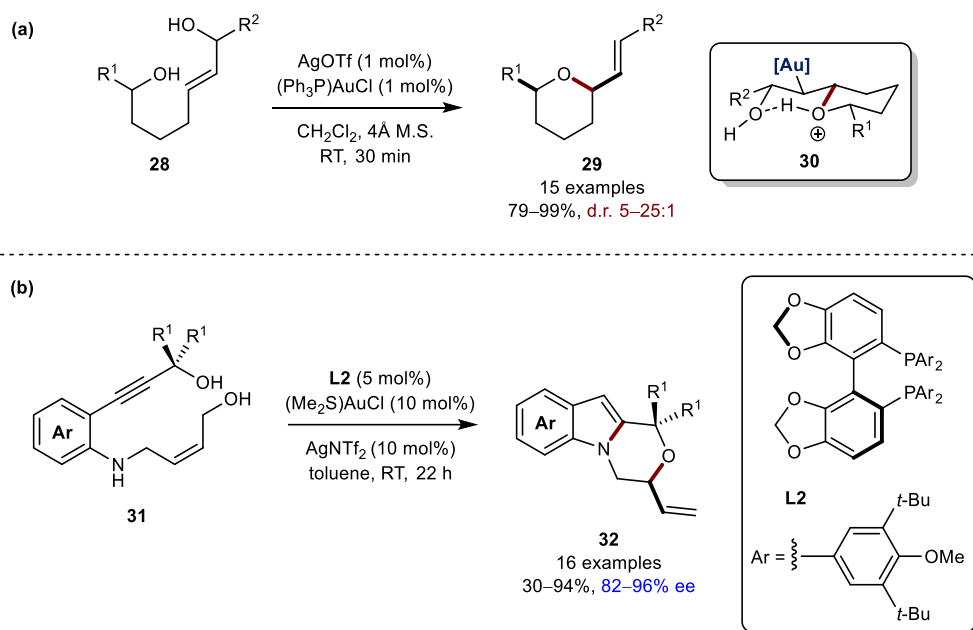


Scheme 11: Proposed mechanism for the formation of **27**.

Previous reports involved C-C bond formation exclusively; however, in 2008, Aponick pioneered a gold-catalysed allylation reaction forming tetrahydropyrans in high yields with good diastereocontrol, forming the *cis*-adduct exclusively (Scheme 12a).⁴¹ To achieve good diastereoselectivity, lower temperatures were required. DFT calculations were later conducted by Aponick to reveal a potential mechanism.⁴² This involves an intramolecular carbon-oxygen (C-O) bond formation *via* an *anti*-addition to the gold-coordinated alkene complex, generating intermediate **30**. This C-O bond forming step adopts a chair-like conformation, governing the stereochemical outcome of the reaction. This is followed by a concerted hydrogen transfer and *anti*-elimination, forming water as the sole by-product. This two-step pathway is extremely facile due to favourable hydrogen bonding between the diol functionalities. In 2011, Aponick reported a variant of this process, accessing tetrahydropyrans in a highly stereoselective fashion when utilising enantioenriched chiral allylic alcohols.⁴³ Moreover, enantioselective variants were later reported by both Bandini,⁴⁴ and Rueping.⁴⁵ In 2017, Hong and co-workers applied this chemistry towards the total synthesis of (+)-laurencin.⁴⁶

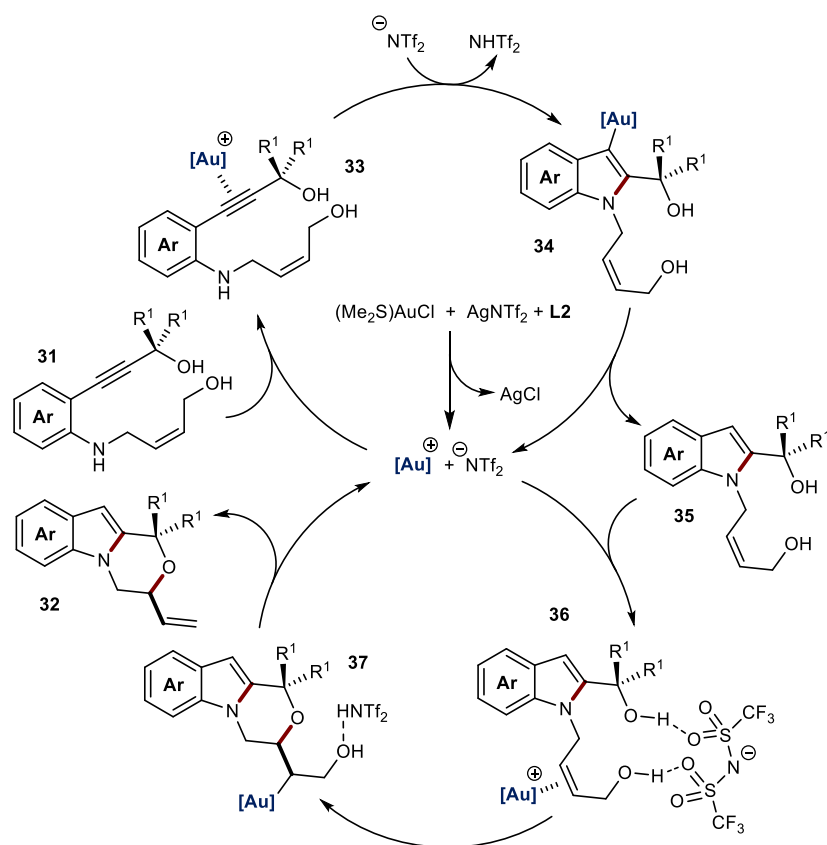
In 2013, Bandini and co-workers reported a one-pot intramolecular enantioselective synthesis of functionalised indoles (**32**) using gold(I) catalysis (Scheme 12b).⁴⁷ Interestingly, the use of a single gold complex enabled the synthesis of both the pyrrolyl

core and the subsequent enantioselective alkoxylation. As seen previously, the counterion had a profound effect on the enantioselectivity of the reaction.



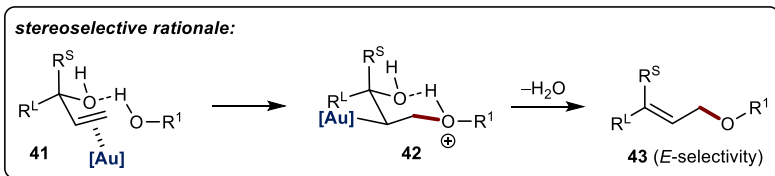
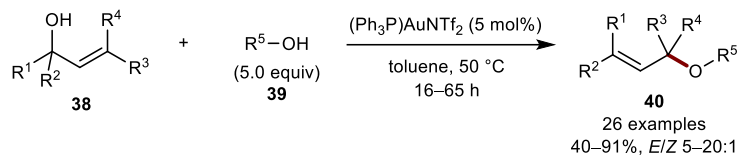
Scheme 12: Gold-catalysed C-O allylations via dehydration.

The proposed mechanism for the formation of **32** in Scheme 12b is initiated by the co-ordination of the active gold catalyst with the alkyne moiety of **31**, affording species **33** (Scheme 13). A formal *anti*-addition of the alkyne occurs, assisted by triflimide, forming intermediate **34**. Protodeauration of **34** occurs, regenerating the active catalyst and liberating species **35**. Co-ordination of the gold catalyst with the alkene of species **35** furnishes intermediate **36**. The authors propose the triflimide counterion exerts a ‘folding effect’ forcing both reactive partners into a favourable geometry. This C-O bond forming step is similar to previous examples (see Scheme 7), occurring *via* an *anti*-addition, followed by hydrogen atom transfer furnishing **37**. *Anti*-elimination occurs, forming water as the sole by-product, liberating the desired product **32** and regenerating the active gold catalyst.

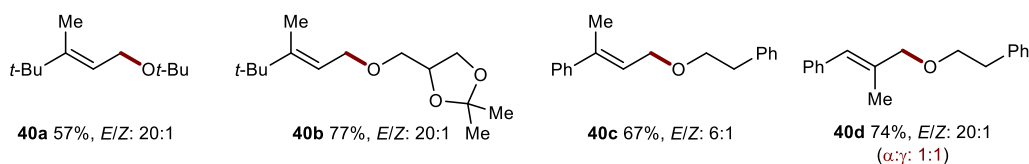


Scheme 13: Proposed mechanism for the formation of **32**.

Intermolecular allylic etherification of alcohols was reported by Lee and co-workers (Scheme 14).⁴⁸ Alkyl alcohols are poor nucleophiles and therefore typically do not participate in allylic substitution reactions.⁴⁹ Nevertheless, the authors demonstrated that gold was able to promote reactivity enabling the synthesis of allylic ethers in good yields with high regio- and stereoselectivity. The substrate scope was modest, with primary (**40a**), secondary and tertiary alcohols generating the desired products in good yields. Reducing steric hinderance around the alkene gave lower (*E*)-selectivity (**40c**). Moreover, highly substituted allylic alcohols gave mixtures of regioisomers (**40d**) with respect to the allylic alcohol (**38**). The reaction proceeds *via* gold-assisted activation of the alkene (**41**), followed by nucleophilic attack of the external alcohol, forming intermediate **42**. The high (*E*)-selectivity arises due to the formation of a 6 membered chair-like transition state.

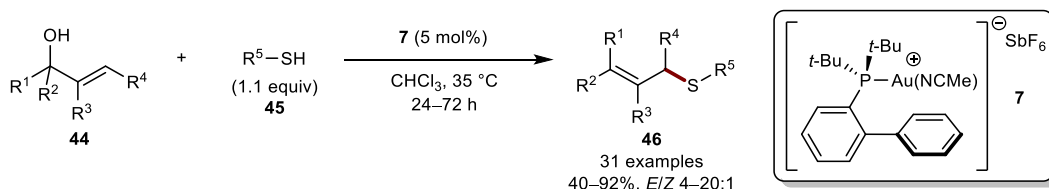


selected examples



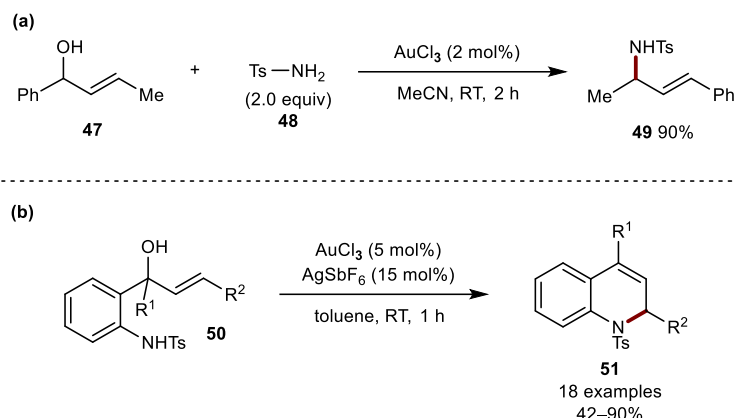
Scheme 14: Gold-catalysed allylic etherification.

Lee extended this concept, reporting the coupling of allylic alcohols and thiols (Scheme 15).⁵⁰ This methodology gave access to the $\text{S}_{\text{N}}2'$ regioselective product (**46**), which was unobtainable using conventional transition metal catalysis. The reaction was tolerant to both alkyl and aryl-derived thiols, with alkyl derivatives requiring longer reaction times. DFT calculations indicated the observed regiocontrol was indicative of the thermodynamic stability of the product.



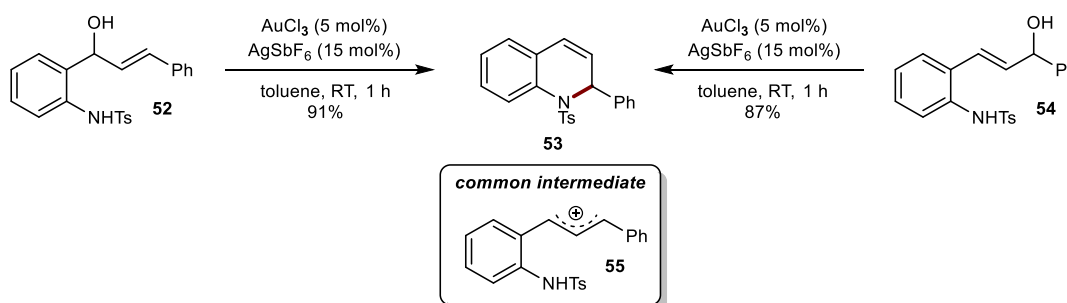
Scheme 15: Gold-catalysed allylic thioetherification.

Liu and co-workers demonstrated the first direct synthesis of allylic amines from allylic alcohols using gold catalysis (Scheme 16a).⁵¹ Utilising AuCl_3 gave the desired allylic amine **49** in 90% yield. The authors propose an $\text{S}_{\text{N}}1$ pathway due to the observation of mixtures of regioisomers with respect to the allylic alcohol. In 2009, Chan and co-workers expanded this methodology, developing an intramolecular allylic amination, synthesising 1,2-dihydropyridines in excellent yields (Scheme 16b).⁵² A concise synthesis of (\pm)-angustureine was performed, demonstrating the applicability of this chemistry.



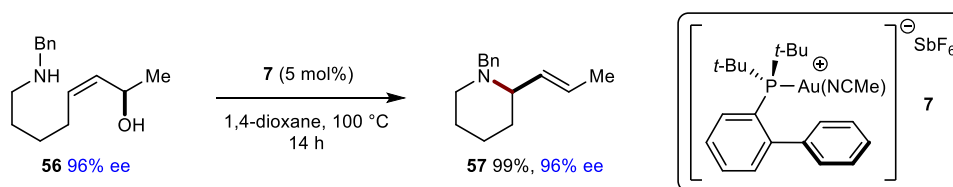
Scheme 16: Gold-catalysed allylic aminations.

Evidence towards an S_N1 pathway was demonstrated by the authors, suggesting the involvement of an allylic carbocation (Scheme 17). Subjecting both regioisomeric compounds **52** and **54** to the reaction conditions gave the same product **53** in 91% and 87% yield respectively. This provides evidence toward common intermediate **55**, indicative of a S_N1 pathway.



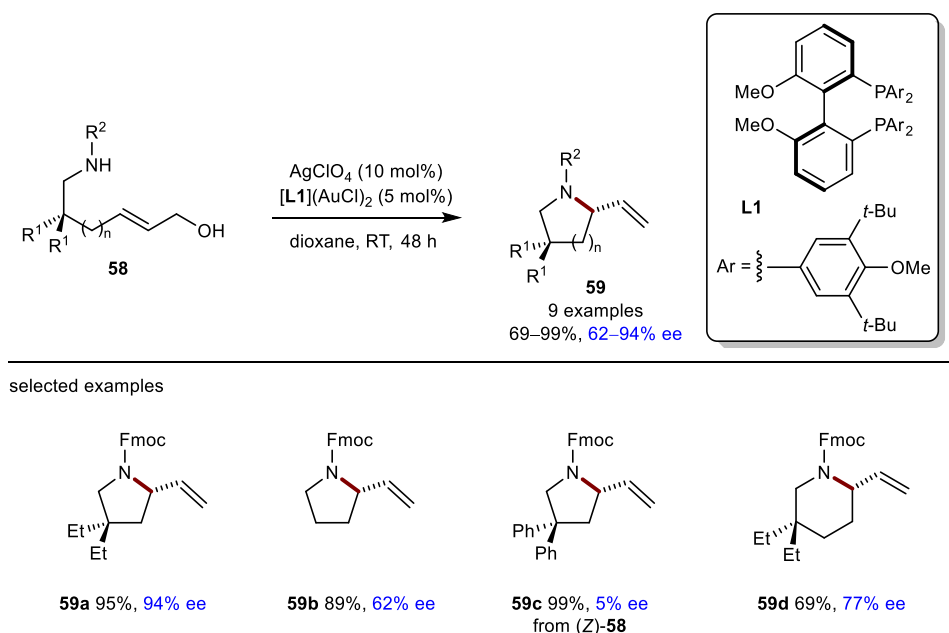
Scheme 17: Common mechanistic carbocation intermediate.

Further applications of this work was reported by Widenhoefer, demonstrating the synthesis of enantioenriched piperidines from enantioenriched allylic alcohols (Scheme 18).⁵³ Subjecting **56** to their optimised reaction conditions gave the desired piperidine **57** in 96% ee, with no loss in optical purity. These products can be easily derivatised to access naturally occurring alkaloids.



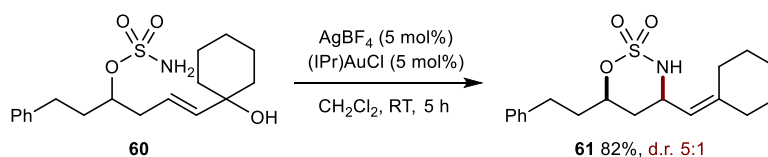
Scheme 18: Gold-catalysed C-N allylation via dehydration.

Widenhoefer and co-workers later developed an enantioselective variant, coupling allylic alcohols and carbamates, forming nitrogen heterocycles in high yields and enantioselectivities (Scheme 19).⁵⁴ Utilising AgClO_4 was crucial in amplifying stereinduction within the reaction system. The substrate scope was modest with allylic alcohols bearing no *gem*-dialkyl substitution (**59b**) generating the desired product in reduced enantioselectivity. Furthermore, subjecting (*Z*)-alkenes to the reaction conditions generated the desired product **59c** in high yield but low enantioselectivity, demonstrating the requirement of (*E*)-alkenes for stereinduction. However, the reaction was applicable towards the synthesis of six-membered nitrogen heterocycles (**59d**). The proposed mechanism is analogous to that of Scheme 7.



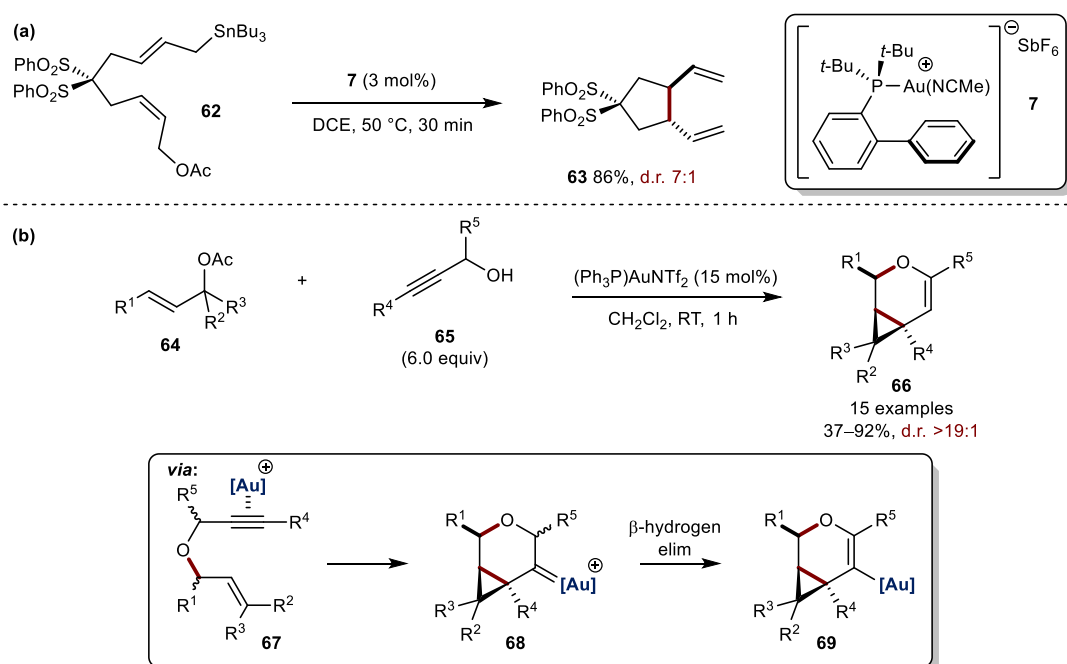
Scheme 19: Gold-catalysed intramolecular allylic amination.

In 2021, Ryu and co-workers reported the intramolecular amination of sulfamate esters (**60**) with allylic alcohols, producing cyclic sulfamides in high yields with modest diastereocontrol (Scheme 20).⁵⁵ Alternating the silver salt additive drastically changed both the reaction yield and diastereoselectivity, with AgBF_4 showing the best performance.



Scheme 20: Gold-catalysed C-N allylation via dehydration.

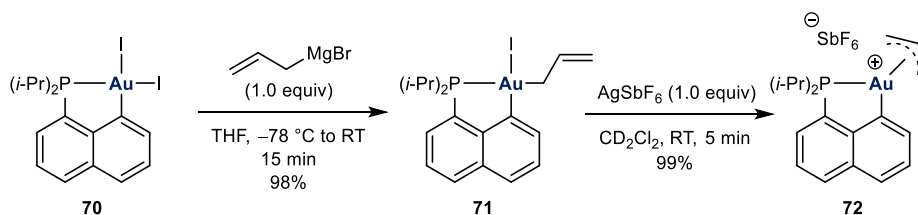
Allylic acetates have been shown to participate in similar reactivity to that of allylic alcohols in a seminal report by Echavarren (Scheme 21a).⁵⁶ Screening various metal catalysts, the authors found cationic gold complex **7** could efficiently promote reactivity over more traditional transition metals such as rhodium and palladium, forming the desired allyl-allyl coupled product in 86% yield. Direct evidence of an allylgold(I) complex *via* transmetalation with the allylic stannane could not be identified, with the authors suggesting complexation between the gold catalyst and alkene being more favourable. This forms an allylic cation *via* an S_N1 pathway, that is quenched with the corresponding allylstannane. Moreover, an oxidative addition pathway between the gold catalyst and the allylic acetate could not be observed. Guo and co-workers extended this concept of utilising allylic acetates *via* an allylation and cycloisomerisation cascade reaction (Scheme 21b).⁵⁷ Intermolecular allylation occurs between allylic acetate **64** and propargyl alcohol **65** forming allylated intermediate **67**. Subsequent cycloisomerisation yields **68**, followed by β-H elimination and protodeauration generates the desired product. Similar examples of this reactivity have been later reported.^{58,59}



Scheme 21: Gold-catalysed allylations from allylic acetates.

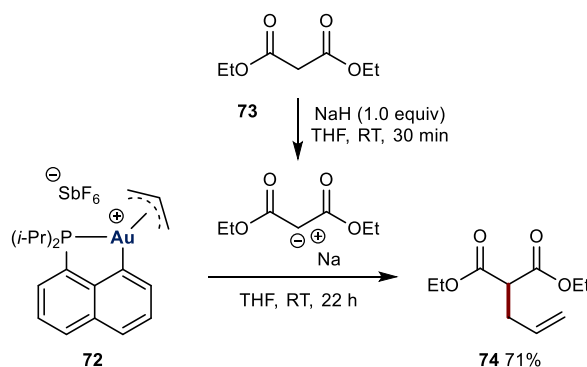
Previous examples discussed demonstrated the reactive allylating partner as an intermediate within the reaction pathway; however, in 2020, both Tilset and Bourissou independently reported the first isolated example of an π -allylgold complex (Scheme 22).^{60,61} Of note, σ -allylgold complexes have been characterised since the 1980's;

however, their direct synthetic utility has been underexploited.^{62,63} Gold complex **71** was synthesised *via* transmetalation with allylmagnesium bromide. This was further reacted with AgSbF₆, releasing a coordination site for the alkene double bond, forming gold complex **72**. Upon heating no rotation from the η^3 -coordination complex to the η^1 -coordination complex was observed, indicating rigid coordination. Furthermore, DFT calculations demonstrated that η^1 -coordinated gold complexes are less stable than η^3 -coordinated gold complexes.



Scheme 22: Formation of cationic gold species **72**.

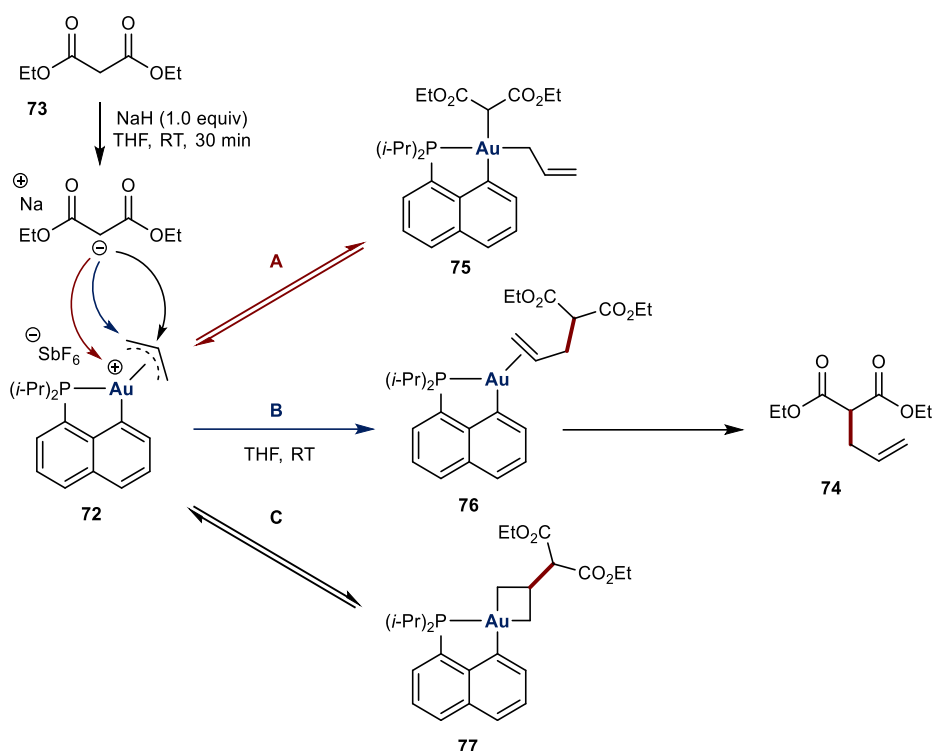
Reactivity studies were conducted to compare such gold complexes to the well-known palladium-catalysed Tsuji-Trost reaction (Scheme 23). Complex **72** reacted with diethylmalonate, affording the desired product in 71% yield. Interestingly, complex **71** was unable to generate the desired product.



Scheme 23: Gold-catalysed allylation of malonate **73**.

In 2021, Bourissou and co-workers extended this concept, performing in-depth experimental and computational analysis on the reactivity of π -allylgold complexes and comparing them to similar electrophiles found in the palladium-catalysed Tsuji-Trost reaction (Scheme 24).⁶⁴ The authors found that the addition of the nucleophile can occur at the central and terminal positions of the π -allyl, as well as the gold centre, in stark contrast to the preference of the terminal position in the palladium-catalysed Tsuji-Trost reaction. This indicates that both outer and inner sphere mechanisms are operating

congruently within the reaction system. σ -Allyl complex **75** and auracyclobutane **77** were isolated and fully characterised. Nucleophilic addition to the central position of the π -allyl and to the gold centre were found to be reversible over time, congregating into the π -alkene complex **76** and generating the desired product **74**.



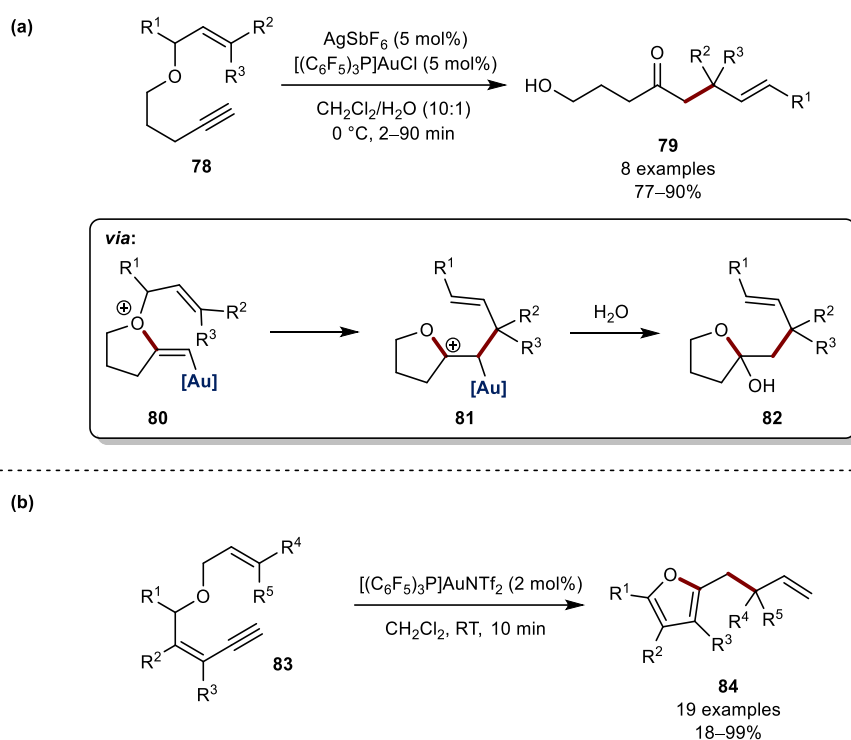
Scheme 24: Nucleophilic addition to π -allylgold(III) complex **72**.

1.2.1.2 Rearrangement Cascades

Gold-catalysed rearrangement cascades proceed *via* multistep transformations that can generate complex molecular scaffolds from simple precursors. These reactions are advantageous due to their mildness, high selectivities and well-understood reactivity.^{65,66} Gold-catalysed rearrangements involving allyl moieties typically comprises of an initial gold-catalysed transformation which facilitates a concerted or stepwise allylic transfer.

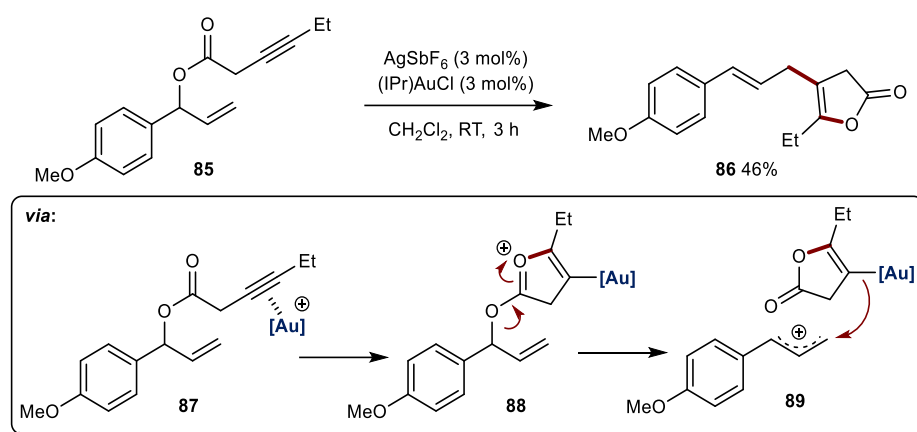
In 2011, Rhee and co-workers reported the gold-catalysed synthesis of γ -hydroxyketones *via* a sigmatropic allyl transfer domino sequence (Scheme 25a).⁶⁷ The reaction required a highly electrophilic catalyst to enable reactivity, generating the corresponding products in good yields. The proposed mechanism is initiated by

coordination of the active gold catalyst to the alkyne, followed by *anti*-nucleophilic attack of the ether linkage, generating species **80**. A sigmatropic rearrangement occurs, forming oxocarbenium **81** via migration of the allyl fragment. Nucleophilic attack by water followed by protodeauration furnishes species **82** which ring-opens to form the desired γ -hydroxyketone product. Later that year, Gagosz reported a similar process, synthesising poly-substituted furans in high yields (Scheme 25b).⁶⁸ The substrate scope was modest with complex allylic fragments participating in this transformation efficiently. The reaction mechanism is similar to the mechanism shown in Scheme 25a. Further expansion of this work in terms of its application towards different scaffolds were later reported.^{69,70}



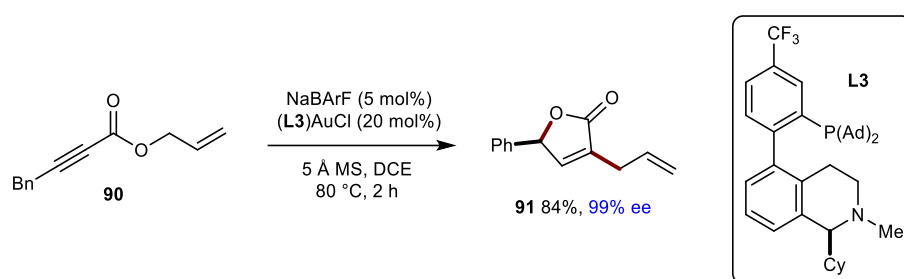
Scheme 25: Gold-catalysed alkoxyacylation and sigmatropic allyl migration.

Hashmi extended this concept towards the synthesis of γ -butyrolactone **86** via a 5-*endo-dig* cyclisation of propargyl ester **85** (Scheme 26).⁷¹ The reaction proceeds via an *anti*-nucleophilic addition to gold-bound species **87**, forming oxonium intermediate **88**. Intermediate **88** collapses into a stabilised carbocation, furnishing **89**. Coupling of the two fragments occurs, producing the desired γ -butyrolactone product.



Scheme 26: Gold-catalysed synthesis of γ -butyrolactone **86**.

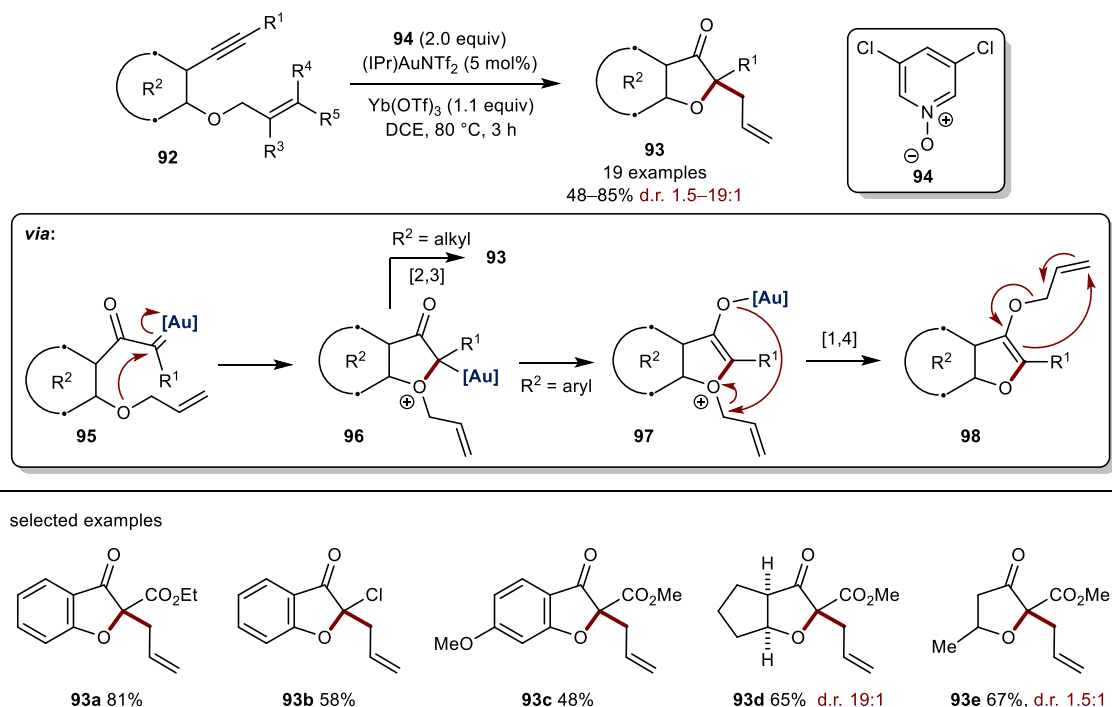
Zhang and co-workers later reported an extension of this work, initially describing the racemic synthesis of allylbutenolides *via* a Claisen rearrangement,⁷² followed by an enantioselective variant (Scheme 27).⁷³ Crucial for reactivity is the incorporation of the amine functionality within **L3**, enabling the isomerisation of the alkyne of **90** to an allene. Subsequent cycloisomerisation, followed by a Claisen rearrangement and alkene isomerisation yields the desired product **91**.



Scheme 27: Gold-catalysed synthesis of γ -butyrolactone **91**.

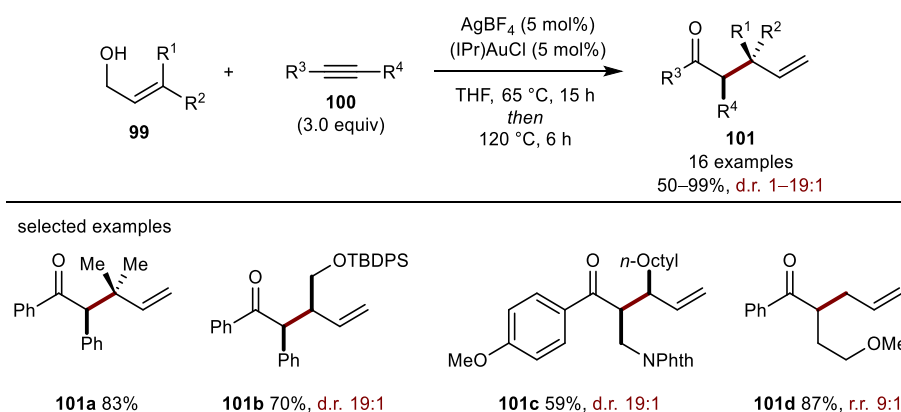
Given the hazardous nature surrounding diazo compounds, methods that avoid their preparation are advantageous. Tang reported such a procedure, showing the rearrangement of allylic oxonium ylides, generating dihydrofuran-3-ones in high yields. (Scheme 28).⁷⁴ The proposed mechanism involves *N*-oxide **94** as an oxygen source, forming species **95** *in-situ*. Nucleophilic attack onto species **95**, generates oxonium ylide **96**. When substrate **96** contains an alkyl backbone, a concerted [2,3]-sigmatropic rearrangement occurs, delivering the desired product **93**. When substrate **96** contains an aryl backbone, tautomerisation to the more thermodynamically stable intermediate **97** ensues, followed by a 1,4-allyl migration and subsequent Claisen rearrangement, furnishing the desired product **93**. The reaction tolerated a wide array of functionality,

with electron-donating substituents leading to lower overall yields (**93c**). Moreover, modest to good diastereocontrol was observed when using substrates containing an alkyl backbone (**93d** and **93e**).



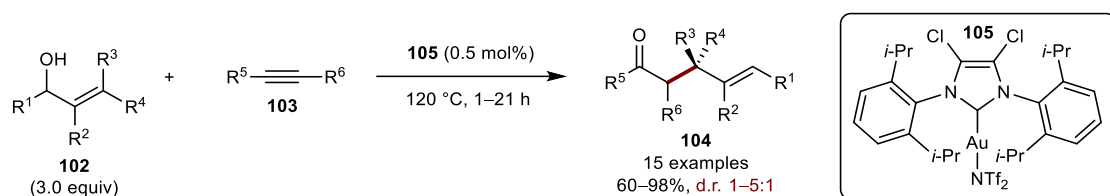
Scheme 28: Gold-catalysed rearrangement of allylic oxonium ylides.

Aponick reported an intermolecular variant, utilising a Claisen rearrangement to form γ , δ -unsaturated ketones in high yields and diastereoselectivities (Scheme 29).⁷⁵ The reaction generated the desired products **101b** and **101c** with exclusive *syn*-selectivity in good yields. However, regioisomeric mixtures were observed when using unsymmetrical alkynes (**101d**). The reaction proceeds *via* a gold-catalysed intermolecular hydroalkoxylation of the substituted alkyne, followed by a Claisen rearrangement.



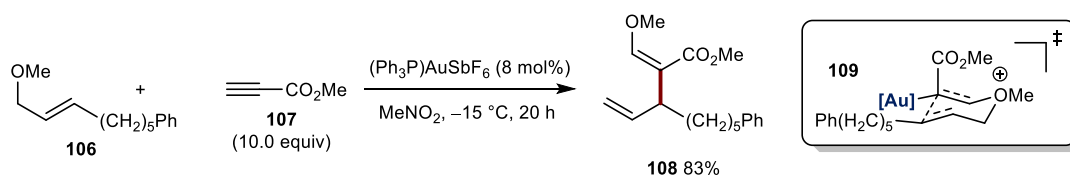
Scheme 29: Gold-catalysed intermolecular hydroalkoxylation/Claisen rearrangement.

A more sustainable variant was later reported by Nolan and co-workers (Scheme 30).⁷⁶ Modification of Aponick's initial conditions by reducing the catalyst loading, avoiding the use of additives and performing the reaction neat with respect to the allylic alcohol, generated the desired products (**104**) in good yields but with modest diastereocontrol. Similar regioselectivity issues with respect to utilising unsymmetrical alkynes were encountered as previously observed in Aponick's work.



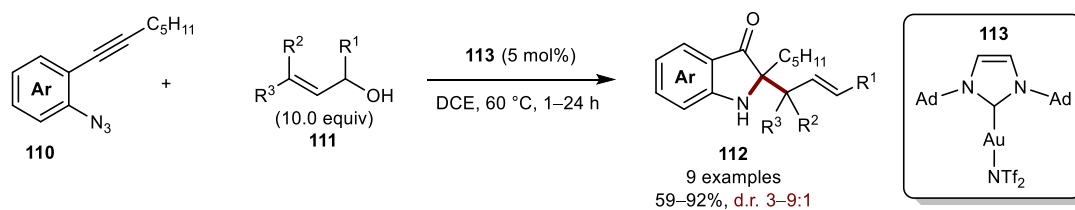
Scheme 30: Gold-catalysed synthesis of homoallylic ketones.

Allylic ethers have been shown to demonstrate similar reactivity to allylic alcohols. Rhee and co-workers reported the coupling of allylic ethers and alkynes *via* a [3,3]-sigmatropic rearrangement, generating the desired product **108** in 83% yield (Scheme 31).⁷⁷ Notable was the lack of alkene-alkyne coupling, indicating good chemoselectivity. Furthermore, the product was obtained as the (*Z*)-isomer exclusively. The authors propose transition state **109**, accounting for exclusive branch selectivity.

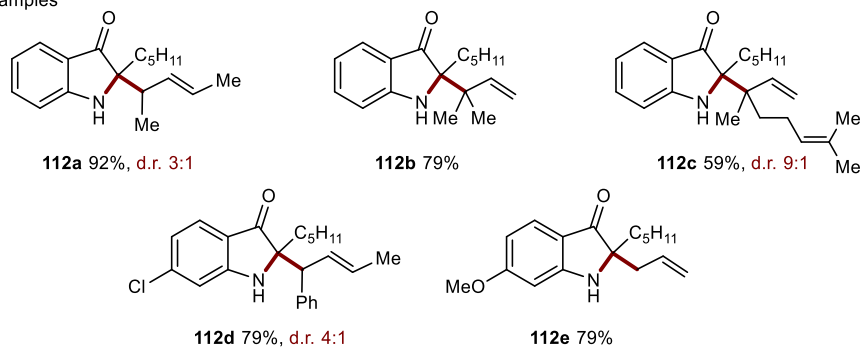


Scheme 31: Gold-catalysed intermolecular coupling of alkynoates and allylic ethers.

In 2011, Gagosz and co-workers reported the intermolecular synthesis of indolyl cores *via* a gold-mediated [3,3] Claisen rearrangement (Scheme 32).⁷⁸ The reaction accommodated multiple substitution patterns with respect to the allylic alcohol (**111**); however, limited diastereocontrol was observed. Remarkably, the construction of two quaternary contiguous stereocentres was feasible without any significant loss in yield (**112c** and **112d**). Moreover, both electron-withdrawing (**112d**) and electron-donating substituents (**112e**) were tolerated in the reaction conditions. Later that year, Zhang reported an extension of this work, expanding on the nucleophilic component, synthesising indole frameworks.⁷⁹

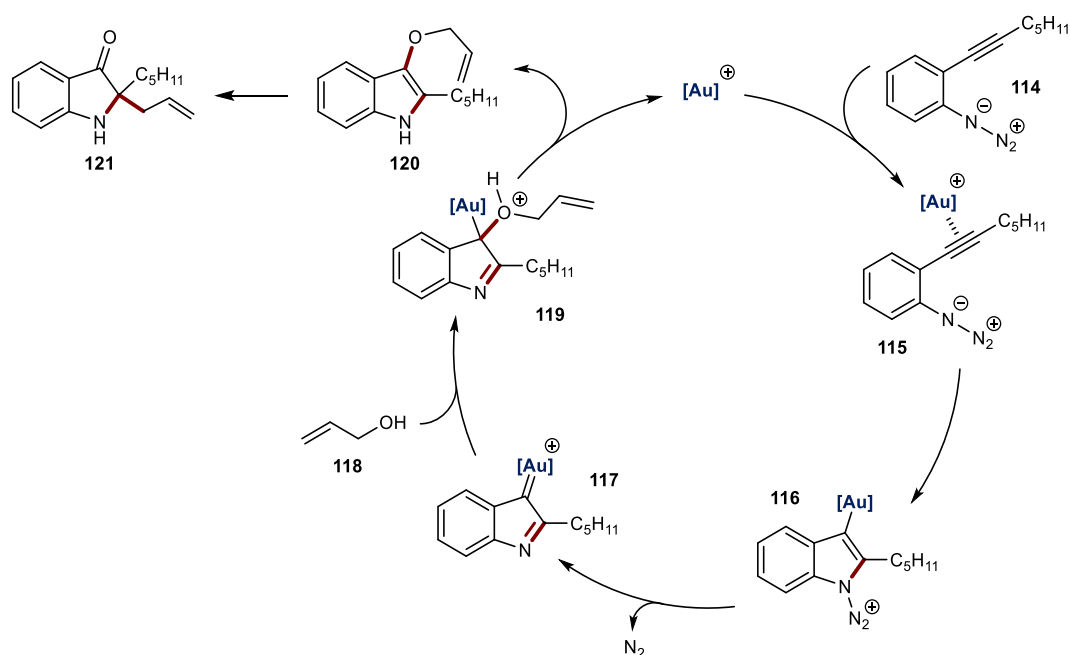


selected examples



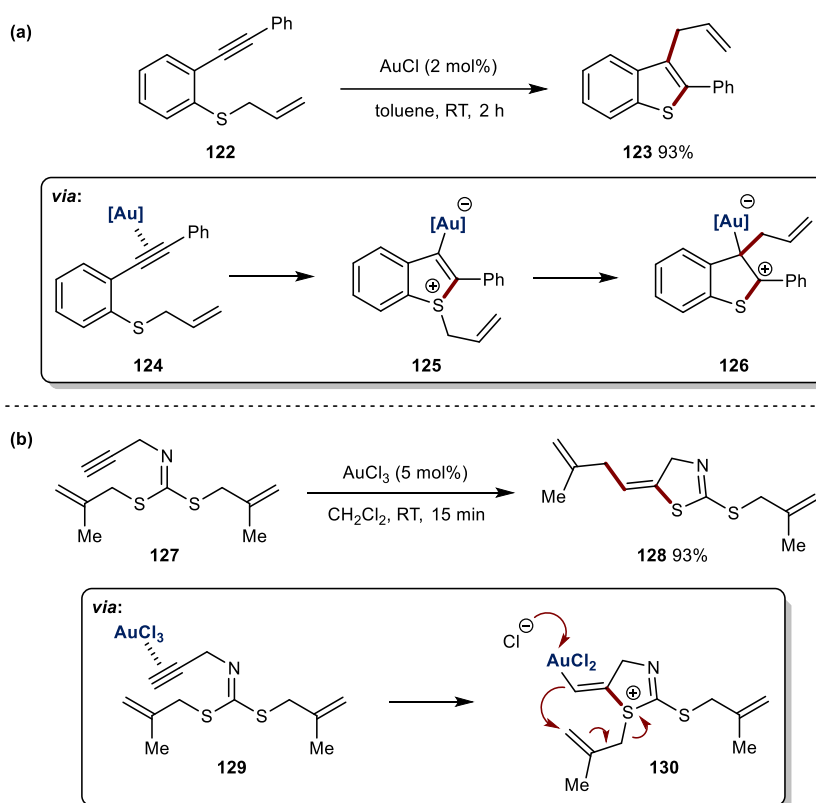
Scheme 32: Gold-catalysed synthesis of substituted indolyl cores.

The proposed mechanism is initiated by activation of the alkyne functionality of azide **114**, via gold catalyst **113** (Scheme 33). *Anti*-nucleophilic attack between the azide and alkyne occurs, followed by gold-assisted extrusion of N₂, forming gold carbene **117**. Subsequent nucleophilic addition of the allylic alcohol generates species **119**. Protodeauration and rearomatisation gives intermediate **120**. The authors propose a gold-mediated Claisen rearrangement in contrast to a thermal pathway due to the mild reaction conditions, generating the desired allylated product **121**.



Scheme 33: Proposed mechanism for the formation of **121**.

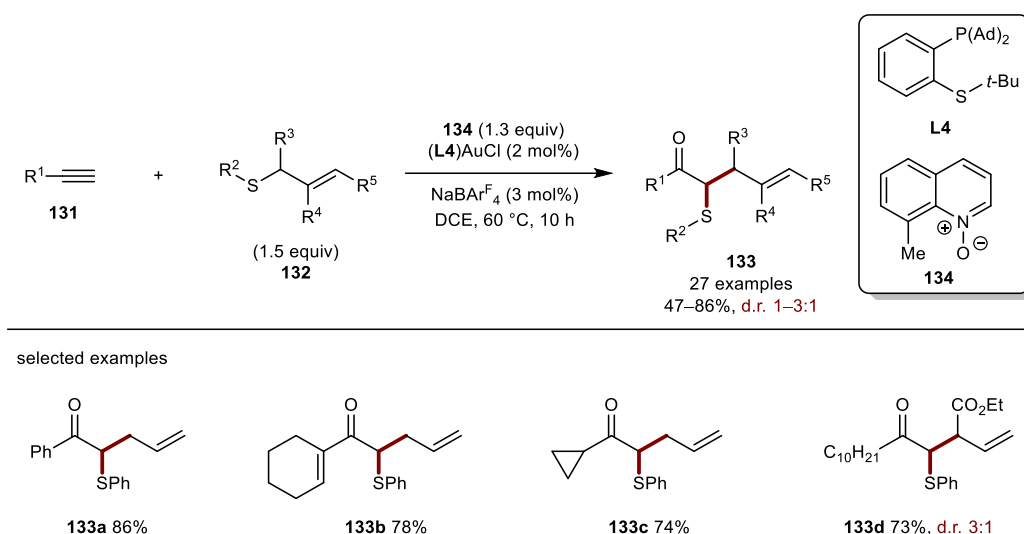
In a seminal report by Nakamura and co-workers, allylic sulfides have been shown to undergo similar reactivity to that of allylic ethers *via* the generation of sulfonium intermediates (Scheme 34a).⁸⁰ Reacting allylic sulfide **122** with catalytic AuCl₃ gave allylbenzothiophene **123** in 93% yield. A proposed mechanism is initiated by coordination of the active gold catalyst with the alkyne moiety of **122**, affording species **124**. *Anti*-addition of the alkyne occurs, forming intermediate **125**. Migration of the allyl group, followed by aromatisation gives the desired product. In 2011, Stevens expanded this work to synthesise thiazoles in high yields (Scheme 34b).⁸¹ The reaction suffered from poor functional group tolerance, with limited examples reported. The reaction proceeds through a 5-*exo-dig* pathway, forming species **130**. Chloride-promoted addition onto the terminal position of the allyl moiety generates the desired product **128**.



Scheme 34: Gold-catalysed rearrangements of allylic sulfonium species.

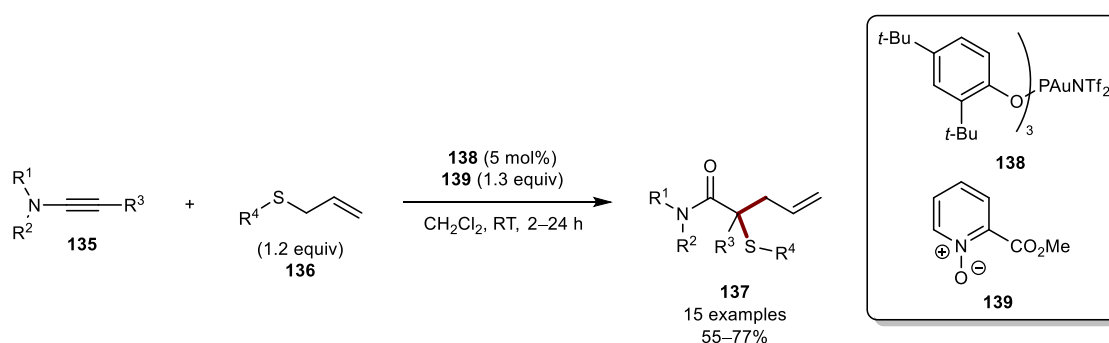
An intermolecular variant was later reported by Zhang and co-workers (Scheme 35).⁸² Coupling allylic sulfides and alkynes under gold(I) catalysis generated the desired products (**133**) in excellent yields, but with poor diastereocontrol. Critical to reactivity was the utilisation of novel *P,S*-bidentate ligand **L4**. The reaction proceeds *via* the generation of a α -oxo gold carbene intermediate. Substrate scope was good, with aryl-

(**133a**), alkenyl- (**133b**) and alkyl-substituted (**133c**) alkynes generating the desired products in good yields. However, poor diastereocontrol was observed when using substituted allylic sulfides (**133d**).



Scheme 35: Gold-catalysed coupling of alkynes and allylic sulfides.

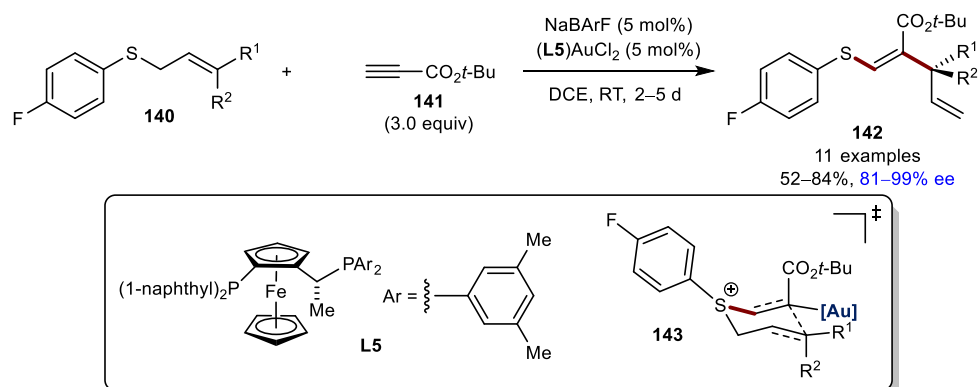
Zhang's work was expanded upon by Davies to incorporate ynamides (**135**) (Scheme 36).⁸³ Modification of the *N*-oxide and gold catalyst was required to enable reactivity. The reaction proceeds *via* the a [2,3]-sigmatropic rearrangement. This reaction offers an alternative to the Doyle-Kirmse reaction.⁸⁴



Scheme 36: Gold-catalysed coupling of ynamides and allylic sulfides.

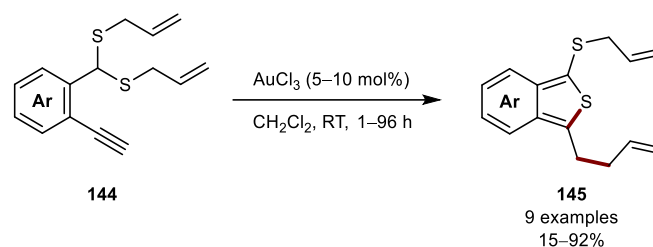
In 2020, Shin reported an enantioselective variant, coupling allylic sulfides and alkynes to generate the corresponding products (**142**) in high yields and enantioselectivities (Scheme 37).⁸⁵ Interestingly, the authors propose the sulfonium-induced [3,3]-sigmatropic rearrangement (**143**) minimises allyl dissociation, rendering the reaction enantioselective. The substrate scope was extremely broad, forming optically active quaternary centres with no significant loss in yield. The reaction required an

electron-deficient aryl sulfide to enhance enantioselectivity. The authors propose that reducing electron-density on the sulfur atom results in a tighter transition state.



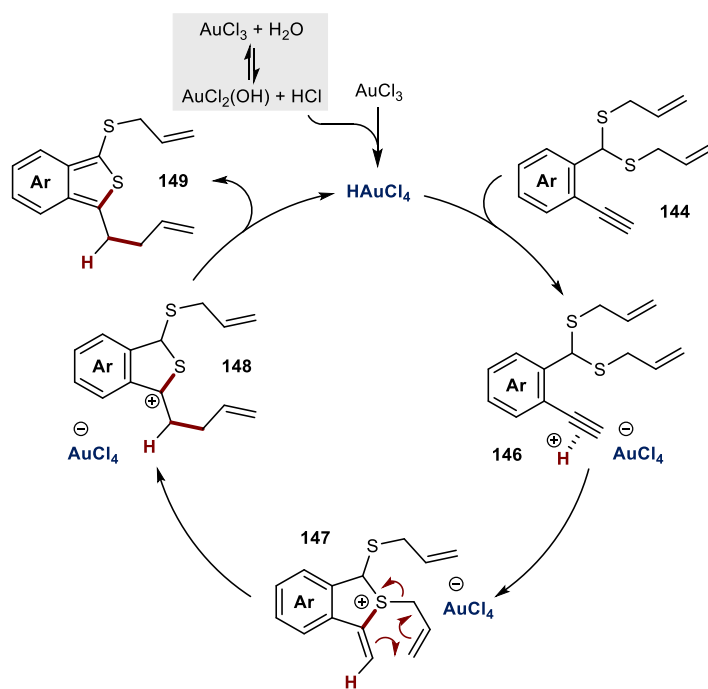
Scheme 37: Gold-catalysed thioallylation of propiolates with allyl sulfides.

A select few gold catalysts have been shown to act as superacids, allowing for unique modes of reactivity to be established. One such example was reported by Stevens and co-workers, demonstrating the synthesis of benzo[*c*]thiophenes (**145**) in good yields (Scheme 38).⁸⁶ The reaction has a modest substrate scope, being restricted to terminal alkynes.



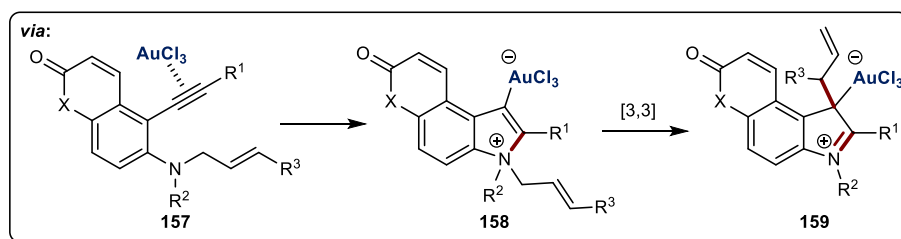
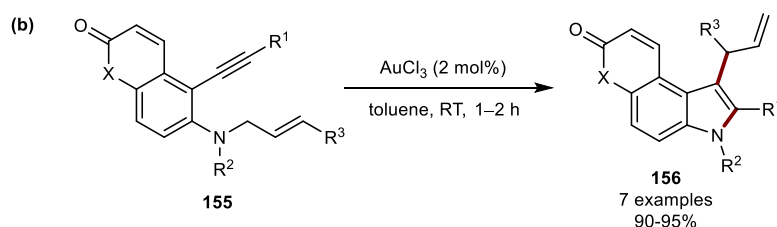
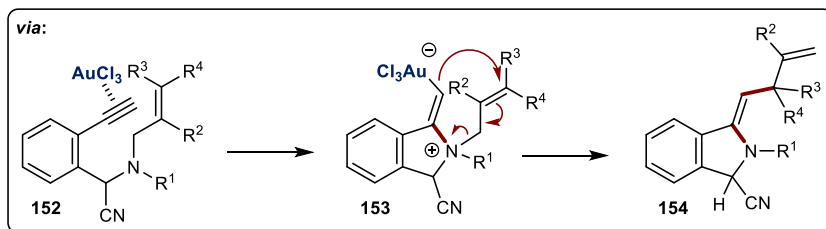
Scheme 38: Gold-catalysed synthesis of benzo[*c*]thiophenes.

Mechanistic investigations revealed the requirement for strongly acidic conditions to promote reactivity. Moreover, utilising strong acids that contained a nucleophilic counterion gave undesired side-products. This culminated in the following proposed cycle (Scheme 39). The active catalyst is formed *via* the addition of water to AuCl₃, forming the active H[AuCl₄] species. Acidic activation of the alkyne moiety of **144** occurs, forming intermediate **146**. A 5-*exo-dig* cyclisation ensues, followed by a Claisen rearrangement, furnishing species **148**. Aromatisation yields the desired product, regenerating the active gold catalyst.



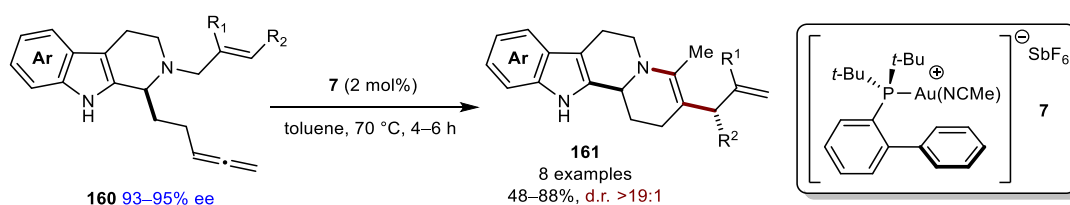
Scheme 39: Proposed mechanism for the formation of **149**.

Allylic amines have been shown to participate in similar reactivity, first reported by Stevens.⁸⁷ Stevens and co-workers demonstrated the intramolecular synthesis of indoles by utilising 1 mol% AuCl₃ in CH₂Cl₂. (Scheme 40a). The key reactive step is a 5-*exo-dig* cyclisation producing intermediate **153**. Addition onto the terminal position of the allyl moiety occurs, generating species **154**. Aromatisation *via* a [1,5]-prototropic shift furnishes the desired product **151**. An extension of this work was later reported by Roy and co-workers, synthesising highly substituted indoles (Scheme 40b).⁸⁸ First, coordination of the gold catalyst to the alkyne moiety occurs, followed by nucleophilic attack of the amine, producing species **158**. A [3,3]-sigmatropic rearrangement ensues, with subsequent aromatisation generating the desired product **154**.

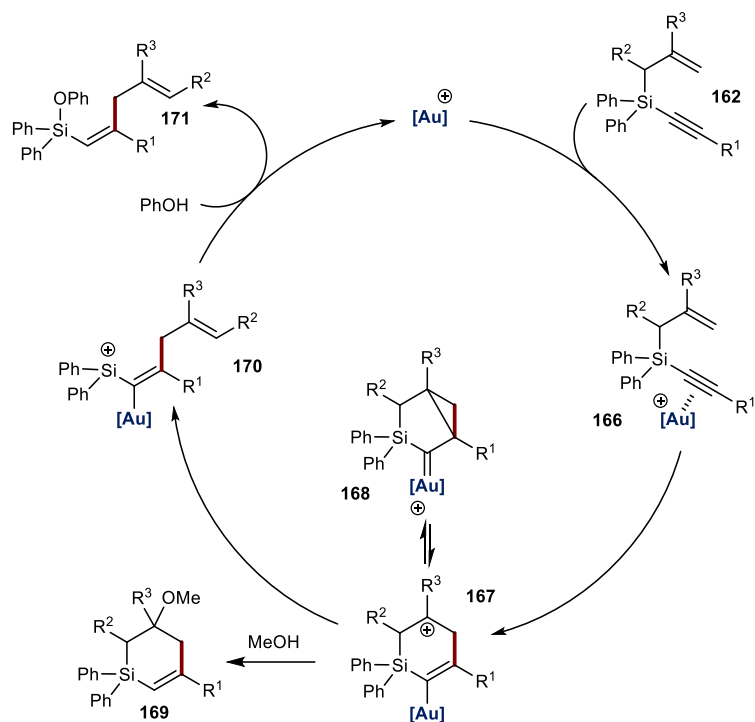


Scheme 40: Gold-catalysed rearrangements of allylic amines.

In 2018, Guinchard reported the intramolecular cyclisation of enantioenriched allylic amines (**160**) onto allenes, furnishing the desired products in good yields and excellent diastereoselectivities (Scheme 41).⁸⁹ Migration of the allyl fragment from the nitrogen atom to the carbon backbone occurs *via* an analogous mechanism to that of scheme 40b.

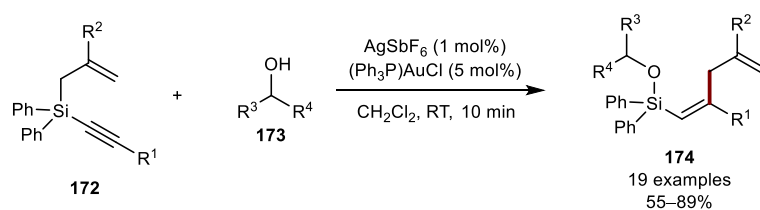


Scheme 41: Gold-catalysed rearrangements of allylic amines.



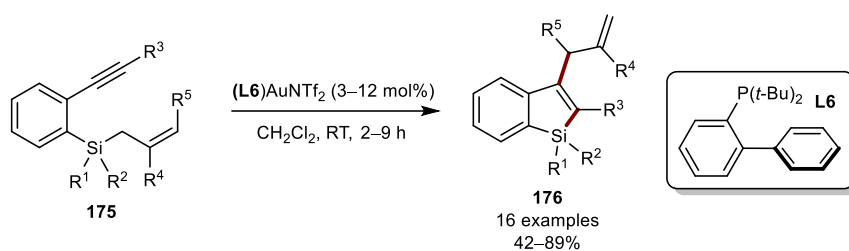
Scheme 43: Proposed mechanism for the formation of **169** and **171**.

That same year, Lee and co-workers extended this approach *via* modification of Toste's original reaction conditions, forming exclusively the acyclic product **174**, with high (*Z*)-selectivity (Scheme 44).⁹¹ The authors propose an identical cycle to Scheme 43. Utilising sterically encumbered alcohols, promotes ring-opening over direct nucleophilic quenching.



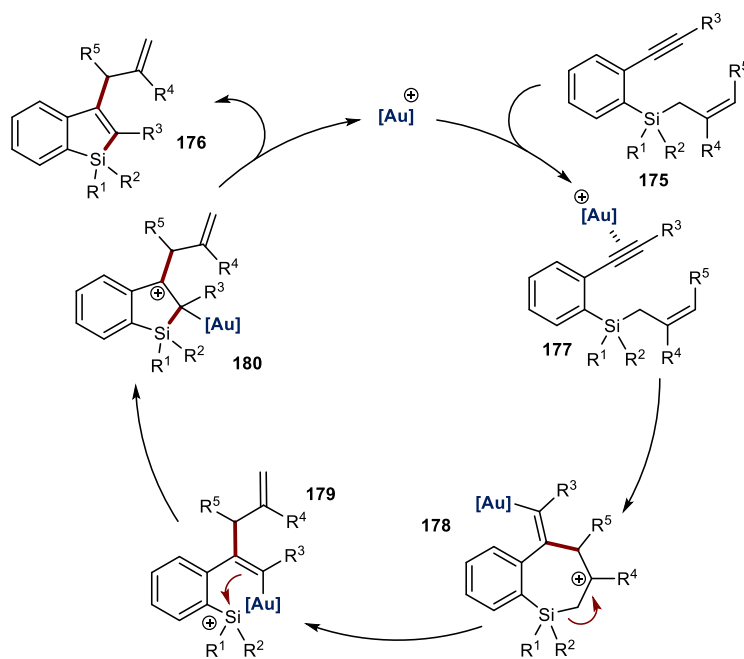
Scheme 44: Gold-catalysed sila-Cope rearrangement forming acyclic product **174**.

In 2008, Murakami reported the synthesis of silole cores *via* an intramolecular *trans*-allylsilylation reaction, forming the desired products in high yields under mild reaction conditions (Scheme 45).⁹² Crucial to reactivity was the incorporation of ligand **L6**, increasing product formation significantly. The functional group compatibility of the reaction was good, with both electron-donating and electron-withdrawing substituents providing the product in appreciable yields.



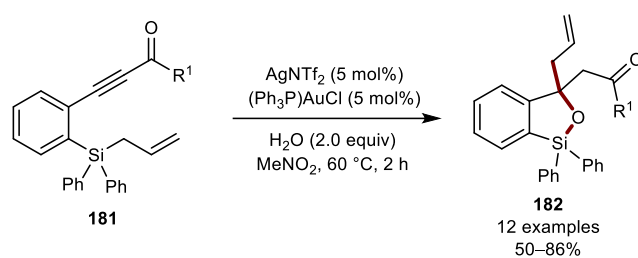
Scheme 45: Gold-catalysed synthesis of 3-allyl-1-silaindenes.

The proposed mechanism is initiated by the activation of the alkyne moiety of **175**, forming intermediate **177** (Scheme 46). A 7-*exo-dig* cyclisation occurs *via* nucleophilic attack of the allylsilane onto the alkyne component of **177**, generating species **178**. β -silyl fragmentation occurs, forming allylated intermediate **179**. Subsequent electrophilic ring closure furnishes cationic species **180**. Aromatisation gives the desired product, regenerating the active gold catalyst. DFT calculations performed by Ujaque in 2010 provide further evidence towards the proposed catalytic cycle.⁹³



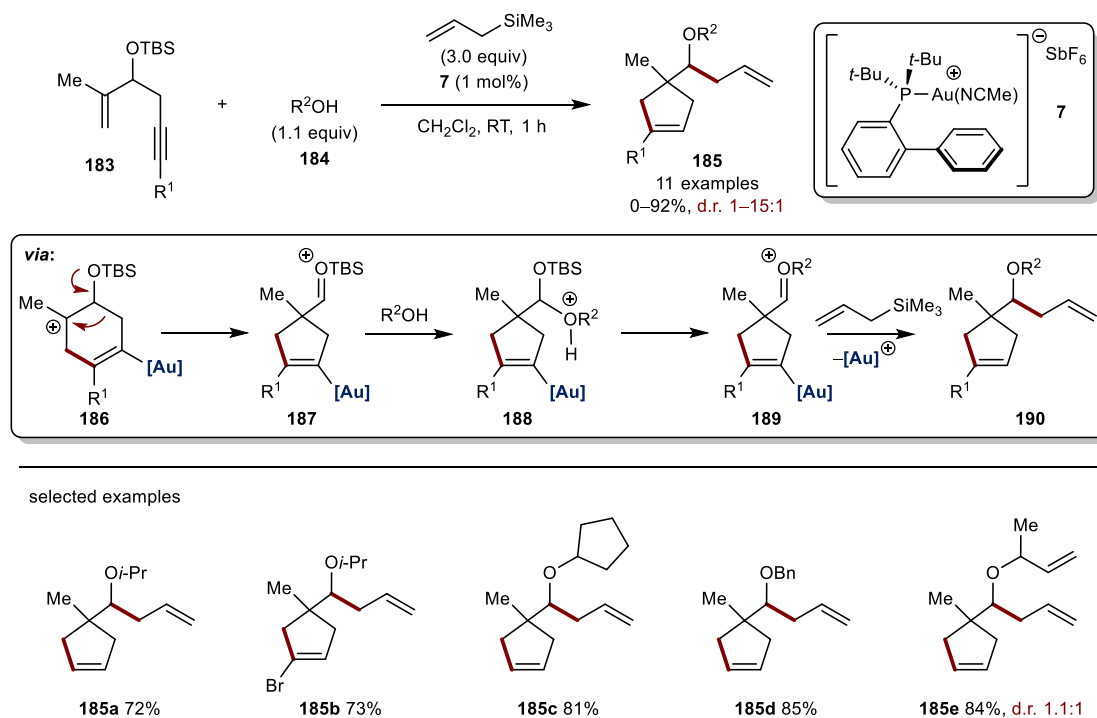
Scheme 46: Proposed mechanism for the formation of **176**.

Horino and co-workers extended this concept by incorporating water, intercepting the silyl cation intermediate **179** proposed by Murakami in Scheme 46. Subsequent nucleophilic ring-closure gave the desired bezoxasiloles in high yields (Scheme 47).⁹⁴



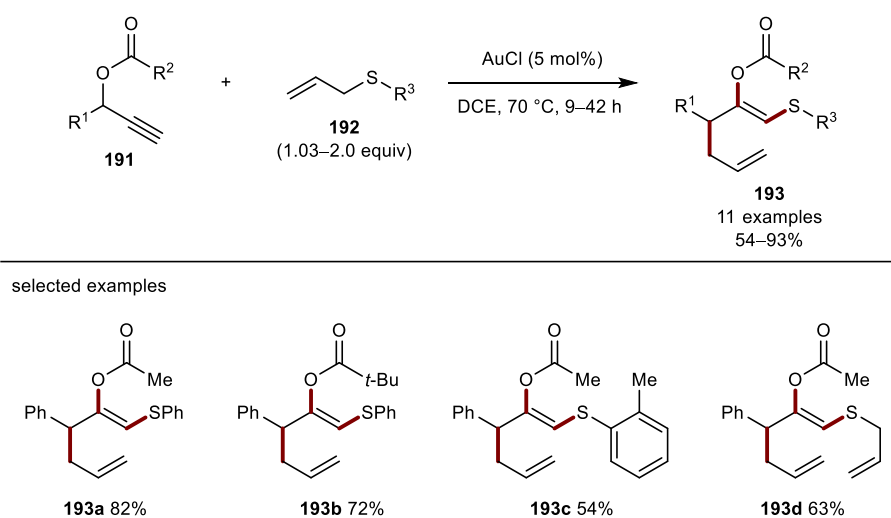
Scheme 47: Gold-catalysed synthesis of bezoxasiloles.

An intermolecular variant was reported by Lee and co-workers, coupling allylsilanes with 1,5-enynes, synthesising cyclised product **185** in high yields with modest levels of diastereocontrol (Scheme 48).⁹⁵ The reaction is initiated *via* a 6-*endo-dig* cyclisation, assisted by gold, affording intermediate **186**. A pinacol-type rearrangement occurs, generating species **187**. Nucleophilic attack of the alcohol arises, forming acetal **188**. Subsequent reformation of an oxonium species ensues, followed by nucleophilic addition of the allylsilane generating the desired product (**190**). Exploration of the substrate scope was modest, with various alcohols participating in the reaction (**185b** and **185c**). Variation with respect to the alkyne was poor, with reactivity shutting down upon introducing steric bulk. Furthermore, poor diastereocontrol was observed when subjecting 3-buten-2-ol (**185e**) to the reaction conditions.



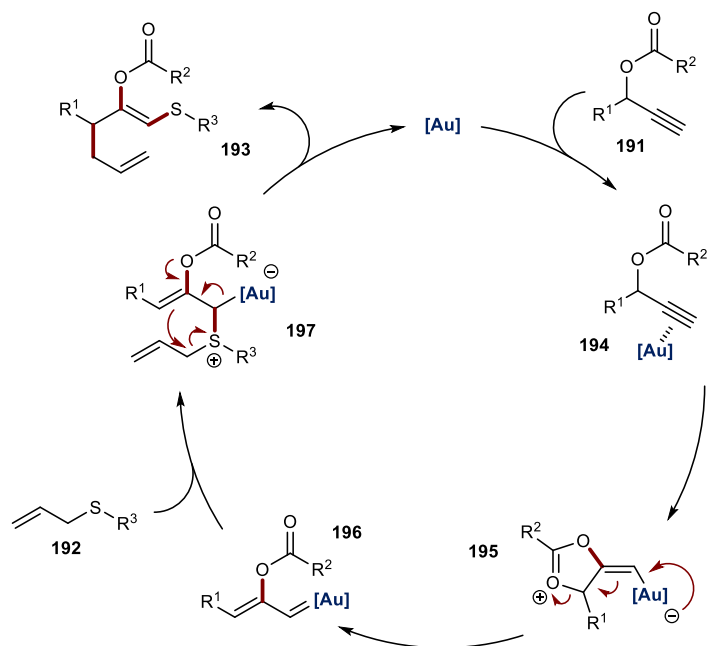
Scheme 48: Gold-catalysed carbocyclisation of enynes.

Gold-catalysed rearrangements containing propargylic carboxylates have been shown to undergo cascade reactions, building molecular complexity from simple precursors.⁹⁶ Furthermore, they have been shown to participate in allylic rearrangements, furnishing net allylated products. A seminal report by Davies and co-workers coupling propargylic carboxylates and allylic sulfides *via* gold-catalysis was reported (Scheme 49).⁹⁷ The reaction tolerated various propargylic carboxylates (**193a** and **193b**), affording the desired products in 82% and 72% yield respectively. Moreover, both aryl (**193c**) and alkyl (**193d**) allylic sulfides were well tolerated, delivering the aforementioned products in good yields.



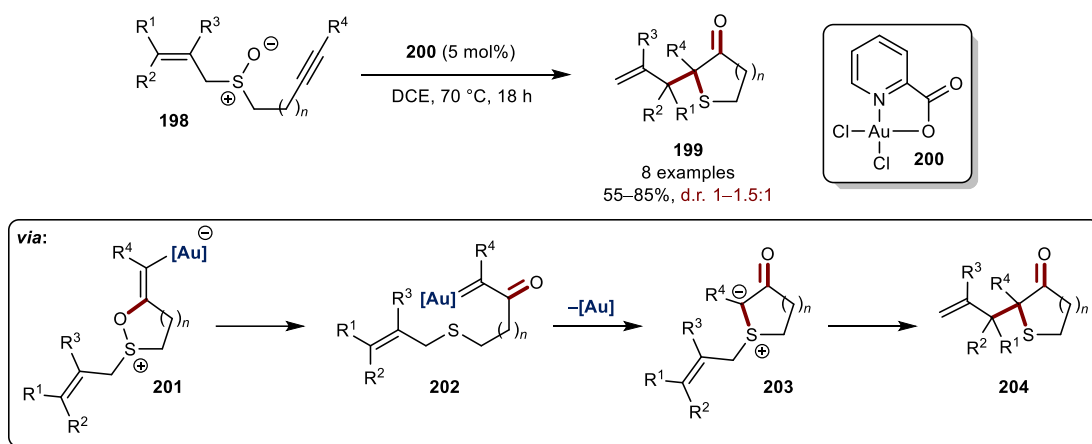
Scheme 49: Gold-catalysed intermolecular coupling of propargylic esters and allylic sulfides.

The authors propose the following catalytic cycle shown in Scheme 50. First, activation of the alkyne moiety of **191** occurs *via* coordination to AuCl, forming species **194**. Nucleophilic attack of the propargylic carboxylate ensues, followed by back-donation from the gold metal centre, generating carbenoid **196**. Nucleophilic attack from the allylic sulfide to the gold carbenoid intermediate generates species **197**. A subsequent 1,4-shift yields the desired product, regenerating the active gold catalyst.



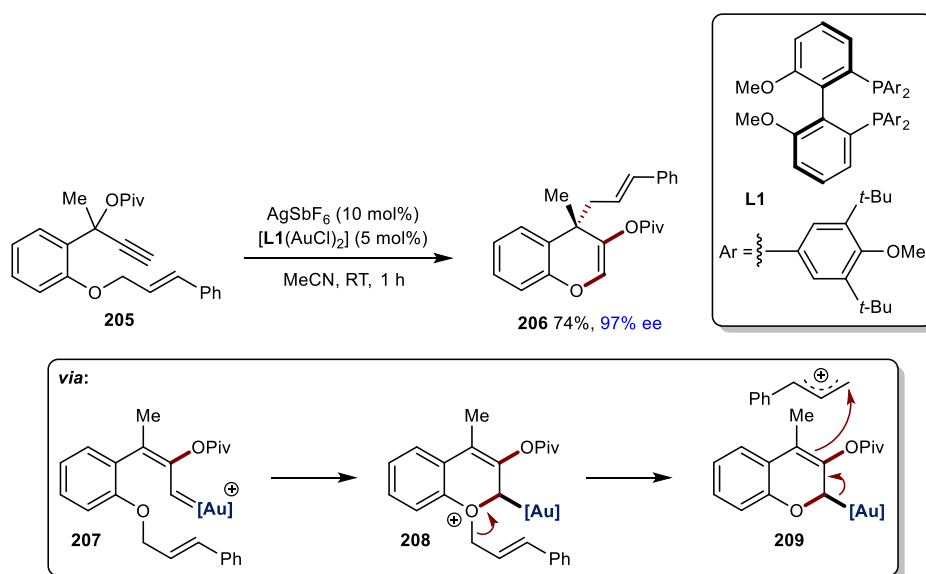
Scheme 50: Proposed mechanism for the formation of **193**.

Davies later reported an intramolecular variant coupling sulfoxides with *in-situ* generated sulfur ylides (Scheme 51).⁹⁸ Cycloisomerisation of sulfoxides which contain a tethered alkyne and allyl fragment generates **199** in high yields but poor diastereocontrol. The mechanism is similar to Scheme 50 and proceeds *via* the *anti*-nucleophilic attack of the sulfoxide group to the gold-activated alkyne moiety of **198**, affording intermediate **201**. Back-donation from the metal centre ensues, forming gold carbenoid **202**. Subsequent nucleophilic attack from the allylic sulfide followed by ylide formation occurs. A [2,3]-sigmatropic rearrangement furnishes the desired product.



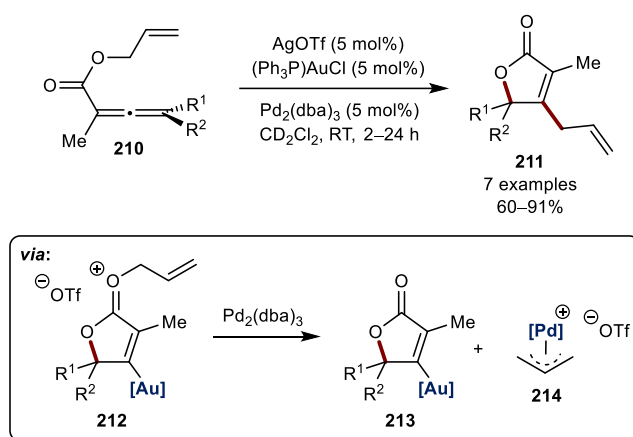
Scheme 51: Gold-promoted cycloisomerisation of **198**.

In 2009, Toste and co-workers reported the first enantioselective gold-catalysed synthesis of benzopyrans by utilising propargylic carboxylates, furnishing products that contain a quaternary centre in high enantioselectivities (Scheme 52).⁹⁹ Crucial for high levels of enantiocontrol was the implementation of bulky substituents on the phosphine aryl rings of **L1**. As seen previously, gold carbenoid species **207** is formed. This intermediate is intercepted by the allylic ether moiety of **207**, forming enantioenriched oxonium species **208**. Subsequent rearrangement of this oxonium species ensues, involving the formation of an allyl cation, affords the desired product.



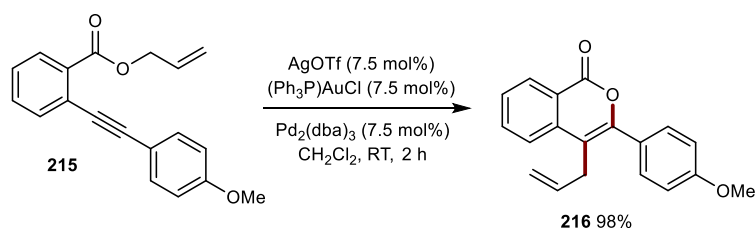
Scheme 52: Gold-catalysed intramolecular propargylic carboxylate rearrangements.

Dual-catalysed transformations promote unique reaction pathways due to synergistic behaviours between two different metal centres. Gold-catalysed transformations often produce reactive intermediates that potentially could be intercepted by other metal centres. This was first realised by Blum and co-workers, reporting the gold/palladium-catalysed synthesis of butenolides (Scheme 53).¹⁰⁰ Gold-catalysed cyclisation of **210** affords allyl oxonium species **212**. This species is susceptible to oxidation addition by $\text{Pd}_2(\text{dba})_3$, forming species **213** and **214**. Transmetalation followed by reductive elimination furnishes the desired product.



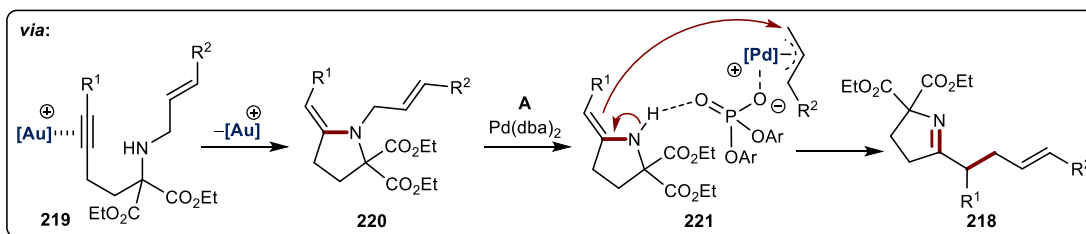
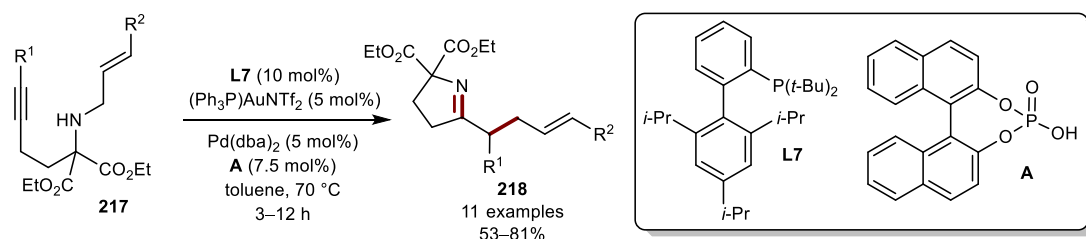
Scheme 53: Gold- and palladium-catalysed synthesis of butenolides.

Hashmi and co-workers extended this concept reporting the cycloisomerisation of alkynylbenzoate ester **215**, generating the cross-coupled product **216** in 98% yield (Scheme 54).¹⁰¹

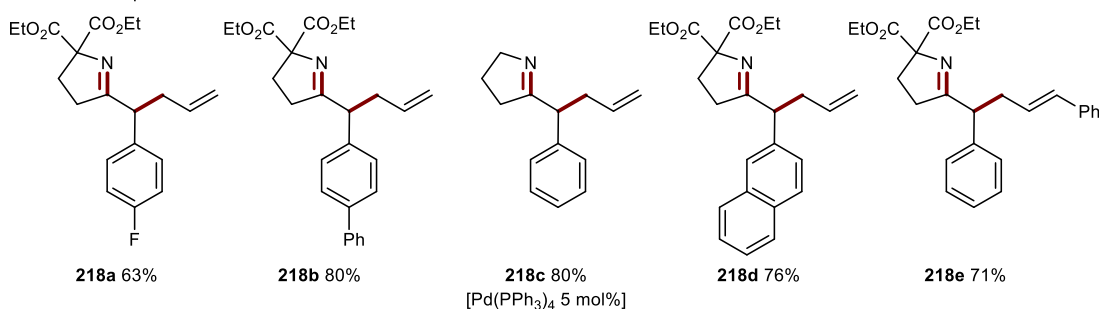


Scheme 54: Gold- and palladium-catalysed cyclisation of alkynylbenzoate esters.

In 2012, Gong reported a ternary system involving gold, palladium and Brønsted acid catalysts, synthesising allylic pyrrolidine derivatives in modest to high yields (Scheme 55).¹⁰² The reaction is initiated *via* activation of the alkyne fragment of **217**. *Anti*-nucleophilic addition followed by protodeauration yields intermediate **220**. Assisted by TRIP, palladium-catalysed oxidative addition occurs, forming species **221**. Nucleophilic attack to the cationic palladium allyl species ensues, forming the desired allylated pyrrolidine product **218**. The reaction scope was good, with electron-withdrawing substituents (**218a**) generating the desired products in reduced yields. Bulkier bi-aryl (**218b**) and naphthyl (**218d**) derivatives furnished the desired products in 80% and 76% respectively. Furthermore, substrates that had no substituents at the α -carbon of the amine fragment, gave the desired product in drastically reduced yield. However, modification of the palladium catalyst gave the aforementioned product in 80% yield (**218c**).

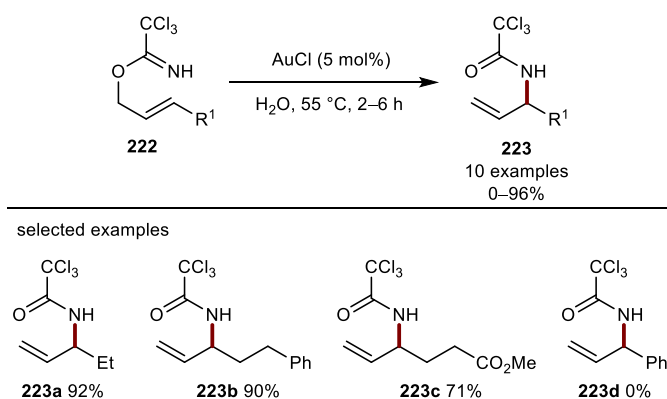


selected examples



Scheme 55: Gold-, palladium- and Brønsted acid-catalysed hydroamination/allylic alkylation.

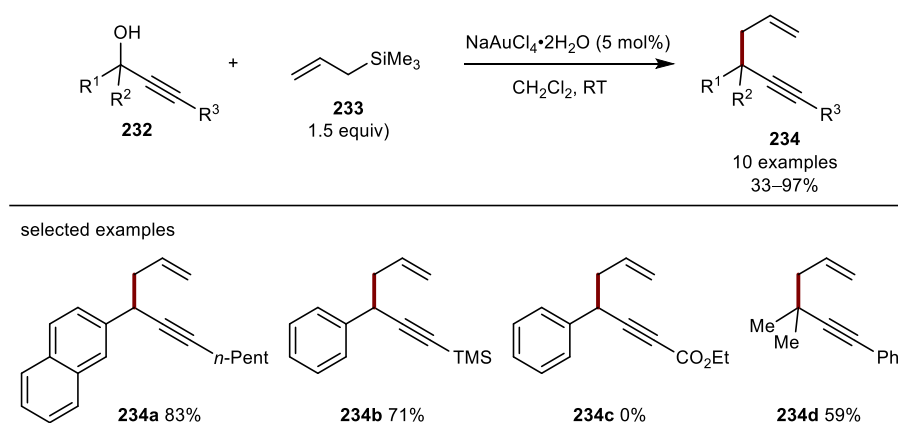
Intramolecular additions to alkenes are a viable synthetic strategy towards the conversion of allylic alcohols to allylic amines. Dang and co-workers reported a highly efficient gold-catalysed Overman rearrangement, forming trichloroacetimidates (**223**) in high yields (Scheme 56).¹⁰³ Remarkably, the reaction could be performed in water without any significant decrease in yield. The reaction tolerated alkyl (**223a**) and ester moieties (**223c**), furnishing the desired products in excellent yields. However, substrates containing phenyl-substituted alkenes (**223d**) diminished reactivity.



Scheme 56: Gold-catalysed Overman rearrangement.

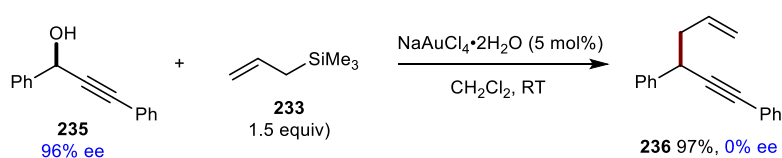
1.2.1.3 Addition of Nucleophilic Allylating Agents to Electrophiles

The addition of nucleophilic allylating agents to electrophiles catalysed by gold is much less commonly reported than the addition of nucleophiles to electrophilic allylating agents. However, several examples have been described and they commonly utilise allylic silanes. A pioneering report by Campagne coupling allylic silanes and propargyl alcohols was described (Scheme 60).¹⁰⁶ The reaction operates under mild reaction conditions and tolerated electron-rich (**234a** and **234b**) aromatic propargyl alcohols; however, electron-poor substituents (**234c**) gave no reactivity. Moreover, alkyl-derived (**234d**) propargyl alcohols were well tolerated.



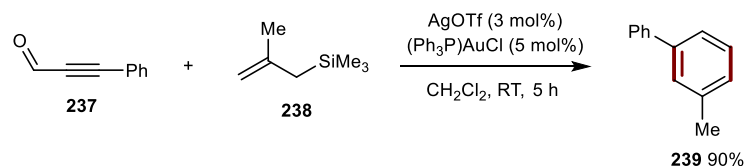
Scheme 60: Gold-catalysed nucleophilic allylation of propargylic alcohols.

Subjecting enantioenriched propargyl alcohol **235** to their optimised reaction conditions generated the corresponding allylated product **236** in 97% yield with no asymmetric induction (Scheme 61). The authors propose the involvement of an *in-situ* generated carbocation *via* a S_N1 reaction pathway.



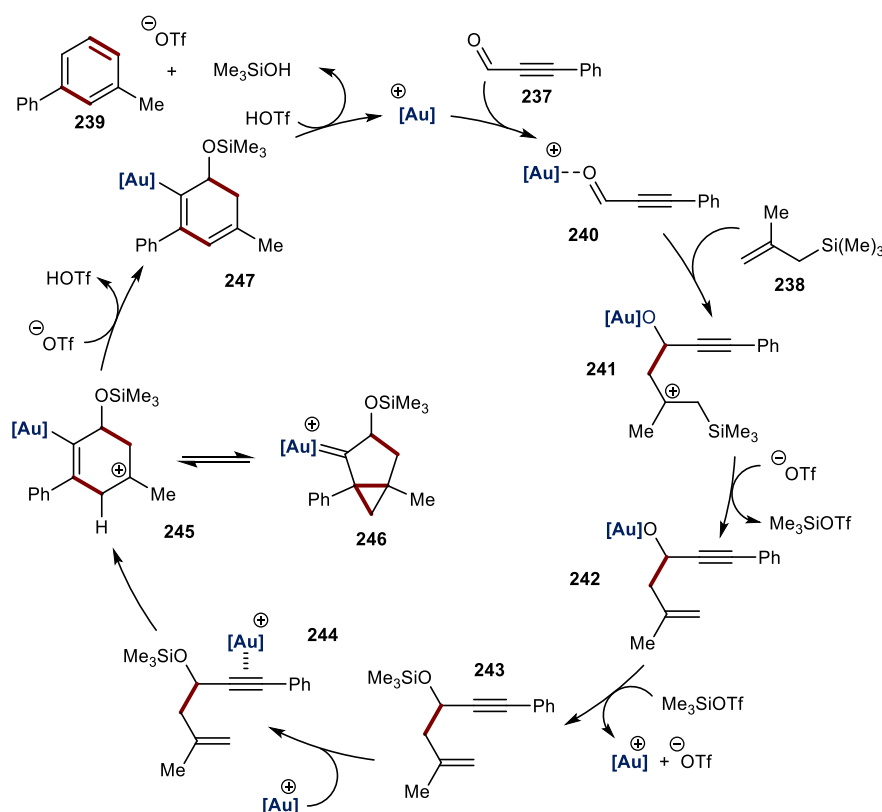
Scheme 61: Gold-catalysed nucleophilic allylation of propargylic alcohol **235**.

In 2009, Liu and co-workers reported the first gold-catalysed addition of allylsilanes to aldehydes, followed by cycloisomerisation affording 1,3-disubstituted aryl rings in excellent yields (Scheme 62).¹⁰⁷ Alkynal **237** was transformed into product **239** in 90% yield using $(\text{Ph}_3\text{P})\text{AuCl}$ as the catalyst in CH_2Cl_2 for 5 h.



Scheme 62: Gold-catalysed nucleophilic allylation of aldehydes.

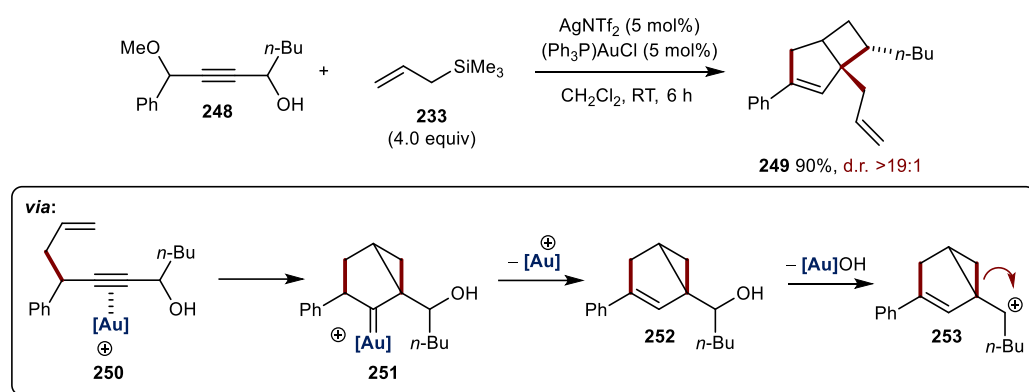
A plausible mechanism begins with coordination of the gold catalyst to the aldehyde of **237** (Scheme 63). Addition of allylsilane **238** occurs, forming carbocation **241**. Elimination of Me₃SiOTf *via* a triflate anion ensues, forming gold-bound allylated product **242**. Exchange of the gold-bound intermediate **242** with Me₃SiOTf, regenerates the active gold catalyst which in turn, coordinates to the alkyne of **243**, forming species **244**. A 6-*endo-dig* cyclisation generates carbocation **245** which can be in resonance with its gold carbenoid form (**246**). Subsequent deprotonation of **245** occurs, forming gold-bound cyclohexadienyl **247**. Elimination of Me₃SiOH followed by protodeauration generates the desired disubstituted aryl product **239**.



Scheme 63: Gold-catalysed formation of **239**.

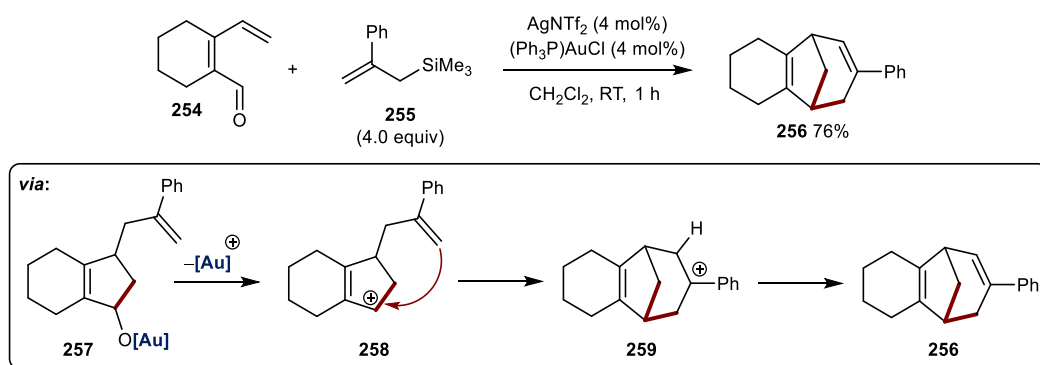
Liu and co-workers extended this concept, reporting a cascade reaction *via* the [3+2] annulation of allylic silanes to form complex highly strained bicyclic frameworks (**249**)

in excellent yields and diastereoselectivities (Scheme 64).¹⁰⁸ The suggested mechanism for the formation of 1,5-enyne **250** is analogous to that proposed by Campagne (Scheme 61). Supported by deuterium studies, the authors propose a cycloisomerisation pathway followed by a 1,2-hydride shift yielding **252**. Formation of carbocation **253** ensues. Subsequent ring expansion and nucleophilic trapping by allylsilane delivers the desired product.



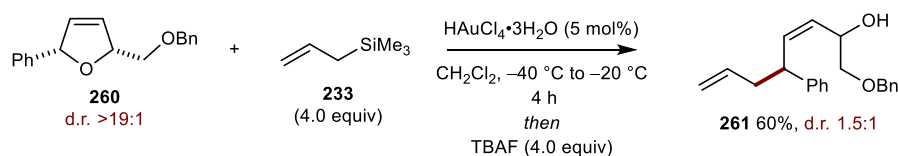
Scheme 64: Gold-catalysed nucleophilic allylation/cycloisomerisation.

Liu reported another intramolecular deoxygenative cyclisation followed by a nucleophilic addition cascade, generating polycyclic frameworks from simple precursors (Scheme 65).¹⁰⁹ First, cyclisation *via* nucleophilic addition of the alkene to the gold-bound aldehyde forms a cationic intermediate that is intercepted by allylic silane **255**, garnishing species **257**. Subsequent gold-mediated deoxygenation occurs, furnishing cationic species **258**. Intramolecular cyclisation forms stabilised intermediate **259**, followed by alkene formation affording the desired polycyclic product. This methodology was applied towards the synthesis of biologically relevant targets from the brazilane family and could be applied to a range of other electrophiles and nucleophiles.^{110,111}



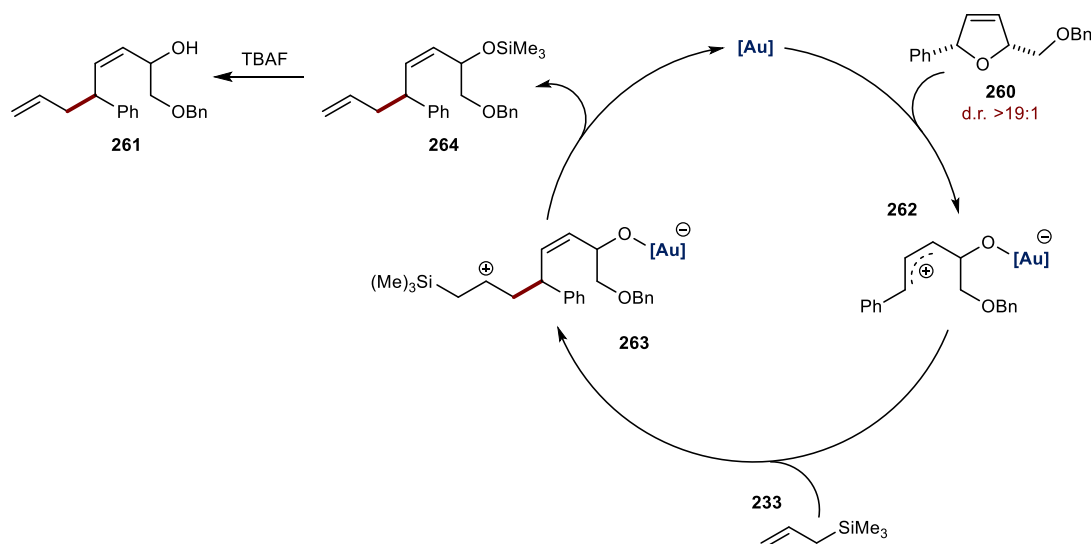
Scheme 65: Gold-catalysed deoxygenated cyclisation.

In 2009, Krause and co-workers demonstrated a robust methodology involving the gold-catalysed ring-opening allylation of dihydrofurans (Scheme 66).¹¹² Gold-catalysed epimerisation of dihydrofurans is known to operate *via* a zwitterionic intermediate, therefore, the authors propose that trapping this intermediate with a nucleophile would generate complex acyclic products. The reaction was regioselective towards the 2-position of furan **260**, affording the desired product **261** in 60% yield. However, loss of diastereocontrol was observed due to the formation of a cationic intermediate.



Scheme 66: Gold-catalysed ring-opening allylation of dihydrofurans.

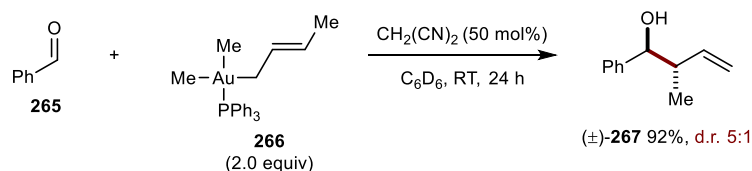
The reaction is initiated by the gold-mediated ring-opening of **260**, forming zwitterionic intermediate **262** (Scheme 67). Nucleophilic attack of the allylic silane occurs at the 2-position, forming species **263**. Cleavage of the carbon-silicon bond forms intermediate **264**, regenerating the active gold catalyst. Remove of the silyl group using TBAF affords the desired product.



Scheme 67: Proposed mechanism for the formation of **261**.

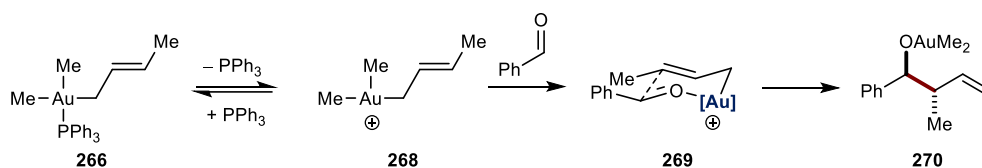
The isolation and characterisation of allylic gold(III) complexes was first reported by Komiyama in 1988.⁶² The first application of these complexes was later reported by

Komiya, demonstrating the nucleophilic allylation of aldehyde **265**, generating homoallylic alcohol **267** in high yield with modest diastereocontrol (Scheme 68).¹¹³ Gold(III) allylic complex **266** was synthesised *via* Grignard displacement from the corresponding gold halide counterpart. The reaction is γ -selective with respect to the allylic gold(III) complex.



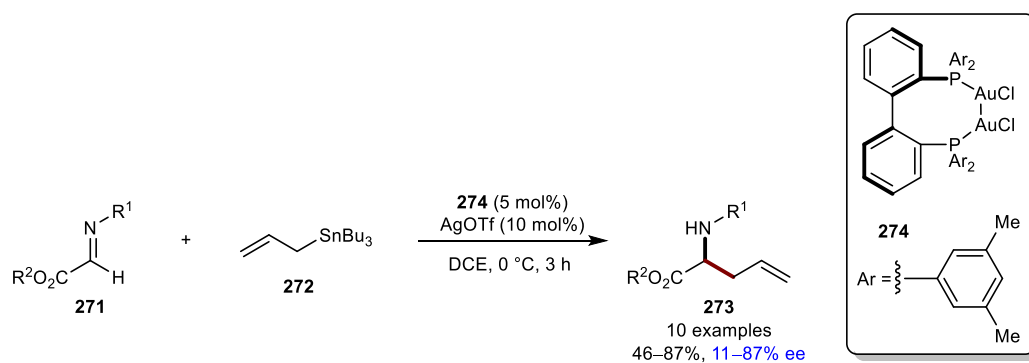
Scheme 68: Allylation of aldehydes using allylgold reagents.

Due to preliminary mechanistic considerations by the authors, a hypothesised closed six-membered chair-like transition state (**269**) was proposed, whereby the gold(III) centre adopts trigonal planar geometry due to the dissociation of PPh₃ (Scheme 69).

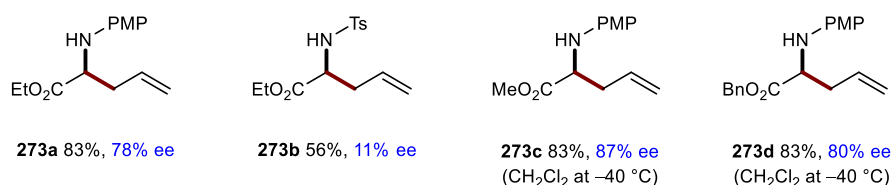


Scheme 69: Mechanistic rationale for the formation of **270**.

Enantioselective variants incorporating nucleophilic allylating agents under gold catalysis are extremely rare. One such example was reported by Mikami and co-workers, demonstrating the nucleophilic allylation of glyoxylate imines with allylic stannanes (Scheme 70).¹¹⁴ Utilisation of the BIPHEP-gold complex **274** rendered the reaction enantioselective, showing increased catalytic activity in comparison to BINAP derivatives. This may be due to the Au-Au intramolecular interaction that gold complex **274** exhibits, providing a more rigid transition state. The substrate scope was poor, with variation with respect to the nitrogen substituent (**273a** and **273b**) forming the desired homoallylic amines in good yields but modest to good enantioselectivities. Furthermore, modification of the reaction conditions was required when varying the ester moiety of the glyoxylate imine (**273c** and **273d**). However, only modest enantioselectivities were observed.

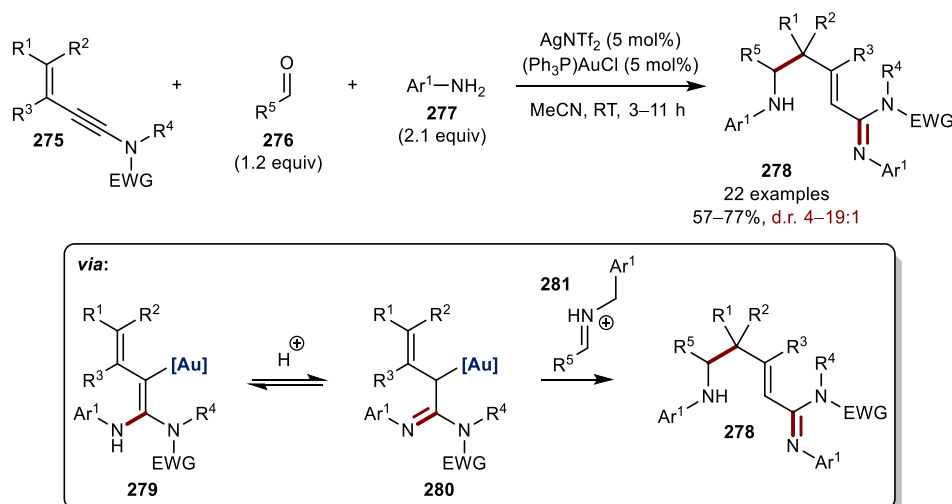


selected examples



Scheme 70: Enantioselective gold-catalysed allylation of glyoxylate imines.

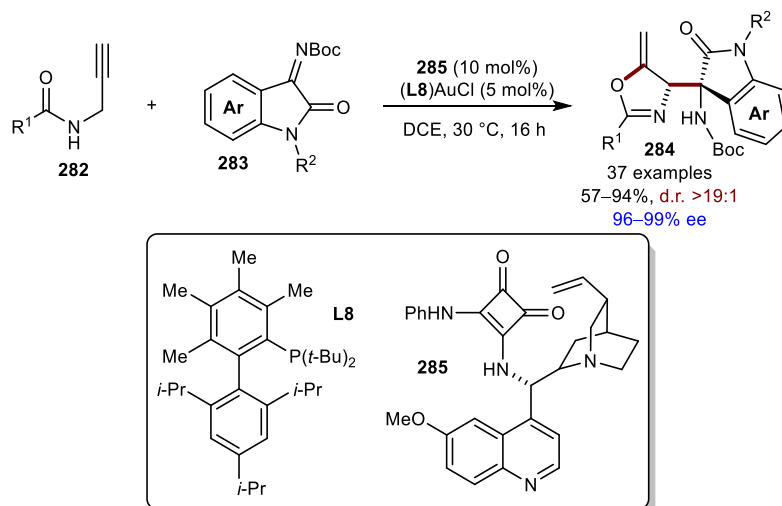
In 2016, Liu and co-workers reported a one-pot gold-catalysed three-component coupling of enynes, aldehydes and amines, generating densely functionalised homoallylic amines in good yields and modest to good diastereoselectivities (Scheme 71).¹¹⁵ The reaction proceeds by *anti*-nucleophilic attack of aniline **277** onto enyne **275**, forming intermediate **279**. Proton transfer forms allylgold species **280**. Nucleophilic allylation of imine **281**, formed *via* condensation between **276** and **277** affords the desired product. The reaction is γ -selective with respect to the allylic gold(I) intermediate **280**.



Scheme 71: Gold-catalysed Mannich cascade reaction.

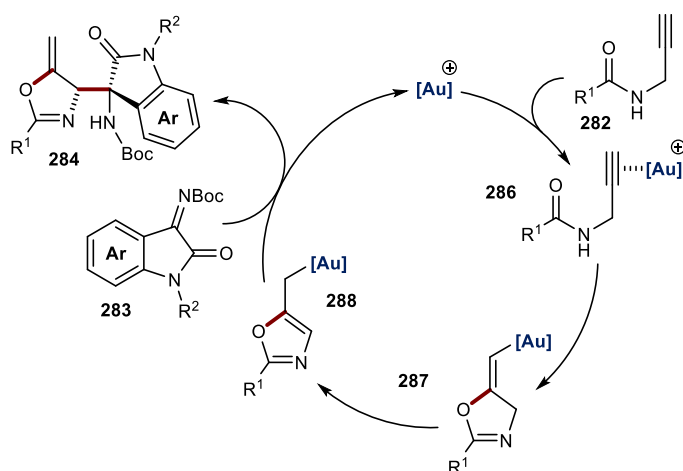
Xu and co-workers reported the first isolation of an allylic gold(I) complex, displaying its capability to allylate isatin-derived ketimines (Scheme 72).¹¹⁶ The reaction

utilises a cooperative catalysis approach involving a gold catalyst and an enantioenriched chiral organocatalyst (**285**), furnishing products that contain vicinal stereocentres. The reaction delivered the desired products in excellent yields, diastereoselectivities and enantioselectivities. Furthermore, the reaction could be extended to include isatins, affording homoallylic alcohols with excellent enantiocontrol.



Scheme 72: Enantioselective gold-catalysed allylation of isatins.

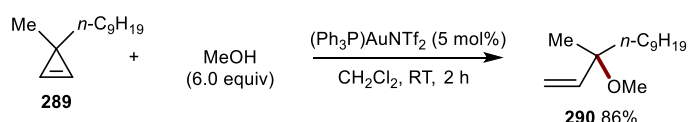
The authors propose the following mechanism (Scheme 73). Coordination of the gold catalyst to the alkyne of **282** occurs, forming species **286**. A 5-*endo-dig* cyclisation ensues *via anti-nucleophilic* addition affording vinylgold intermediate **287**. Aromatisation assisted by quinone-derived squaramide catalyst **285** forms allylgold(I) complex **288**. S_E2' allylation facilitated by the organocatalyst occurs *via* a formal heteroene reaction producing the desired product (**284**), regenerating the active gold catalyst.



Scheme 73: Proposed mechanism for the formation of **284**.

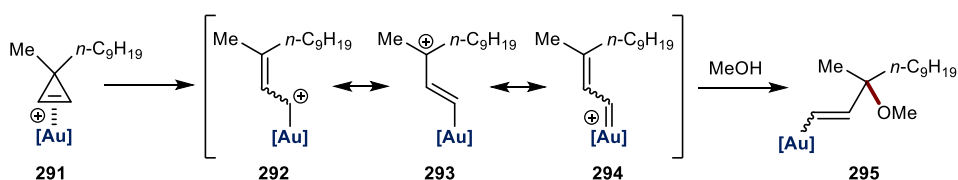
1.2.1.4 Miscellaneous Additions of Allyl Fragments

Gold-catalysed ring-opening of cyclopropenes is an alternative methodology to incorporate allyl moieties. This was first realised by Lee and co-workers, reporting the regioselective ring-opening of cyclopropenes followed by coupling with MeOH to give *tert*-allylic ether **290** in 86% yield (Scheme 74).¹¹⁷ Increasing the steric bulk surrounding the alcohol generates mixtures of regioisomers.



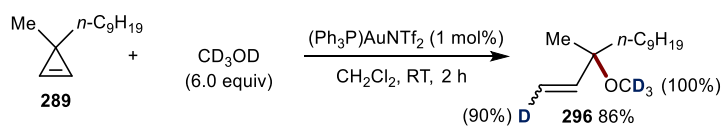
Scheme 74: Gold-catalysed ring-opening of cyclopropenes.

The authors propose initial activation of the cyclopropene, forming intermediate **291** (Scheme 75). Subsequent ring-opening ensues, affording species **292**. Delocalisation of the positive charge of intermediate **292** between the C-1 (**292**), C-3 (**293**) and Au atoms can occur. Regioselective addition of MeOH ensues; however, the identity of the nucleophile can alter the regioselectivity of the reaction. When utilising Ph_2SO as the nucleophile, exclusive attack at the C-1 carbon occurs. Protodeauration furnishes the desired product **290**.



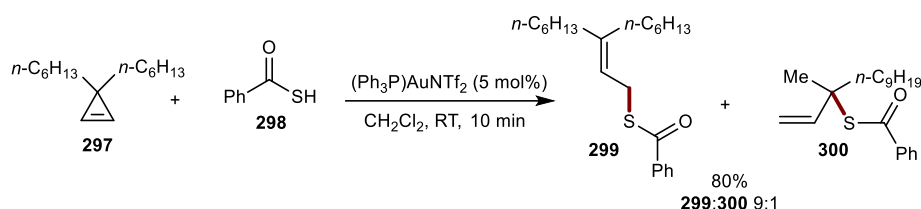
Scheme 75: Mechanistic Rationale for the formation of **290**.

To support their mechanism, the authors subjected CD_3OD to their reaction conditions, observing high deuterium incorporation at the vinylic position of **296** (Scheme 76).



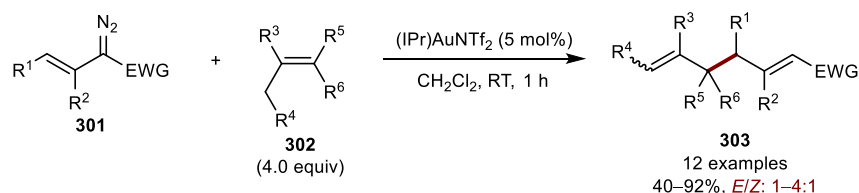
Scheme 76: Deuterium mechanism evaluation.

An extension of this work was later reported incorporating thioacids as the nucleophilic component (Scheme 77).¹¹⁸ Intercepting the ring-opened intermediate with thioacid **298** gave a 9:1 mixture of C-1 (**299**) vs. C-3 (**300**) allylated products in 80% yield. The regioselectivity of the reaction was highly dependent on the nucleophile.



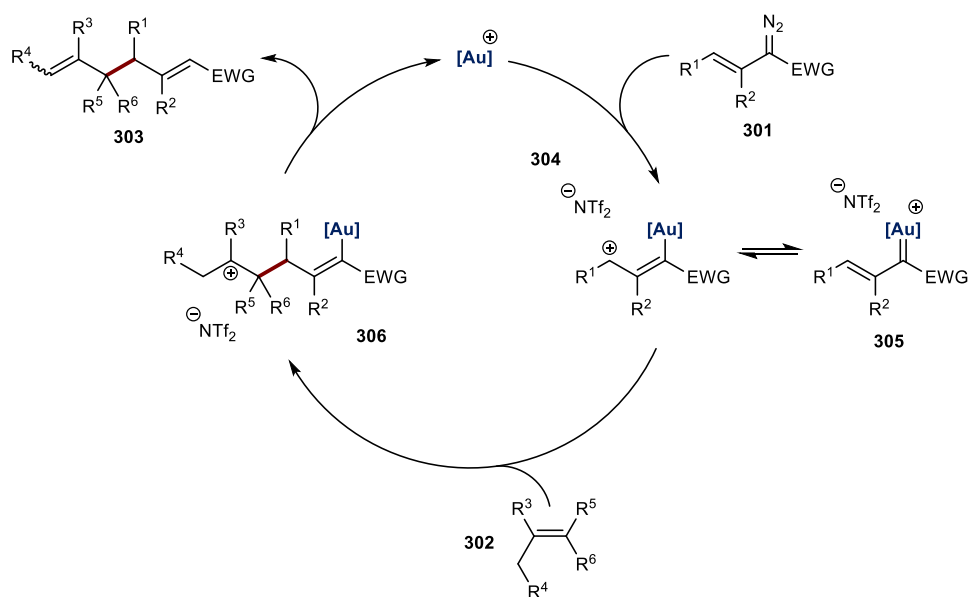
Scheme 77: Gold-catalysed addition of thioacids.

Stabilised vinyl diazo derivatives have found use within gold-catalysed allylations. In 2013, Barluenga and co-workers demonstrated the regioselective coupling of diazo derivatives and alkenes, furnishing allylated products (**303**) in modest to good yields (Scheme 78).¹¹⁹ Neither the [2+1] cyclopropane product nor the allylic C-H insertion product were observed. The authors propose that diazo derivative **301** acts as an allylic cation in the reaction, allowing for the regioselective synthesis of γ -substituted compounds. The reaction could be extended to activated arenes, affording allylated phenyl derivatives in excellent yields.



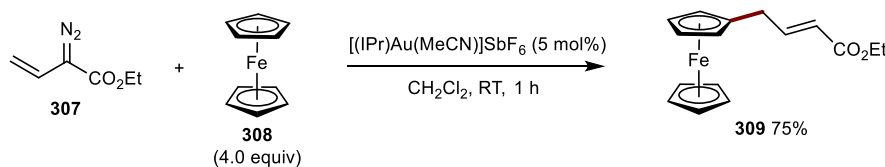
Scheme 78: Gold-catalysed allylation using vinyl diazo derivatives.

The reaction is initiated by the interaction of vinyl diazo derivative **301** with the gold catalyst, forming carbenoid intermediate **305** (Scheme 79), which can be in resonance between its carbenoid form (**305**) and its allylic cation form (**304**). Nucleophilic addition at the C-3 position occurs, furnishing the most stable carbocation **306**. Deprotonation, followed by protodeauration gives the desired product, regenerating the active gold catalyst.



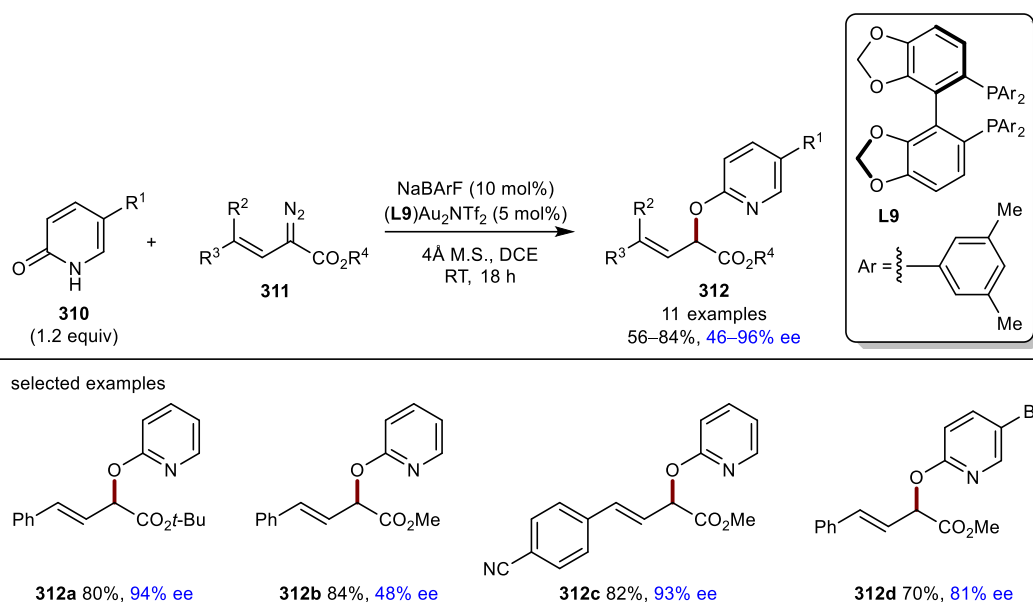
Scheme 79: Proposed mechanism for the formation of **303**.

López and co-workers extended this concept to incorporate ferrocenes, exploiting the unique reactivity of gold carbenoid intermediates initially reported by Barluenga (Scheme 80).¹²⁰ Coupling stabilised diazo species **307** with ferrocene gave the desired C-H functionalised allylated derivative **309** in 75% yield.



Scheme 80: Gold-catalysed allylation of ferrocene.

An enantioselective variant was later reported by Sun and co-workers (Scheme 81).¹²¹ The authors demonstrated the gold-catalysed regioselective insertion of 2-pyridones into stabilised diazo compounds, forming allylic ethers (**312**) in modest to excellent yields. The reaction was rendered enantioselective using bisphosphine ligand **L9**. The reaction tolerated several functionalised diazo intermediates (**312a**), affording the desired products in excellent yields and good enantioselectivities. Reducing the steric bulk surrounding the ester moiety (**312b**) gave reduced enantioselectivity. Limited functional group tolerance was observed for the 2-pyridone, resulting in diminished enantioselectivities (**312d**).

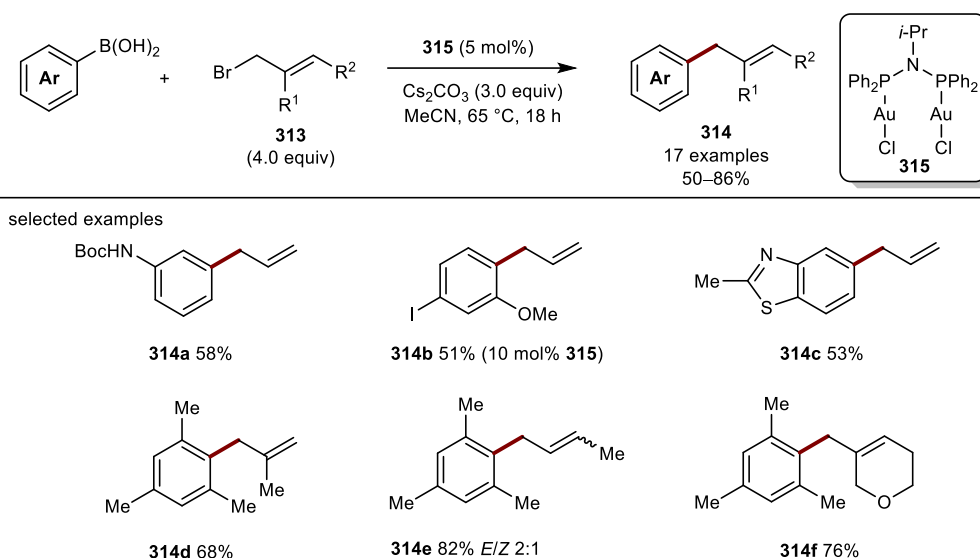


Scheme 81: Enantioselective gold-catalysed vinylcarbene insertion.

1.2.2 Redox Active Gold-Catalysed Allylations

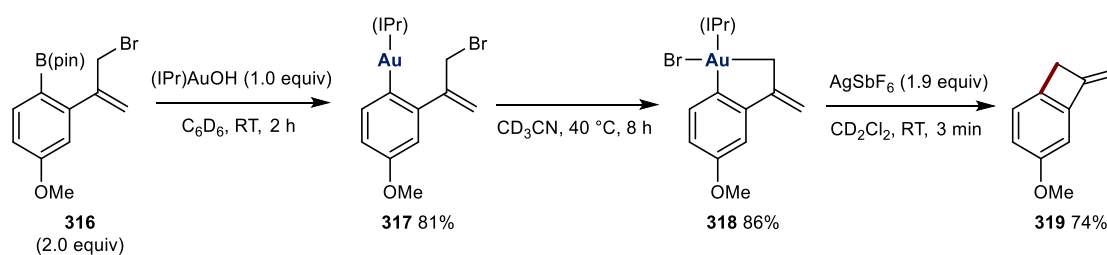
Two electron redox cycles involving gold ($\text{Au}^{\text{I}}/\text{Au}^{\text{III}}$) typically require harsh stoichiometric oxidants to enable reactivity due to the high redox potential of $\text{Au}^{\text{I}}/\text{Au}^{\text{III}}$.²⁷ However, several synthetic applications of gold catalysis involving two electron cycles that incorporate stoichiometric oxidants have been reported.^{122,123} More recently, methods that avoid these stoichiometric oxidants have been developed and have shown promising applications in several allylation reactions.^{124–128}

In 2014, Toste reported a pioneering example of a gold-catalysed cross-coupling between aryl boronic acids and allyl bromides in the absence of a stoichiometric oxidant (Scheme 82).¹²⁴ This methodology provides access to $\text{sp}^2\text{-sp}^3$ cross-coupled products under mild reaction conditions. Crucial for reactivity was the bimetallic gold complex **315**. The reaction tolerated both electron-rich (**314a**) and heteroaromatic (**314c**) boronic acids. Interestingly, substrates containing halides (**314b**) reacted with complete regioselectivity for the external bromide. Furthermore, sterically demanding substrates (**314d**) generated the desired products in good yields. Utilising substituted allylic bromides gave the linear product (**314e**) exclusively, albeit in poor *E/Z* selectivity. The reaction did not tolerate basic or nucleophilic functionality.



Scheme 82: Gold-catalysed allylation of boronic acids.

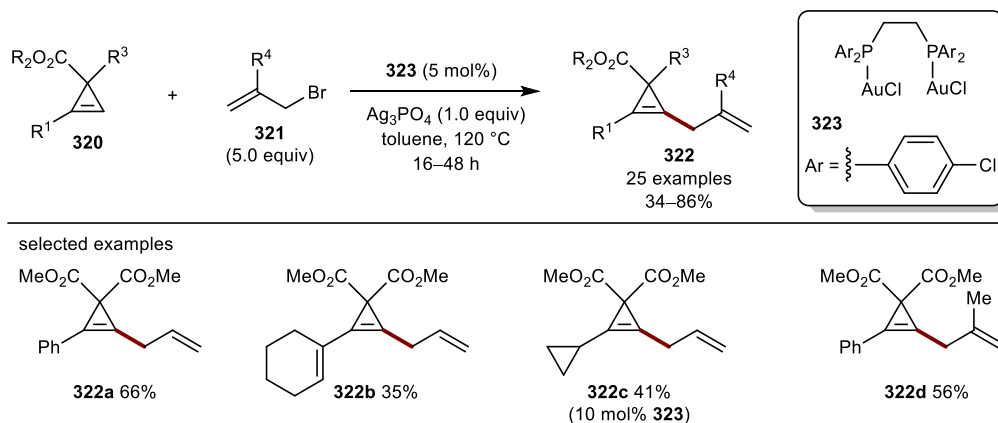
To elucidate the mechanism, the authors synthesised substrate **316** (Scheme 83). Transmetalation upon treatment with (IPr)AuOH ensues, forming gold complex **317** in 81% yield. Heating in CD₃CN afforded oxidative aurocycle **318**. This strained complex exhibited hampered reductive elimination, allowing for its direct observation. Finally, halide abstracting facilitates reductive elimination, furnishing the desired product. With this information, the authors propose base-assisted transmetalation, oxidative addition and rapid reductive elimination as the most favourable reaction pathway.



Scheme 83: Isolated products of oxidative addition/reductive elimination pathway.

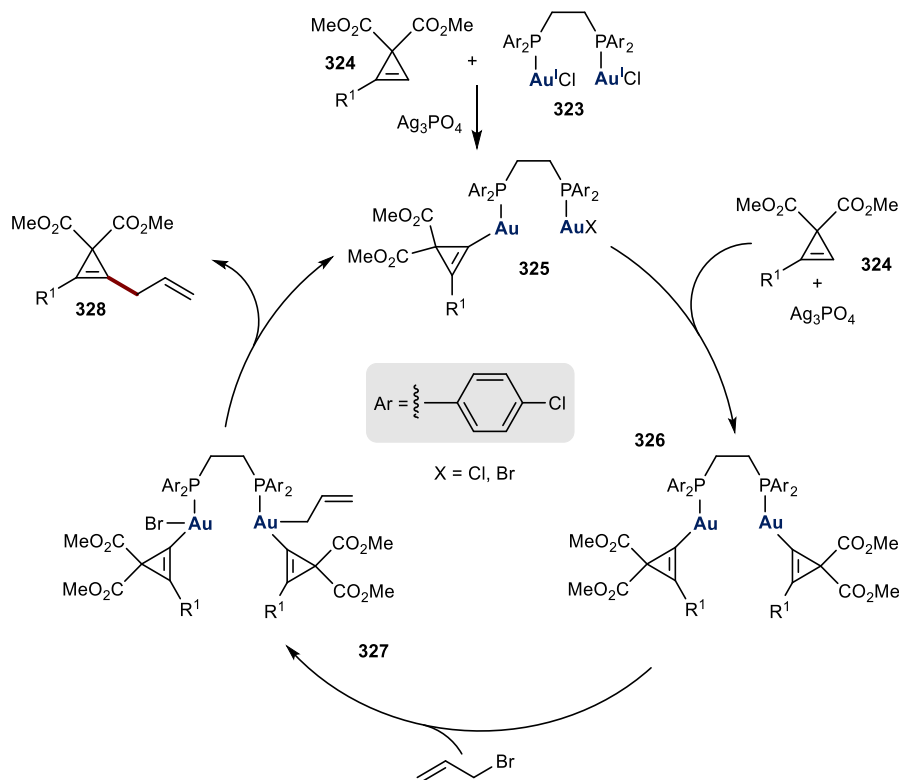
Xie and co-workers later extended this methodology towards the C-H activation of cyclopropenes, avoiding the use of stoichiometric oxidants (Scheme 84).¹²⁵ Similar to Toste's original paper, the use of dinuclear gold complex **323** was crucial for reactivity. The authors propose that Ag₃PO₄ facilitates the C-H activation step and acts as a halide scavenger, increasing reaction efficiency. The reaction scope was modest, with electron-rich substituents shutting down reactivity. The reaction tolerated both aryl- (**322a**) and alkenyl- (**322b**) substituted cyclopropenes, generating the desired products in poor to

modest yields. Alkyl-derived cyclopropenes (**322c**) required increased catalyst loadings to improve product formation. Variation of the allyl fragment was limited (**322d**).



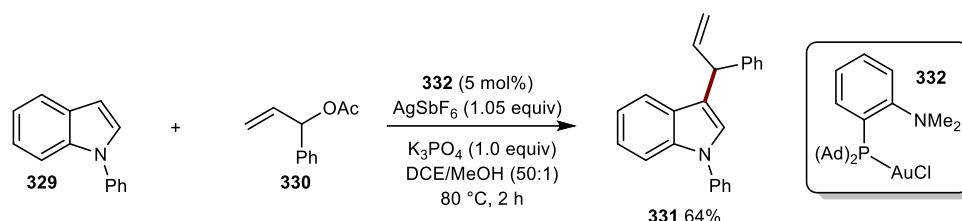
Scheme 84: Gold-catalyzed C-H activation of cyclopropenes.

The proposed mechanism is detailed in Scheme 85. Reacting cyclopropene **324** and gold complex **323** in the presence of Ag_3PO_4 forms intermediate **325**. This process repeats itself, forming complex **326**. This dinuclear gold complex was isolated and fully characterised. Oxidative addition with allyl bromide ensues, affording intermediate **327**. Reductive elimination furnishes the desired product, regenerating dinuclear catalyst **325**.



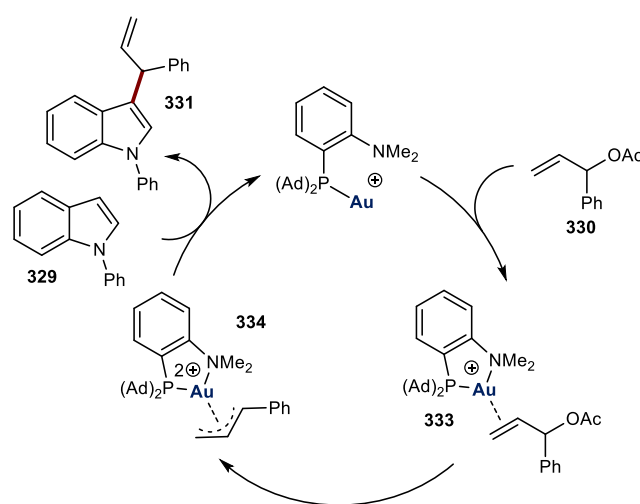
Scheme 85: Proposed mechanism for the formation of **328**.

Rodriguez and co-workers reported an analogous procedure to Toste's original paper, coupling indoles and allylic acetates under gold catalysis, generating C-3 allylated indoles in good yields (Scheme 86).¹²⁶ Starting from either α -(**330**) or γ -substituted allylic acetates afforded the α -allylated product (**331**) exclusively, suggesting the involvement of a π -allylgold complex.



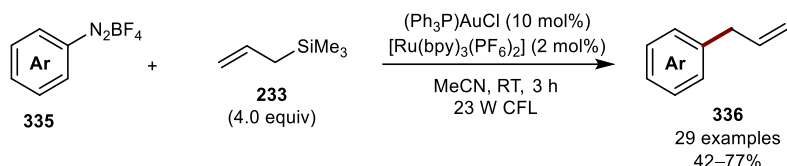
Scheme 86: Gold-catalysed allylation of indoles

The reaction is initiated *via* the coordination of the gold complex to allylic acetate **330**, forming species **333** (Scheme 87). Oxidative cleavage of the C-O bond occurs, generating π -allylgold(III) intermediate **334**. This intermediate was confirmed spectroscopically. Nucleophilic attack of the indole ensues, generating the desired product.



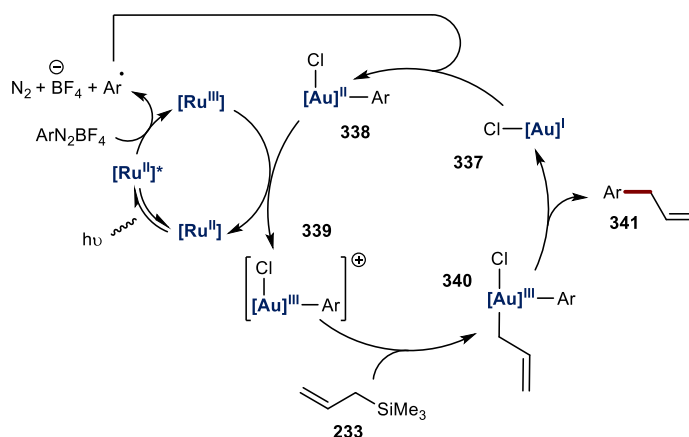
Scheme 87: Proposed mechanism for the formation of **331**.

Metallophotoredox catalysis is another approach to avoid stoichiometric oxidants. One such report demonstrated the sp^2 - sp^3 coupling of aryldiazonium reagents (**335**) and allylsilanes, yielding allylarenes in modest to excellent yields (Scheme 88).¹²⁷ The reaction proceeds under mild reaction conditions and has modest functional group tolerance. The reaction did not tolerate any functionality with respect to the allylic silane, and the authors attribute this to steric factors.



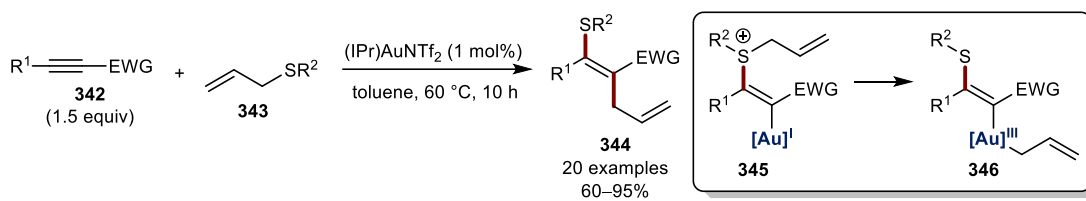
Scheme 88: Gold-catalysed allylation of aryl diazonium salts.

The reaction is initiated by the photoexcitation of the ruthenium(II) catalyst (Scheme 89). Quenching of the photoexcited catalyst by the aryldiazonium salt occurs, extruding nitrogen gas, forming an aryl radical, that is intercepted by gold complex **337**, forming species **338**. A single electron transfer between species **338** and the now oxidised ruthenium(III) catalyst, affords cationic species **339** and regenerates the ruthenium(II) catalyst. Transmetalation ensues, followed by subsequent reductive elimination, furnishing the desired cross-coupled product **341**.

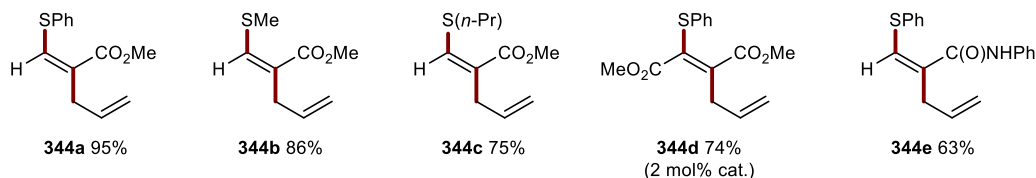


Scheme 89: Proposed mechanism for the formation of **341**.

In 2018, Shi reported the thioallylation of alkynes in the absence of an external stoichiometric oxidant (Scheme 90).¹²⁸ The reaction furnished stereoselectively tri- and tetra-substituted alkenes in modest to high yields. The gold catalyst acts as a π -acid for alkyne activation and as a redox catalyst, whereby the *in-situ* generated sulfonium cation **345** operates as a mild oxidant, forming intermediate **346**. The reaction displayed good functional group tolerance, with both aryl- (**344a**) and alkyl- (**344b**) substituted thiols affording the desired products in good yields. Increasing the catalyst loading was required for di-substituted alkynes (**344d**). The authors propose catalyst deactivation when using amides (**344e**), accounting for the decrease in isolated yield.



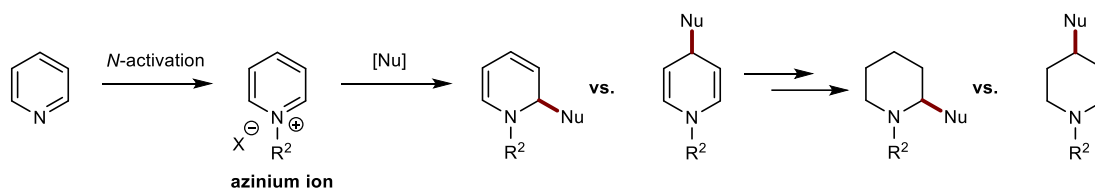
selected examples



Scheme 90: Gold-catalysed thioallylation of alkynes.

1.3 Nucleophilic Dearomatisation of Azinium Salts *via* Allyl Reagents

Functionalisation of pyridines represents a powerful tool for the construction of complex biologically relevant targets.¹²⁹ However, the direct modification of pyridine is challenging, most notably due to chemoselectivity issues and its comparatively low π -energy relative to benzene, therefore, requiring substituents to activate the pyridine scaffold towards electrophilic aromatic substitution.¹³⁰ Nucleophilic aromatic substitution relies on the installation of good leaving groups.¹³¹ Furthermore, organometallic alternatives are typically unstable and difficult to access.¹³² The nucleophilicity of the nitrogen substituent can be exploited to synthesise cationic intermediates that exhibit increased electrophilic character, known as azinium ions (Scheme 91). Due to their increased electrophilicity, azinium ions can undergo nucleophilic dearomatisation *via* the addition of either a hydride or a nucleophile, forming dihydropyridine derivatives, which serve as direct precursors to piperidine cores.^{133–135}



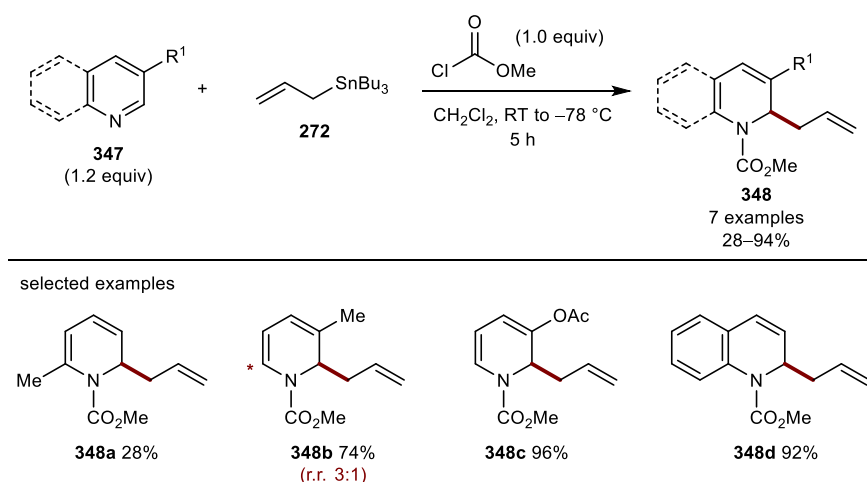
Scheme 91: Functionalising azinium salts.

Azinium ions contain reactive sites at the C2-, C4- and C6-positions of the pyridine ring. Regioselectivity is governed by the nature of the nucleophile. In general, hard nucleophiles, such as Grignard reagents are selective towards 1,2-additions, while soft nucleophiles such as organocuprates are selective towards 1,4-additions.¹³³ Moreover, increasing the steric hinderance of the activating agent can further increase regiocontrol.¹³³ High regioselectivity is desired as further modification of the corresponding dihydropyridine product provides access to distinct molecular scaffolds. Azinium ions containing stabilising electron-withdrawing substituents at the 3-position have shown increased selectivity towards the 1,4-adduct.¹³⁶

Over the past few decades, a plethora of nucleophiles have been used in the dearomatisation of azinium ions, with the most common being the addition of aryl,¹³⁷ alkenyl¹³⁸ and alkyl organometallic reagents,¹³⁹ cyanide reagents¹⁴⁰ and enolates.¹⁴¹ However, the addition of allyl reagents is comparably underdeveloped.¹³³ This section of the review will solely focus on the nucleophilic dearomatisation of azinium ions *via* allyl reagents, categorised by the allylic precursor utilised.

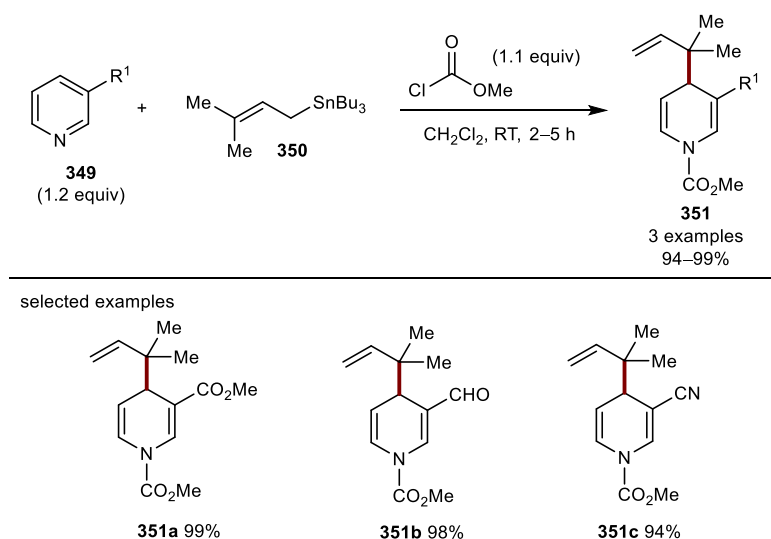
1.3.1 Addition of Allylstannanes

Nucleophilic allylation of azinium ions to access allylated dihydropyridine derivatives is not well described within the scientific literature. Yamaguchi and co-workers reported one of first examples, coupling allylic stannanes with *in-situ* generated azinium ions, accessing the 2-allylated product (**348**) in modest to excellent yields (Scheme 92).¹⁴² Functional group compatibility was modest, with only seven examples reported. Moreover, an inseparable mixture of regioisomers was obtained for a significant majority of examples (**348b**). The reaction tolerated quinolinium ions (**348d**), affording the desired product in 92% yield.



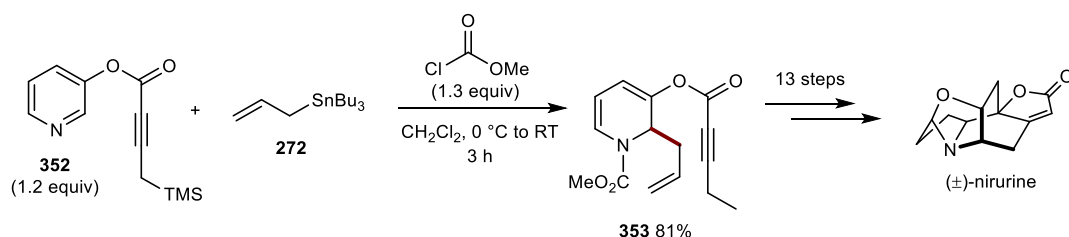
Scheme 92: Addition of allylstannanes to azinium ions.

Yamaguchi and co-workers later extended this methodology, examining the allylic stannane scope (Scheme 93).¹⁴³ Interestingly, when using prenyl allylic stannane **350**, the 4-allylated product was observed exclusively, affording γ -allylated product **351** in excellent yields. The substrate scope was not explored thoroughly, with only four examples reported. However, the reaction was tolerant towards esters (**351a**), aldehydes (**351b**) and nitriles (**351c**), generating the desired products in excellent yields. Unfortunately, the products were not stable and had to be hydrogenated using PtO_2 and H_2 , affording the corresponding piperidine derivatives. The switch in regioselectivity can be explained by the Hard Soft Acid Base theory (HSAB).¹³³ Prenyl stannane is a softer nucleophile than allyl stannane, therefore, it preferentially attacks at the 4-position of the *in-situ* generated azinium ion.¹⁴³



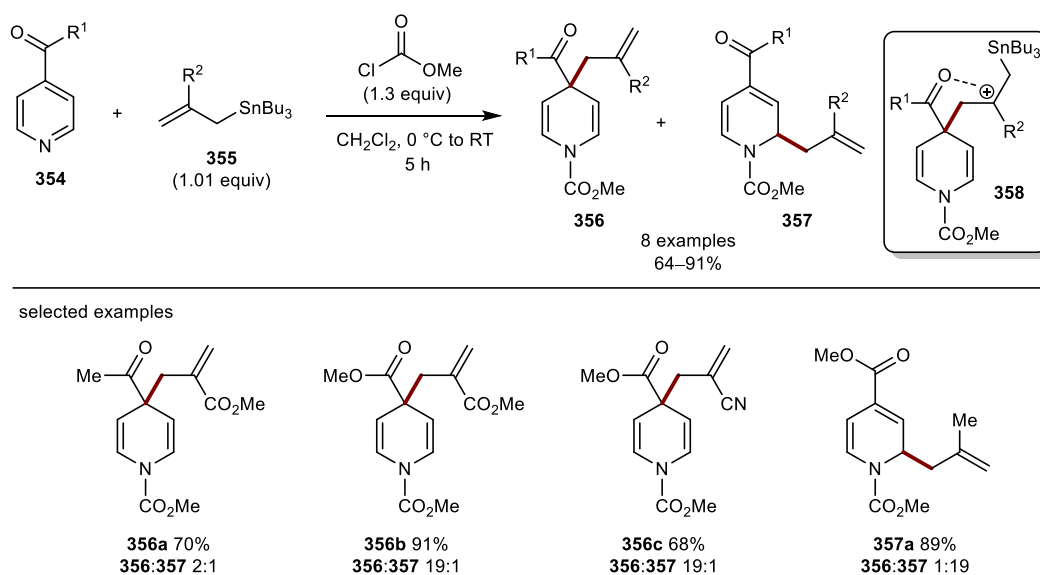
Scheme 93: Addition of substituted allylstannanes to azinium salts.

Magnus and co-workers applied Yamaguchi's methodology towards the synthesis of (±)-nirurine (Scheme 94).¹⁴⁴ Nucleophilic dearomatisation of **352** via the addition of allylstannane generated the desired product in 81% yield. Further transformations furnished (±)-nirurine.



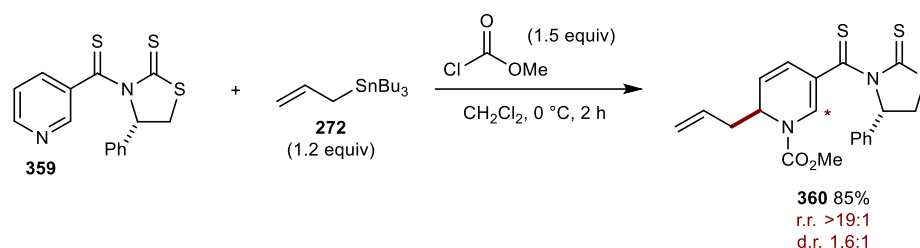
Scheme 94: Total synthesis of (±)-nirurine.

In 1993, Yamaguchi and co-workers discovered that pyridines containing an electron-withdrawing substituent at the 4-position gave the 4-allylated product as the major regioisomer, regardless of the hardness of the nucleophile (Scheme 95).¹⁴⁵ This was due to a stabilisation effect within reactive intermediate **358**. Once again, an inseparable mixture of regioisomers was reported for the majority of examples. Allylic stannanes containing an electron-withdrawing substituent (**356a**, **356b** and **356c**) were required for maintaining high levels of regiocontrol. Reacting 2-methylallyl stannane (**357a**) gave the reverse selectivity, favouring the 2-allylated product. This is due to the stabilisation of the carbocation by the methyl substituent on the allylic fragment.



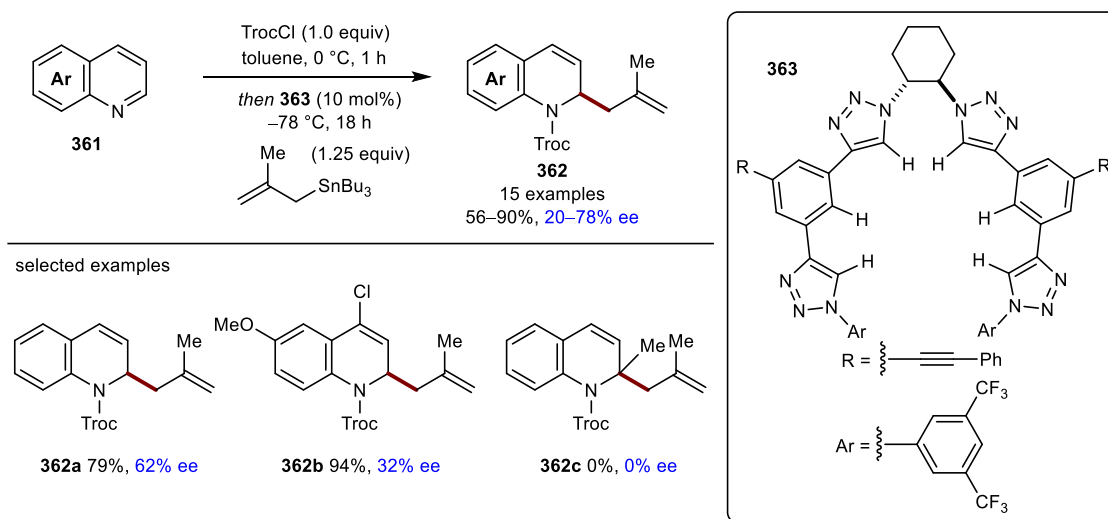
Scheme 95: Addition of allylstannanes to 4-substituted azinium salts.

An asymmetric variant was later reported by Yamada and co-workers (Scheme 96).¹⁴⁶ Utilising an enantioenriched chiral auxiliary (**359**), the diastereoselective addition of allylstannane was reported, generating the 6-allylated product (**360**) in 85% yield, with good regiocontrol but poor diastereocontrol.



Scheme 96: Addition of allyl stannanes to substituted pyridines.

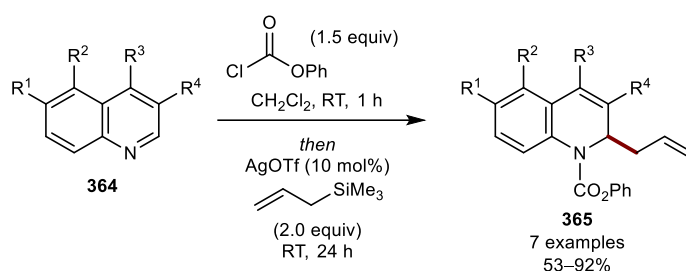
Very recently, an anion-binding strategy was applied towards the allylation of azinium ions *via* allylic stannanes (Scheme 97).¹⁴⁷ Utilising organocatalyst **363**, the reaction could be rendered enantioselective, forming the desired allylated products in good yields and modest to good enantioselectivities. The reaction scope was modest with substituted quinolinium ions affording the desired products in varying enantioselectivities (**362a**). The reaction did tolerate both electron-donating and halide functionalities (**362b**), generating the desired product in 94% yield and 32% ee. However, reaction inhibition was observed when attempting to form quaternary centres (**362c**).



Scheme 97: Enantioselective dearomatisation of azinium ions.

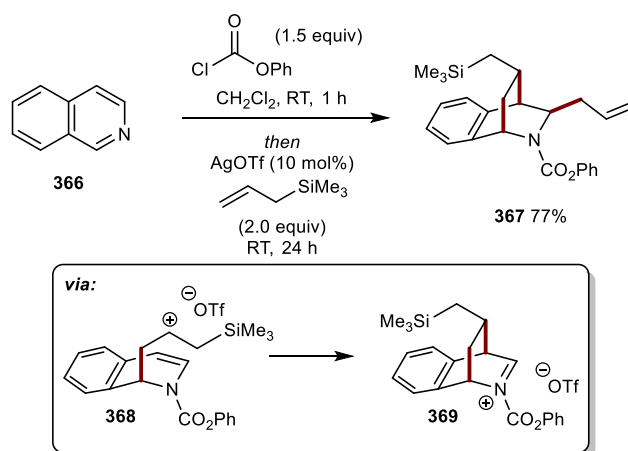
1.3.2 Addition of Allylsilanes

Allylic silanes are generally less toxic and exhibit better functional group tolerance than allylic stannanes. Therefore, methodologies that utilise allylic silanes are highly advantageous. However, allylic silanes are less nucleophilic, and often need additives to facilitate reactivity. Yamaguchi and co-workers demonstrated the first example of coupling allylic silanes with quinolinium ions, affording the desired allylated products (**365**) in good yields (Scheme 98).¹⁴⁸ AgOTf was required to enable reactivity, as it is proposed to replace the chloride ion of the quinolinium ion, increasing its electrophilicity.



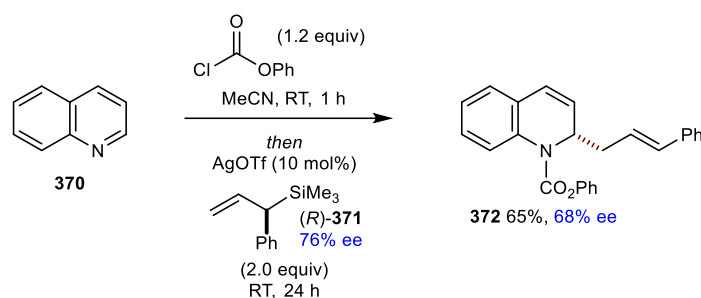
Scheme 98: Addition of allylsilanes to substituted quinolines.

An expansion of this methodology to include isoquinolines was later investigated (Scheme 99).¹⁴⁹ Interestingly, bicyclic product **367** was obtained in 77% yield under their standard reaction conditions. The reaction proceeds *via* the addition of the allylic silane to the *in-situ* generated isoquinolinium ion, forming species **368**. Intramolecular addition of the enamide ensues, forming iminium ion **369**. A second equivalent of allylic silane quenches the iminium ion, forming the desired bicyclic product.



Scheme 99: Addition of allylsilanes to isoquinolines.

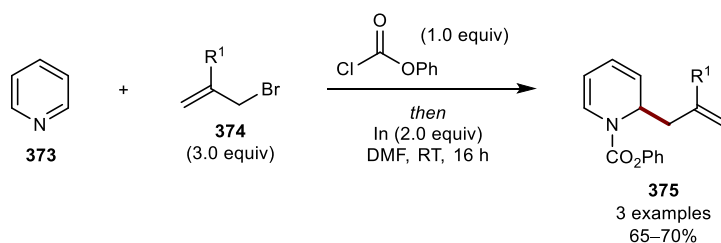
In 2002, Yamaguchi and co-workers reported the regioselective addition of enantioenriched allylic silanes (**371**) to quinolinium ions, generating the 2-allylated product **372** in modest yields and enantioselectivities (Scheme 100).¹⁵⁰ Utilising enantioenriched allylic silanes delivered the corresponding products with good enantiospecificity. The authors propose a *si*-face attack through an *anti*-S_E2' mechanism, supported by the exclusive formation of the (*E*)-alkene.



Scheme 100: Addition of enantioenriched allylsilanes to substituted quinolines.

1.3.3 Addition of Allyl Halides

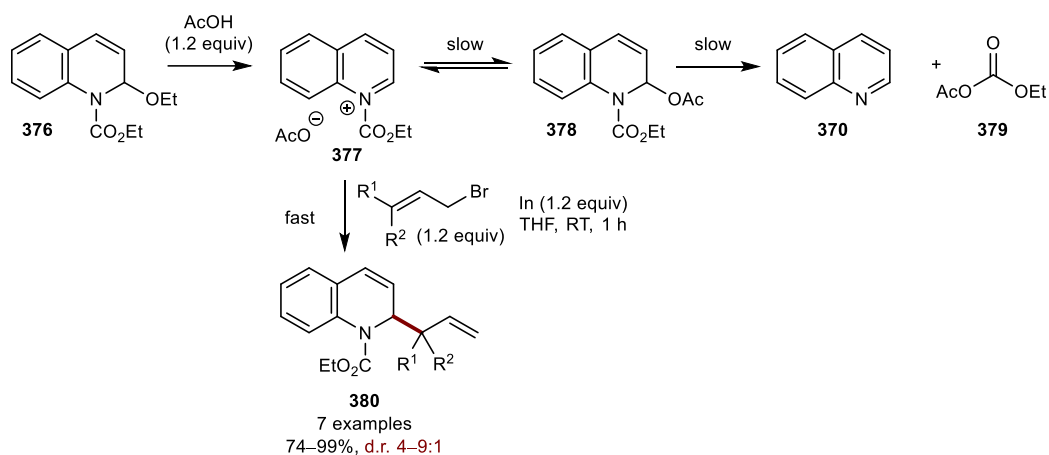
Nucleophilic allylations of azinium ions involving allylic halides typically incorporate stoichiometric quantities of indium and proceed under the Barbier-type mechanism, which couples together an alkyl halide with an electrophile. Loh and co-workers reported the first indium-mediated regioselective allylation of azinium ions by allylic halides, furnishing the desired products in good yields (Scheme 101).¹⁵¹ This was the first example of complete regiocontrol when using pyridine (**373**). The substrate scope was not explored thoroughly, with few examples reported.



Scheme 101: Allylation of pyridine using allylic indium reagents.

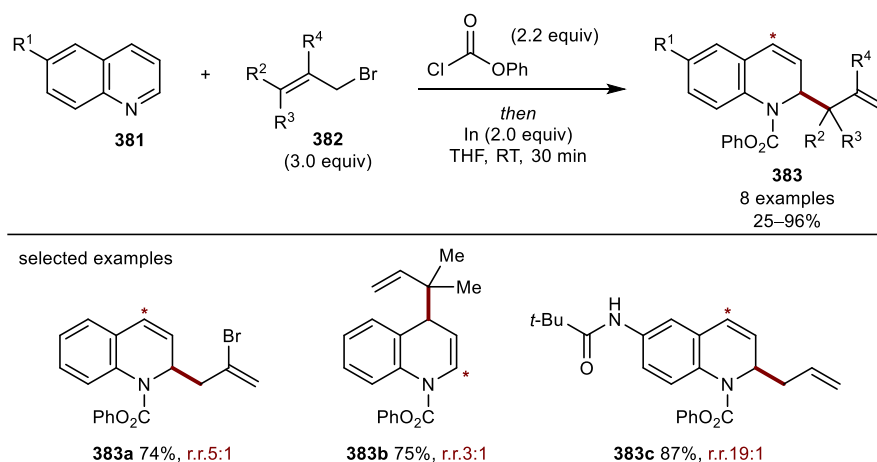
In 2002, Yoon and co-workers demonstrated the indium-mediated coupling of allylic halides with 1-ethoxy-1-(ethoxycarbonyl)-1,2-dihydroquinoline (EEDQ) in the

presence of acetic acid to give the corresponding allylated products (**380**) with excellent α -selectivities with respect to the allylic indium reagent (Scheme 102).¹⁵² Reacting EEDQ (**376**) with acetic acid, forms quinolinium ion **377**, whereby the anion can act as a nucleophile attacking the quinolinium ion forming intermediate **378**. Fragmentation yields quinoline and amide coupling reagent **379**. The rate of nucleophilic attack of the *in-situ* generated allylic indium reagent is sufficient to trap quinolinium intermediate **377**, forming allylated products.



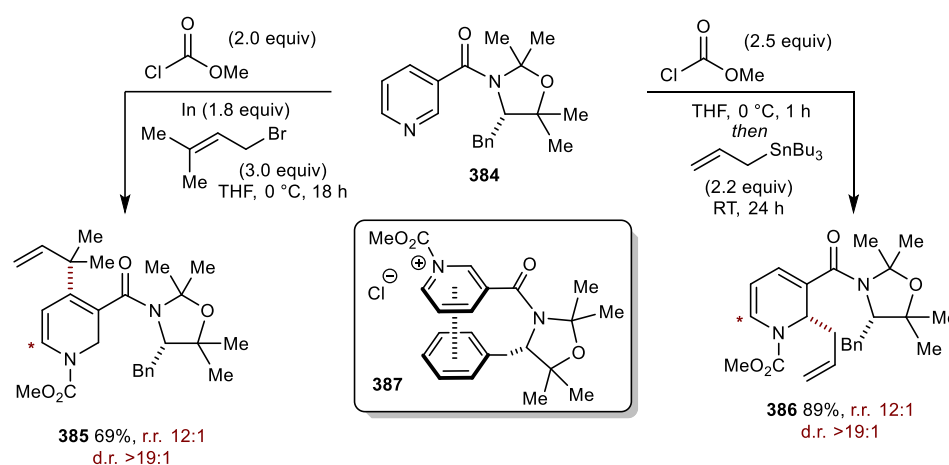
Scheme 102: Allylation of EEDQ using allylic indium reagents.

Yoon and co-workers later reported an extension of Loh's initial finding, exploring the effect of substituted allylic halides on the regioselectivity of the reaction with respect to the quinolinium ion (Scheme 103).¹⁵³ Poor regiocontrol was observed for the majority of examples, with 2-bromoallyl bromide giving the corresponding product **383a** in a 5:1 mixture of regioisomers. Utilising prenyl bromide reversed the regioselectivity (**383b**).



Scheme 103: Allylation of substituted quinolines using allyl indium reagents.

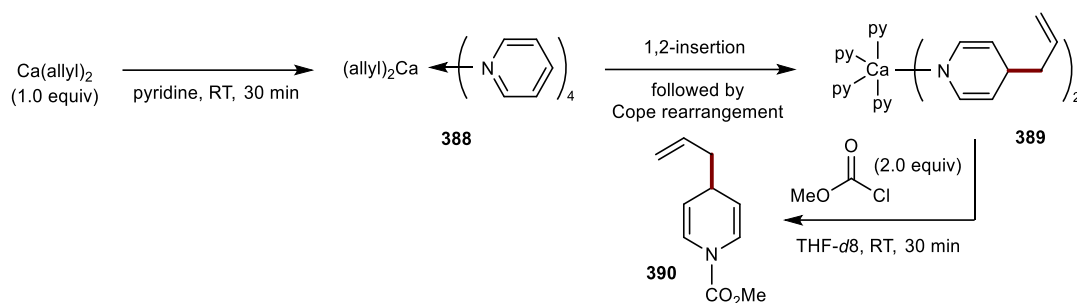
In 2007, Yamada demonstrated the regioselective addition of allylic reagents to *in-situ* generated azinium ions (Scheme 104).¹⁵⁴ Utilising enantioenriched chiral auxiliary **384**, the diastereoselective addition of allylic stannane was reported, generating the 2-allylated product **386** in 89% yield. Furthermore, a change in regioselectivity was observed when utilising allylic indium reagents, generating the 4-allylated product (**385**) in 69% yield with good regiocontrol and diastereocontrol. DFT calculations indicated transition state **387** as the most stable conformer, allowing for the selective addition of the allylic reagent from the least hindered face.



Scheme 104: Regioselective addition of allyl nucleophiles to substituted pyridines.

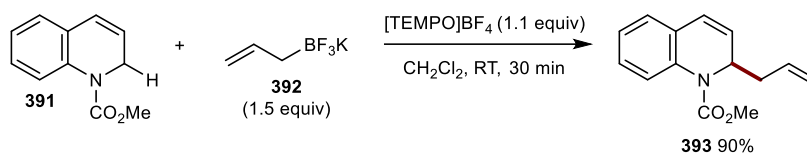
1.3.4 Addition of Miscellaneous Allyl Reagents

Maron reported the insertion of pyridine derivatives into allyl calcium, generating the 4-allylated product (Scheme 105).¹⁵⁵ Supported by DFT calculations and NMR spectroscopy, the mechanism is initiated by the coordination of pyridine to calcium, affording activated intermediate **388**. Nucleophilic dearomatisation at the C2-position occurs, followed by a Cope rearrangement, generating calcium-bound intermediate **389**, which can further react with methyl chloroformate to afford the desired allylated product **390**.



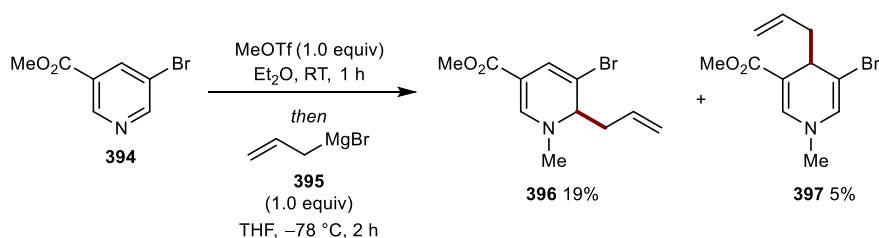
Scheme 105: Calcium-catalysed allylation of azinium ions.

In 2017, Liu and co-workers reported a metal-free oxidative C-H allylation of 1,2-dihydroquinolines, forming the desired product in 90% yield (Scheme 106).¹⁵⁶ The reaction utilises an oxidant and occurs *via* an initial hydrogen atom extraction, forming a quinolinium ion. Subsequent nucleophilic addition by potassium allyltrifluoroborate generates the desired product (**393**).



Scheme 106: Oxidative allylation of 1,2-dihydroquinoline.

The addition of allylmagnesium reagents to *in-situ* generated azinium ions has been reported extensively; however, its widespread utility has been hindered due to the reaction producing mixtures of inseparable regioisomers and its poor functional group compatibility. Smith and co-workers reported a predictive model for the addition of Grignard reagents to azinium ions (Scheme 107).¹⁵⁷ In general, the selectivity of the reaction is affected by numerous factors including the substituent pattern of the azinium ion (**394**) and the nature of the nucleophile.



Scheme 107: Addition of Grignard reagent **395** to azinium ion **394**.

1.4 Summary

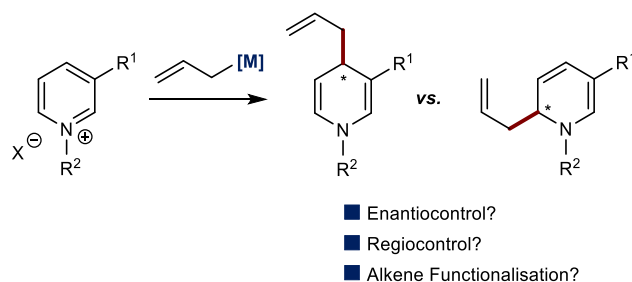
In summary, gold-catalysed allylations have been extensively researched over the past two decades. In particular, the addition of nucleophiles to electrophilic allylating agents and allylations resulting from rearrangement cascades are well-known. In contrast, gold-catalysed additions of nucleophilic allylating agents to electrophiles are comparatively underdeveloped. Moreover, accessing nucleophilic allylating agents *via* transmetalation from an allyl precursor could give access to unique reaction pathways.

The nucleophilic dearomatisation of azinium ions by allyl reagents is a powerful tool to access functionalised dihydropyridines cores. However, there are no robust methodologies for the regioselective allylation of azinium ions. Furthermore, current synthetic strategies favour the 1,2-adduct, often forming inseparable mixtures of regioisomers, therefore, there is a need for methodologies favouring the 1,4-adduct exclusively. As a result, the development of a gold-catalysed nucleophilic allylation of azinium ions, forming the 1,4-adduct with high levels of regiocontrol and stereocontrol, would be beneficial to synthetic chemists.

2.0 Results and Discussion

2.1 Aims and Objectives

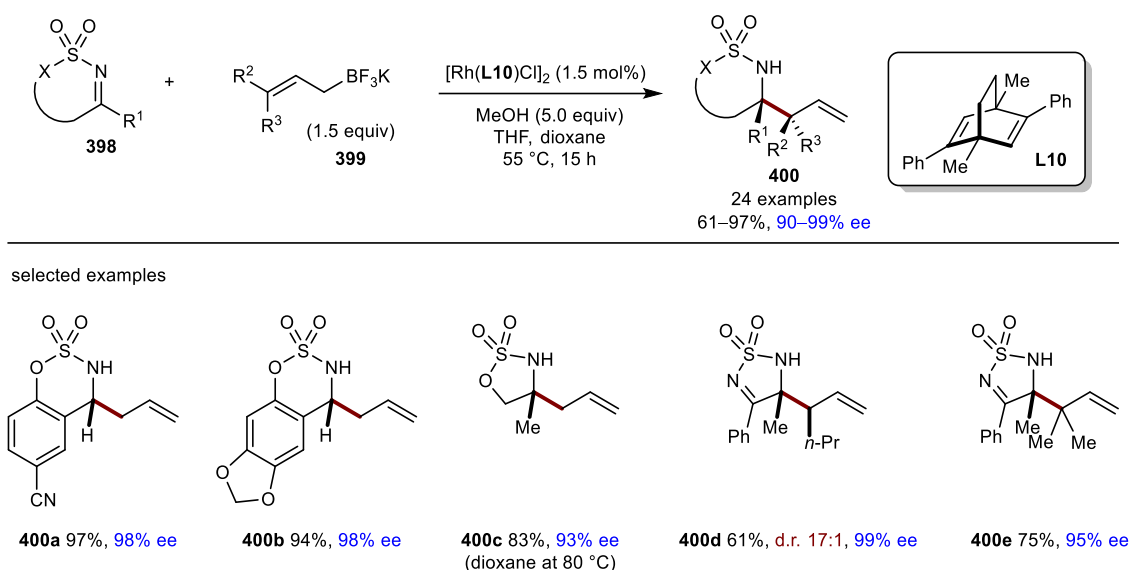
As summarised, it is evident that a nucleophilic allylation of azinium ions, with high levels of regio- and stereocontrol, would be highly desirable. We were interested in utilising allylic boronates as the allylic precursor as they are readily prepared, stable, and have broad functional group tolerance. Our aim was to demonstrate the first metal-catalysed highly regioselective coupling of azinium ions with allylic boronates which would operate under mild conditions and have good functional group tolerance (Scheme 108).



Scheme 108: Reaction principle.

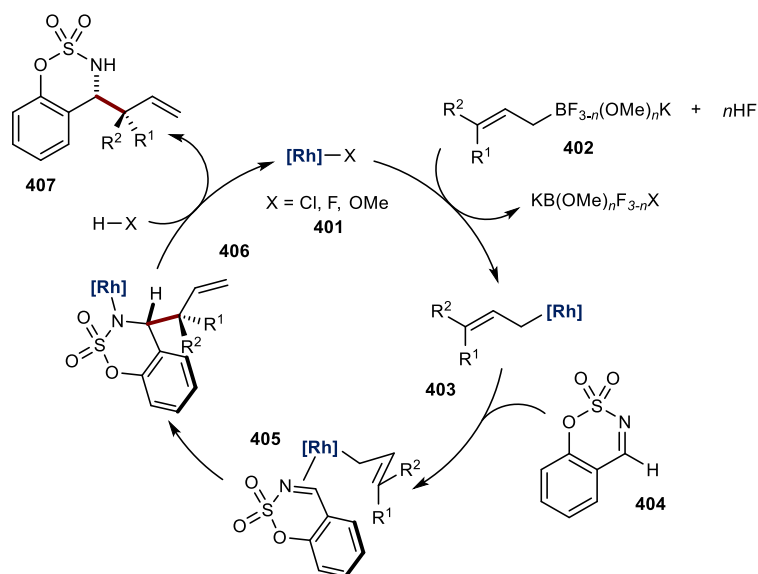
2.2 Reaction Optimisation

In 2012, Lam and co-workers reported the first enantioselective rhodium-catalysed allylation of ketimines, generating homoallylic amines in high yields and enantioselectivities (Scheme 109).¹⁵ The reaction scope incorporated various cyclic aldimines (**400a** and **400b**) and cyclic ketimines (**400c** and **400d**), with a variety of electron-donating and electron-withdrawing substituents, generating the corresponding homoallylic amines in good yields and excellent enantioselectivities. Highly substituted allylic boronates (**400d** and **400e**) gave the *anti*-adduct in high diastereoselectivities, with γ -selectivity.



Scheme 109: Rhodium-catalysed allylation of cyclic imines.

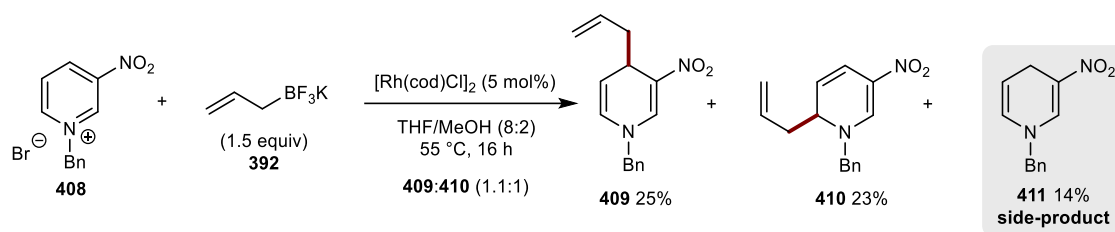
In the presence of methanol, potassium allyltrifluoroborates undergo reversible methanolysis, generating species **402** (Scheme 110).¹⁵ Transmetalation ensues, forming allylrhodium species **403**. Coordination of aldimine **404** occurs, proceeding through a cyclic chair-like transition state, generating intermediate **406**. Protonolysis of **406** releases the desired product, regenerating the active rhodium catalyst **401**.



Scheme 110: Proposed mechanism for the formation of **407**.

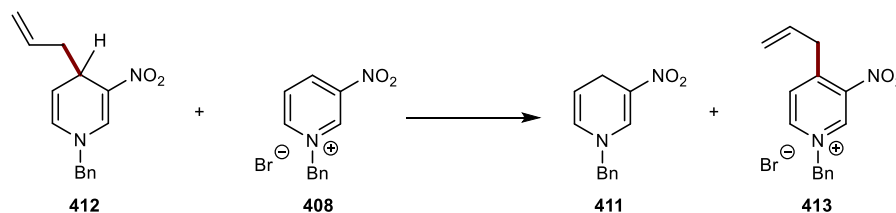
The similarities between the described cyclic imine system and our targeted azinium ion led us to utilise the reported reaction conditions as a foundation to establish initial reactivity. However, modification of the solvent system was required to increase the

solubility of the azinium salt. Pleasingly, subjecting azinium salt **408** and potassium allyltrifluoroborate **392** to a slight modification of Lam's previous conditions gave the corresponding 4-allylated (**409**) and 6-allylated (**410**) dihydropyridines in 25% and 22% yield respectively (Scheme 111).



Scheme 111: Rhodium-catalysed allylation of **408**.

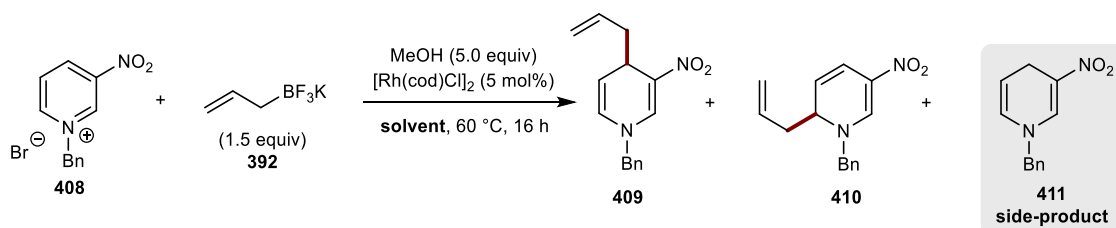
Notably, side-product **411** was isolated in 14% yield. Mechanistically, the formation of side-product **411** may proceed *via* a hydride addition from **412**, analogous to NADPH within biological systems (Scheme 112).¹⁵⁸ This forms side-product **411** and allylated azinium ion **413** as a by-product. However, the presence of **413** could only be observed by mass spectrometry.



Scheme 112: Speculative formation of side-product **411**. Only one regioisomer is shown for clarity.

Having established the feasibility of our process, certain reaction parameters were investigated to increase regiocontrol. A preliminary solvent screen was conducted (Table 1). Regrettably, solvents such as EtOAc, acetone and DCE (entries 1,2 and 5) gave diminished yields. Pleasingly, using TFE (entry 3) gave the desired allylated products in a 6.2:1 ratio of 4-allylated vs. 6-allylated. During optimisation, side-product **411** was observed within the majority of reactions. For all screening reactions, the remaining mass balance is attributed to unreacted starting material. TFE was chosen as the solvent for further reaction optimisation.

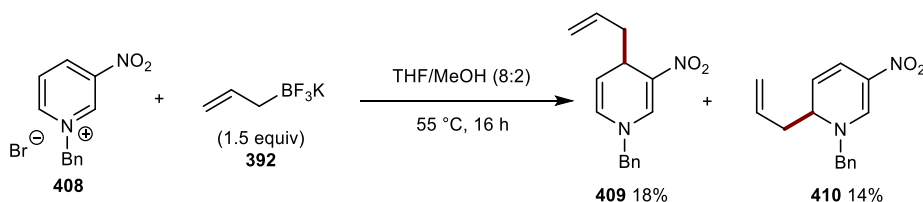
Table 1: Solvent screening.



Entry	Solvent	Yield (%)				Ratio of 409:410
		409	410	411	Total	
1	EtOAc	16	18	40	74	1:1.1
2	acetone	-	-	-	-	-
3	TFE	31	5	22	58	6.2:1
4	HFIP	9	2	32	43	4.5:1
5	DCE	12	9	40	61	1.3:1

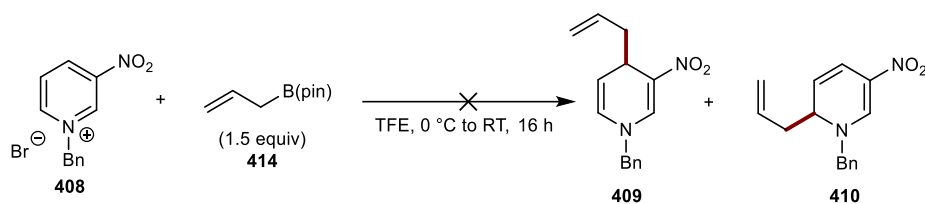
Reactions conducted with 0.1 mmol of **408**. Yields determined by ^1H NMR spectroscopy using 1,3,5-trimethoxybenzene as the internal standard.

Before conducting additional optimisation reactions, a control reaction was performed without the addition of the rhodium catalyst (Scheme 113). Unfortunately, comparable yields and regioselectivities were observed, suggesting that rhodium does not effectively promote reactivity. Therefore, using rhodium as the catalyst was not explored further.



Scheme 113: Catalyst free allylation of 408. Isolated yields.

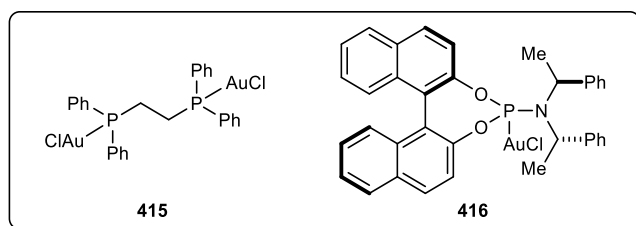
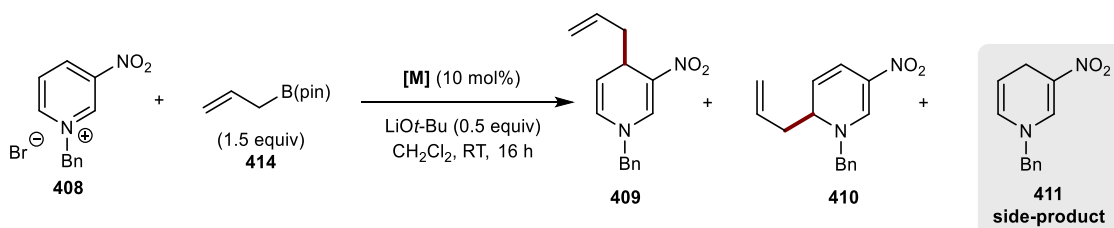
We hypothesised that allyl pinacolboronate **414**, which is less nucleophilic than its organotrifluoroborate equivalent,¹⁵⁹ could minimise the competitive racemic background allylation. Therefore, allyl pinacolboronate **414** was subjected to the rhodium free reaction conditions at room temperature and pleasingly, no reactivity was observed (Scheme 114). As such, allyl pinacolboronate was chosen as the boronate coupling partner for all further reactions.



Scheme 114: Allylation of **408** using allyl pinacolboronate **414**.

The screening of various metal catalysts to establish reactivity was first investigated utilising allyl pinacolboronate **414** (Table 2). CH_2Cl_2 was chosen as the solvent to increase the solubility of the azinium ion. LiOt-Bu was added to activate the allyl pinacolboronate, promoting transmetalation with the metal catalyst. Subjecting either $[\text{Ir}(\text{cod})\text{Cl}]_2$ (entry 1) or $\text{NiBr}_2\cdot\text{glyme}$ (entry 2) to the reaction conditions gave no conversion of azinium salt to the desired allylated product. Moreover, palladium catalysis gave no desired product formation (entry 5). Our first significant breakthrough came with the use of $(\text{Me}_2\text{S})\text{AuCl}$ (entry 4). Remarkably, this catalyst gave the 4-allylated product exclusively, albeit in poor yield. This is surprising since gold catalysis is not commonly associated with nucleophilic allylation reactions utilising allyl pinacolboronates. Achiral bis-phosphine based bimetallic gold catalyst **415** (entry 9) was synthesised and utilised in the reaction, affording the corresponding allylated products in poor yields. Moreover, enantioenriched phosphoramidite-derived gold catalyst **416** was utilised in the reaction, affording the corresponding products in reduced yields and as a racemic mixture. Shibasaki and co-workers have reported several copper-catalysed allylations of either alcohols or amines utilising allyl pinacolboronates.^{17,160,161} However, when applying their optimised conditions to our reaction system, no reactivity was observed (entry 6). Furthermore, modifying the solvent (entry 7) or copper catalyst (entry 8) gave no product formation. For all screening reactions, significant formation of side-product **411** was observed within the crude ^1H NMR spectra.

Table 2: Metal screening.



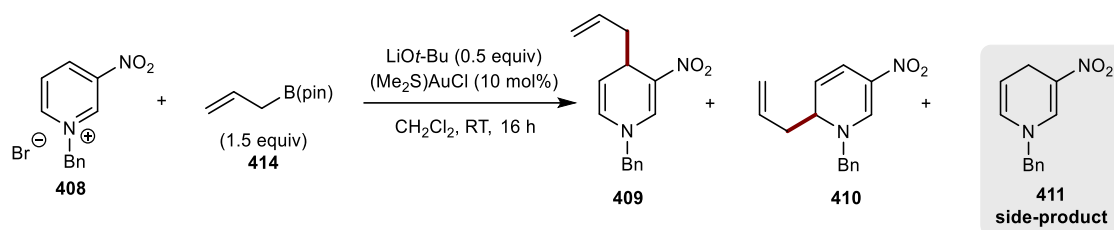
Entry	Metal	Yield (%)				Ratio of 409:410
		409	410	411	Total	
1 ^[a]	[Ir(cod)Cl] ₂	-	-	-	-	-
2	NiBr ₂ ·glyme	-	-	42	42	-
3 ^[a]	AgNO ₃	-	-	38	38	-
4	(Me ₂ S)AuCl	23	-	44	67	>19:1
5	Pd(PPh ₃) ₄	-	-	14	14	-
6 ^[b]	CuOAc	-	-	35	35	-
7 ^[c]	CuOAc	-	-	14	14	-
8 ^[d]	CuTc	-	-	19	19	-
9 ^[e]	415	trace	trace	6	6	-
10 ^[e]	416	13	6	15	34	2.2:1

Reactions conducted with 0.1 mmol of **408**. Yields determined by ¹H NMR spectroscopy using 1,3,5-trimethoxybenzene as the internal standard. [a] Reaction conducted using 5 mol% metal catalyst, [b] Using 5 mol% CuOAc and 6 mol% BINAP, [c] Conducted in MeCN using 5 mol% CuOAc and 6 mol% BINAP, [d] Using 5 mol% CuTc and 12 mol% phosphoramidite, [e] Conducted in MeCN at -20 °C.

Having established the feasibility of our reaction, various control reactions were conducted to confirm the requirement of all reagents. (Table 3). Reducing the temperature (entry 1) exclusively gave the 4-allylated product, with no formation of side-product **411**. In the absence of LiOt-Bu (entries 2 and 3), reactivity shut down, thereby suggesting its requirement to activate the allyl pinacolboronate towards transmetalation. Crucially, in the absence of the gold catalyst (entry 4) no product formation was

observed. Gold exhibits Lewis acidic characteristics, therefore, various transition metal based Lewis acids were explored (entries 5, 6, and 7). Interestingly, reactivity shut down when utilising other Lewis acidic metals; however, diminished yields were observed when employing both Au(SMe₂)Cl and La(OTf)₃. This suggests that gold does not act as a Lewis acid to facilitate the allylation of the azinium ion.

Table 3: Control reactions.



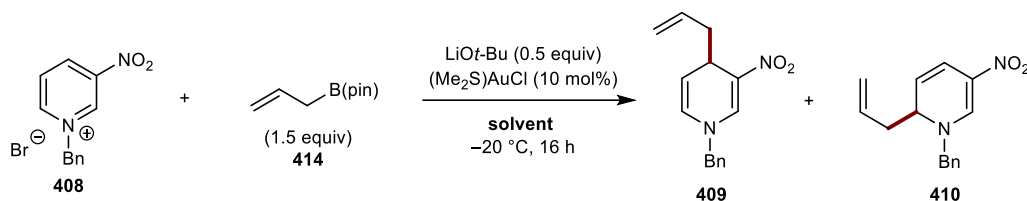
Entry	Alteration	Yield (%)				Ratio of 409:410
		409	410	411	Total	
1	at 0 °C	21	-	-	21	>19:1
2	no LiOt-Bu	-	-	-	-	-
3 ^[a]	no LiOt-Bu	-	-	-	-	-
4	no [Au]	-	-	23	23	-
5 ^[b]	La(OTf) ₃ , no [Au]	-	-	-	-	-
6 ^[b]	La(OTf) ₃	12	-	-	12	>19:1
7 ^[c]	Sc(OTf) ₃ , no [Au]	-	-	6	6	-

Reactions conducted with 0.1 mmol of **408**. Yields determined by ¹H NMR spectroscopy using 1,3,5-trimethoxybenzene as the internal standard. [a] Conducted at -10 °C, [b] Using La(OTf)₃ 10 mol%, [c] Using Sc(OTf)₃ 10 mol%.

To optimise yields, an extensive solvent screen was performed at -20 °C to avoid the formation of side-product **411** (Table 4). Conducting the reaction in MeCN (entry 2) gave a drastic increase in yield, albeit lowering the regioselectivity to 4.5:1. Interestingly, utilising DCE (entry 3), an analogous solvent to CH₂Cl₂ diminished reactivity. MeOH (entry 5) reversed the regioselectivity, affording the 6-allylated product in 30% yield. Utilising either Et₂O (entry 8) or benzonitrile (entry 10) generated the corresponding 4-allylated dihydropyridine in 13% and 52% yield respectively, with modest levels of regiocontrol. THF (entry 6) and EtOAc (entry 11) generated the desired product in modest to excellent yields with 7:1 ratio of 4- vs. 6-allylated dihydropyridine. A combination of EtOAc/CH₂Cl₂ (1:1) gave the highest regioselectivity with excellent

yields (entry 12) and was therefore chosen as the solvent system for further optimisation reactions.

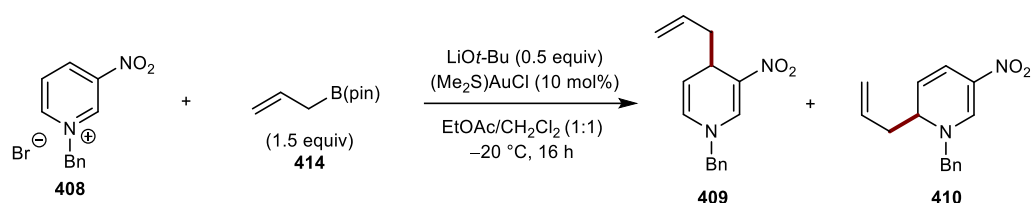
Table 4: Solvent screening.



Entry	Solvent	Yield (%)			Ratio of 409:410
		409	410	Total	
1	CH ₂ Cl ₂	21	-	21	>19:1
2	MeCN	68	15	83	4.5:1
3	DCE	4	trace	4	>19:1
4	acetone	41	16	57	2.6:1
5	MeOH	20	30	50	1:1.5
6	THF	49	7	56	7:1
7	DMF	16	9	25	1.8:1
8	Et ₂ O	13	-	13	>19:1
9	MeO(CH ₂) ₂ OH	55	16	71	3.4:1
10	PhCN	52	20	72	2.6:1
11	EtOAc	85	12	97	7:1
12	EtOAc/CH ₂ Cl ₂ (1:1)	80	7	87	11:1

Reactions conducted with 0.1 mmol of **408**. Yields determined by ¹H NMR spectroscopy using 1,3,5-trimethoxybenzene as the internal standard.

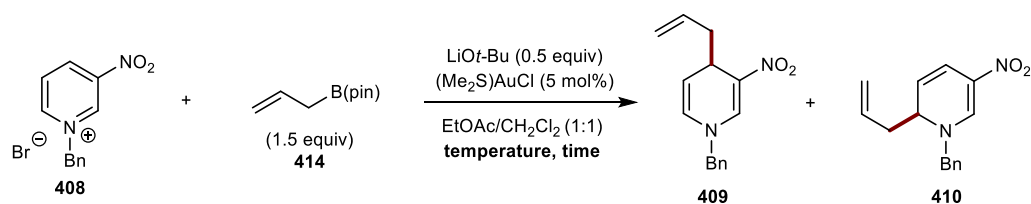
A second series of control reactions were conducted (Table 5). Pleasingly, the catalyst loading could be lowered from 10 mol% to 2.5 mol% without any significant loss of yield and regiocontrol (entries 1 and 2). All previous optimisation reactions were performed under an inert atmosphere, using deoxygenated anhydrous solvents. Fortunately, conducting the reaction in an open flask without special precautions to exclude air or moisture gave no significant loss in yield (entries 3, 4, and 5), thus, highlighting the robustness of this methodology. Repeat experiments revealed optimised conditions with 5 mol% catalyst loading gave the most consistent results at this scale.

Table 5: Control reactions.

Entry	Alteration	Yield (%)			Ratio of 409:410
		409	410	Total	
1	5 mol% [Au]	81	9	90	9:1
2	2.5 mol% [Au]	79	7	86	11:1
3	no degassing sol.	79	8	87	10:1
4	no drying/degassing sol.	81	9	90	9:1
5	open to air	80	8	88	10:1
6	no [Au]	trace	trace	-	-

Reactions conducted with 0.1 mmol of **408**. Yields determined by ^1H NMR spectroscopy using 1,3,5-trimethoxybenzene as the internal standard.

Encouraged by our findings, the temperature and duration of the reaction were then varied (Table 6). Performing the reaction at room temperature for 16 hours gave a decrease in both yield and regioselectivity (entry 1), with formation of side-product **411**. However, the reaction time could be lowered from 16 hours to 90 minutes without any loss in yield (entry 2).

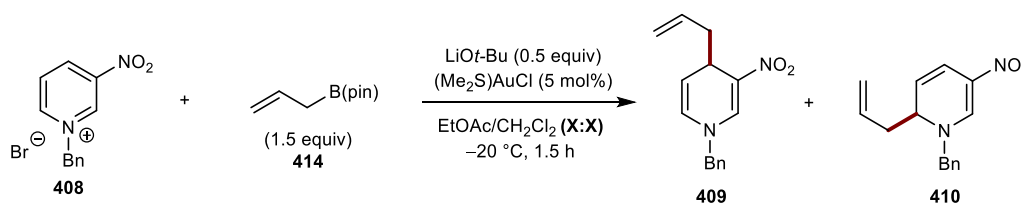
Table 6: Temperature and reaction time screening.

Entry	Alteration	Yield (%)			Ratio of 409:410
		409	410	Total	
1	at RT for 16 h	55	7	62	8:1
2	at -20 °C for 1.5 h	84	7	91	12:1

Reactions conducted with 0.1 mmol of **408**. Yields determined by ^1H NMR spectroscopy using 1,3,5-trimethoxybenzene as the internal standard.

Mixed-solvent systems were then investigated (Table 7). Increasing the ratio of EtOAc to CH₂Cl₂ resulted in slightly diminished yields and regioselectivities (entries 1, 2 and 3). Increasing the ratio of CH₂Cl₂ to EtOAc (entries 4, 5, and 6) gave a slight increase in regiocontrol; however, lower overall yields were observed. The results indicate an independence on the ratio of EtOAc to CH₂Cl₂ with respect to the regioselectivity of the reaction. Therefore, EtOAc/CH₂Cl₂ (1:1) remained as the optimum mixed solvent system for our reaction conditions.

Table 7: Solvent mixture screening.

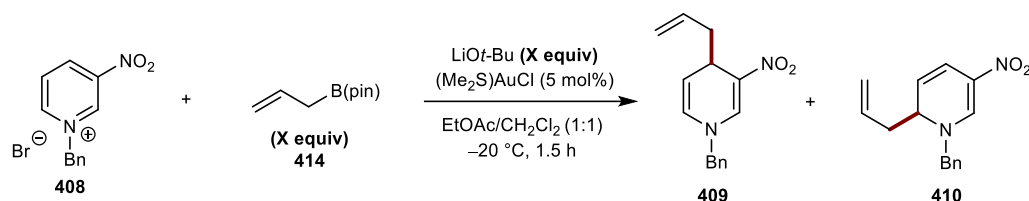


Entry	Solvent System	Yield (%)			Ratio of 409:410
		409	410	Total	
1	EtOAc/CH ₂ Cl ₂ (2:1)	67	7	74	10:1
2	EtOAc/CH ₂ Cl ₂ (4:1)	75	8	83	9:1
3	EtOAc/CH ₂ Cl ₂ (9:1)	65	7	72	9:1
4	EtOAc/CH ₂ Cl ₂ (1:2)	75	8	83	9:1
5	EtOAc/CH ₂ Cl ₂ (1:4)	69	7	76	10:1
6	EtOAc/CH ₂ Cl ₂ (1:9)	69	5	74	14:1
7	EtOAc/CH ₂ Cl ₂ (1:1)	80	7	87	11:1

Reactions conducted with 0.1 mmol of **408**. Yields determined by ¹H NMR spectroscopy using 1,3,5-trimethoxybenzene as the internal standard.

Finally, a series of reactions concerning the equivalents of each reagent were performed (Table 8). Either increasing or decreasing the equivalents of base gave no increase in overall yield (entries 1, 2 and 3). Additionally, lowering the equivalents of allyl pinacolboronate in the reaction system proved detrimental for the yield (entries 4 and 5). Further experiments investigating the use of phosphine substituted gold catalysts such as (Ph₃P)AuCl and (Me₃P)AuCl were also attempted. However, any deviation from the “standard” reaction conditions diminished reactivity, with only trace amounts of product being observed in the crude ¹H NMR spectra.

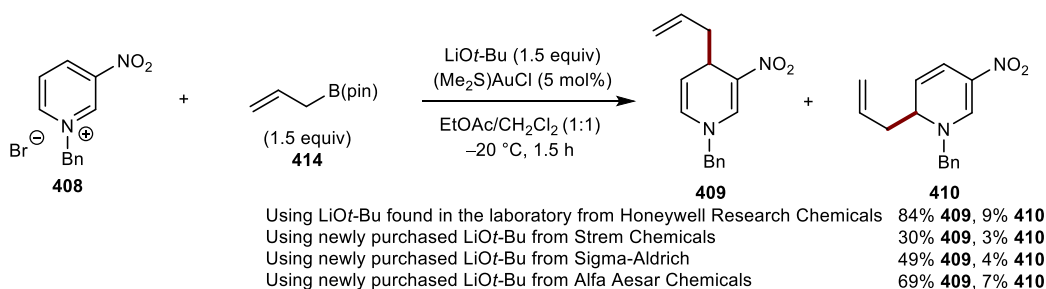
Table 8: Equivalents of allylic boronate and base screening.



Entry	Equivalents		Yield (%)			Ratio of 409:410
	Allylic Boronate	Base	409	410	Total	
1	1.5	1.0	85	9	94	9:1
2	1.5	0.3	52	7	59	7:1
3	1.5	0.2	38	4	42	9:1
4	1.2	0.5	65	7	72	9:1
5	1.1	0.5	56	5	61	11:1

Reactions conducted with 0.1 mmol of **408**. Yields determined by ¹H NMR spectroscopy using 1,3,5-trimethoxybenzene as the internal standard.

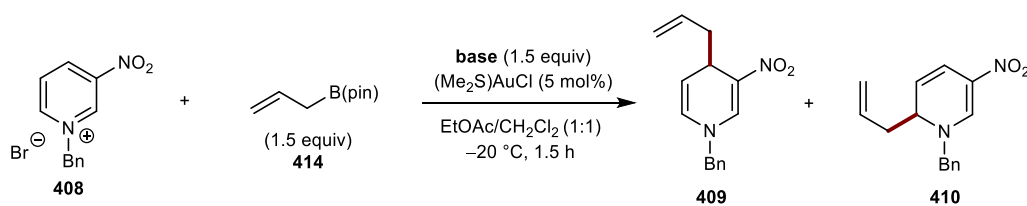
With our optimised conditions in hand, exploration of the substrate scope was the next logical step; however, reproducibility issues were encountered when using a newly purchased bottle of LiOt-Bu (Scheme 115). A drastic decrease in yield was observed when using newly purchased LiOt-Bu from various manufacturers. This suggests that an impurity in the original bottle of LiOt-Bu was impacting the reaction efficiency. LiOt-Bu is known to decompose to LiOH and Li₂CO₃ when exposed to moisture over significant periods of time.¹⁶² However, subjecting both LiOH and Li₂CO₃ gave a decrease in yield. ¹H NMR spectroscopy of the original LiOt-Bu from Honeywell Research Chemicals identified slight irregularity in the associated peaks; however, no significant conclusions could be drawn from this. Further experiments investigating H₂O as an additive gave reduced yields, while variation in the equivalents of base gave no increase in yield.



Scheme 115: Examination of different suppliers for LiOt-Bu.

A base screen was conducted to find an alternative to LiOt-Bu (Table 9). Subjecting NaOt-Bu (entry 1) to the reaction conditions gave the desired product in 36% yield with respectable levels of regiocontrol. Switching to KOt-Bu (entry 2) gave trace product, suggesting the cation may influence reactivity. LiOt-Bu is known to decompose to LiOH, therefore, NaOH and KOH (entries 3 and 4) were examined. Both gave reduced yields and regioselectivities. Alternative alkoxides were analysed (entries 5, 6, and 7). Fortunately, LiOi-Pr (entry 5) gave an outstanding yield of 97% with an excellent 13:1 ratio of 4- vs. 6-allylated dihydropyridine. Utilising carbonates as bases (entries 8, 9 and 10) resulted in diminished yields in comparison to LiOt-Bu. Therefore, LiOi-Pr was selected for the remainder of our studies, circumventing any issues associated with using LiOt-Bu. However, any attempts to render LiOi-Pr sub-stoichiometric as observed with LiOt-Bu proved unsuccessful.

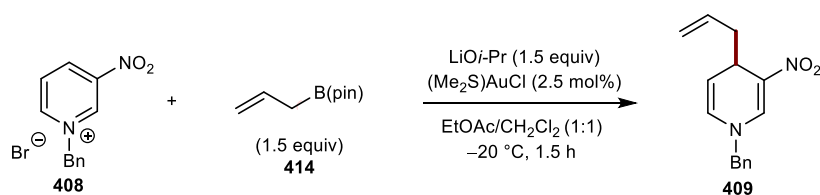
Table 9: Base screening.



Entry	Base	Yield (%)			Ratio of 409:410
		409	410	Total	
1	NaOt-Bu	36	5	41	7:1
2	KOt-Bu	trace	-	-	-
3	NaOH	46	4	50	11:1
4	KOH	19	4	23	5:1
5	LiOi-Pr	90	7	97	13:1
6	NaOMe	trace	-	-	-
7	KOAc	trace	-	-	-
8	Na ₂ CO ₃	-	-	-	-
9	K ₂ CO ₃	-	-	-	-
10	Cs ₂ CO ₃	trace	-	-	-
11	K ₃ PO ₄	-	-	-	-

Reactions conducted with 0.1 mmol of **408**. Yields determined by ¹H NMR spectroscopy using 1,3,5-trimethoxybenzene as the internal standard.

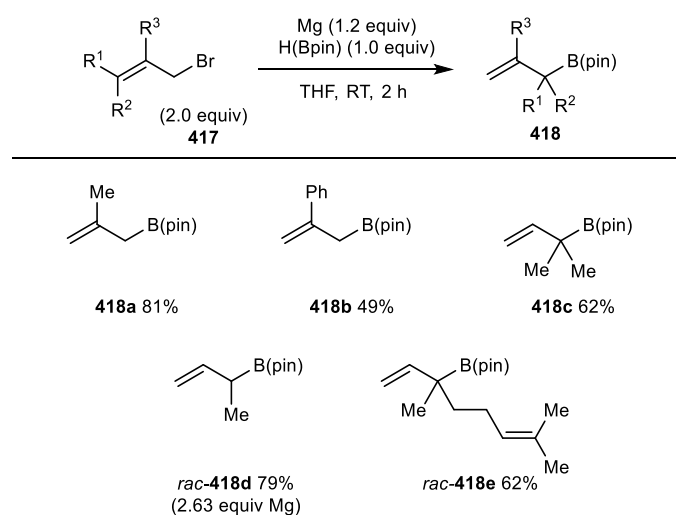
A final set of conditions were settled upon to investigate the substrate scope (Scheme 116). A lower catalyst loading of 2.5 mol% was preferred when exploring the substrate scope given the use of a precious metal catalyst.



Scheme 116: Optimised conditions.

2.3 Reaction Scope

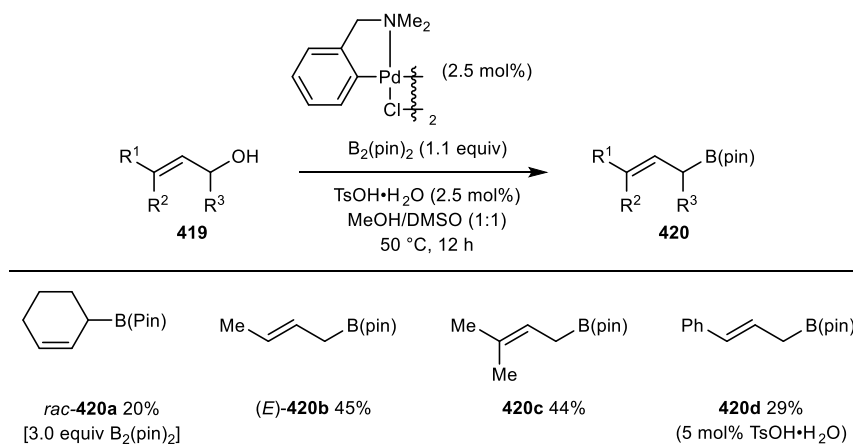
First, various substituted allyl pinacolboronates were synthesised. Allyl pinacolboronates featuring α - or β -substitution (**418**) were synthesised according to the methods of Singaram (Scheme 117).¹⁶³ Under Barbier conditions, formation of an allylic Grignard reagent occurs, followed by attack on pinacolborane, eliminating hydridomagnesium bromide to form the corresponding allyl pinacolboronate **418**.



Scheme 117: Synthesis of functionalised allyl pinacolboronates.

Allyl pinacolboronates featuring γ -substitution (**420**) were synthesised *via* a one-step procedure from commercially available allylic alcohols (Scheme 118).¹⁶⁴ Due to the preference for π -allylpalladium species to undergo nucleophilic substitution at the least

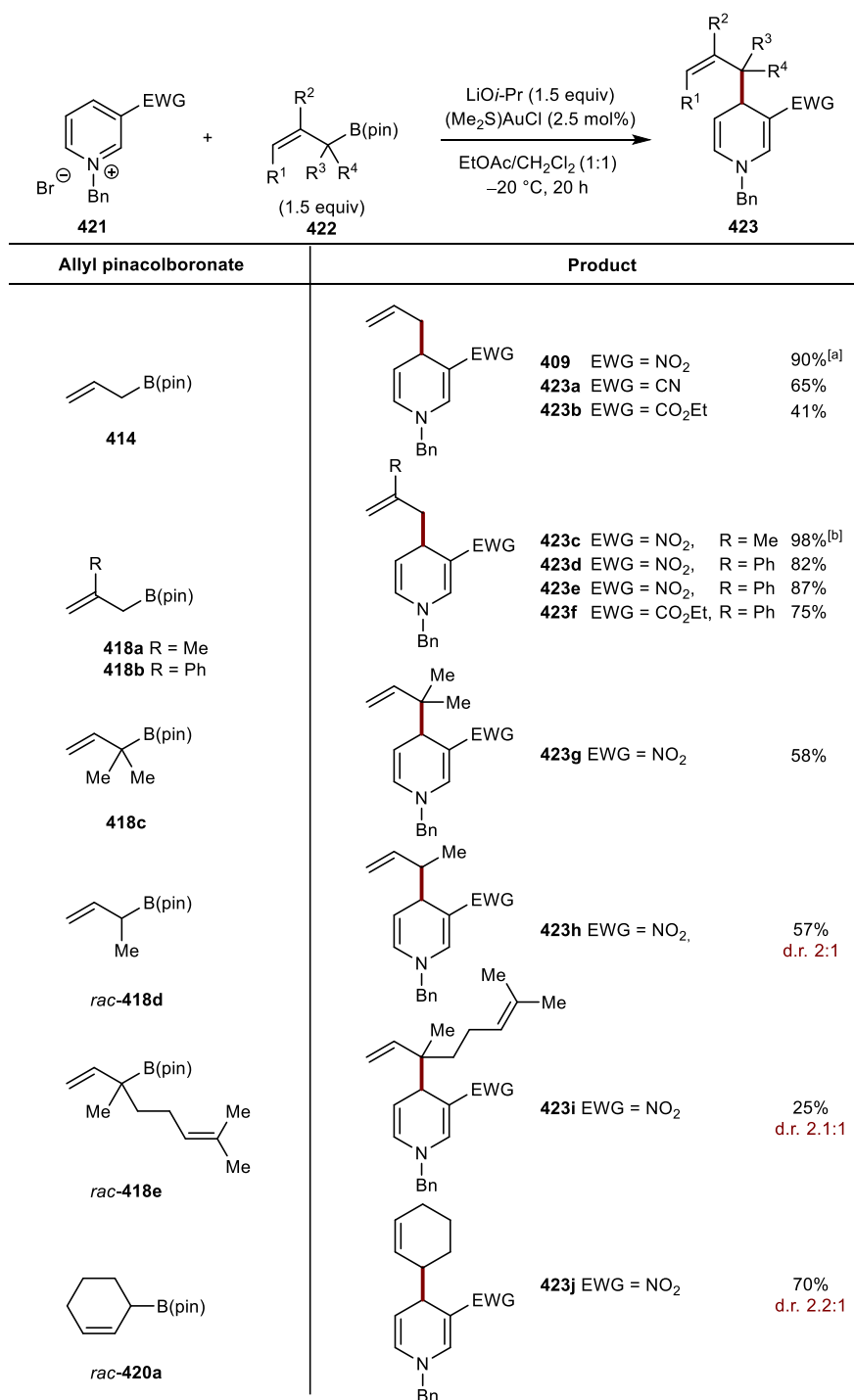
hindered carbon, regioisomeric allylic alcohols could be utilised, forming exclusively the (*E*)-allyl pinacolboronate.



Scheme 118: Palladium-catalysed synthesis of functionalized allyl pinacolboronates.

With our optimised conditions and a range of functionalised allyl pinacolboronates in hand, the scope of the reaction was explored (Table 10). Allyl pinacolboronate **414** reacted successfully with various 3-substituted *N*-benzylpyridinium bromides to give **409–423b** in 41–90% yield. In most cases, the reaction time was extended to 20 hours to achieve full consumption of starting material with only one single regioisomer being observed. 2-Methylallyl pinacolboronate (**418a**) and 2-phenylallyl pinacolboronate (**418b**) are effective allylating agents and provided **423c–423f** in excellent yields. These yields are higher than those of the corresponding reactions with allyl pinacolboronate (**409–423b**), this may be attributed to the higher nucleophilicity of 2-methylallyl pinacolboronate and 2-phenylallyl pinacolboronate. Interestingly, the reaction of α,α -dimethylallyl pinacolboronate (**418c**) occurred with high α -regioselectivity (with respect to the allylating agent) to give the reverse-prenylated 1,4-dihydropyridine **423g** in 58% yield, and none of the alternative prenylation product resulting from γ -allylation was observed. High α -regioselectivities were also observed with α -methyl-substituted allyl pinacolboronate *rac*-**418d** and the geranyl-bromide-derived α,α -disubstituted allyl pinacolboronate *rac*-**418e**, which gave 1,4-dihydropyridines **423h** and **423i** in 57% and 25% yield, respectively, as mixtures of inseparable diastereomers. Cyclohexenyl allyl pinacolboronate *rac*-**420a** gave 1,4-dihydropyridine **423j** in 70% yield as a 2.2:1 mixture of inseparable diastereomers.

Table 10: Allyl pinacolboronate scope.



Reactions conducted on 0.5 mmol scale. Isolated yields. [a] 1.5 h, [b] 4.5 h.

Pleasingly, a single crystal of **423c** was grown using a CH₂Cl₂/petroleum ether solvent system and submitted for X-ray crystal analysis, confirming the regioselectivity of the allylated dihydropyridine (Figure 1).

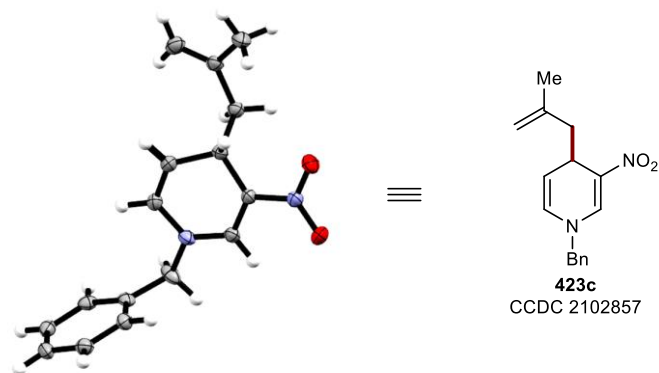
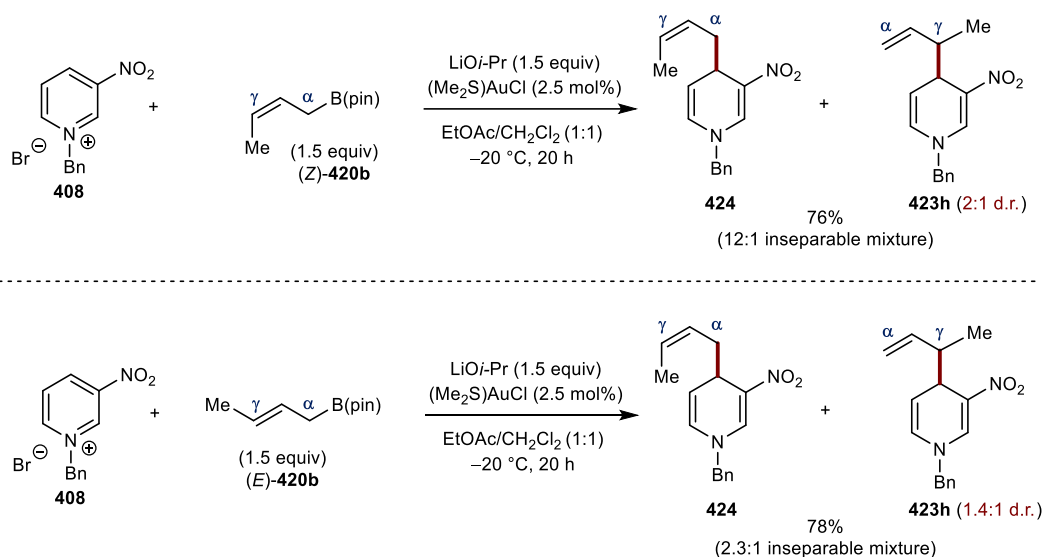


Figure 1: X-ray crystal structure for **423c** at 50% atomic probability distributions for ellipsoids.

Additional experiments revealed examples where lower $\alpha:\gamma$ selectivity with respect to the allyl pinacolboronate were observed (Scheme 119). Regioisomeric mixtures were detected in the reactions of azinium salt **408** with crotyl pinacolboronates. Subjecting (*Z*)-crotyl pinacolboronate to the reaction conditions gave a 12:1 mixture of regioisomers in 76% yield, favoring the α -allylation product **424** over the γ -allylation product **423h**, the latter of which was formed in 2:1 diastereoselectivity. In contrast, when subjecting (*E*)-crotyl pinacolboronate to the reaction conditions, the $\alpha:\gamma$ selectivity decreased to 2.3:1 and interestingly, the α -addition product **424** was isolated as the *Z*-isomer, with **423h** being formed in 1.4:1 diastereoselectivity.



Scheme 119: Alkylation of **408** using (*Z*)- and (*E*)-crotyl pinacolboronate.

X-ray crystallographic data was collected for **424** (Figure 2) using a CH_2Cl_2 /petroleum ether solvent system, confirming the geometry of the olefin.

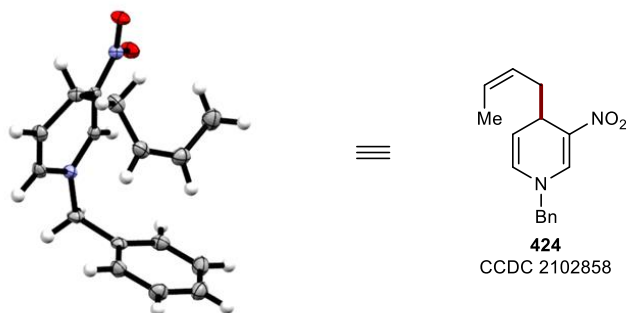
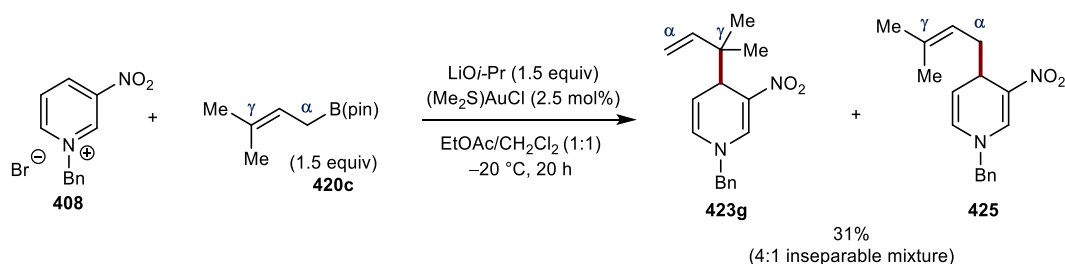


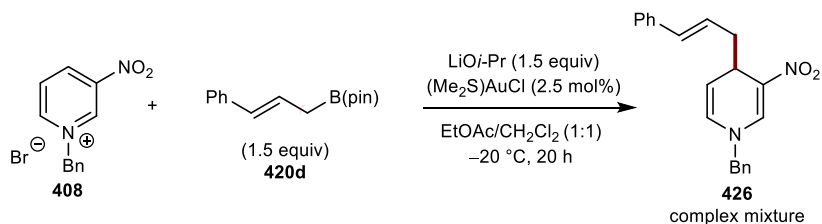
Figure 2: X-ray crystal structure for **424** at 50% atomic probability distributions for ellipsoids.

Comparatively to the preference of α -substitution observed with crotyl pinacolboronates, prenyl pinacolboronate **420c** (Scheme 120) gave a 4:1 mixture of inseparable regioisomers **423g** and **425** favoring the reverse prenylated product **423g**. This result should be contrasted with the reaction using α,α -dimethylallyl pinacolboronate (**418c**) (Table 10), which gave only the reverse prenylation product **423g**. The rationale behind this switch in regioselectivity with respect to prenyl pinacolboronate **420c** is explained by DFT calculations shown in section 2.5.



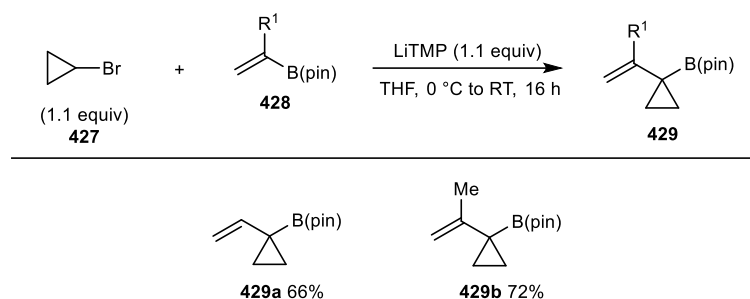
Scheme 120: Alkylation of **408** using prenyl pinacolboronate **420c**.

(*E*)-Allyl pinacolboronate **420d** displayed poor reactivity, with modest starting material consumption, while producing a complex crude ^1H NMR spectrum (Scheme 121). Product isolation proved challenging, with characterisation not possible by NMR techniques due to the complex nature of the spectra.



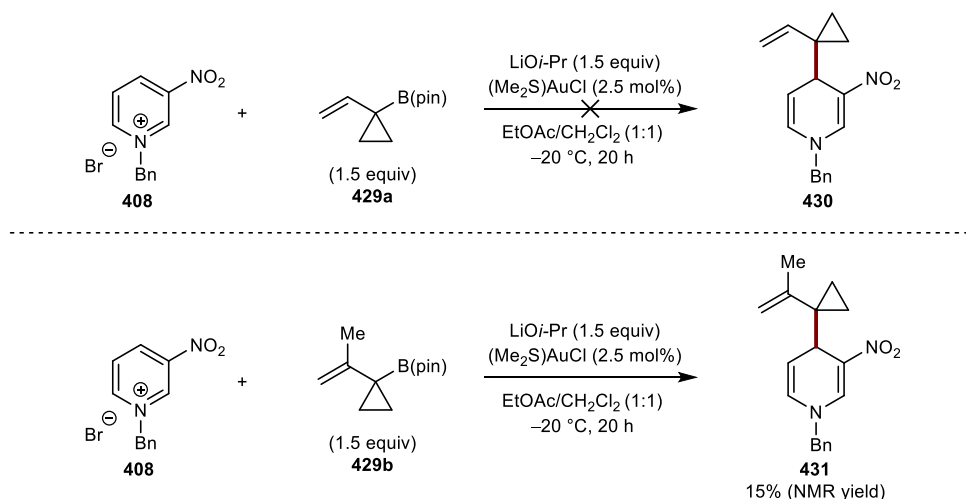
Scheme 121: Alkylation of **408** using allyl pinacolboronate **420d**.

Allyl pinacolboronates featuring an α -cyclopropyl substituent were synthesised according to Aggarwal and co-workers (Scheme 122).¹⁶⁵ Deprotonation followed by reaction with vinyl pinacolboronate **428** generates a boronate intermediate which undergoes a 1,2-metalate rearrangement to afford the desired product.



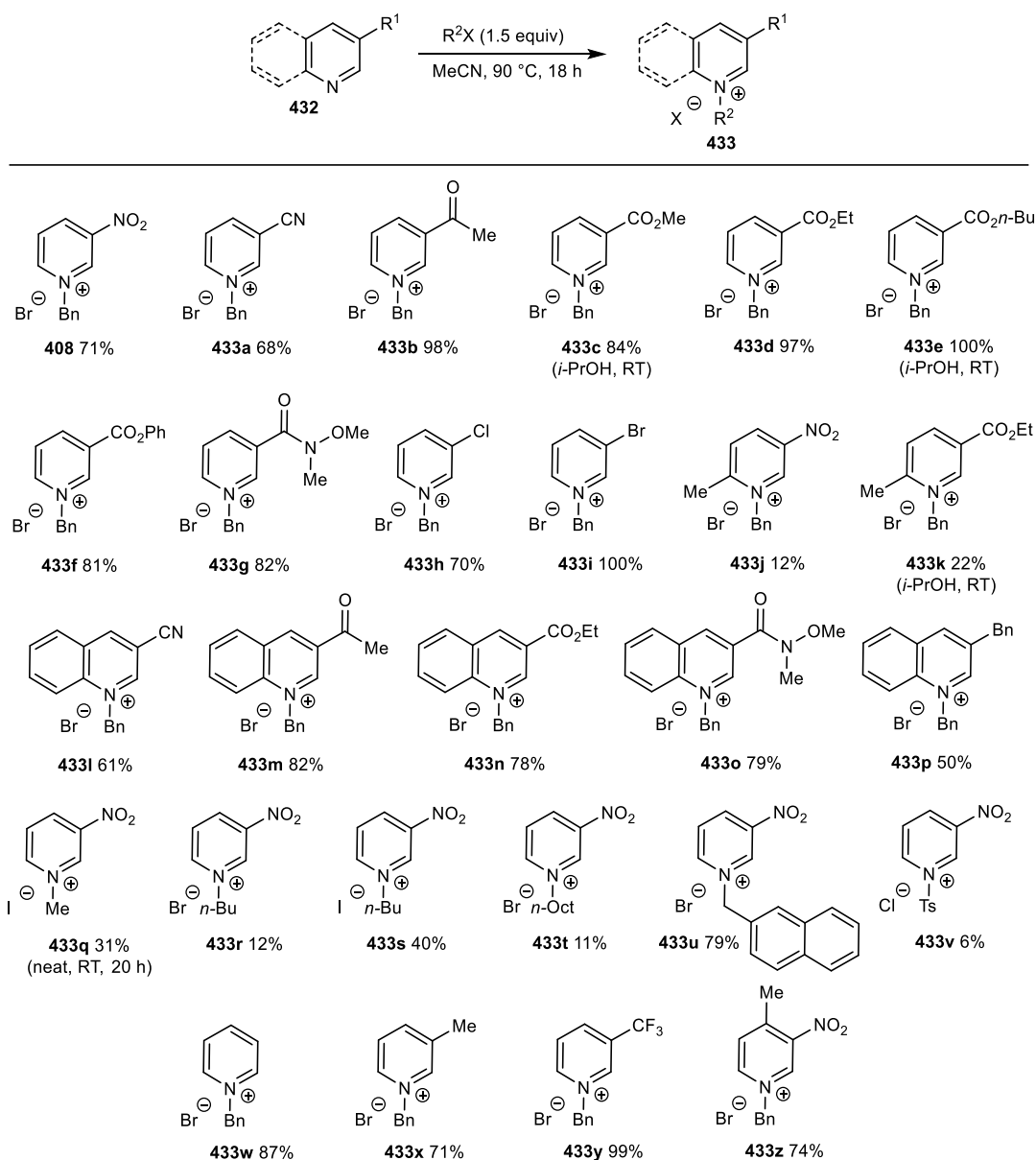
Scheme 122: Synthesis of α -cyclopropylallyl pinacolboronates.

Subjecting α -cyclopropylallyl pinacolboronate **429a** to our optimised reaction conditions gave no desired product formation, with the recovery of starting material accounting for mass balance (Scheme 123). Interestingly, α -cyclopropylallyl pinacolboronate **429b** gave the desired product in 15% yield. This change in reactivity may be attributed to the higher nucleophilicity of **429b** in comparison to **429a**.



Scheme 123: Allylation of **408** using allyl pinacolboronates **429a** and **429b**. Yield determined by ¹H NMR spectroscopy using 1,3,5-trimethoxybenzene as the internal standard.

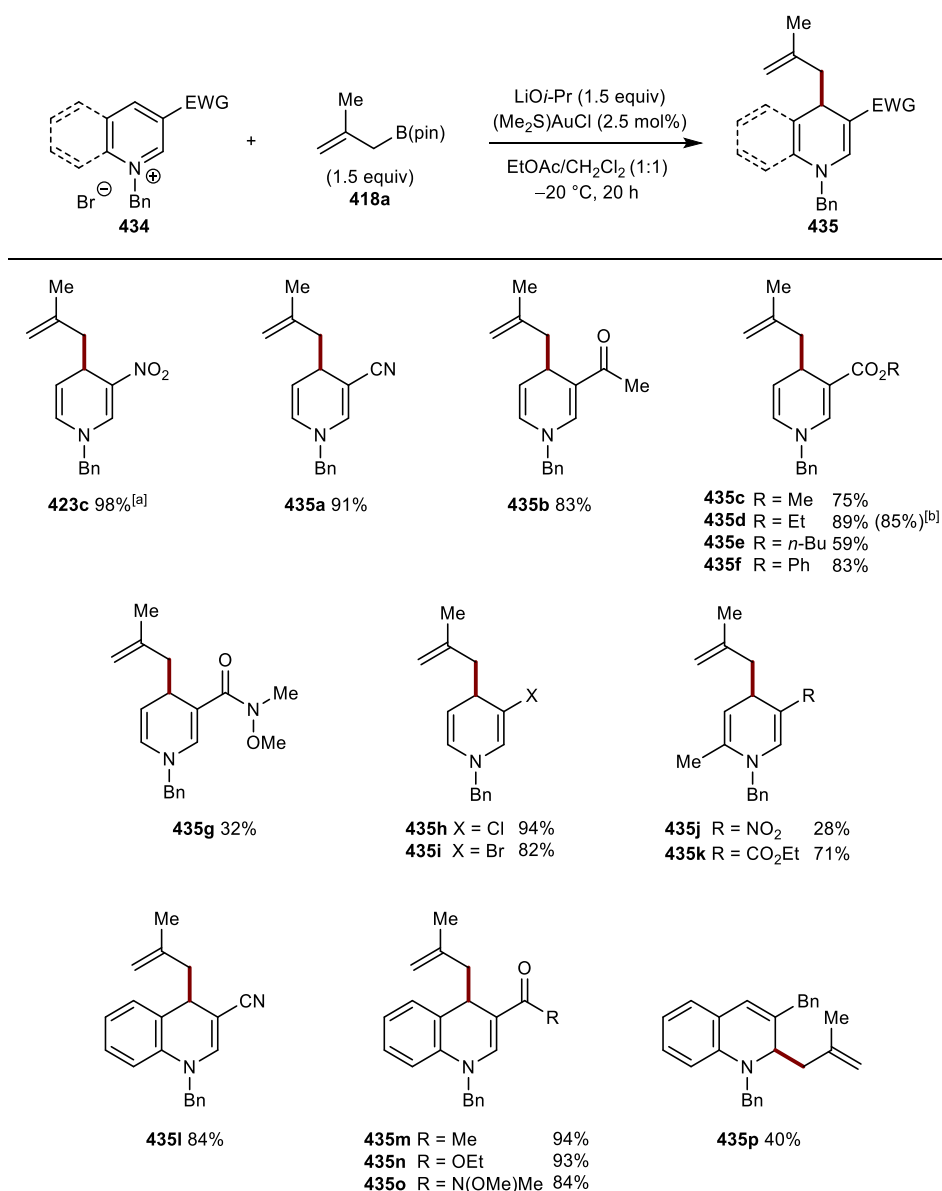
Next, the substrate scope with respect to the azinium salt was investigated. First, a range of azinium salts were synthesised from commercially available substituted pyridines *via* *N*-alkylation using benzyl bromide (Scheme 124). This process could be performed on a multi-gram scale, requiring no purification by column chromatography.



Scheme 124: Synthesis of azinium salts.

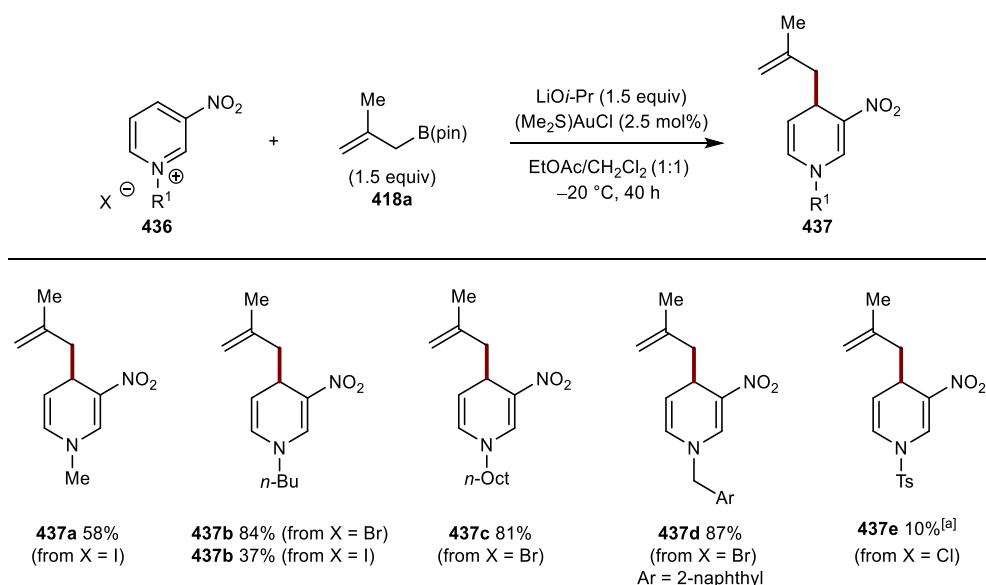
The scope of the reaction with respect to the azinium salt was examined using 2-methylallyl pinacolboronate (**418a**), as it provided superior yields in comparison to allyl pinacolboronate (**414**) (Scheme 125). In all reported examples, complete regiocontrol was observed, allylating exclusively at the 4-position of the azinium salt, with the exception of **435p**. In addition to the high-yielding reaction to form **423c**, the reaction was successful with *N*-benzyl azinium salts containing various electron-withdrawing groups at the 3-position, such as cyano (**435a**), acetyl (**435b**) and a variety of esters (**435c–435f**). 1,4-Dihydropyridine **435d** could also be synthesised on gram scale with no significant loss in yield. Lower yields were observed for both *N*-benzyl azinium salts

containing an *n*-butyl ester (**435e**) and Weinreb amide (**435g**) at the 3-position. Notably, substrates containing chloro- or bromo- groups at the 3-position also reacted successfully to give 1,4-dihydropyridines **435h** and **435i** in 94% and 82% yield, respectively. *N*-Benzyl-2-methyl-5-nitropyridinium bromide provided 1,4-dihydropyridine **435j** in a poor 28% yield, most likely due to the modestly electron-donating methyl group reducing the electrophilicity of the substrate. Pleasingly, a range of *N*-benzylquinolinium salts also reacted efficiently to give 1,4-dihydroquinolines **435l–435p** in 40–94% yield; these substrates contained a cyano (**435l**), acetyl (**435m**), ester (**435n**), Weinreb amide (**435o**), or benzyl (**435p**) group at the 3-position. Interestingly, *N*-benzylquinolinium salt containing a benzyl substituent gave the 2-allylated product **435p** exclusively.



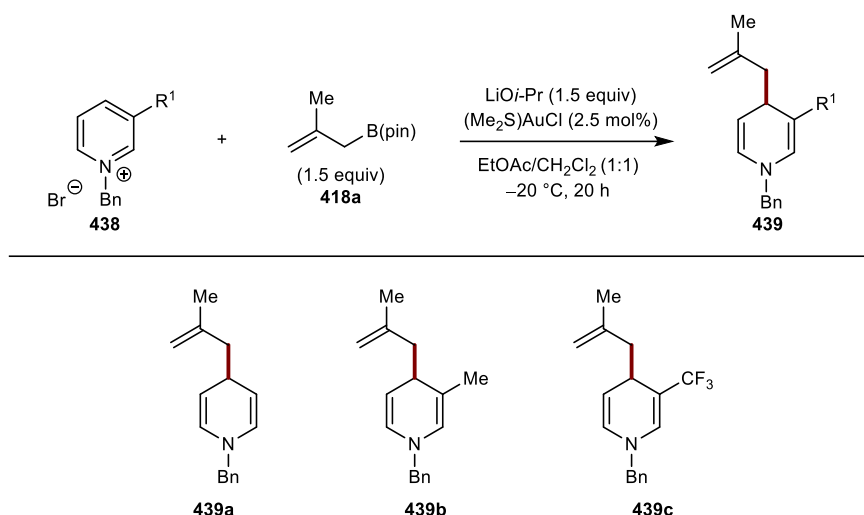
Scheme 125: Azinium salt scope. Reactions conducted on 0.5 mmol scale. Isolated yields. [a] 4.5 h, [b] Reaction conducted on 4.0 mmol scale.

Following the azinium salt scope, variation of the nitrogen substituent and counterion was briefly investigated (Scheme 126). The addition of 2-methylallyl pinacolboronate (**418a**) to *N*-methyl-3-nitropyridinium iodide provided 1,4-dihydropyridine **437a** in 58% yield, which is lower than that obtained with *N*-benzyl-3-nitropyridinium bromide (**423c**). Changing the *N*-substituent to an *n*-butyl fragment gave the desired product in 84% from the bromide salt (**433r**); however, the iodide salt (**433s**) gave reduced yield, attributed to solubility issues. Increasing the carbon chain to an *n*-octyl substituent afforded 1,4-dihydropyridine **437c** in excellent yield. *N*-(2-Naphthylmethyl)-3-nitropyridinium bromide was an effective substrate and gave **437d** in 87% yield. *N*-Tosyl-3-nitropyridinium bromide **437e** gave the desired product in 10% yield by crude ¹H NMR spectroscopy, with fragmentation of the nitrogen-tosyl bond accounting for the majority of mass balance.



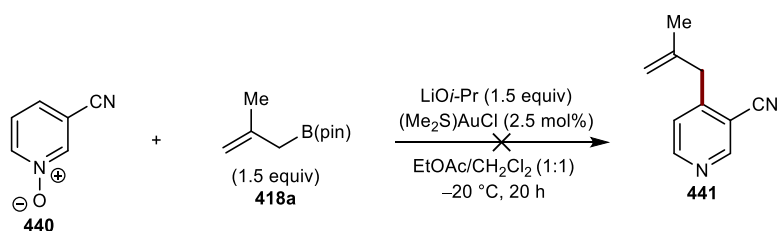
Scheme 126: Protecting group scope. Reactions conducted on 0.5 mmol scale. Isolated yields. [a] Reaction conducted on 0.1 mmol scale, yield determined by ¹H NMR spectroscopy using 1,3,5-trimethoxybenzene as the internal standard.

No reactivity was observed when substrates containing either a proton or methyl group at the 3-position of the azinium salt were subjected to the reaction conditions (Scheme 127). Furthermore, 3-trifluoromethyl azinium salt gave the desired product as a mixture of regioisomers; however, purification of **439c** proved challenging with significant decomposition on silica.



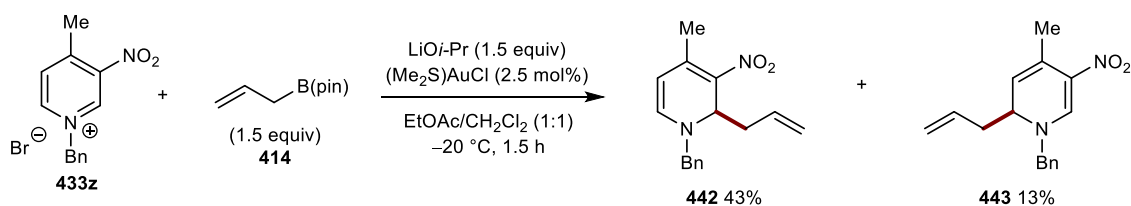
Scheme 127: Unsuccessful allylation of azinium salts.

We postulated that utilising *N*-oxide **440** could provide allylated pyridine **441** (Scheme 128). However, upon reacting **440** under our standard reaction conditions, no product formation was observed.



Scheme 128: Unsuccessful allylation of *N*-oxide **440**. Substrate **440** was synthesised by H. Green.

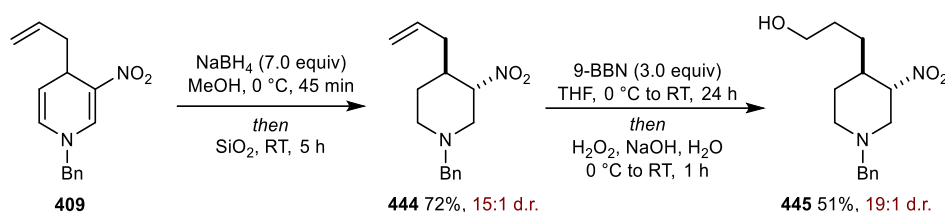
On further assessment of the reaction scope, it was postulated that subjecting azinium salt **433z**, which contains a methyl group at the 4-position, would potentially block allylation at this site (Scheme 129). Indeed, reaction of **433z** with allyl pinacolboronate (**414**) gave a mixture of the allylated product **442** in 43% yield and the allylated product **443** in 13% yield.



Scheme 129: Gold-catalysed allylation of **433z** using **414**. Isolated yields.

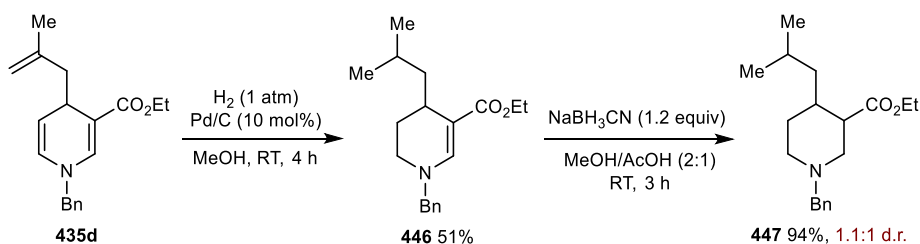
2.4 Product Manipulations

The synthetic utility of the corresponding dihydropyridine products was briefly investigated (Scheme 130). Enamide reduction of dihydropyridine **409** using NaBH₄, followed by epimerisation with silica gel gave piperidine **444** in 72% yield as a 15:1 inseparable mixture of diastereoisomers. A *trans*-diaxial relationship was observed, allowing the two bulky substituents to occupy the more favourable equatorial positions. Hydroboration and oxidation of the remaining alkene afforded primary alcohol **445** in 51% yield as a 19:1 inseparable mixture of diastereoisomers.



Scheme 130: Product derivatisation of 409.

Further product manipulations are shown in Scheme 131. Hydrogenation of dihydropyridine **435d** selectively reduced the 1,1-disubstituted exocyclic alkene and the less substituted enamide, furnishing tetrahydropyridine **446** in modest yield. Reduction of the remaining enamide using NaBH₃CN gave piperidine **447** in 94% yield.

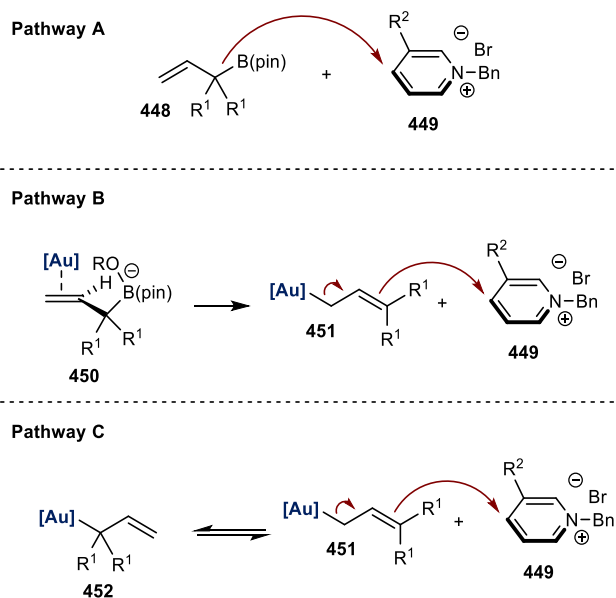


Scheme 131: Product derivatisation of 435d.

2.5 Mechanistic Studies

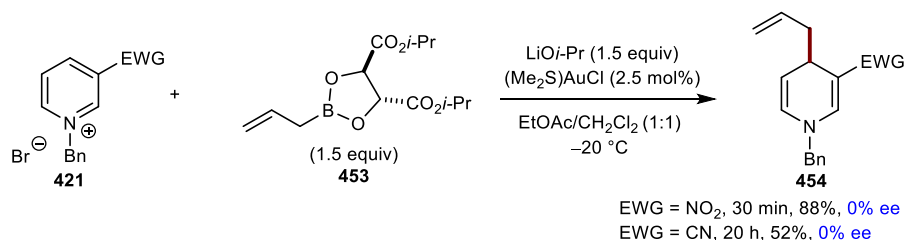
Our substrate scope indicated a complex reaction mechanism not yet described in the literature; therefore, we hypothesised three potential reaction pathways (Scheme 132). Pathway A involves the direct addition of allyl pinacolboronate **448** to the azinium ion. Pathway B involves transmetalation between the allyl pinacolboronate and the gold

catalyst, generating allylgold intermediate **451**, that cannot interconvert between its two σ -allyl isomers. This intermediate then undergoes nucleophilic addition onto the azinium ion. Pathway C involves a similar process to that of pathway B, except allylgold intermediate **451** can interconvert between its two σ -allyl isomers (**451** and **452**).



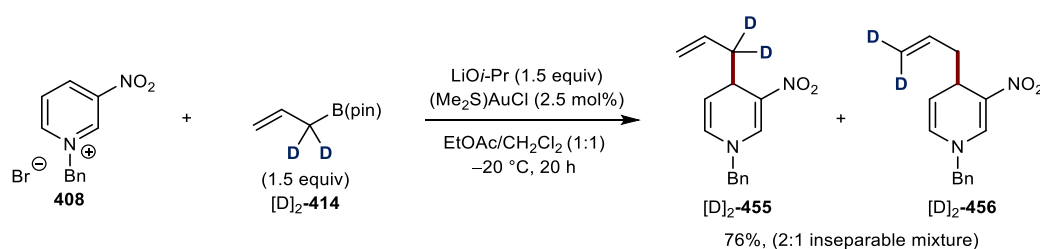
Scheme 132: Viable mechanistic pathways.

To provide evidence for transmetalation between the allyl pinacolboronate and gold catalyst, enantiopure allyl pinacolboronate **453** was subjected to our optimised reaction conditions (Scheme 133). Utilising 3-nitro- or 3-cyano-*N*-benzyl pyridinium bromide generated the desired product with no asymmetric induction. The loss of enantiospecificity with respect to allyl pinacolboronate suggests that boron is not involved in the C-C bond forming step. This indicates that pathway A may not be operating within our reaction conditions. Thus, the two more likely pathways are either pathway B or pathway C, suggesting transmetalation is likely occurring.



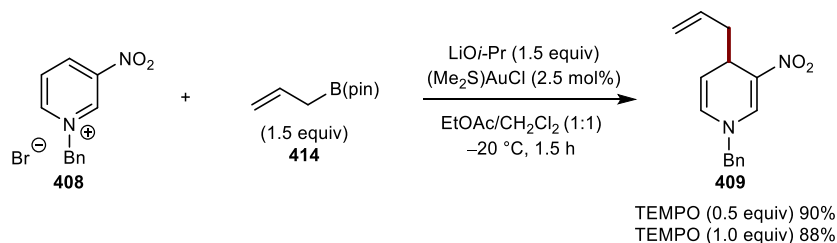
Scheme 133: Investigating the effect of using enantiopure allyl pinacolboronate **453**. Yields determined by ¹H NMR spectroscopy using 1,3,5-trimethoxybenzene as the internal standard.

To discern between pathway B and C, the reaction of **408** with α,α -dideuterated allyl pinacolboronate ($[D]_2$ -**414**) was conducted (Scheme 134). This reaction gave a 2:1 mixture of regioisomers $[D]_2$ -**455** and $[D]_2$ -**456** in 76% yield, in favour of the α -allylation product $[D]_2$ -**455**. This scrambling of the deuterium label strongly suggests that pathway C is in operation and that the allylgold species can interconvert between its σ -allyl isomers post-transmetalation. Alternative mechanisms involving allyl pinacolboronates as the nucleophilic component would be expected to furnish $[D]_2$ -**455** exclusively, providing further evidence against pathway A. To observe an unequal mixture of products suggests that, either one of the σ -allylgold isomers is more reactive, leading to the formation of a major allylation product or the rate of isomerisation between the two σ -allylgold isomers is slower than that of nucleophilic addition. However, at this moment it is important to state that these results provide no evidence to support or disprove whether transmetalation is a α - or γ -selective process.



Scheme 134: Gold-catalysed allylation of **408** using $[D]_2$ -**414**.

Allylic radicals may account for the formation of the regioisomeric products observed in Scheme 120, therefore, TEMPO studies were conducted to investigate this (Scheme 135). The addition of stoichiometric TEMPO gave no change in yield, nor could any radical adducts be detected. This is highly suggestive of a non-radical process.

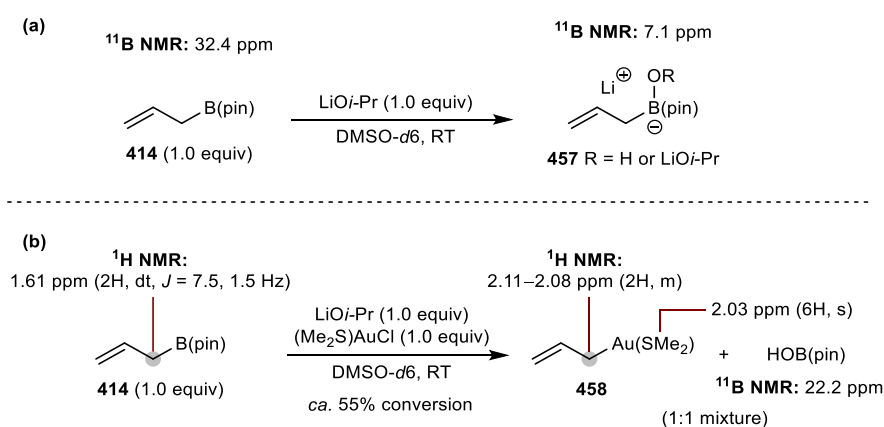


Scheme 135: Investigating the effect of TEMPO on the allylation of **408**. Reaction conducted on 0.1 mmol scale, yields determined by 1H NMR spectroscopy using 1,3,5-trimethoxybenzene as the internal standard.

To provide further evidence for the formation of an allylgold(I) intermediate, several equimolar control reactions were performed and analysed by 1H and ^{11}B NMR

spectroscopy (Scheme 136). First, equimolar quantities of allyl pinacolboronate **414** and Li*Oi*-Pr in the absence of (Me₂S)AuCl were mixed in DMSO-*d*₆ (Scheme 136a). By ¹H spectroscopy, minute changes were detected; however, no significant conclusions could be established due to broadening of the signals, attributable to the incomplete solubility of Li*Oi*-Pr. A new signal was observed by ¹¹B spectroscopy at 7.1 ppm, which is consistent with either a hydroxide or isopropoxide boronate complex.^{166,167} The presence of H₂O in DMSO-*d*₆ likely accounts for the hydroxide group which would react with Li*Oi*-Pr to give LiOH.

Next, equimolar quantities of allyl pinacolboronate **414**, Li*Oi*-Pr, and (Me₂S)AuCl were mixed in DMSO-*d*₆ (Scheme 136b). Full consumption of allyl pinacolboronate **414** was not observed; however, new signals consistent with the formation of a 1:1 mixture of allylgold(I) species **458** and HOB(pin) emerged. ¹¹B NMR spectroscopy provided further evidence for the formation of HOB(pin) at 22.2 ppm. This peak may contain trace quantities of *i*-PrOB(pin), resulting from Li*Oi*-Pr; however due to the large presence of H₂O in DMSO-*d*₆, HOB(pin) is expected to be the major boron-containing by-product. The formation of ClB(pin) (*ca.* 28 ppm) was not observed.^{168,169}



Scheme 136: Observation of **458**.

In the annotated ¹H NMR spectrum (Figure 3) for the reaction described in Scheme 136b, a new multiplet appeared at 2.11–2.08 ppm, attributable to the methylene protons adjacent to the gold centre. A broad singlet appeared at 7.99 ppm, referable to the hydroxyl proton of HOB(pin). The alkenyl protons of allylgold species **458** were assigned; however, due to the incomplete consumption of allyl pinacolboronate **414**, minute overlap of signals was observed.

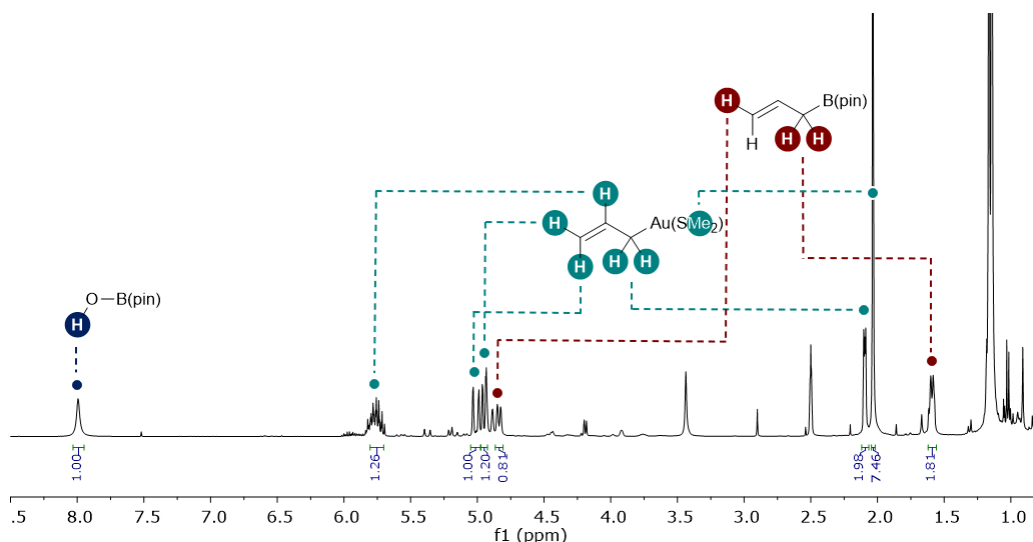
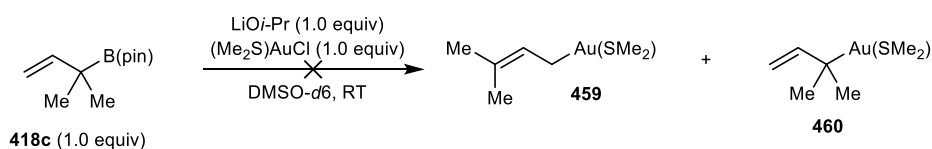


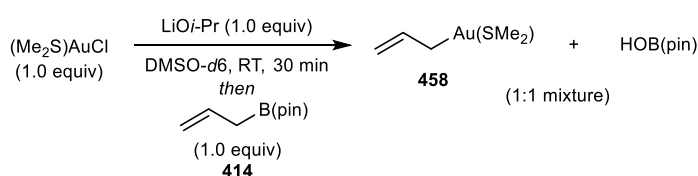
Figure 3: Annotated ^1H spectrum of reaction described in scheme 136b.

To investigate the equilibria between the σ -allylgold isomers as seen in Scheme 132, equimolar quantities of allyl pinacolboronate **418c**, LiOi-Pr, and $(\text{Me}_2\text{S})\text{AuCl}$ were mixed in DMSO-*d*6 (Scheme 137). This reaction produced a very complex crude ^1H NMR spectrum, with product identification proving extremely challenging due to the complex nature of the spectra. No significant conclusions could be drawn from this experiment.



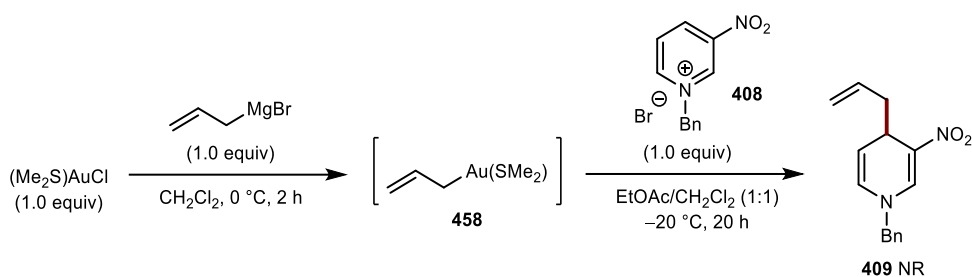
Scheme 137: Attempted observation of isomerisation.

An additional experiment was performed whereby equimolar quantities of LiOi-Pr and $(\text{Me}_2\text{S})\text{AuCl}$ were mixed in DMSO-*d*6 for 30 min in the absence of allyl pinacolboronate **414** (Scheme 138). The ^1H NMR spectrum was extremely complex, and no conclusions could be drawn concerning the equilibria between gold chloride, hydroxide, and isopropoxide intermediates. Subsequent addition of allyl pinacolboronate **414** led to identical results as seen previously (Scheme 136b), whereby, the formation of a 1:1 mixture of allylgold(I) species **458** and HOB(pin) was directly observed.



Scheme 138: Sequential addition to observe **458**.

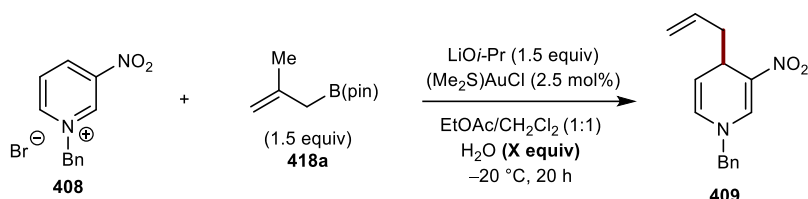
The delayed addition of azinium salt **408** to *in-situ* generated allylgold(I) species **458** was investigated (Scheme 139). Generation of allylgold(I) intermediate **458** via the addition of allylmagnesium bromide to $(\text{Me}_2\text{S})\text{AuCl}$,⁶⁰ followed by subsequent addition of azinium salt **408** did not produce the desired product. This lack of reactivity may be attributed to the instability of allylgold(I) species **458**. The remaining mass balance of the reaction was unreacted starting material **408**.



Scheme 139: *In-situ* formation of **409**.

Since we are suggesting HOB(pin) as a by-product after transmetalation between the allyl pinacolboronate and $(\text{Me}_2\text{S})\text{AuCl}$, we looked to investigate the effect of water on our reaction (Table 11). All previously mentioned reactions utilise solvents that were undried, obtained from commercial vendors and used without further purification. Utilising anhydrous solvents (entry 1) without the addition of water as an additive gave a drastic decrease in yield to 36%. Increasing the equivalents of water (entries 2 and 3) increased the yield, indicating the important role of water within our reaction. However, further increasing the equivalents of water (entries 4, 5 and 6), shut down reactivity due to the formation of an emulsion within our system

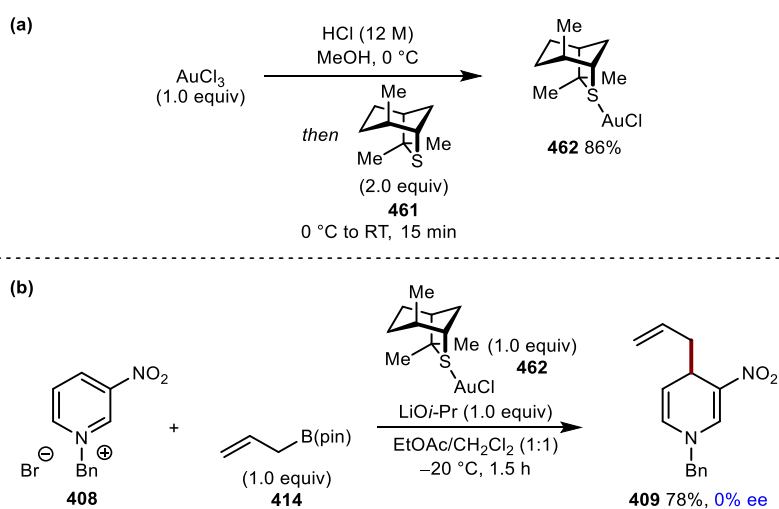
Table 11: Investigation of H₂O as an additive.



Entry	H ₂ O	Yield (%)
1	anhydrous solvents	36
2	0.2	66
3	0.5	51
4	1	42
5	2	11
6	5	10

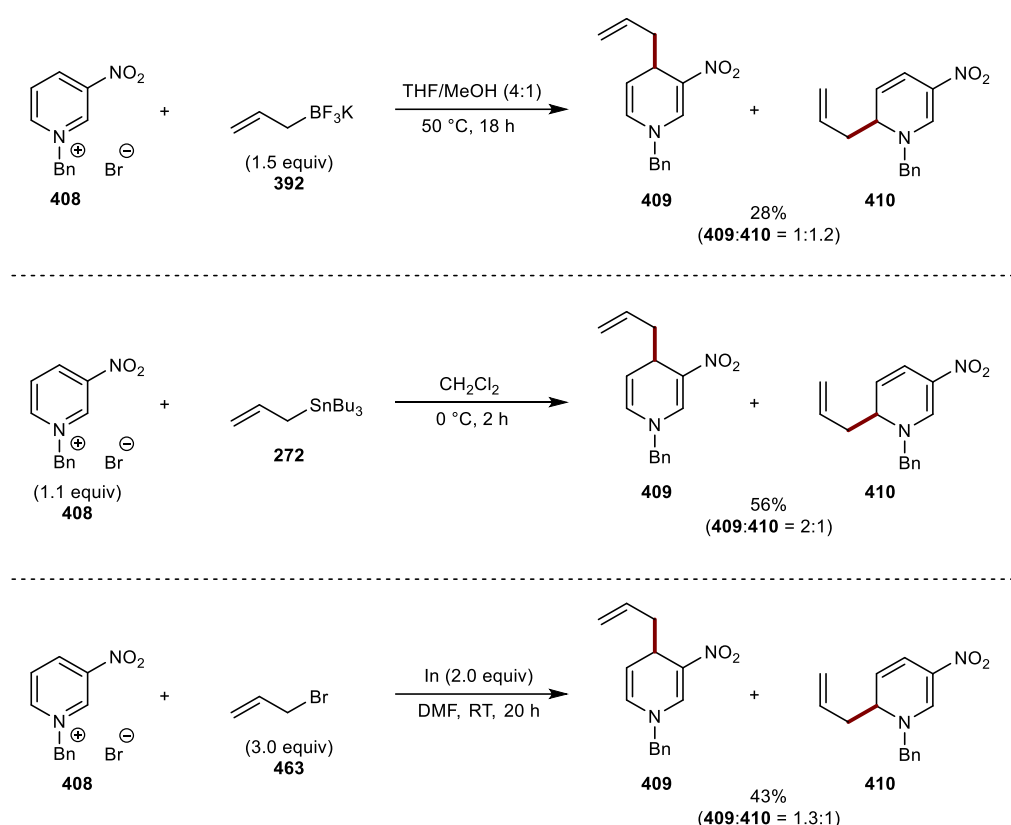
Reactions conducted with 0.1 mmol of **408**. Yields determined by ¹H NMR spectroscopy using 1,3,5-trimethoxybenzene as the internal standard.

To probe whether the dimethyl sulfide ligand of our gold catalyst was bound throughout the course of the reaction, gold catalyst **462** was synthesised as dissociation of ligand **461** could be observed by ¹H NMR spectroscopy (Scheme 140a). Subjecting one equivalent of catalyst **462** to our optimised reaction conditions gave the desired product **423a** in 78% yield and 0% ee (Scheme 140b). Upon analysis of the ¹H NMR spectrum, no un-bound ligand could be detected, suggesting no dissociation of the ligand.



Scheme 140: Evidence against ligand displacement.

To provide clarity on the role of gold with respect to regioselectivity within the reaction, several uncatalysed addition reactions were performed (Scheme 141). The addition of potassium allyltrifluoroborate gave the desired products in 28% yield as a 1:1.2 mixture of regioisomers, favouring the 6-allylated product. Allyltributylstannane and allylindium bromide gave increased formation of the desired products; however, poor regiocontrol was observed in both instances, favouring the 4-allylated product. These results suggest that a combination of both the C3-electron withdrawing group on the azinium ion and the gold metal centre are responsible for high regioselectivity.

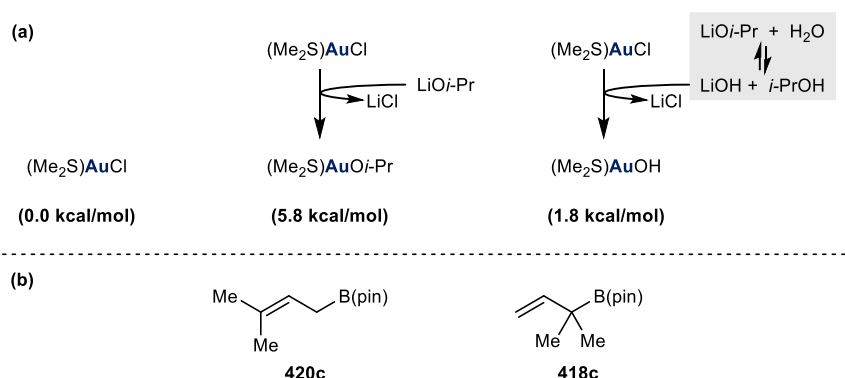


Scheme 141: Probing the effect of gold on regioselectivity.

To gain additional mechanistic insight, computational studies were performed at the PBE0¹⁷⁰/def2-TZVP^{171,172}/SMD-(CH₂Cl₂)¹⁷³ level by Dr. Kristaps Ermanis. All quantum mechanical calculations were carried out using Gaussian 16. All DFT structure optimisations and frequency calculations were done with the implicit SMD solvent model. The molecular geometries were optimised at the DFT level of theory using the PBE0 functional with the def2-TZVP basis set. Frequency calculations were performed on all structures and confirmed to contain no imaginary frequencies or just one imaginary frequency for ground states and transition states, respectively. The free energies were

corrected using quasi-harmonic approximation and corrections were done using the GoodVibes script.¹⁷⁴

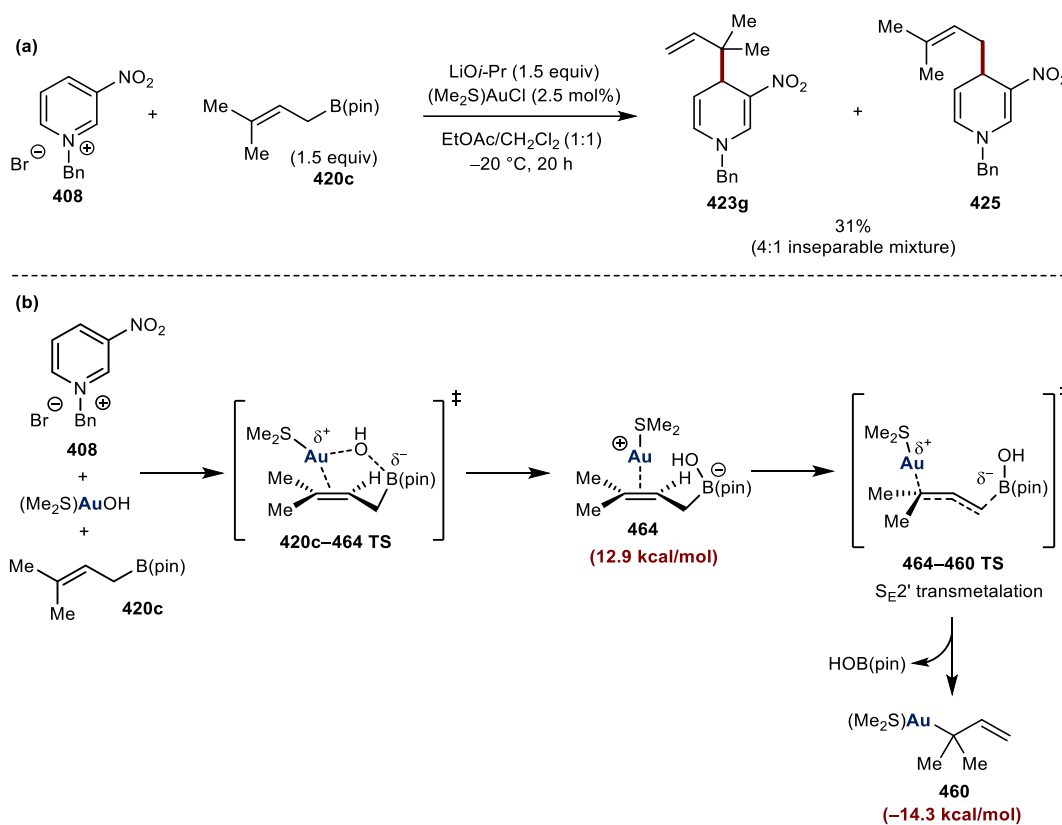
First, we investigated the structure of the active catalytic species within our reaction (Scheme 142a). Three catalytic species were considered: $(\text{Me}_2\text{S})\text{AuCl}$, $(\text{Me}_2\text{S})\text{AuO}i\text{-Pr}$ and $(\text{Me}_2\text{S})\text{AuOH}$. $(\text{Me}_2\text{S})\text{AuO}i\text{-Pr}$ is formed *via* ligand exchange between $(\text{Me}_2\text{S})\text{AuCl}$ and $\text{LiO}i\text{-Pr}$. As we take no precaution to exclude moisture or air from the reaction, LiOH may be present, formed by reaction of $\text{LiO}i\text{-Pr}$ with H_2O . Therefore, $(\text{Me}_2\text{S})\text{AuOH}$ may be formed by reaction with LiOH . The relative computational free energies of $(\text{Me}_2\text{S})\text{AuCl}$, $(\text{Me}_2\text{S})\text{AuO}i\text{-Pr}$ and $(\text{Me}_2\text{S})\text{AuOH}$ were calculated to be 0.0 kcal/mol, 5.8 kcal/mol, and 1.8 kcal/mol, respectively. This suggests $(\text{Me}_2\text{S})\text{AuO}i\text{-Pr}$ is not the active catalyst. As $(\text{Me}_2\text{S})\text{AuCl}$ is unable to catalyse the reaction itself (Table 3, entry 2), $(\text{Me}_2\text{S})\text{AuOH}$ is assumed to be the active catalyst for all further computational calculations. The reaction of both primary allyl pinacolboronate **420c** and tertiary allyl pinacolboronate **418c** (Scheme 142b) were investigated computationally to compare their transmetalation, interconversion between their σ -allylgold isomers and to gain an insight into the α : γ allylation regioselectivity of the reaction.



Scheme 142: Investigation of the active metal catalyst. Free energies are calculated at $\text{PBE0/def2-TZVP/SMD}-(\text{CH}_2\text{Cl}_2)$.

First, the reaction of primary allyl pinacolboronate **420c** was modelled computationally (Scheme 143a). Transmetalation was calculated to be most favourable *via* an $\text{S}_{\text{E}}2'$ mechanism (Scheme 143b). Transmetalation was found to occur through complex **464**, whereby, the alkene moiety of **420c** is coordinated to $[(\text{Me}_2\text{S})\text{Au}]^+$. Transition state **420c**–**464** gives rise to complex **464** *via* a *syn* pathway allowing for the facile transfer of the hydroxide ligand from the gold centre to the boron centre with minimal ion separation. Transmetalation can be completed *via* an $\text{S}_{\text{E}}2'$ mechanism from

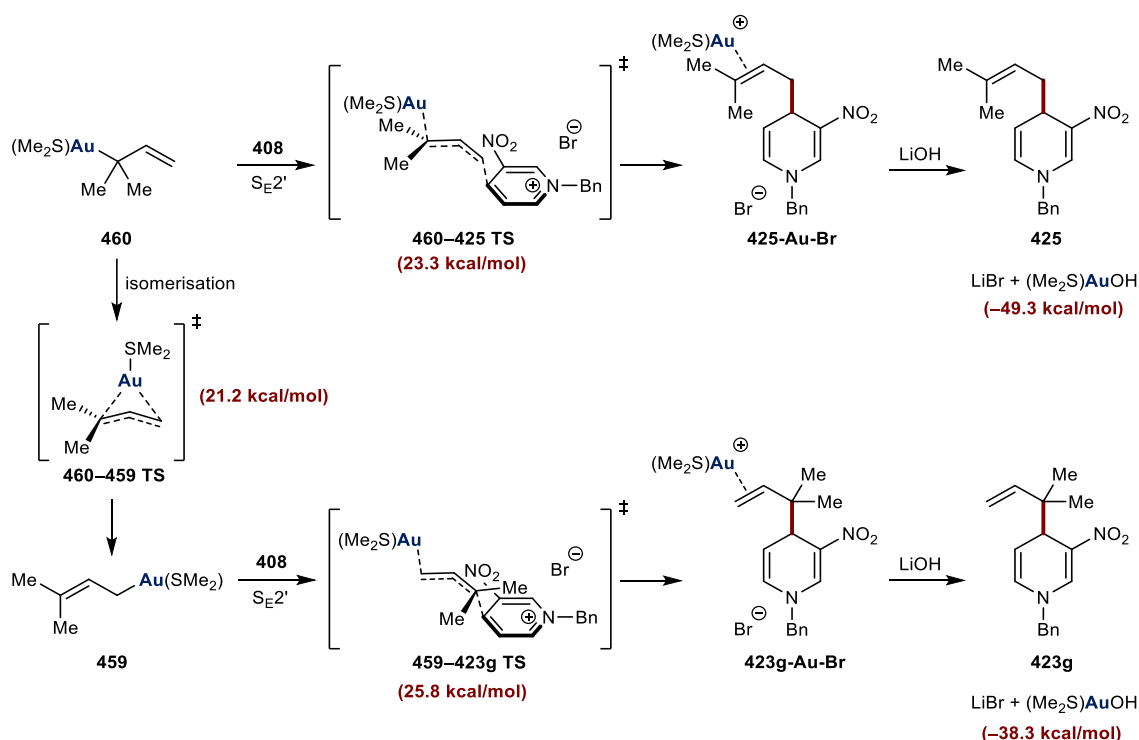
intermediate **464**, forming a carbon-gold bond, extruding HOB(pin) as a stoichiometric by-product. The formation of tertiary gold species **460** occurs through transition state **464–460** with a relatively low barrier of 17.9 kcal/mol with respect to the starting materials. Transmetalation is thermodynamically favourable.



Scheme 143: Modelling of transmetalation between $(\text{Me}_2\text{S})\text{AuOH}$ and **420c**.

From here (Scheme 144), tertiary gold species **460** can be intercepted by azinium salt **408** via an $\text{S}_{\text{E}}2'$ allylation to give intermediate **425-Au-Br**. This occurs via transition state **460–425** with a barrier of 23.3 kcal/mol. Liberation of gold-bound intermediate **425-Au-Br** with LiOH ensues, forming prenylated product **425**. However, this was the minor product observed experimentally (see Scheme 143a), with the reverse-prenylated isomer (**423g**) being the major product. This reverse-prenylated isomer may arise via the isomerisation of tertiary gold species **460**. This can occur through π -allylgold transition state **460–459** with a barrier of 21.2 kcal/mol, forming primary gold species **459**. This pathway was found to be 2.1 kcal/mol lower in energy than the competing $\text{S}_{\text{E}}2'$ nucleophilic allylation of tertiary gold species **460** and was determined to be thermodynamically favourable. Primary gold species **459** reacts with azinium salt **408** via a nucleophilic $\text{S}_{\text{E}}2'$ allylation. Liberation of gold-bound intermediate **423g-Au-Br**

with LiOH forms product **423g**. Independently, computational studies predicted the reverse-prenylated isomer (**423g**) as the major product which coincides with experimental findings.



A free-energy diagram (Figure 4) clearly represents the previously discussed information, showing that isomerisation (red line) is more favourable than the competing nucleophilic $S_{E2'}$ allylation (blue line) even though we are forming the less thermodynamically stable product ($\Delta G = -38.3$ kcal/mol for **423g** vs. $\Delta G = -49.3$ kcal/mol for **425**). The stabilities of primary and tertiary allylgold complexes seen within our calculations are consistent with a previous report by Hashmi and co-workers.¹⁷⁵

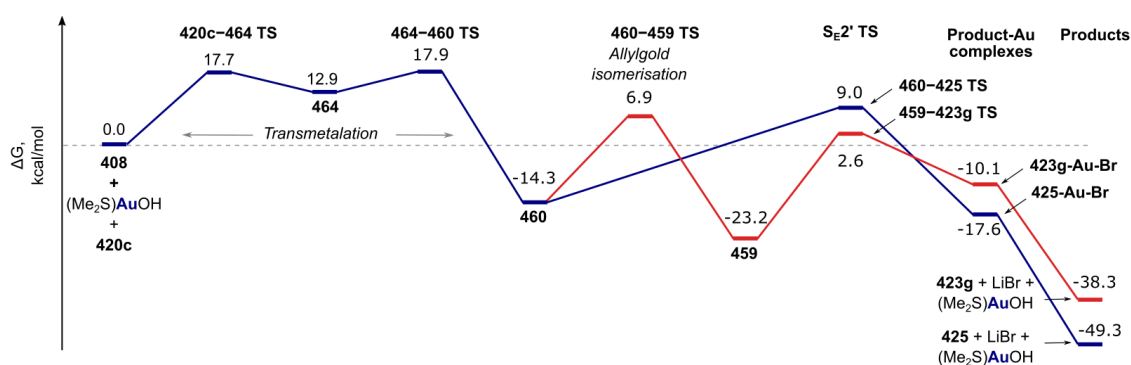
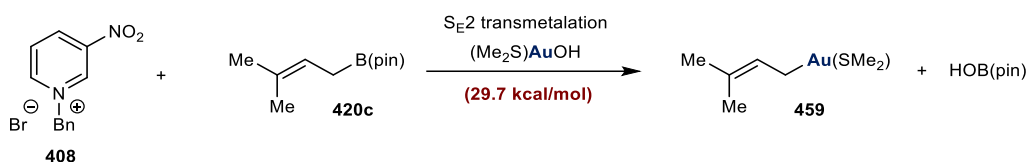


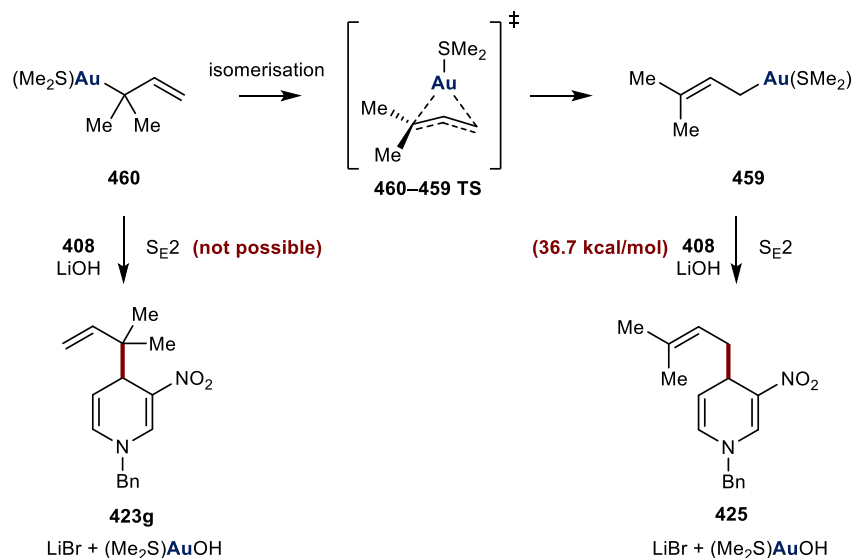
Figure 4: Free-energy plot for the reaction between **420c** and **408**. Free energies shown are relative to the starting materials and calculated at PBE0/def2-TZVP/SMD(CH₂Cl₂).

Additional mechanistic pathways were mapped computationally (Scheme 145). Direct S_{E2} transmetalation from allyl pinacolboronate **420c** was found to have a very high barrier of 29.7 kcal/mol in comparison to 17.7 kcal/mol for S_{E2}' transmetalation. Therefore, it is likely that this pathway is not operational within our reaction system.



Scheme 145: Computational modelling for direct S_{E2} transmetalation from **420c**. Free energies shown are relative to the starting materials and calculated at PBE0/def2-TZVP/SMD- (CH_2Cl_2) .

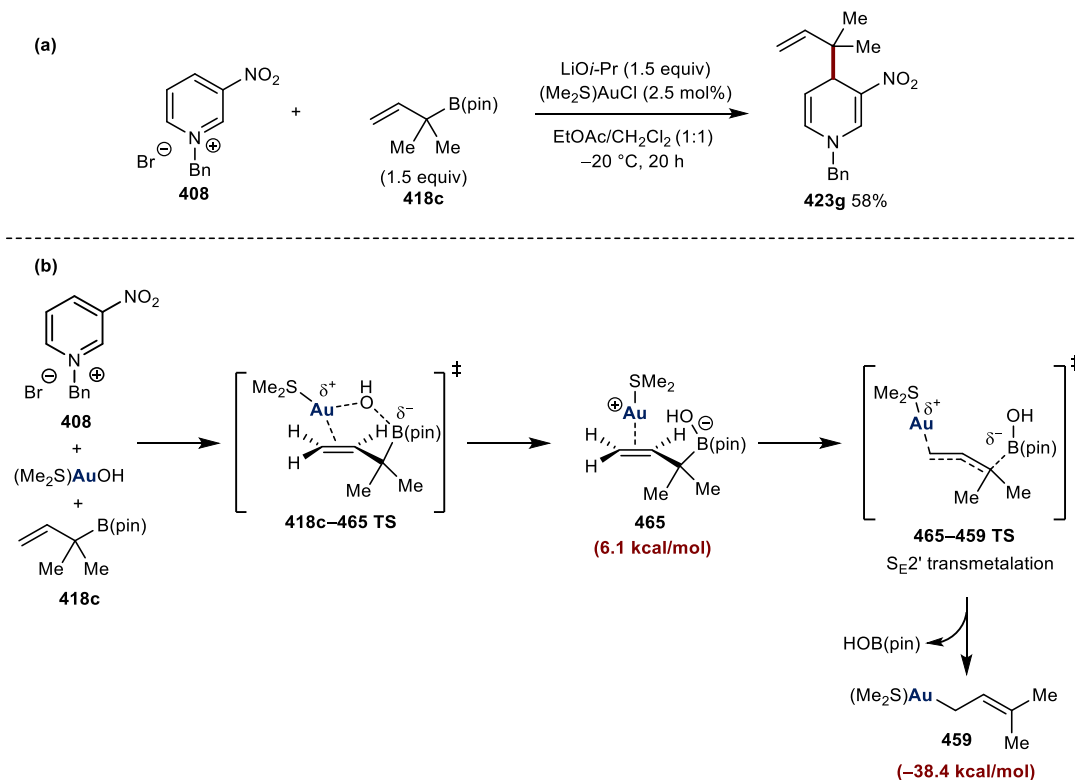
An alternative pathway for producing either reverse-prenylated product **423g** or prenylated product **425** via direct nucleophilic S_{E2} allylation from **460** or **459** respectively was investigated (Scheme 146). Direct nucleophilic S_{E2} allylation from tertiary gold species **460** was found to be impossible. Alternatively, the tertiary gold species isomerises upon approach towards the azinium salt to form primary allylgold species **459**. Direct nucleophilic S_{E2} allylation from primary gold species **459** was found to have a high barrier of 36.7 kcal/mol in comparison to 25.8 kcal/mol for nucleophilic S_{E2}' allylation. Therefore, nucleophilic S_{E2} allylation is not a productive pathway.



Scheme 146: Computational modelling for direct S_{E2} allylation. Free energies shown are relative to the starting materials and calculated at PBE0/def2-TZVP/SMD- (CH_2Cl_2) .

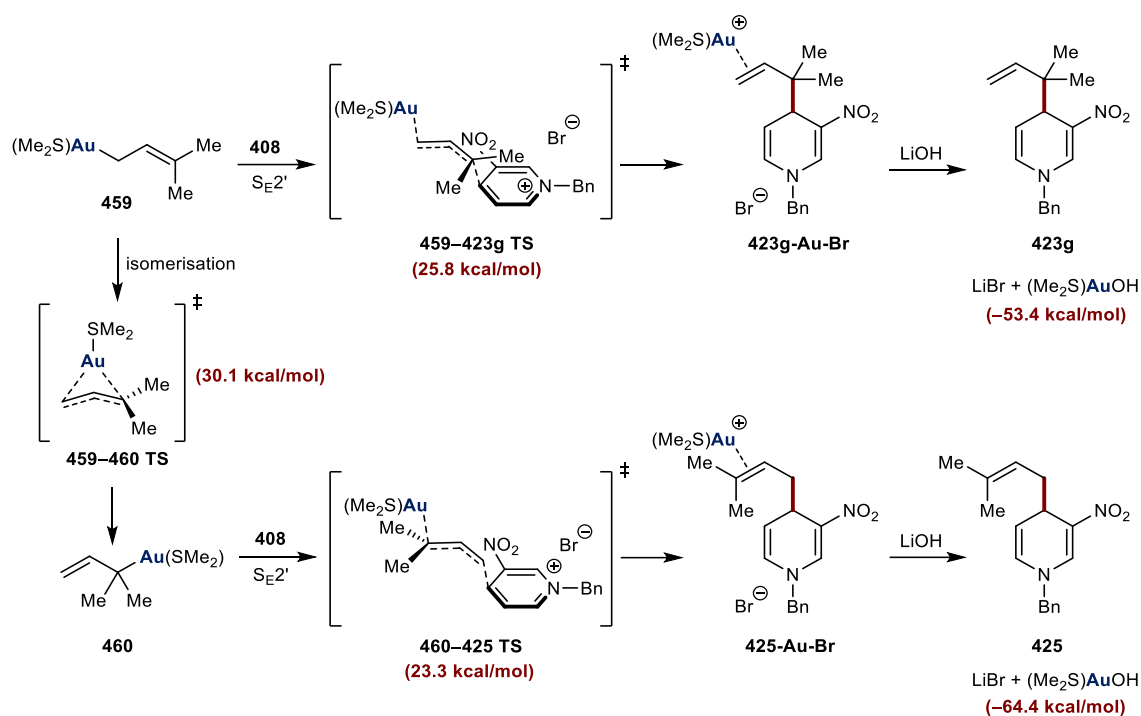
Next, we investigated tertiary allyl pinacolboronate **418c** computationally which gave the reverse-prenylated product **423g** exclusively (Scheme 147a). Transmetalation

via intermediate **465** was found to be thermodynamically favourable ($\Delta G = -38.4$ kcal/mol) (Scheme 147b). As seen previously (see Scheme 143), transmetalation occurs via an $S_{E2'}$ mechanism from intermediate **465**, forming a carbon-gold bond, extruding HOB(pin). There is a high thermodynamic driving force due to the formation of a more stable primary gold species relative to tertiary allyl pinacolboronate **418c**.



Scheme 147: Modelling of transmetalation between $(Me_2S)AuOH$ and **418c**.

From here (Scheme 148), primary gold species **459** can be coupled with azinium salt **408** via an $S_{E2'}$ allylation to give gold-bound intermediate **423g-Au-Br**. This occurs via transition state **459-423g** with a barrier of 25.8 kcal/mol. Liberation of gold-bound intermediate **423g-Au-Br** with LiOH ensues forming reverse-prenylated product **423g**. Isomerisation from **459** to **460** was found to be 4.3 kcal/mol higher in energy than the direct $S_{E2'}$ nucleophilic allylation of primary gold species **459**. Therefore, the production of the tertiary gold species **460** followed by nucleophilic $S_{E2'}$ allylation to give prenylated product **425** is much less feasible. Once again, both our experimental and computational studies are consistent since the computational study predicted the reverse-prenylated isomer exclusively.



Scheme 148: Modelling of the allylation between **418c** and **408**.

A free-energy diagram (Figure 5) clearly represents the previously discussed information, showing that isomerisation (red line) to the tertiary allylgold complex is less favourable than competing nucleophilic $S_{E2'}$ allylation (blue line) of the primary allylgold species.

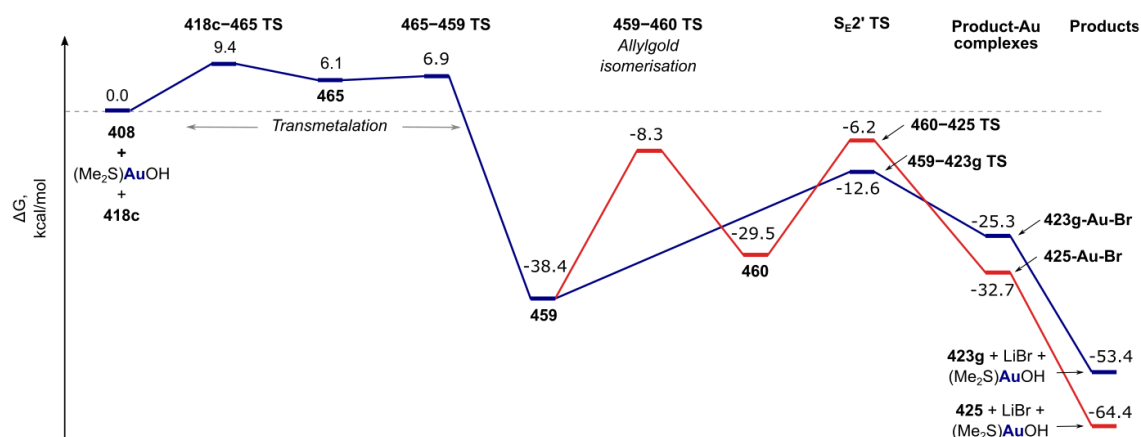


Figure 5: Free-energy plot for the reaction between **418c** and **408**. Free energies shown are relative to the starting materials and calculated at PBE0/def2-TZVP/SMD-(CH_2Cl_2).

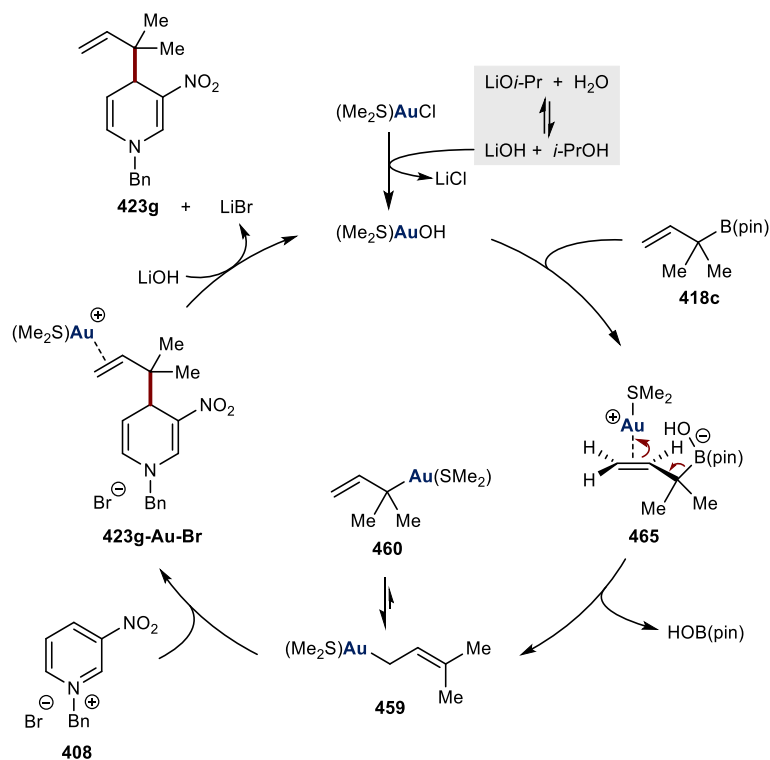
As seen in Scheme 149, direct S_{E2} transmetalation from tertiary allyl pinacolboronate **418c** was considered and found to be not possible due to steric hindrance surrounding the boron centre. Therefore, it is likely that this pathway is not operational. Moreover, direct nucleophilic S_{E2} allylation from primary gold species **459**

had a very high barrier of 36.7 kcal/mol in comparison to nucleophilic S_E2' allylation at 25.8 kcal/mol.



Scheme 149: Computational modelling for direct S_E2 transmetalation from **418c**. Free energies shown are relative to the starting materials and calculated at PBE0/def2-TZVP/SMD-(CH₂Cl₂).

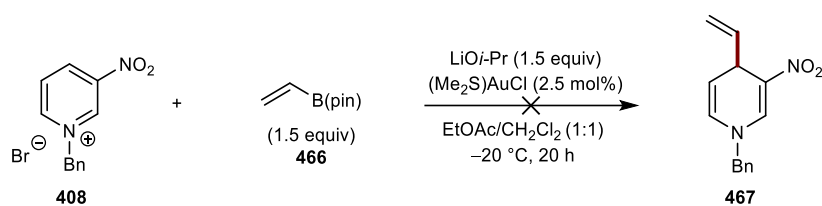
With all the previously discussed information, a catalytic cycle is proposed (Scheme 150). First, the reaction of Li*i*-Pr with H₂O yields LiOH, which in turn reacts with (Me₂S)AuCl to form (Me₂S)AuOH. Transmetalation with allyl pinacolboronate **418c** occurs through intermediate **465** via an S_E2' pathway generating primary allylgold intermediate **459**. Isomerisation to tertiary gold species **460** is unfavorable. Direct S_E2' nucleophilic allylation ensues producing gold-bound complex **423g-Au-Br**. Reaction with LiOH releases the desired product, regenerating the active gold catalyst and forming LiBr as a stoichiometric by-product.



Scheme 150: Proposed catalytic cycle.

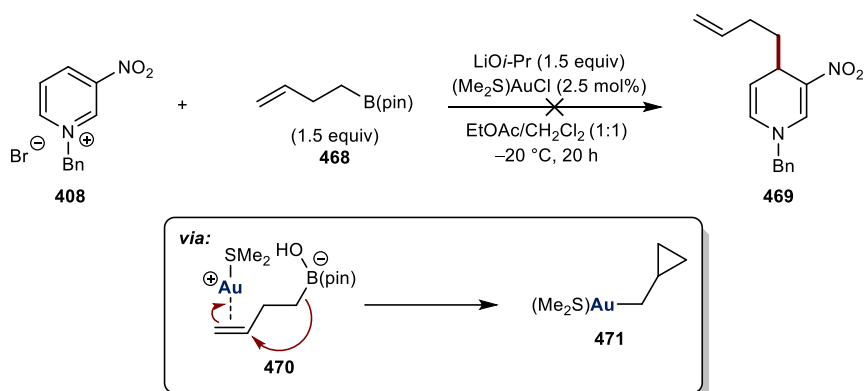
2.6 Extension to Other Nucleophiles

Having successfully developed the regioselective allylation of azinium ions with allyl pinacolboronates, we were curious to explore the viability of utilising alternative nucleophiles. Logically, we began with the alkenylation of azinium ions using vinyl pinacolboronate **466** (Scheme 151). However, upon subjecting this to our optimised reaction conditions, no product formation could be observed, with retention of unreacted starting material.



Scheme 151: Gold-catalysed alkenylation of 408 using 466.

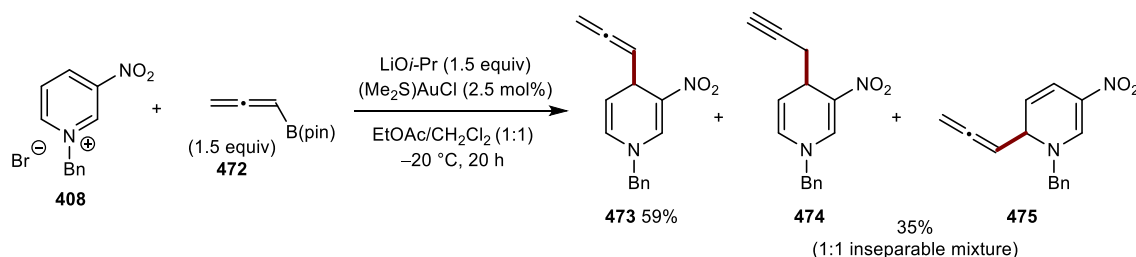
Next, the homoallylation of azinium ions was investigated (Scheme 152). We postulated accessing cyclopropyl gold species **471** via an S_E2' transmetalation as seen previously in Scheme 143. Unfortunately, the product of this reaction was not detected, with only starting material being observed within the crude ¹H NMR spectrum. A brief screening of the reaction conditions yielded no promising results; therefore, this was not explored further.



Scheme 152: Gold-catalysed homoallylation of 408 using 468.

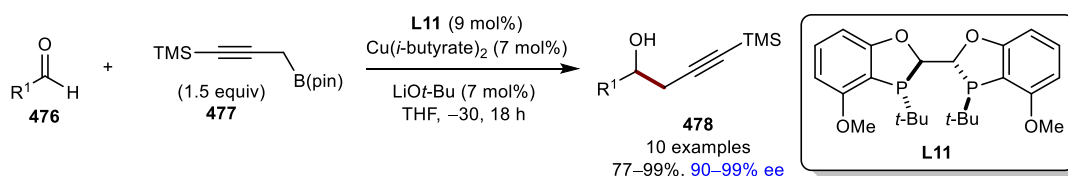
The addition of allenyl-derived nucleophiles to azinium ions has not been previously reported. As such, we sought to develop this area by subjecting allenyl pinacolboronate **472** to our reaction conditions (Scheme 153). Fortunately, the desired 4-allenylated

product **473** was isolated in 59% yield along with a 1:1 inseparable mixture of 4-propargylated product **474** and 6-allenylated product **475**. The observation of both allenylated (**473**) and propargylated (**474**) products suggests an isomerisation pathway post-transmetalation between both the σ -propargyl and σ -allenylgold(I) intermediates. To observe an unequal mixture of products suggests that, either one of the σ -gold isomers is more reactive, leading to the formation of a major product or the rate of isomerisation between the two σ -gold isomers is slower than that of nucleophilic addition.



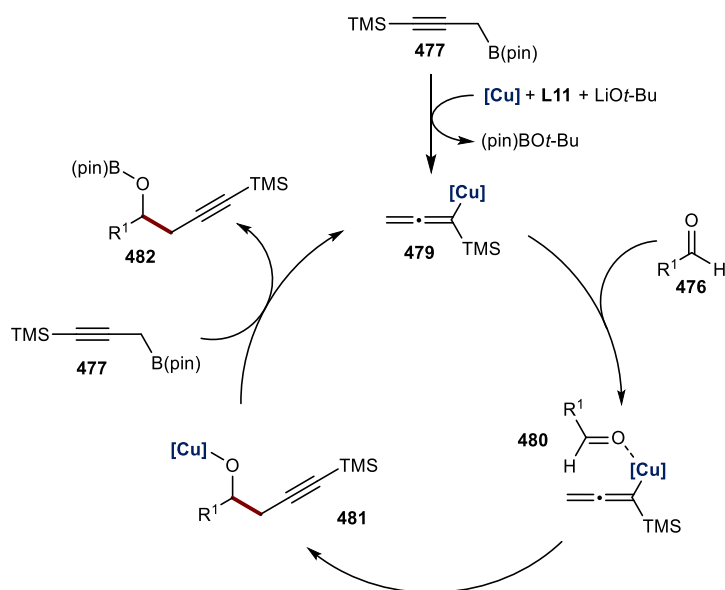
Scheme 153: Gold-catalysed allenylation of **408** using **472**.

Having observed the formation of **474** from allenyl pinacolboronate, we considered whether the direct propargylation of azinium ions would be feasible. In 2010, Fandrick and co-workers reported the enantioselective copper-catalysed propargylation of aldehydes, generating the desired alcohols in excellent yields and enantioselectivities (Scheme 154).¹⁷⁶ The reaction utilises propargyl pinacolboronate **477** and has been further extended to include both ketones and aldimines.^{177,178}



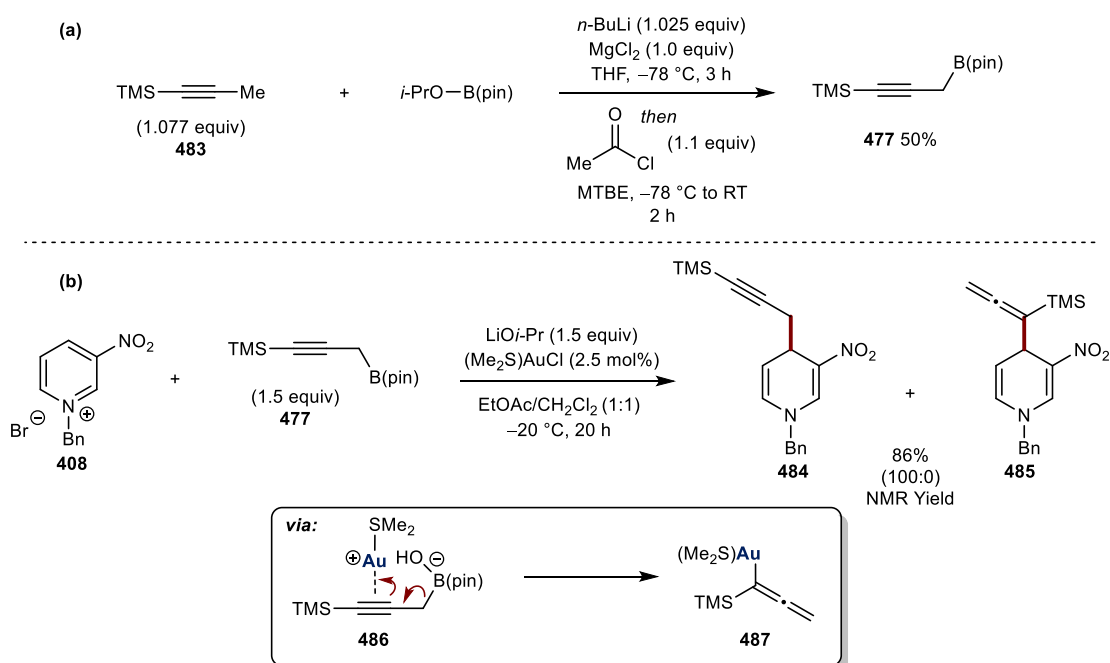
Scheme 154: Copper-catalysed enantioselective propargylation of **476** using **477**.

The proposed mechanism is initiated *via* transmetalation of propargyl pinacolboronate **477** with the copper catalyst, assisted by LiOt-Bu , forming allenyl copper intermediate **479** (Scheme 155). Coordination of aldehyde **476** ensues, affording species **480**, followed by subsequent propargylation yielding copper alkoxide species **481**. Transmetalation between species **481** and propargyl pinacolboronate **477** regenerates the active allenyl copper intermediate and yields the desired product after work-up.



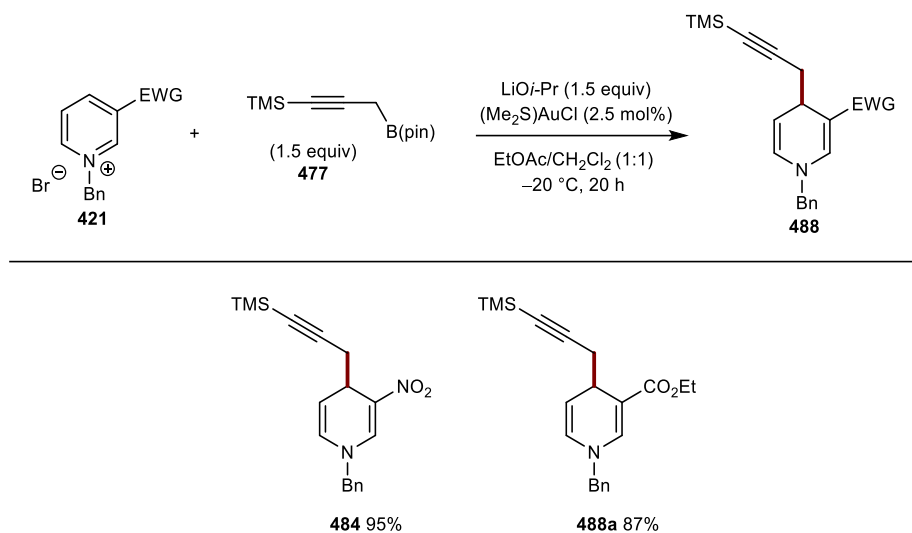
Scheme 155: Proposed mechanism for the formation of **482**.

Considering this precedent, we synthesised propargyl pinacolboronate **477** (Scheme 156a). Upon subjecting this coupling partner to our reaction conditions, we were pleased to observe an 86% ^1H NMR yield of 4-propargylated product **484** and none of the allenylated product **485** (Scheme 156b). We propose the reaction occurs *via* the formation of allenyl gold species **487** through a $\text{S}_{\text{E}}2'$ transmetalation mechanism.



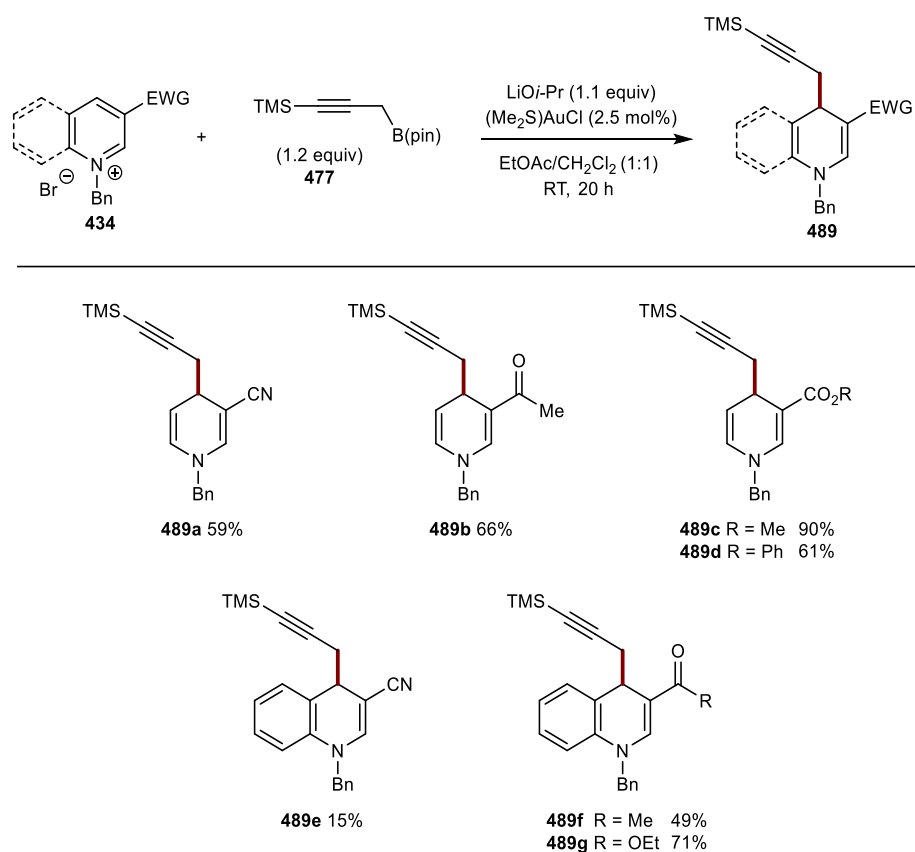
Scheme 156: Gold-catalysed propargylation of **408** using **477**. Yield determined by ^1H NMR spectroscopy 1,3,5-trimethoxybenzene as the internal standard.

A small preliminary scope of the reaction with respect to the azinium salt was examined (Scheme 157). In both reported examples (**484** and **488a**), complete regiocontrol was observed, propargylating exclusively at the 4-position of the azinium salt. Azinium salts containing either a nitro (**484**) or ester (**488a**) substituent were well tolerated.



Scheme 157: Azinium salt scope. Reactions conducted on 0.5 mmol scale. Isolated yields.

The optimisation and scope of the propargylation reaction was further examined within our group by Jack Smithson (Scheme 158). The equivalents of both LiO*i*-Pr and propargyl pinacolboronate **477** could be lowered without any significant loss in yield. Furthermore, the reaction could be performed at room temperature without any loss in regiocontrol. *N*-Benzyl azinium salts containing various electron-withdrawing groups at the 3-position, such as cyano (**489a**), acetyl (**489b**) and a variety of esters (**489c–489d**) were well tolerated. Pleasingly, a range of *N*-benzylquinolinium salts also reacted efficiently to give 1,4-dihydroquinolines **489e–489g** in 15–71% yield; these substrates contained a cyano (**489e**), acetyl (**489f**), and ester (**489g**) group at the 3-position. Further attempts to expand the substrate scope are ongoing.



Scheme 158: Azinium salt scope. Reactions conducted on 0.5 mmol scale. Isolated yields. All reactions performed by J. Smithson.

2.7 Development Towards an Enantioselective Variant

Following our investigations towards a racemic gold-catalysed regioselective allylation of azinium ions, we were interested in whether an enantioselective variant would be feasible. Asymmetric gold(I) catalysis is extremely challenging due to the linear coordination favoured by gold(I) catalysts (Figure 6a).¹⁷⁹ This linear geometry places the chiral ligand and substrate on opposite sides of the gold metal centre. Moreover, both the substrate bond and the chiral ligand bond to the gold catalyst are free to rotate. As discussed previously, our reaction system adopts a linear transition state with regards to the C-C bond forming step. Consequently, the chiral inducing environment is distant from this event, rendering an enantioselective variant challenging.

Nevertheless, there are four main strategies for rendering gold(I) catalysis enantioselective (Figure 6b). Two of the most widely utilised strategies involve either bimetallic gold complexes in conjunction with asymmetric bis-phosphine based ligands

or monodentate chiral phosphoramidites. Both strategies use commercially available ligands with tuneable steric and electronic properties. More recently, chiral NHC based ligands and chiral counteranions have emerged as potential alternatives to govern enantioselectivity within gold(I)-catalysed reactions.

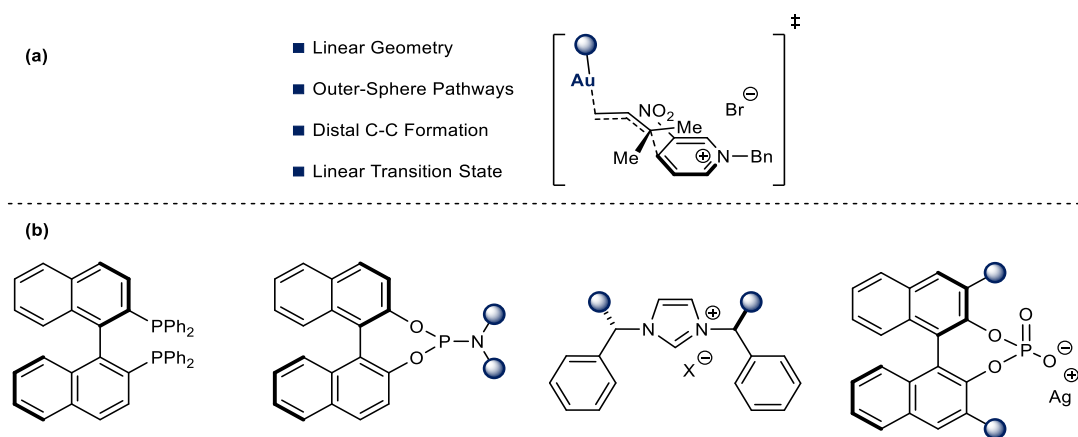
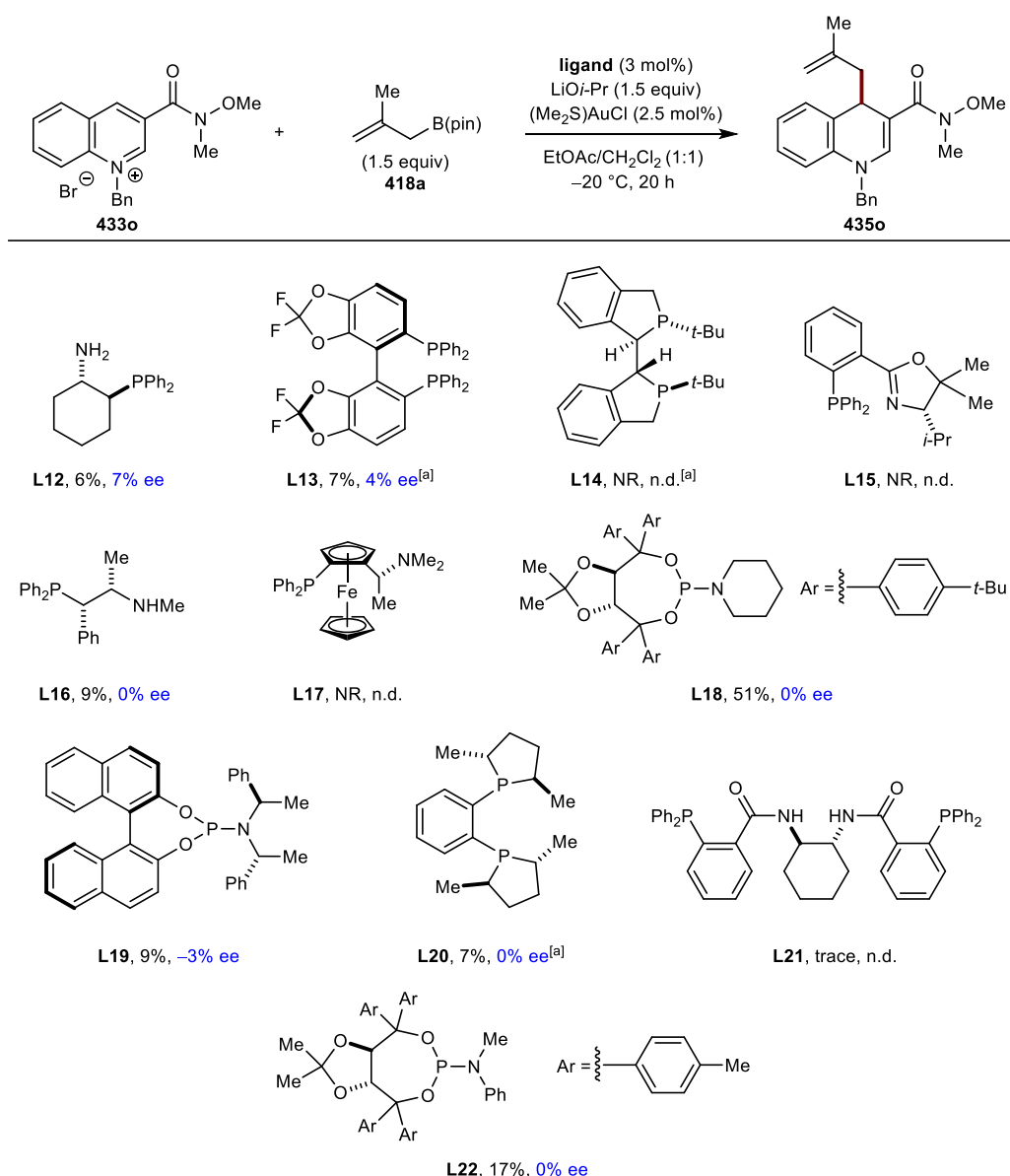


Figure 6: Challenges with rendering the reaction enantioselective and typical ligand classes for governing enantioselectivity using gold(I) catalysts.

We began our investigation with a ligand screen (Table 12). Regrettably, when subjecting both mono-phosphine (**L12**, **L15**, **L16**, and **L17**) and bis-phosphine (**L13**, **L14**, **L20** and **L21**) ligands to our reaction conditions, no enantioselectivity was observed. Phosphoramidite-derived ligands (**L18**, **L19** and **L22**) generated the desired product in poor yields and very poor enantioselectivity. For all screening reactions mentioned, regioselectivity with respect to the azinium salt remained high. A further sixty examples of enantiopure chiral ligands were evaluated; however, they all gave similar results as seen in Table 12. To investigate whether the poor enantioselectivities were due to substrate **433o**, several alternative azinium salts were subjected to identical reaction conditions with no improvement to enantioselectivity.

Table 12: Ligand screening using 433o.

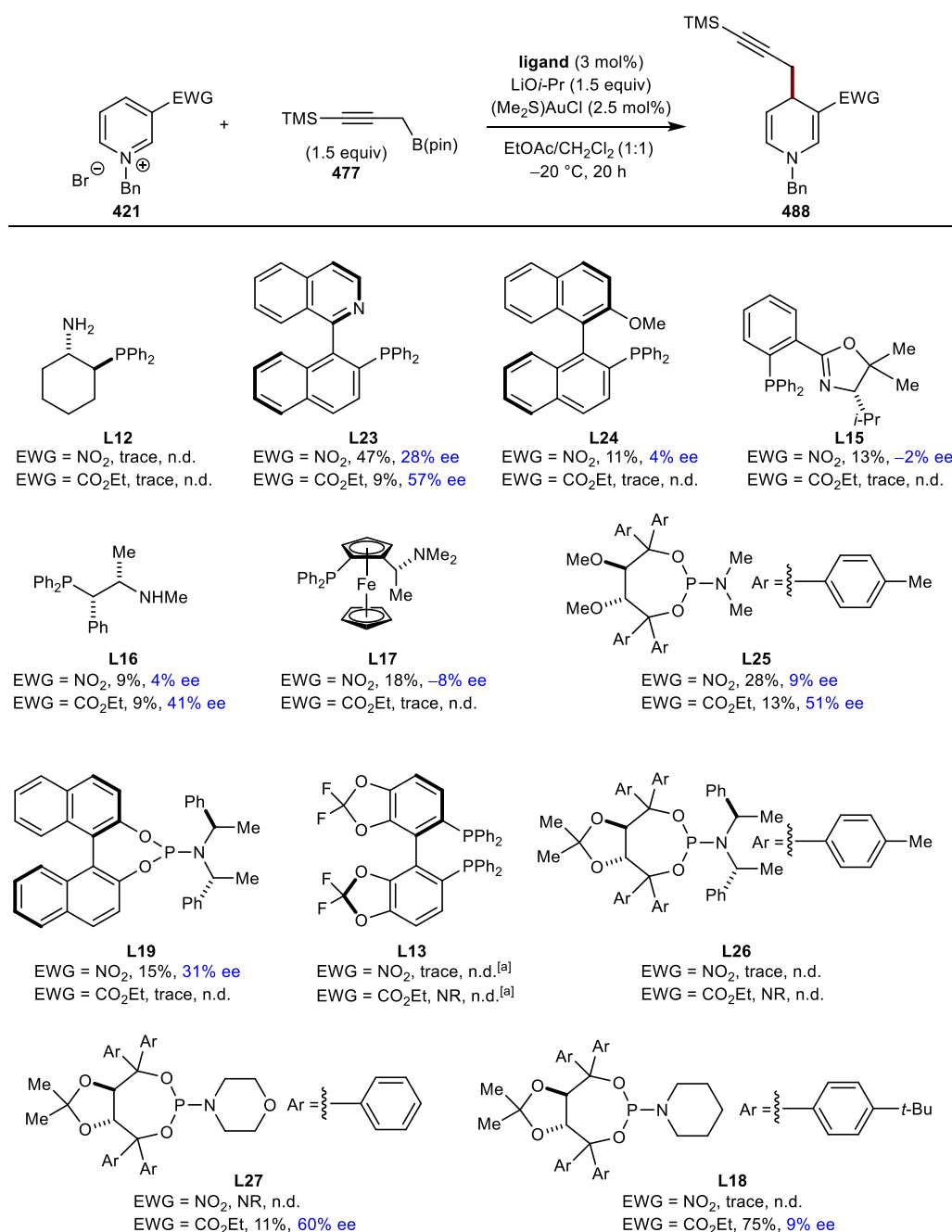


Yields determined by ¹H NMR spectroscopy using 1,3,5-trimethoxybenzene the internal standard. Reactions conducted using 0.1 mmol of **433o**. [a] (Me₂S)AuCl (5 mol%).

Having demonstrated the successful propargylation of azinium salts (see Scheme 158), we were interested in developing an enantioselective variant. Due to the proposed formation of an allenyl intermediate, we hypothesised that this may be more influenced by chiral ligands, allowing for greater enantiocontrol in comparison to the allylation reaction. We began our investigation with a ligand screen (Table 13). Pleasingly moderate to good enantioselectivities were observed, albeit with a significant reduction in product formation. *N*-Benzylpyridinium bromide containing a nitro substituent gave higher yields due to its increased electrophilicity, while *N*-benzylpyridinium bromides containing an ester substituent gave higher enantioselectivities. Several classes of

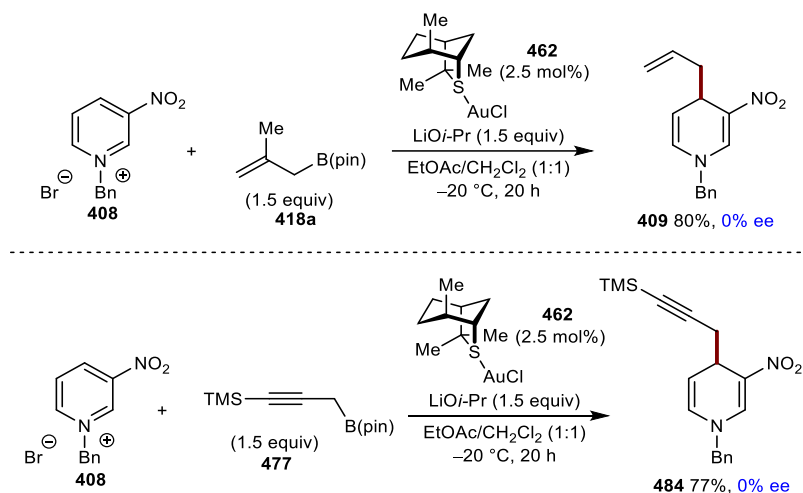
privileged ligands were examined, including mono-phosphines (**L12**, **L23**, **L24**, **L15**, **L16** and **L17**), bis-phosphines (**L13**) and phosphoramidites (**L25**, **L19**, **L26** and **L27**). QUINAP (**L23**) gave the best combination of both yield and enantioselectivity. A further sixty examples of privileged ligands were evaluated; however, they all gave inferior results as compared to QUINAP (**L23**). As a result, we began to optimise our reaction using QUINAP as the chiral ligand; however, any deviations from the standard conditions shown in Table 13 gave poorer results.

Table 13: Ligand screening using 421.



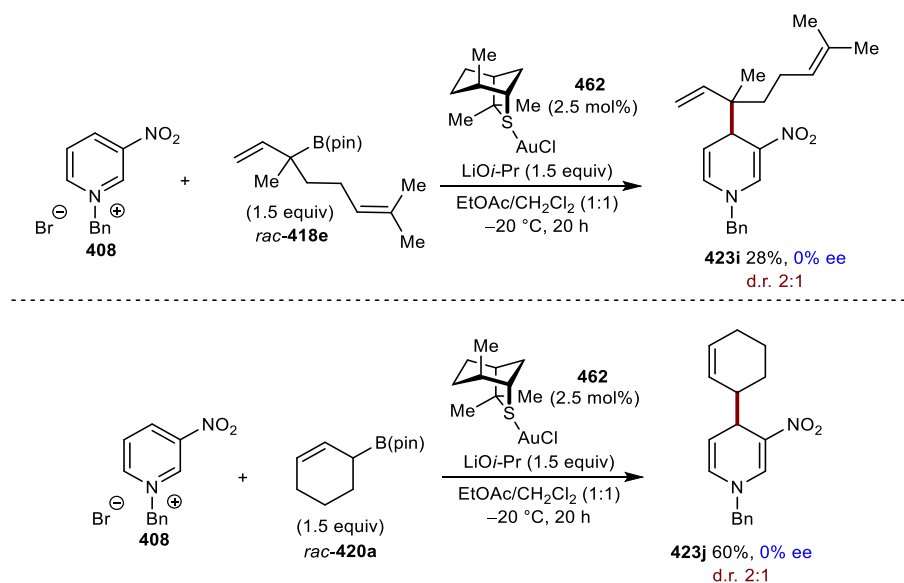
Yields determined by ¹H NMR spectroscopy using 1,3,5-trimethoxybenzene the internal standard. Reactions conducted using 0.1 mmol of **421**. [a] (Me₂S)AuCl (5 mol%).

Due to the limited success when utilising phosphorus containing ligands, we turned our attention towards sulfur-containing ligands as the racemic reaction utilises $(\text{Me}_2\text{S})\text{AuCl}$ as the catalyst. Asymmetric alternatives to $(\text{Me}_2\text{S})\text{AuCl}$ may generate the desired products with greater enantiocontrol. Asymmetric sulfur ligands have been utilised for enantioselective catalysis extensively.^{180–182} Sulfur is considered soft and can have strong interactions with soft metals such as copper, palladium and gold. In comparison to phosphine containing ligands, sulfur derivatives are inferior σ -donor and π -acceptors.¹⁸² However, sulfur-containing ligands are widely available from either chiral pools or direct modification of other heteroaromatic ligands. We began by synthesising gold catalyst **462** (Scheme 159). Subjecting this catalyst to our reaction conditions generated the desired product **409** in good yield and regioselectivity, but the product was racemic. Near identical reactivity was observed when utilising propargyl pinacolboronate **477** as the nucleophilic partner. However, we were encouraged by these results due to significant increases in yield as compared to phosphine containing ligands.



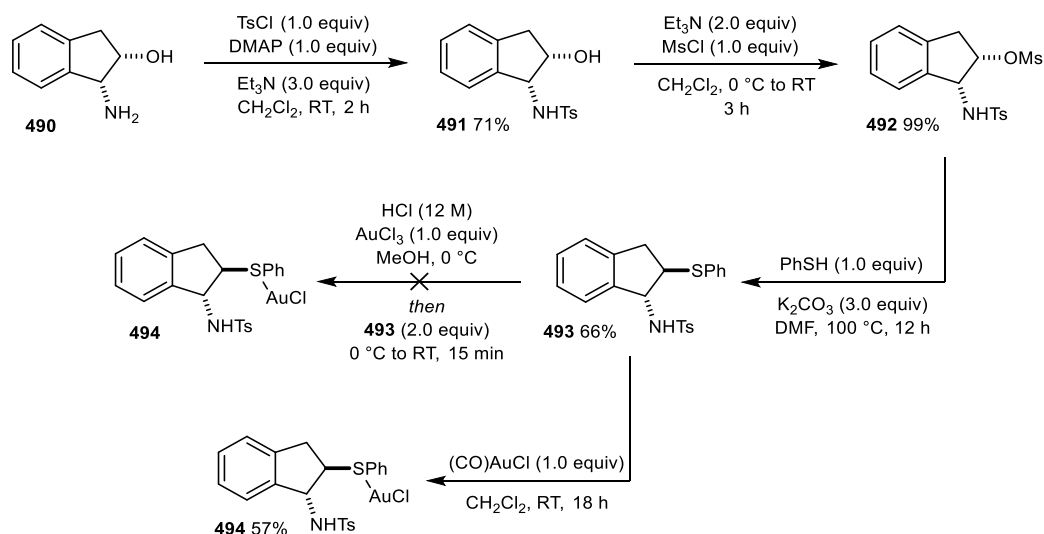
Scheme 159: Investigating catalyst **462** for generating enantioenriched products.

We hypothesised that increasing the steric bulk surrounding the pinacolboronate may increase enantiocontrol within the reaction. Therefore, we subjected both geranyl-bromide-derived α,α -disubstituted allyl pinacolboronate *rac*-**418e** and cyclohexenyl allyl pinacolboronate *rac*-**420a** to the reaction conditions using gold catalyst **462** (Scheme 160). Unfortunately, no enantiocontrol was observed nor any significant increase in diastereocontrol.



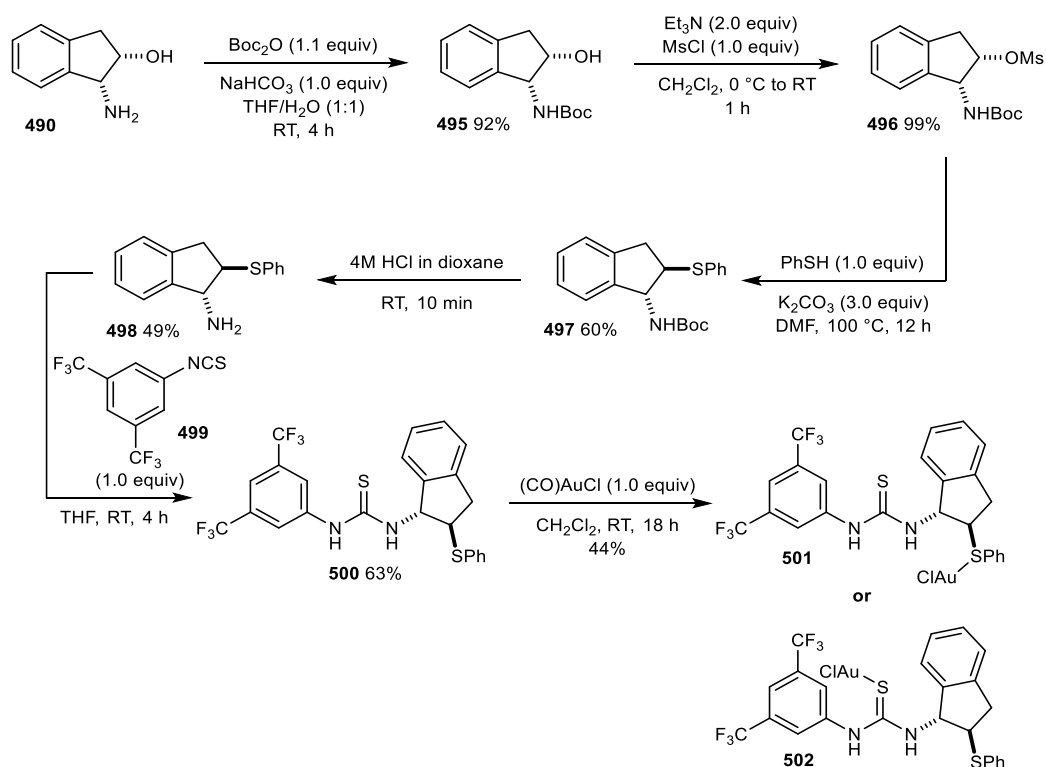
Scheme 160: Increasing steric bulk for generating enantioenriched products.

Next, we began to synthesise alternative sulfur-containing ligand scaffolds from commercially available chiral pools. The Zhao group have utilised ligand **493** (Scheme 161) for various enantioselective cyclisation cascade reactions.^{183,184} A modified synthetic route gave access to the desired ligand in four steps. First, *N*-tosyl protection of amino alcohol **490** followed by *O*-mesyl protection afforded product **492**. S_N2 displacement using thiophenol yields compound **493**. Treatment under acidic conditions with $AuCl_3$ did not yield the corresponding gold complex **494** due to solubility issues with regards to ligand **493** in methanol. Fortunately, treatment with $(CO)AuCl$ followed by precipitation gave the desired gold complex in 57% yield.



Scheme 161: Synthesis of **494**.

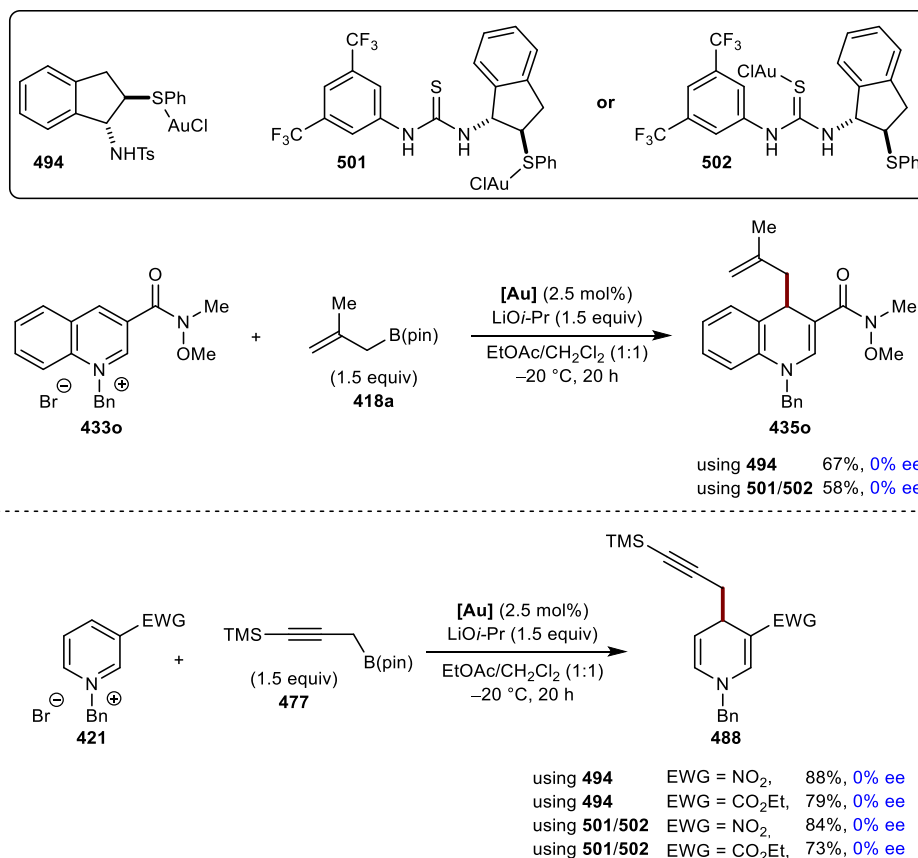
We sought to incorporate an additional binding mode using the same scaffold as seen in Scheme 161 to restrict conformational changes and enhance rigidity within the reaction transition state. The Jacobsen group have shown that electron-deficient thioureas can promote regio- and enantiocontrol *via* the formation of multiple hydrogen bonds.^{185–188} We hypothesise that ligands bearing an electron-deficient thiourea may coordinate to the anion of the azinium salt, inducing an asymmetric environment within the reaction system. Our synthesis began (Scheme 162) with the *N*-Boc protection of amino alcohol **490**, followed by mesylation of the alcohol affording product **496**. S_N2 displacement using thiophenol yields compound **497**. Boc deprotection under acidic conditions followed by subsequent addition of isothiocyanate **499** generated the desired ligand **500**. Treatment with (CO)AuCl followed by precipitation gave the desired gold complex. However, the exact position of the gold metal centre within the complex could not be identified (**501** or **502**). Furthermore, any attempts to perform X-ray crystallography *via* the growth of a single crystal were unsuccessful. An alternative route involving an electron-deficient urea would circumvent this problem.



Scheme 162: Synthesis of **501** or **502**. All reactions performed by H. Green.

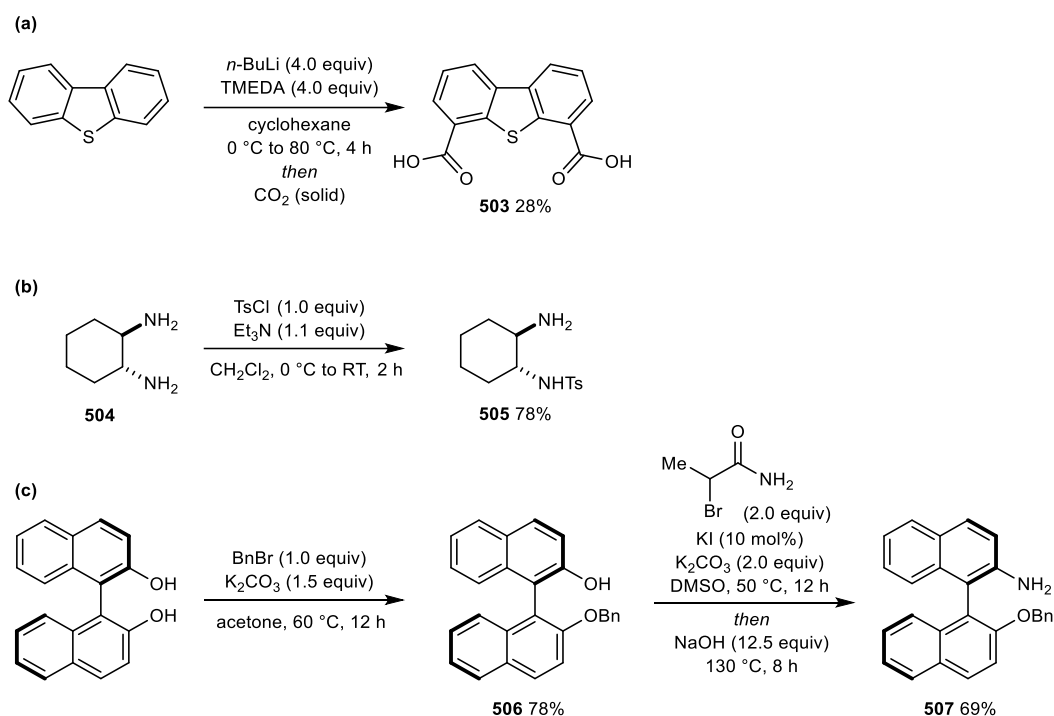
Unfortunately, when replacing (Me₂S)AuCl with sulfur-containing ligand **494** in both our allylation and propargylation reaction (Scheme 163), no enantioselectivity was

observed. Furthermore, ligand **501/502** gave similar results, forming the desired product in modest to good yields but as a racemate. Evaluation of various reaction conditions gave no improvement to yield nor enantioselectivity.



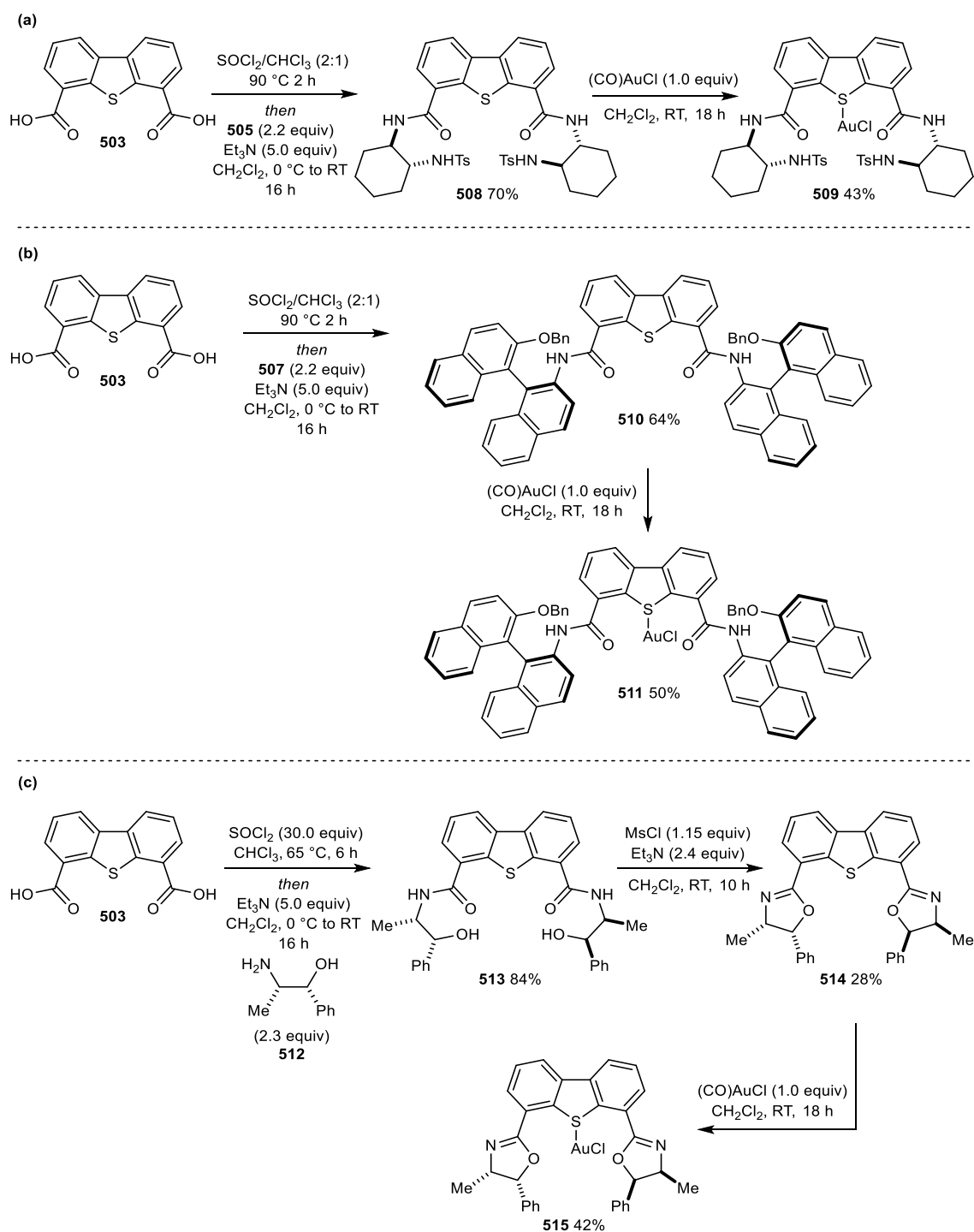
Scheme 163: Evaluation of ligands **494** and **501/502**.

Our second iteration of ligand design focussed on significantly increasing the steric bulk surrounding the gold metal centre by utilising a C₂-symmetric scaffold. Dibenzothiophene as a core scaffold has been utilised in asymmetric catalysis,¹⁸⁹ in particular palladium-catalysed allylic substitutions. This scaffold is easily derivatised, with chirality being introduced by coupling chiral auxiliaries adjacent to the sulfur centre, giving access to a diverse range of C₂-symmetric ligands. Our synthetic route began with the synthesis of each core component of the ligand structure (Scheme 164). First, commercially available dibenzothiophene was bislithiated and quenched with CO₂ forming dicarboxylic acid **503** (Scheme 164a). Chiral auxiliary **505** was prepared by mono *N*-tosyl protection of diamine **504** (Scheme 164b). Finally, chiral auxiliary **507** was prepared in two steps *via* a mono *O*-benzyl protection/Smiles rearrangement sequence (Scheme 164c).



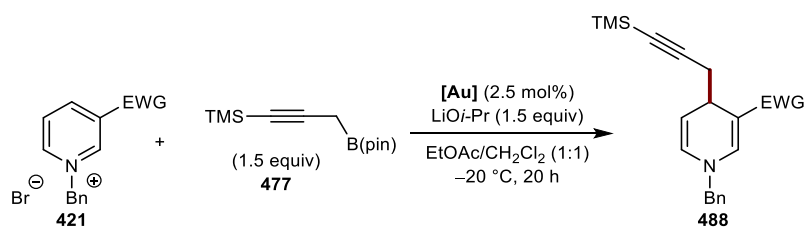
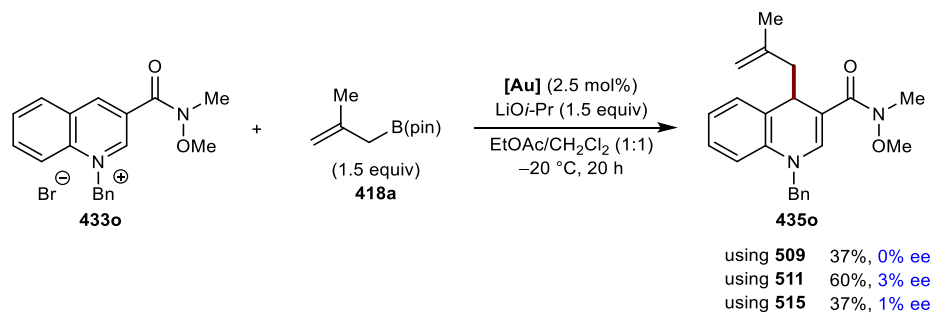
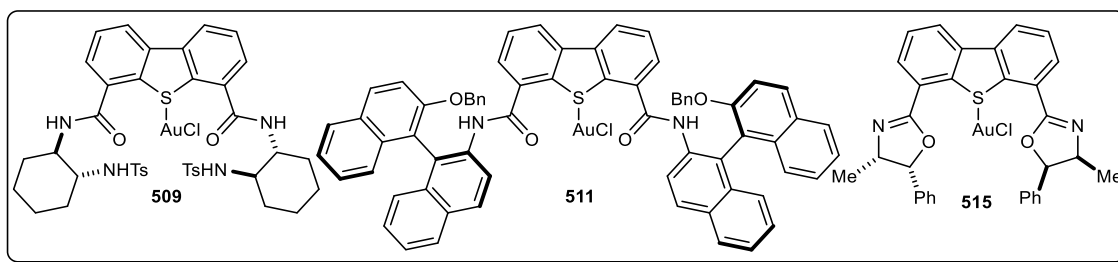
Scheme 164: Synthesis of ligand fragments **503**, **505** and **507**. Synthesis of **503** was performed by H. Green.

The final ligands could be assembled *via* the formation of an acid chloride from **503** followed by quenching with the appropriate chiral amine precursor (Scheme 165). Coupling of dicarboxylic acid **503** and **505** gave ligand **508** in 70% yield, followed by treatment with (CO)AuCl affording the desired gold complex **509** (Scheme 165a). An analogous procedure was utilised for the formation of gold complex **511** (Scheme 165b). Finally, gold complex **515** (Scheme 165c) was prepared *via* a three-step procedure. First, amide formation by coupling of amino alcohol **512** with dicarboxylic acid **503** using thionyl chloride. Mesylation of the alcohol and subsequent dehydrative cyclisation generates oxazoline **514**. Complexation using (CO)AuCl gave the desired product in 42% yield.



Scheme 165: Synthesis of ligands **509**, **511** and **515**. All reactions for the synthesis of **515** were performed by H. Green.

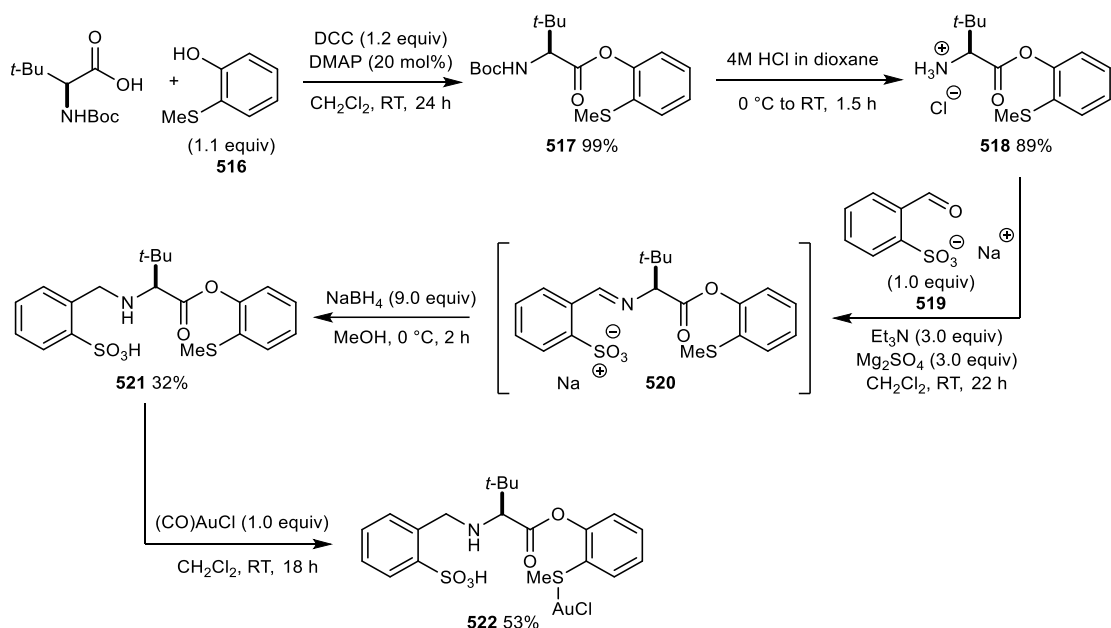
Unfortunately, when replacing $(\text{Me}_2\text{S})\text{AuCl}$ with our C2-symmetric sulfur analogues **509**, **511** and **515** in both our allylation and propargylation reaction (Scheme 166), little to no enantioselectivity was observed. Once again, optimisation of various reaction parameters gave no improvement to enantioselectivity.



using 509	EWG = NO ₂ ,	94%	0% ee
using 509	EWG = CO ₂ Et,	79%	4% ee
using 511	EWG = NO ₂ ,	69%	0% ee
using 511	EWG = CO ₂ Et,	56%	0% ee
using 515	EWG = NO ₂ ,	84%	2% ee
using 515	EWG = CO ₂ Et,	58%	0% ee

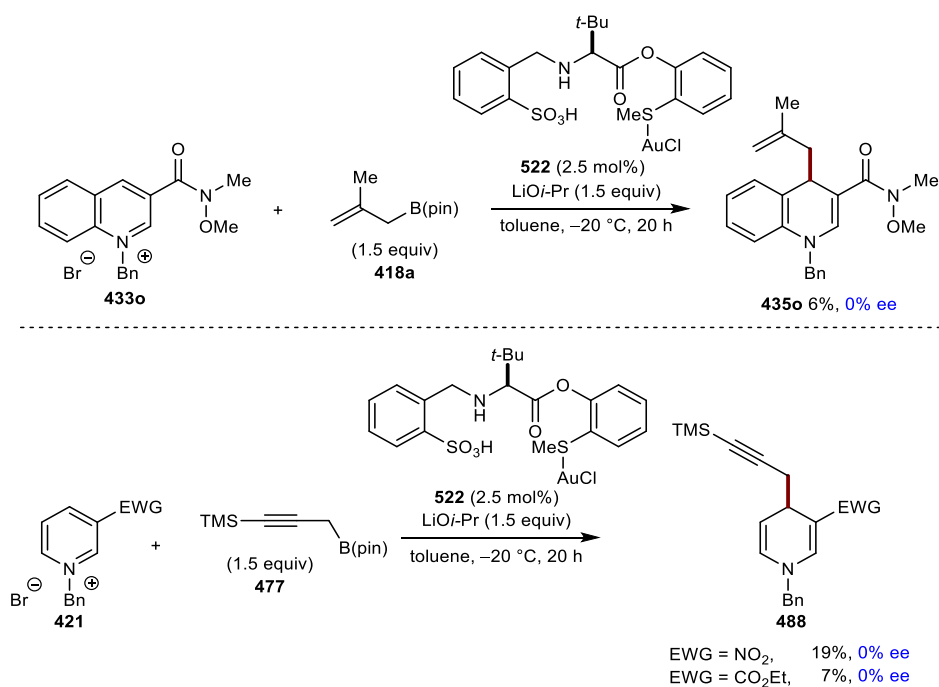
Scheme 166: Evaluation of ligands **509**, **511** and **515**.

Our final attempt to render these reactions enantioselective involves exploiting the low solubility of azinium salts in apolar organic solvents, an asymmetric phase-transfer catalytic approach.^{190,191} This approach has been utilised previously in conjunction with azinium salts forming the desired products in high yields and enantioselectivities.¹³⁶ This methodology utilises a coordinating anionic catalyst, whereby specific interactions towards the cationic azinium ion may allow a phase transfer to occur, transferring the previously insoluble azinium ion into the organic phase where reactivity can occur. By incorporating an asymmetric fragment within this catalyst, the reaction may be rendered enantioselective. Our synthetic route began with the coupling of Boc-Tle-OH with alcohol **516**, affording product **517** (Scheme 167). Boc deprotection followed by condensation with aldehyde **519** and subsequent reduction gave the desired ligand **521**. Complexation using (CO)AuCl afforded catalyst **522**. The active anionic catalyst should be formed *in-situ* via reacting with excess LiOi-Pr in the reaction medium.



Scheme 167: Synthesis of ligand **522**.

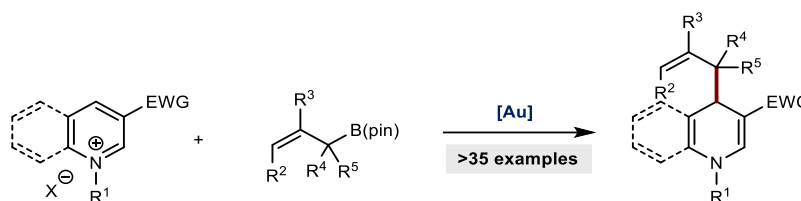
However, upon subjecting phase-transfer catalyst **522** to our optimised allylation and propargylation reaction conditions in toluene as the apolar solvent, limited product formation was observed, with no enantioselectivity (Scheme 168). Any attempt to optimise the reaction with respect to solvent, base and temperature was unsuccessful, with the majority of mass balance attributed to unreacted starting material. Furthermore, alternative phase-transfer catalysts did not effectively promote reactivity.



Scheme 168: Evaluation of ligand **522**.

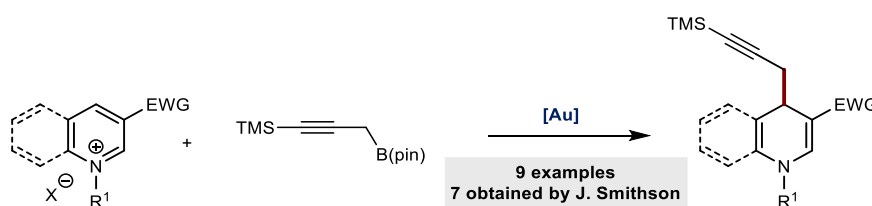
2.8 Conclusions and Future Work

In summary, the gold-catalysed regioselective nucleophilic allylation of azinium salts by allyl pinacolboronates has been achieved in excellent yields and regioselectivities (Scheme 169). This methodology gives access to a broad range of functionalised 1,4-dihydropyridines and 1,4-dihydroquinolines, which were previously difficult to access with existing established methodologies. The reaction operates with exclusive regioselectivity for the 4-position of the azinium salt. The reactive species have been elucidated with a combination of both experimental and computational studies. This research demonstrates the first example of accessing allylgold(I) species from allyl pinacolboronates.



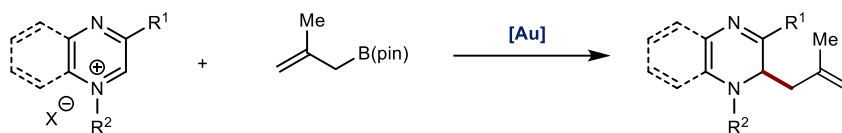
Scheme 169: Gold-catalysed regioselective nucleophilic allylation of azinium salts.

Furthermore, this mode of reactivity has been extended to include other nucleophilic coupling partners. In particular, the gold-catalysed regioselective nucleophilic addition of propargyl pinacolboronates has been established (Scheme 170). The reaction requires no precautions to exclude air or moisture and shows exquisite regioselectivity for the 4-position of the azinium salts.



Scheme 170: Gold-catalysed regioselective nucleophilic propargylation of azinium salts.

Future work would comprise of expanding the substrate scope of the reactions to include alternative electrophiles. One such avenue to explore is pyrazinium salts (Scheme 171). Utilising pyrazinium salts within our reaction conditions would give access to unique molecular scaffolds.



Scheme 171: Gold-catalysed nucleophilic allylation of pyrazinium salts.

Other classes of nucleophiles could also be explored (Figure 7). These may include the addition of aryl boronic acids and functionalised allenyl silanes. Furthermore, propargylic silanes may be of interest as to expand the scope of the propargylation reaction.

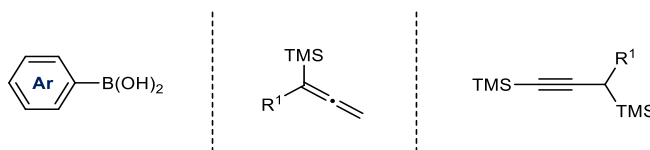
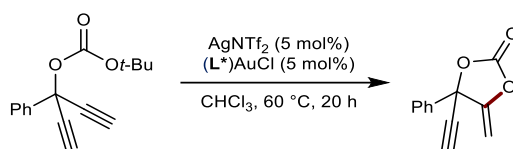


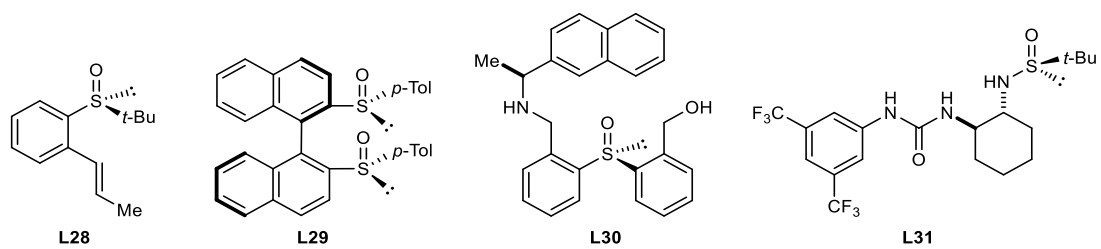
Figure 7: Alternative coupling partners.

Various novel asymmetric gold catalysts have been synthesised. Applications of these catalysts may be extended to other gold-catalysed transformations that have not yet been rendered enantioselective. One such example was reported by the Guo group, demonstrating the racemic synthesis of cyclic carbonates in high yields under gold catalysis. (Scheme 172).¹⁹² If preliminary results were successful, further modifications of these asymmetric catalysts are achievable.



Scheme 172: Gold-catalysed synthesis of cyclic carbonates.

An improvement to the enantioselective variant of our reaction may also be investigated. Enantiopure sulfoxides are an attractive scaffold due to their conformational stability and they can be easily prepared by a variety of methodologies.¹⁸² They have proven to be excellent asymmetric ligands for synthetic transformations and some examples can be seen in Scheme 173. Sulfoxides **L28** and **L29** are excellent asymmetric ligands for the addition of boronic acids to electron-deficient alkenes,^{193,194} while sulfoxides **L30** and **L31** could render both Mannich and cycloadditions reactions enantioselective.^{195,196}



Scheme 173: Potential sulfoxide ligands for enantioselective variant.

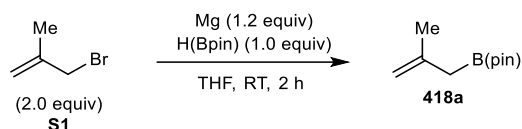
3.0 Experimental

3.1 General Information

All air-sensitive reactions were carried out under an inert atmosphere using oven-dried apparatus. All commercially available reagents were used as received unless otherwise stated. Petroleum ether refers to Sigma-Aldrich product 24587 (petroleum ether boiling point 40-60 °C). Thin layer chromatography (TLC) was performed on Merck DF-Alufoilien 60F254 0.2 mm precoated plates. Compounds were visualized by exposure to UV light or by dipping the plates into solutions of potassium permanganate, ninhydrin, phosphomolybdic acid or vanillin followed by gentle heating. Flash column chromatography was carried out using silica gel (Fisher Scientific 60 Å particle size 35-70 micron or Fluorochem 60 Å particle size 40-63 micron). Melting points were recorded on a Gallenkamp melting point apparatus and are uncorrected. The solvent of recrystallisation is reported in parentheses. Infrared (IR) spectra were recorded on Bruker platinum alpha FTIR spectrometer on the neat compound using the attenuated total reflection technique. NMR spectra were acquired on Bruker Ascend 400 or Ascend 500 spectrometers. ¹H and ¹³C NMR spectra were referenced to external tetramethylsilane *via* the residual protonated solvent (¹H) or the solvent itself (¹³C). ¹¹B, ¹⁹F and ³¹P NMR spectra were referenced through the solvent lock (²H) signal according to the IUPAC-recommended secondary referencing method following Bruker protocols. All chemical shifts are reported in parts per million (ppm). For CDCl₃, the shifts are referenced to 7.26 ppm for ¹H NMR spectroscopy and 77.16 ppm for ¹³C NMR spectroscopy. For DMSO-*d*₆, the shifts are referenced to 2.50 ppm for ¹H NMR spectroscopy and 39.52 ppm for ¹³C NMR spectroscopy. Coupling constants (*J*) are quoted to the nearest 0.1 Hz. High-resolution mass spectra were recorded using electrospray ionization (ESI) techniques. X-ray diffraction data were collected at 120 K on an Agilent SuperNova diffractometer using CuKα radiation.

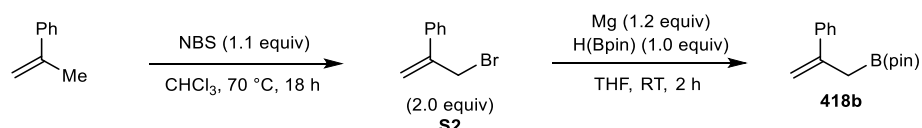
3.2 Preparation of Pinacolboronates

4,4,5,5-Tetramethyl-2-(2-methylallyl)-1,3,2-dioxaborolane (418a)



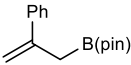
Following a modification of a reported procedure,¹⁶³ an oven-dried flask equipped with a magnetic stir bar was charged with magnesium turnings (146 mg, 6.00 mmol) and was purged with argon for 30 min. Anhydrous THF (9 mL) was added, followed by pinacolborane (725 μ L, 5.00 mmol). 3-Bromo-2-methylprop-1-ene (**S1**) (504 μ L, 5.00 mmol) was added dropwise over 5 min. The solution was stirred at room temperature for 30 min, then additional 3-bromo-2-methylprop-1-ene (**S1**) (504 μ L, 5.00 mmol) was added dropwise over 5 min and the solution was stirred at room temperature for an additional 1.5 h. The reaction was diluted with petroleum ether (7 mL) and quenched carefully with the slow addition of 0.1 M aqueous HCl solution (15 mL). The reaction mixture was extracted with petroleum ether (3 \times 20 mL) and the organic layers were combined, dried (MgSO₄), and concentrated *in vacuo* to give the title compound **418a** as a colourless oil (735 mg, 81%). ¹H NMR (400 MHz, CDCl₃) δ 4.69-4.65 (2H, m, CH₂=), 1.77 (3H, s, =CCH₃), 1.72 (2H, s, CH₂B), 1.25 (12H, s, 2 \times C(CH₃)₂); ¹³C NMR (101 MHz, CDCl₃) δ 143.0 (C), 110.3 (CH₂), 83.4 (2 \times C), 24.9 (4 \times CH₃), 24.6 (CH₃), the secondary carbon (CH₂) next to boron was not observed due to quadrupolar coupling effects of ¹¹B. Data consistent with previously reported literature.¹⁶³

Preparation of substrate 418b



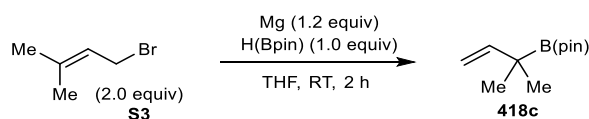
(3-Bromoprop-1-en-2-yl)benzene (**S2**). To a solution of α -methylstyrene (1.30 mL, 10.0 mmol) in CHCl₃ (5 mL) was added NBS (1.96 g, 11.0 mmol). The mixture was stirred at 70 $^{\circ}$ C for 18 h and cooled to room temperature. The reaction mixture was filtered and concentrated *in vacuo*. Purification of the residue by column chromatography (100% petroleum ether) gave the title compound **S2** as a colourless oil

(964 mg, 49%). ¹H NMR (400 MHz, CDCl₃) δ 7.52-7.48 (2H, m, ArH), 7.41-7.31 (3H, m, ArH), 5.57 (1H, s, CH_aH_b=), 5.50 (1H, s, CH_aH_b=), 4.39 (2H, s, CH₂Br); ¹³C NMR (101 MHz, CDCl₃) δ 144.4 (C), 137.7 (C), 128.6 (2 × CH), 128.4 (CH), 126.2 (2 × CH), 117.3 (CH₂), 34.3 (CH₂). Data consistent with previously reported literature.¹⁹⁷

 **4,4,5,5-Tetramethyl-2-(2-phenylallyl)-1,3,2-dioxaborolane (418b).**

Following a literature procedure for similar compounds,¹⁶³ an oven-dried flask equipped with a magnetic stir bar was charged with magnesium turnings (58.3 mg, 2.40 mmol) and was purged with argon for 30 min. Anhydrous THF (5 mL) was added, followed by pinacolborane (290 μL, 2.00 mmol). (3-Bromoprop-1-en-2-yl)benzene (**S2**) (394 mg, 2.00 mmol) was added dropwise over 5 min. The solution was stirred at room temperature for 30 min, then additional (3-bromoprop-1-en-2-yl)benzene (**S2**) (394 mg, 2.00 mmol) was added dropwise over 5 min and the solution was stirred at room temperature for an additional 1.5 h. The reaction was diluted with petroleum ether (7 mL) and quenched carefully with the slow addition of 0.1 M aqueous HCl solution (15 mL). The reaction mixture was extracted with petroleum ether (3 × 20 mL) and the organic layers were combined, dried (MgSO₄), and concentrated *in vacuo*. Purification of the residue by column chromatography (0 to 2% Et₂O/petroleum ether) gave the title compound **418b** as a colourless oil (238 mg, 49%). ¹H NMR (500 MHz, CDCl₃) δ 7.48-7.45 (2H, m, ArH), 7.32-7.28 (2H, m, ArH), 7.25-7.21 (1H, m, ArH), 5.36 (1H, d, *J* = 1.4 Hz, CH_aH_b=), 5.11-5.10 (1H, m, CH_aH_b=), 2.16 (2H, s, CH₂B), 1.17 (12H, s, 2 × C(CH₃)₂); ¹³C NMR (101 MHz, CDCl₃) δ 144.5 (C), 142.0 (C), 128.2 (2 × CH), 127.3 (CH), 126.0 (2 × CH), 112.3 (CH₂), 83.5 (2 × C), 24.7 (4 × CH₃), the secondary carbon (CH₂) next to boron was not observed due to quadrupolar coupling effects of ¹¹B. Data consistent with previously reported literature.¹⁹⁸

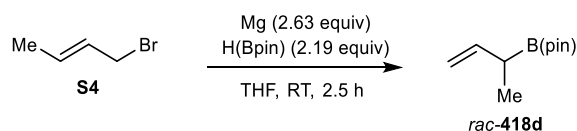
4,4,5,5-Tetramethyl-2-(2-methylbut-3-en-2-yl)-1,3,2-dioxaborolane (418c)



Following a modification of a reported procedure,¹⁶³ an oven-dried flask equipped with a magnetic stir bar was charged with magnesium turnings (146 mg, 6.00 mmol) and was

purged with argon for 30 min. Anhydrous THF (9 mL) was added, followed by pinacolborane (725 μL , 5.00 mmol). 1-Bromo-3-methylbut-2-ene (**S3**) (578 μL , 5.00 mmol) was added dropwise over 5 min. The solution was stirred at room temperature for 30 min, then additional 1-bromo-3-methylbut-2-ene (**S3**) (578 μL , 5.00 mmol) was added dropwise over 5 min and the solution was stirred at room temperature for an additional 1.5 h. The reaction was diluted with petroleum ether (7 mL) and quenched carefully with the slow addition of 0.1 M aqueous HCl solution (15 mL). The reaction mixture was extracted with petroleum ether (3×20 mL) and the organic layers were combined, dried (MgSO_4), and concentrated *in vacuo*. Purification of the residue by column chromatography (0 to 2% Et_2O /petroleum ether) gave the title compound **418c** as a colourless oil (612 mg, 62%). ^1H NMR (400 MHz, CDCl_3) δ 5.99-5.93 (1H, m, =CH), 4.93-4.91 (1H, m, CH_aH_b =), 4.90-4.87 (1H, m, CH_aH_b =), 1.22 (12H, s, $2 \times \text{C}(\text{CH}_3)_2$), 1.06 (6H, s, $\text{BC}(\text{CH}_3)_2$); ^{13}C NMR (101 MHz, CDCl_3) δ 146.8 (CH), 110.1 (CH_2), 83.3 ($2 \times \text{C}$), 24.7 ($4 \times \text{CH}_3$), 23.6 ($2 \times \text{CH}_3$), the quaternary carbon (C) next to boron was not observed due to quadrupolar coupling effects of ^{11}B . Data consistent with previously reported literature.¹⁶³

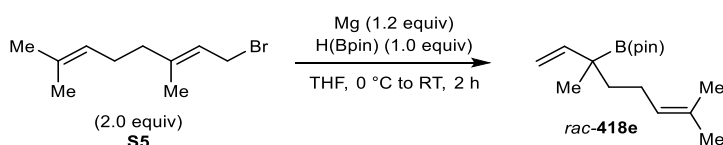
2-(But-3-en-2-yl)-4,4,5,5-tetramethyl-1,3,2-dioxaborolane (*rac*-**418d**)



Following a modification of a reported procedure,¹⁶³ an oven-dried flask equipped with a magnetic stir bar was charged with magnesium turnings (292 mg, 12.0 mmol) and was purged with argon for 30 min. Anhydrous THF (17.5 mL) was added, followed by pinacolborane (1.45 mL, 10.0 mmol). (*E*)-1-Bromobut-2-ene (**S4**) (0.70 mL, 4.56 mmol) was added dropwise over 5 min. The solution was stirred at room temperature for 2 h. The reaction was diluted with petroleum ether (7 mL) and quenched carefully with the slow addition of 0.1 M aqueous HCl solution (15 mL). The reaction mixture was extracted with petroleum ether (3×20 mL) and the organic layers were combined, dried (MgSO_4), and concentrated *in vacuo* to give the title compound *rac*-**418d** as a colourless oil (656 mg, 79%). ^1H NMR (400 MHz, CDCl_3) δ 5.94 (1H, ddd, $J = 17.3, 10.3, 7.1$ Hz, =CH), 5.00-4.90 (2H, m, CH_2 =), 1.94-1.85 (1H, m, CHB), 1.24 (12H, s, $2 \times \text{C}(\text{CH}_3)_2$),

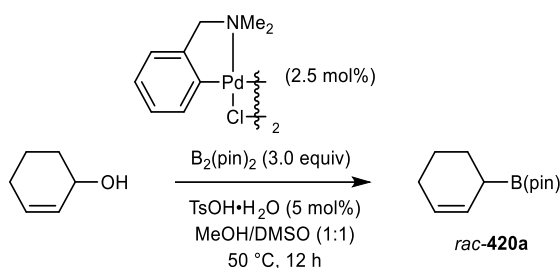
1.10 (3H, d, $J = 7.3$ Hz, CH_3); ^{13}C NMR (101 MHz, CDCl_3) δ 141.1 (CH), 112.1 (CH_2), 83.3 ($2 \times \text{C}$), 24.8 ($4 \times \text{CH}_3$), 14.2 (CH_3), the tertiary carbon (CH) next to boron was not observed due to quadrupolar coupling effects of ^{11}B . Data consistent with previously reported literature.¹⁶³

2-(3,7-Dimethylocta-1,6-dien-3-yl)-4,4,5,5-tetramethyl-1,3,2-dioxaborolane (*rac*-418e)



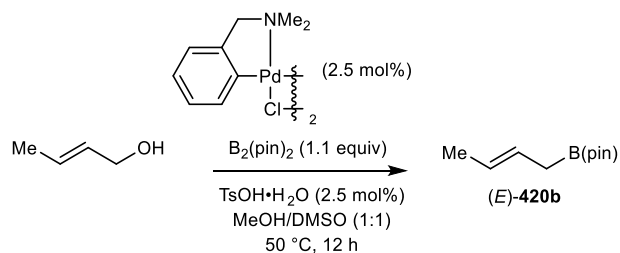
Following a modification of a reported procedure,¹⁹⁹ an oven-dried flask equipped with a magnetic stir bar was charged with magnesium turnings (146 mg, 6.00 mmol) and was purged with argon for 30 min. Anhydrous THF (9 mL) was added at 0 °C, followed by pinacolborane (725 μL , 5.00 mmol). (*E*)-1-Bromo-3,7-dimethylocta-2,6-diene (**S5**) (992 μL , 5.00 mmol) was added dropwise over 5 min. The solution was stirred at room temperature for 30 min, then additional (*E*)-1-bromo-3,7-dimethylocta-2,6-diene (**S5**) (992 μL , 5.00 mmol) was added dropwise over 5 min and the solution was stirred at room temperature for an additional 1.5 h. The reaction was diluted with petroleum ether (7 mL) and quenched carefully with the slow addition of 0.1 M aqueous HCl solution (15 mL). The reaction mixture was extracted with petroleum ether (3×20 mL) and the organic layers were combined, dried (MgSO_4), and concentrated *in vacuo*. Purification of the residue by column chromatography (0 to 2% Et_2O /petroleum ether) gave the title compound *rac*-418e as a colourless oil (819 mg, 62%). ^1H NMR (500 MHz, CDCl_3) δ 5.91 (1H, dd, $J = 17.4, 10.8$ Hz, $\text{CH}_2=\text{CH}$), 5.15-5.10 (1H, m, $\text{CH}_2\text{CH}=\text{}$), 4.97-4.91 (2H, m, $\text{CH}_2=\text{}$), 1.97-1.91 (2H, m, $\text{CH}_2\text{C}=\text{}$), 1.67 (3H, s, $=\text{C}(\text{CH}_3)_2$), 1.59 (3H, s, $=\text{C}(\text{CH}_3)_2$), 1.52 (1H, ddd, $J = 13.3, 11.0, 6.0$ Hz, BCCH_aH_b), 1.36 (1H, ddd, $J = 13.3, 11.0, 6.0$ Hz, BCCH_aH_b), 1.22 (12H, s, $2 \times \text{C}(\text{CH}_3)_2$), 1.07 (3H, s, BCCH_3); ^{13}C NMR (125.8 MHz, CDCl_3) δ 145.5 (CH), 131.2 (C), 125.2 (CH), 111.9 (CH_2), 83.3 ($2 \times \text{C}$), 38.5 (CH_2), 25.9 (CH_3), 24.82 ($2 \times \text{CH}_3$), 24.76 ($2 \times \text{CH}_3$), 24.5 (CH_2), 19.7 (CH_3), 17.7 (CH_3), the quaternary carbon (C) next to boron was not observed due to quadrupolar coupling effects of ^{11}B . Data consistent with previously reported literature.¹⁹⁹

2-(Cyclohex-2-en-1-yl)-4,4,5,5-tetramethyl-1,3,2-dioxaborolane (*rac*-420a)



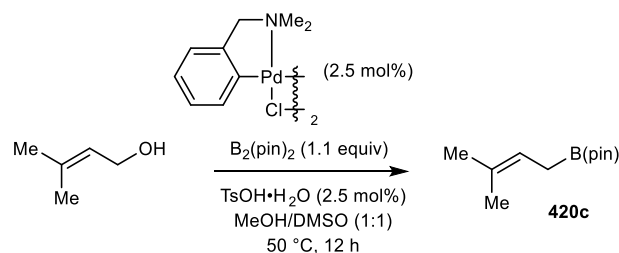
Following a literature procedure for similar compounds,¹⁶⁴ an oven-dried two-necked flask was charged with cyclohex-2-en-1-ol (491 μL , 5.00 mmol) and purged with argon for 30 min. Anhydrous MeOH (10 mL) and anhydrous DMSO (10 mL) (both of which were freshly degassed under a stream of argon for 30 min) were added, followed by $\text{TsOH}\cdot\text{H}_2\text{O}$ (47.6 mg, 0.25 mmol), di- μ -chlorobis{2-[(dimethylamino)methyl]phenyl-C,N}dipalladium(II) (69.0 mg, 0.13 mmol) and bis(pinacolato)diboron (3.81 g, 15.0 mmol). The resulting mixture was stirred at 50 °C for 12 h. The solution was cooled to room temperature and H_2O (15 mL) was added. The solution was extracted with Et_2O (3 \times 30 mL) and the combined organic layers were dried (MgSO_4), filtered and concentrated *in vacuo*. Purification of the residue by column chromatography (2% Et_2O /petroleum ether) gave the title compound *rac*-420a as a colourless oil (208 mg, 20%). ^1H NMR (400 MHz, CDCl_3) δ 5.74-5.64 (2H, m, $\text{CH}_2\text{CH}=\text{}$ and $=\text{CHCH}$), 2.02-1.97 (2H, m, CH_2), 1.83-1.55 (5H, m, CHB , CH_2 , CH_2), 1.24 (12H, s, $2 \times \text{C}(\text{CH}_3)_2$); ^{13}C NMR (101 MHz, CDCl_3) δ 127.7 (CH), 126.2 (CH), 83.3 ($2 \times \text{C}$), 25.2 (CH_2), 24.9 ($2 \times \text{CH}_3$), 24.8 ($2 \times \text{CH}_3$), 24.3 (CH_2), 22.7 (CH_2), the tertiary carbon (CH) next to boron was not observed due to quadrupolar coupling effects of ^{11}B . Data consistent with previously reported literature.¹⁶⁴

(*E*)-2-(But-2-en-1-yl)-4,4,5,5-tetramethyl-1,3,2-dioxaborolane [(*E*)-420b]



Following a literature procedure for similar compounds,¹⁶⁴ an oven-dried two-necked flask was charged with (*E*)-but-2-en-1-ol (427 μ L, 5.00 mmol) and purged with argon for 30 min. Anhydrous MeOH (10 mL) and anhydrous DMSO (10 mL) (both of which were freshly degassed under a stream of argon for 30 min) were added, followed by TsOH·H₂O (23.8 mg, 0.13 mmol), di- μ -chlorobis{2-[(dimethylamino)methyl]phenyl-C,N}dipalladium(II) (69.0 mg, 0.13 mmol) and bis(pinacolato)diboron (1.40 g, 5.50 mmol). The resulting mixture was stirred at 50 °C for 12 h. The solution was cooled to room temperature and H₂O (15 mL) was added. The solution was extracted with Et₂O (3 \times 30 mL) and the combined organic layers were dried (MgSO₄), filtered and concentrated *in vacuo*. Purification of the residue by column chromatography (2% Et₂O/petroleum ether) gave the title compound (*E*)-**420b** as a colourless oil (409 mg, 45%). ¹H NMR (400 MHz, CDCl₃) δ 5.50-5.35 (2H, m, CH₃CH= and =CHCH₂), 1.65-1.62 (5H, m, CH₃ and CH₂B), 1.25 (12H, s, 2 \times C(CH₃)₂); ¹³C NMR (101 MHz, CDCl₃) δ 126.0 (CH), 125.5 (CH), 83.3 (2 \times C), 24.9 (4 \times CH₃), 18.2 (CH₃), the secondary carbon (CH₂) next to boron was not observed due to quadrupolar coupling effects of ¹¹B. Data consistent with previously reported literature.²⁰⁰

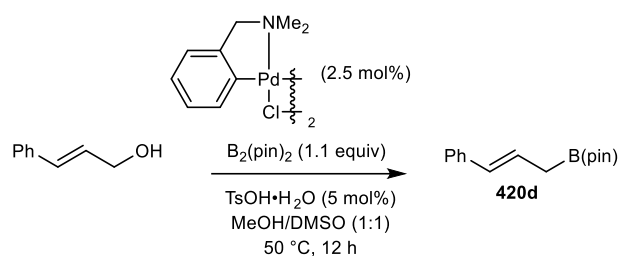
4,4,5,5-Tetramethyl-2-(3-methylbut-2-en-1-yl)-1,3,2-dioxaborolane (**420c**)



Following a literature procedure for similar compounds,¹⁶⁴ an oven-dried two-necked flask was charged with 3-methylbut-2-en-1-ol (508 μ L, 5.00 mmol) and purged with argon for 30 min. Anhydrous MeOH (10 mL) and anhydrous DMSO (10 mL) (both of which were freshly degassed under a stream of argon for 30 min) were added, followed by TsOH·H₂O (23.8 mg, 0.13 mmol), di- μ -chlorobis{2-[(dimethylamino)methyl]phenyl-C,N}dipalladium(II) (69.0 mg, 0.13 mmol) and bis(pinacolato)diboron (1.40 g, 5.50 mmol). The resulting mixture was stirred at 50 °C for 12 h. The solution was cooled to room temperature and H₂O (15 mL) was added. The solution was extracted with Et₂O (3 \times 30 mL) and the combined organic layers were dried (MgSO₄), filtered and concentrated

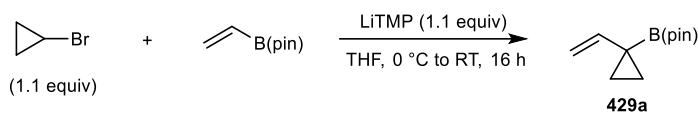
in vacuo. Purification of the residue by column chromatography (2% Et₂O/petroleum ether) gave the title compound **420x** as a colourless oil (430 mg, 44%). ¹H NMR (400 MHz, CDCl₃) δ 5.25-5.19 (1H, m, =CH), 1.69 (3H, s, (CH₃)₂C=), 1.62-1.57 (5H, m, (CH₃)₂C= and CH₂B), 1.24 (12H, s, 2 × C(CH₃)₂); ¹³C NMR (101 MHz, CDCl₃) δ 131.6 (C), 118.6 (CH), 83.2 (2 × C), 25.8 (CH₂), 24.9 (4 × CH₃), 17.8 (2 × CH₃). Data consistent with previously reported literature.¹⁶⁴

2-Cinnamyl-4,4,5,5-tetramethyl-1,3,2-dioxaborolane (**420d**)



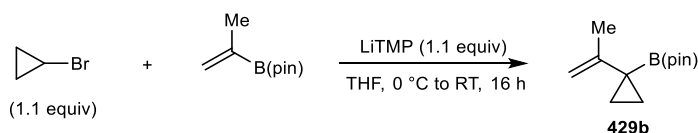
Following a literature procedure for similar compounds,¹⁶⁴ an oven-dried two-necked flask was charged with *trans*-cinnamyl alcohol (643 μL, 5.00 mmol) and purged with argon for 30 min. Anhydrous MeOH (10 mL) and anhydrous DMSO (10 mL) (both of which were freshly degassed under a stream of argon for 30 min) were added, followed by TsOH·H₂O (47.6 mg, 0.25 mmol), di-μ-chlorobis{2-[(dimethylamino)methyl]phenyl-C,N}dipalladium(II) (69.0 mg, 0.13 mmol) and bis(pinacolato)diboron (1.40 g, 5.50 mmol). The resulting mixture was stirred at 50 °C for 12 h. The solution was cooled to room temperature and H₂O (15 mL) was added. The solution was extracted with Et₂O (3 × 30 mL) and the combined organic layers were dried (MgSO₄), filtered and concentrated *in vacuo*. Purification of the residue by column chromatography (2% Et₂O/petroleum ether) gave the title compound **420d** as a colourless oil (352 mg, 29%). ¹H NMR (400 MHz, CDCl₃) δ 7.35-7.31 (2H, m, ArH), 7.29-7.25 (2H, m, ArH), 7.18-7.14 (1H, m, ArH), 6.37 (1H, d, *J* = 15.8 Hz, CCH=), 6.28 (1H, dt, *J* = 15.8, 7.2 Hz, =CHCH₂), 1.97 (2H, d, *J* = 7.2 Hz, CH₂B), 1.26 (12H, s, 2 × C(CH₃)₂); ¹³C NMR (101 MHz, CDCl₃) δ 138.3 (C), 130.4 (CH), 128.5 (2 × CH), 126.6 (CH), 126.4 (CH), 126.0 (2 × CH), 83.5 (2 × C), 24.9 (4 × CH₃), the secondary carbon (CH₂) next to boron was not observed due to quadrupolar coupling effects of ¹¹B. Data consistent with previously reported literature.²⁰⁰

4,4,5,5-Tetramethyl-2-(1-vinylcyclopropyl)-1,3,2-dioxaborolane (**429a**)



To a stirred solution of 2,2,6,6-tetramethylpiperidine in THF (3.0 mL) under argon at 0 °C was added *n*-BuLi (2.5 M in hexanes, 2.2 mL, 5.50 mmol) dropwise over 15 min. The solution was stirred for 30 min at 0 °C, warmed to room temperature and stirred for a further 30 min. A separate flask was charged with cyclopropyl bromide (441 μ L, 5.50 mmol) and vinylboronic ester (848 μ L, 5.00 mmol) and purged with argon for 30 min. Anhydrous THF (17 mL) was added followed by the dropwise addition of the LiTMP solution (see above) at 0 °C over 15 min. The reaction was stirred for 2 h at 0 °C, warmed to room temperature and stirred for a further 14 h. The reaction was quenched with saturated aqueous NaHCO₃ (15 mL) and extracted with Et₂O (3 x 15 mL). The combined organic layers were washed with H₂O (20 mL), brine (20 mL), dried (MgSO₄), filtered and concentrated *in vacuo*. The residue was purified by column chromatography (0 to 10% CH₂Cl₂/*n*-pentane), to give the title compound **429a** as a colourless oil (642 mg, 66%). *Caution: product is volatile.* ¹H NMR (400 MHz, CDCl₃) δ 5.78 (1H, dd, *J* = 17.3, 10.5 Hz, CH₂=CH), 5.10 (1H, dd, *J* = 17.3, 1.7 Hz, CH_aH_b=), 4.87 (1H, dd, *J* = 10.5, 1.7 Hz, CH_aH_b=), 1.22 (12H, s, 2 \times C(CH₃)₂), 0.96-0.93 (2H, m, CCH₂), 0.68-0.66 (2H, m, CCH₂); ¹³C NMR (126 MHz, CDCl₃) δ 142.6 (CH), 111.8 (CH₂), 83.3 (2 \times C), 24.8 (4 \times CH₃), 14.1 (2 \times CH₂), the quaternary carbon (C) next to boron was not observed due to quadrupolar coupling effects of ¹¹B. Data consistent with previously reported literature.¹⁶⁵

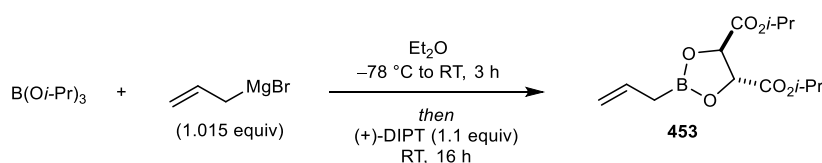
4,4,5,5-Tetramethyl-2-[1-(prop-1-en-2-yl)cyclopropyl]-1,3,2-dioxaborolane (429b)



To a stirred solution of 2,2,6,6-tetramethylpiperidine in THF (3.0 mL) under argon at 0 °C was added *n*-BuLi (2.5 M in hexanes, 2.2 mL, 5.50 mmol) dropwise over 15 min. The solution was stirred for 30 min at 0 °C, warmed to room temperature and stirred for a further 30 min. A separate flask was charged with cyclopropyl bromide (441 μ L, 5.50 mmol) and 4,4,5,5-tetramethyl-2-(prop-1-en-2-yl)-1,3,2-dioxaborolane (940 μ L, 5.00

mmol) and purged with argon for 30 min. Anhydrous THF (17 mL) was added followed by the dropwise addition of the LiTMP solution (see above) at 0 °C over 15 min. The reaction was stirred for 2 h at 0 °C, warmed to room temperature and stirred for a further 14 h. The reaction was quenched with saturated aqueous NaHCO₃ (15 mL) and extracted with Et₂O (3 x 15 mL). The combined organic layers were washed with H₂O (20 mL), brine (20 mL), dried (MgSO₄), filtered and concentrated *in vacuo*. The residue was purified by column chromatography (0 to 5% CH₂Cl₂/*n*-pentane), to give the title compound **429b** as a yellow solid (752 mg, 72%). ¹H NMR (400 MHz, CDCl₃) δ 4.74-4.72 (1H, m, CH_aH_b=), 4.68-4.67 (1H, m, CH_aH_b=), 1.82 (3H, s, CCH₃), 1.21 (12H, s, 2 × C(CH₃)₂), 0.83-0.81 (2H, m, CCH₂), 0.63-0.61 (2H, m, CCH₂); ¹³C NMR (101 MHz, CDCl₃) δ 148.7 (C), 109.9 (CH₂), 83.3 (2 × C), 24.7 (4 × CH₃), 23.2 (CH₃), 11.9 (2 × CH₂), the quaternary carbon (C) next to boron was not observed due to quadrupolar coupling effects of ¹¹B. Data consistent with previously reported literature.¹⁶⁵

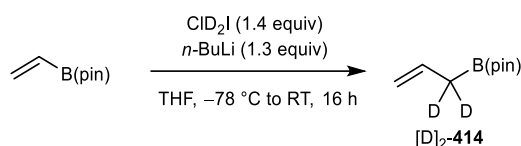
Diisopropyl (4*R*,5*R*)-2-allyl-1,3,2-dioxaborolane-4,5-dicarboxylate (**453**)



An oven-dried flask was purged with argon for 30 min, followed by the addition of anhydrous Et₂O (1.1 mL). B(OiPr)₃ (1.00 mL, 4.33 mmol) in anhydrous Et₂O (1.1 mL) and allylmagnesium bromide (1.0 M in Et₂O, 4.40 mL, 4.40 mmol) were added dropwise simultaneously at -78 °C. The solution was then allowed to warm to room temperature and stirred for 3 h. The slurry was cooled to 0 °C and quenched with 1 M aqueous HCl solution saturated with NaCl and stirred for 15 min. The solution was extracted with anhydrous CH₂Cl₂/Et₂O (1:5, 3 × 6 mL) and to the combined organic layers was added (+)-DIPT (1.00 mL, 4.76 mmol). The resulting mixture was stirred at room temperature for 1 h. Anhydrous Na₂SO₄ was added, and the mixture was stirred for an additional 15 h. The mixture was filtered and concentrated *in vacuo* to give the title compound **453** as a colourless viscous oil (1.18 g, 96%), contaminated with 32% (+)-DIPT. ¹H NMR (400 MHz, CDCl₃) δ 5.94-5.83 (1H, m, =CH), 5.19-5.09 (2H, m, and 2 × CH(CH₃)₂), 5.05-4.97 (2H, m, CH₂=), 4.77 (2H, s, 2 × CHC), 1.92 (2H, d, *J* = 7.2 Hz, CH₂B), 1.29 (12H, d, *J* = 4.5 Hz, 2 × CH(CH₃)₂); ¹³C NMR (101 MHz, CDCl₃) δ 168.9 (2 × C), 132.7 (CH),

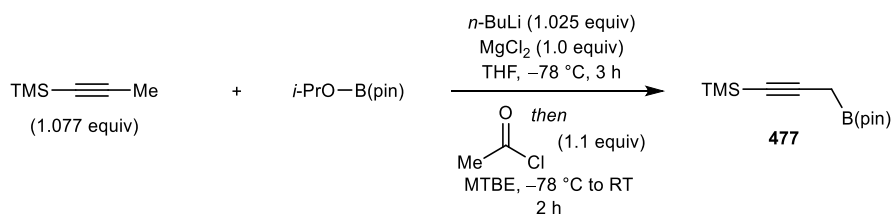
115.8 (CH₂), 77.7 (2 × CH), 77.0 (2 × CH), 21.5 (4 × CH₃), the secondary carbon (CH₂) next to boron was not observed due to quadrupolar coupling effects of ¹¹B. Data consistent with previously reported literature.²⁰¹

2-(Allyl-1,1-*d*₂)-4,4,5,5-tetramethyl-1,3,2-dioxaborolane ([D]₂-414)



An oven-dried flask was purged with argon for 30 min, followed by the addition of vinylboronic acid pinacol ester (678 μL, 4.00 mmol), ClCD₂I (0.99 g, 5.60 mmol), and anhydrous THF (17 mL). *n*-BuLi (2.5 M in hexanes, 2.08 mL, 5.20 mmol) was added dropwise at -78 °C and the solution was allowed to warm to room temperature and stirred for 16 h. H₂O (10 mL) and *n*-pentane (50 mL) were added, and the mixture was passed through a plug of celite (8 cm in height and 2 cm wide) using *n*-pentane (50 mL) as the eluent. The filtrate was washed with saturated aqueous NH₄Cl solution (50 mL), extracted with *n*-pentane (3 × 30 mL), dried (MgSO₄), filtered and concentrated *in vacuo*. Purification of the residue by column chromatography (0 to 1% Et₂O/*n*-pentane) gave the title compound [D]₂-414 as a colourless oil (264 mg, 39%), contaminated with 15% vinylboronic acid pinacol ester. ¹H NMR (400 MHz, CDCl₃) δ 5.86 (1H, dd, *J* = 16.4, 10.6 Hz, =CH), 5.00 (1H, dd, *J* = 17.1, 2.1 Hz, CH_aH_b=), 4.93 (1H, dd, *J* = 10.6, 2.1 Hz, CH_aH_b=), 1.25 (12H, s, 2 × C(CH₃)₂); ²H NMR (77 MHz, CHCl₃) δ 1.72 (2D, d, *J* = 1.2 Hz, CD₂); ¹³C NMR (101 MHz, CDCl₃) δ 137.2 (CH), 115.0 (CH₂), 83.4 (2 × C), 24.9 (4 × CH₃), the quaternary carbon (C) next to boron was not observed due to quadrupolar coupling effects of ¹¹B. Data consistent with previously reported literature.²⁰²

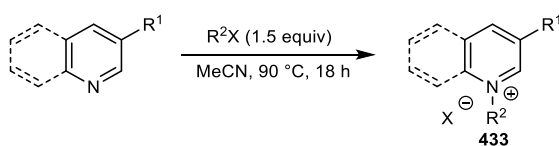
Trimethyl[3-(4,4,5,5-tetramethyl-1,3,2-dioxaborolan-2-yl)prop-1-yn-1-yl]silane (477)



An oven-dried flask was charged with trimethyl(prop-1-yn-1-yl)silane (4.94 mL, 33.4 mmol), and purged with argon for 30 min. Anhydrous THF (30 mL) was added, followed by the dropwise addition of *n*-BuLi (1.9 M in hexanes, 16.7 mL, 31.8 mmol) at -78 °C. The resulting solution was stirred at -78 °C for 1 h. A separate oven-dried flask was charged with MgCl₂ (2.95 g, 31.0 mmol) and purged with argon for 30 min. Anhydrous THF (30 mL) and 2-isopropoxy-4,4,5,5-tetramethyl-1,3,2-dioxaborolane (6.32 mL, 31.0 mmol) were added followed by the dropwise addition of the lithiopypyne solution (see above) at -78 °C. The resulting suspension was warmed to room temperature over 1 h and stirred for an additional 1 h. Acetyl chloride (2.42 mL, 34.1 mmol) in MTBE (2.42 mL) was added to the suspension at -78 °C and the reaction mixture was warmed to room temperature over 1 h and concentrated *in vacuo*. Petroleum ether (75 mL) was added, and the suspension was filtered, washed with petroleum ether (2×25 mL) and the filtrate was concentrated *in vacuo*. The residue was purified by vacuum distillation (100 °C, 1.0 mbar) to give the title compound **477** as a colourless oil (3.97 g, 50%). ¹H NMR (500 MHz, CDCl₃) δ 1.87 (2H, s, CH₂B), 1.27 (12H, s, $2 \times C(CH_3)_2$), 0.13 (9H, s, Si(CH₃)₃); ¹³C NMR (126 MHz, CDCl₃) δ 103.3 (C), 84.2 ($2 \times C$), 83.3 (C), 24.8 ($4 \times CH_3$), 0.4 ($3 \times CH_3$), the secondary carbon (CH₂) next to boron was not observed due to quadrupolar coupling effects of ¹¹B. Data consistent with previously reported literature.²⁰³

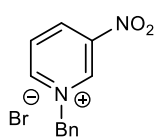
3.3 Preparation of Azinium Salts

General Procedure A: Preparation of Azinium Salts

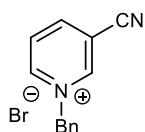


Following a modification of a reported procedure,²⁰⁴ a flask was charged with the appropriate substituted azine (1.0 equiv) and MeCN. The appropriate alkyl halide (1.5

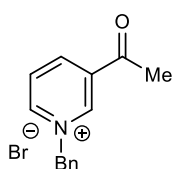
equiv) was added in one portion and the resulting mixture was stirred at 90 °C for 18 h. The mixture was cooled to room temperature and transferred to a beaker which was cooled to 0 °C and stirred vigorously for 5 min. Et₂O (30 mL per mmol of azine) was added portionwise, and the mixture was stirred vigorously at 0 °C for 15 min, at which point the product precipitated. If no precipitation occurred, the mixture was sonicated until precipitation occurred. The precipitated product was removed by vacuum filtration, washed with ice-cold Et₂O (3 × 5 mL per mmol of azine) and dried under vacuum to give the desired product.



1-Benzyl-3-nitropyridin-1-ium bromide (408). The title compound was prepared according to General Procedure A, using 3-nitropyridine (2.00 g, 16.1 mmol), benzyl bromide (2.88 mL, 24.2 mmol) and MeCN (30 mL) to give a dark yellow solid (3.35 g, 71%). m.p. 161-162 °C (Et₂O); IR 2982, 1639, 1528 (NO₂), 1455, 1353 (NO₂), 1125, 1030, 963, 731, 663 cm⁻¹; ¹H NMR (400 MHz, DMSO-*d*₆) δ 10.36 (1H, s, ArH), 9.52 (1H, dd, *J* = 6.2, 1.2 Hz, ArH), 9.38-9.34 (1H, m, ArH), 8.43 (1H, dd, *J* = 8.6, 6.1 Hz, ArH), 7.63-7.59 (2H, m, ArH), 7.49-7.44 (3H, m, ArH), 6.06 (2H, s, NCH₂); ¹³C NMR (101 MHz, DMSO-*d*₆) δ 149.2 (CH), 146.7 (C), 142.5 (CH), 140.2 (CH), 133.6 (C), 129.6 (CH), 129.18 (2 × CH), 128.15 (CH), 129.1 (2 × CH), 63.8 (CH₂); HRMS (ESI) Exact mass calculated for [C₁₂H₁₁N₂O₂]⁺: 215.0815, found 215.0808.

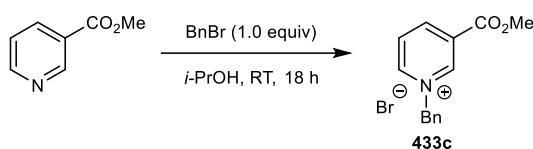


1-Benzyl-3-cyanopyridin-1-ium bromide (433a). The title compound was prepared according to General Procedure A, using 3-cyanopyridine (1.00 g, 9.61 mmol), benzyl bromide (1.71 mL, 14.4 mmol) and MeCN (15 mL) to give a pale pink solid (1.78 g, 68%). ¹H NMR (500 MHz, DMSO-*d*₆) δ 10.05 (1H, s, ArH), 9.47 (1H, dd, *J* = 6.3, 1.3 Hz, ArH), 9.15-9.11 (1H, m, ArH), 8.38 (1H, dd, *J* = 8.1, 6.2 Hz, ArH), 7.63-7.60 (2H, m, ArH), 7.48-7.44 (3H, m, ArH), 5.93 (2H, s, NCH₂); ¹³C NMR (126 MHz, DMSO-*d*₆) δ 149.1 (CH), 149.0 (CH), 148.0 (CH), 133.4 (C), 129.6 (CH), 129.22 (2 × CH), 129.15 (2 × CH), 128.8 (CH), 113.9 (C), 113.2 (C), 63.9 (CH₂). Data consistent with previously reported literature.²⁰⁴

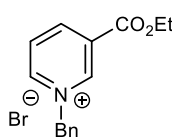


3-Acetyl-1-benzylpyridin-1-ium bromide (433b). The title compound was prepared according to General Procedure A, using 3-acetylpyridine (1.01 mL, 10.0 mmol), benzyl bromide (1.78 mL, 15.0 mmol) and MeCN (20 mL) to give an off-white white solid (2.86 g, 98%). ^1H NMR (400 MHz, DMSO-*d*6) δ 9.85 (1H, s, ArH), 9.39 (1H, d, $J = 6.0$ Hz, ArH), 9.04 (1H, dd, $J = 8.1, 1.4$ Hz, ArH), 8.32 (1H, dd, $J = 8.0, 6.1$ Hz, ArH), 7.63-7.59 (2H, m, ArH), 7.48-7.41 (3H, m, ArH), 6.03 (2H, s, NCH₂), 2.75 (3H, s, CH₃); ^{13}C NMR (101 MHz, DMSO-*d*6) δ 194.1 (C), 147.3 (CH), 145.4 (CH), 144.5 (CH), 135.8 (C), 134.1 (C), 129.4 (CH), 129.2 (2 \times CH), 128.9 (2 \times CH), 128.6 (CH), 63.3 (CH₂), 27.4 (CH₃). Data consistent with previously reported literature.²⁰⁵

1-Benzyl-3-(methoxycarbonyl)pyridin-1-ium bromide (433c)



Following a modification of a reported procedure,²⁰⁶ a flask was charged with methyl nicotinate (1.37 g, 10.0 mmol) and *i*-PrOH (5 mL). Benzyl bromide (1.19 mL, 10.0 mmol) was added dropwise, and the resulting mixture was stirred at room temperature for 18 h. MTBE (20 mL) was added in one portion and the mixture was sonicated until precipitation occurred. The product was removed by vacuum filtration and washed with MTBE (5 \times 10 mL) and dried under vacuum to give the title compound **433c** as an off-white solid (2.58 g, 84%). ^1H NMR (400 MHz, CDCl₃) δ 10.08 (1H, dd, $J = 6.2, 1.4$ Hz, ArH), 9.79 (1H, s, ArH), 8.84 (1H, dt, $J = 8.0, 1.5$ Hz, ArH), 8.25 (1H, dd, $J = 8.1, 6.1$ Hz, ArH), 7.72-7.68 (2H, m, ArH), 7.33-7.29 (3H, m, ArH), 6.48 (2H, s, NCH₂), 3.92 (3H, s, CH₃); ^{13}C NMR (101 MHz, CDCl₃) δ 161.5 (C), 148.7 (CH), 145.5 (CH), 145.2 (CH), 132.6 (C), 130.4 (C), 130.2 (CH), 129.9 (2 \times CH), 129.7 (2 \times CH), 128.7 (CH), 64.5 (CH₂), 53.9 (CH₃). Data consistent with previously reported literature.²⁰⁶



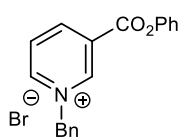
1-Benzyl-3-(ethoxycarbonyl)pyridin-1-ium bromide (433d). The title compound was prepared according to General Procedure A, using ethyl nicotinate (1.37 mL, 10.0 mmol), benzyl bromide (1.78 mL, 15.0 mmol)

and MeCN (20 mL) to give an off-white solid (3.13 g, 97%). ^1H NMR (400 MHz, CDCl_3) δ 10.08-10.05 (1H, m, ArH), 9.76 (1H, s, ArH), 8.83-8.80 (1H, m, ArH), 8.25 (1H, dd, $J = 8.1, 6.1$ Hz, ArH), 7.70-7.67 (2H, m, ArH), 7.32-7.28 (3H, m, ArH), 6.47 (2H, s, NCH_2), 4.37 (2H, q, $J = 7.1$ Hz, CH_2CH_3), 1.34 (3H, t, $J = 7.1$ Hz, CH_3); ^{13}C NMR (101 MHz, CDCl_3) δ 161.0 (C), 148.6 (CH), 145.4 (CH), 145.1 (CH), 132.6 (C), 130.7 (C), 130.1 (CH), 129.9 ($2 \times \text{CH}$), 129.6 ($2 \times \text{CH}$), 128.7 (CH), 64.4 (CH_2), 63.4 (CH_2), 14.2 (CH_3). Data consistent with previously reported literature.²⁰⁷

1-Benzyl-3-(butoxycarbonyl)pyridin-1-ium bromide (433e)



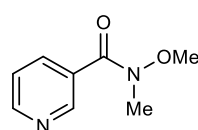
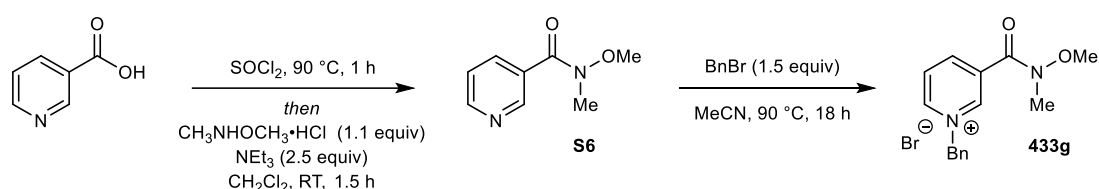
Following a modification of a reported procedure,²⁰⁶ a flask was charged with butyl nicotinate (1.71 mL, 10.0 mmol) and *i*-PrOH (5 mL). Benzyl bromide (1.19 mL, 10.0 mmol) was added dropwise, and the resulting mixture was stirred at room temperature for 18 h. MTBE (20 mL) was added in one portion and the mixture was sonicated until precipitation occurred. The product was removed by vacuum filtration and washed with MTBE (5×10 mL) and dried under vacuum to give the title compound **433e** as an off-white solid (3.50 g, 100%). m.p. 96-97 °C (Et_2O); IR 3041, 3382, 2958, 1726 (C=O), 1629, 1294, 1209, 1105, 750, 708 cm^{-1} ; ^1H NMR (400 MHz, CDCl_3) δ 10.12 (1H, dt, $J = 6.3, 1.3$ Hz, ArH), 9.50 (1H, s, ArH), 8.83 (1H, dt, $J = 8.1, 1.5$ Hz, ArH), 8.29 (1H, dd, $J = 8.1, 6.1$ Hz, ArH), 7.69-7.65 (2H, m, ArH), 7.39-7.35 (3H, m, ArH), 6.44 (2H, s, NCH_2), 4.35 (2H, t, $J = 6.7$ Hz, OCH_2), 1.75-1.70 (2H, m, $\text{CH}_2\text{CH}_2\text{CH}_3$), 1.44-1.34 (2H, m, $\text{CH}_2\text{CH}_2\text{CH}_3$), 0.92 (3H, t, $J = 7.4$ Hz, CH_3); ^{13}C NMR (101 MHz, CDCl_3) δ 161.1 (C), 149.1 (CH), 145.1 (CH), 145.0 (CH), 132.4 (C), 130.8 (C), 130.3 (CH), 130.1 ($2 \times \text{CH}$), 129.8 ($2 \times \text{CH}$), 128.8 (CH), 67.3 (CH_2), 65.0 (CH_2), 30.4 (CH_2), 19.1 (CH_2), 13.7 (CH_3); HRMS (ESI) Exact mass calculated for $[\text{C}_{17}\text{H}_{20}\text{NO}_2]^+$: 270.1489, found 270.1496.



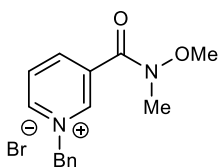
1-Benzyl-3-(phenoxycarbonyl)pyridin-1-ium bromide (433f). The title compound was prepared according to General Procedure A, using phenyl nicotinate (498 mg, 2.50 mmol), benzyl bromide (446 μL , 3.75

mmol) and MeCN (5 mL) to give an off-white solid (750 mg, 81%). m.p. 158-159 °C (Et₂O); IR 3060, 1751 (C=O), 1632, 1585, 1285, 1189, 1088, 729, 694, 668 cm⁻¹; ¹H NMR (400 MHz, CDCl₃) δ 10.05-10.03 (2H, m, ArH), 8.93 (1H, d, *J* = 7.9 Hz, ArH), 8.25 (1H, dd, *J* = 8.1, 6.0 Hz, ArH), 7.74-7.71 (2H, m, ArH), 7.39-7.31 (5H, m, ArH), 7.28-7.23 (3H, m, ArH), 6.50 (2H, s, NCH₂); ¹³C NMR (101 MHz, CDCl₃) δ 159.9 (C), 150.0 (C), 149.0 (CH), 146.1 (CH), 145.6 (CH), 132.6 (C), 130.2 (CH), 130.1 (2 × CH and C), 129.78 (2 × CH), 129.76 (2 × CH), 128.8 (CH), 126.9 (CH), 121.4 (2 × CH), 64.6 (CH₂); HRMS (ESI) Exact mass calculated for [C₁₉H₁₆NO₂]⁺: 290.1176, found 290.1180.

Preparation of substrate 433g



***N*-Methoxy-*N*-methylnicotinamide (S6).** A flask was charged with nicotinic acid (1.48 g, 12.0 mmol). Thionyl chloride (10.0 mL) was added in one portion and the reaction was stirred at 90 °C for 1 h. The reaction was cooled to room temperature and concentrated *in vacuo* to leave a residue, which was dissolved in anhydrous CH₂Cl₂ (10 mL). *N,O*-Dimethylhydroxylamine hydrochloride (1.29 g, 13.2 mmol) was added, followed by the dropwise addition of triethylamine (4.18 mL, 30.0 mmol) at 0 °C. The reaction mixture was stirred at room temperature for 1.5 h. H₂O (30 mL) was added and the resulting mixture was extracted with CH₂Cl₂ (3 × 50 mL), and the combined organic layers were dried (MgSO₄), filtered, and concentrated *in vacuo* to give the title compound **S6** as a brown oil (1.94 g, 97%). ¹H NMR (400 MHz, CDCl₃) δ 8.95-8.93 (1H, m, ArH), 8.67 (1H, dd, *J* = 4.9, 1.7 Hz, ArH), 8.03 (1H, dt, *J* = 8.0, 2.0 Hz, ArH), 7.36 (1H, dd, *J* = 8.0, 4.9 Hz, ArH), 3.54 (3H, s, CH₃), 3.38 (3H, s, CH₃); ¹³C NMR (101 MHz, CDCl₃) δ 167.4 (C), 151.2 (CH), 149.2 (CH), 136.5 (CH), 130.1 (C), 123.2 (CH), 61.4 (CH₃), 33.3 (CH₃). Data consistent with previously reported literature.²⁰⁸

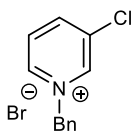


1-Benzyl-3-[methoxy(methyl)carbamoyl]pyridin-1-ium bromide

(433g). The title compound was prepared according to General Procedure A, using **S6** (831 mg, 5.0 mmol), benzyl bromide (892 μL ,

7.5 mmol) and MeCN (10 mL) to give a light brown solid (1.39 g,

82%). m.p. 144-145 $^{\circ}\text{C}$ (Et_2O); IR 3030, 2994, 1646 (C=O), 1627, 1462, 1199, 982, 772, 715, 678 cm^{-1} ; ^1H NMR (400 MHz, CDCl_3) δ 9.99 (1H, d, $J = 5.9$ Hz, ArH), 9.37 (1H, s, ArH), 8.70 (1H, d, $J = 7.9$ Hz, ArH), 8.17 (1H, dd, $J = 8.1, 6.0$ Hz, ArH), 7.70-7.65 (2H, m, ArH), 7.40-7.36 (3H, m, ArH), 6.44 (2H, s, NCH_2), 3.62 (3H, s, CH_3), 3.36 (3H, s, CH_3); ^{13}C NMR (101 MHz, CDCl_3) δ 161.8 (C), 147.0 (CH), 145.1 (CH), 144.5 (CH), 133.9 (C), 132.6 (C), 130.3 (CH), 130.0 (2 \times CH), 129.9 (2 \times CH), 128.2 (CH), 64.9 (CH_2), 62.7 (CH_3), 33.2 (CH_3); HRMS (ESI) Exact mass calculated for $[\text{C}_{15}\text{H}_{17}\text{N}_2\text{O}_2]^+$: 257.1285, found 257.1288.

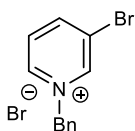


1-Benzyl-3-chloropyridin-1-ium bromide (433h). The title compound

was prepared according to General Procedure A, using 3-chloropyridine

(951 μL , 10.0 mmol), benzyl bromide (1.78 mL, 15.0 mmol) and MeCN (20

mL) to give an off-white solid (1.99 g, 70%). m.p. 137-138 $^{\circ}\text{C}$ (Et_2O); IR 3004, 1621, 1492, 1329, 1169, 1131, 772, 741, 715, 694 cm^{-1} ; ^1H NMR (400 MHz, CDCl_3) δ 9.77 (1H, d, $J = 6.1$ Hz, ArH), 9.72 (1H, s, ArH), 8.37 (1H, dd, $J = 8.7, 1.7$ Hz, ArH), 8.09 (1H, dd, $J = 8.4, 6.1$ Hz, ArH), 7.77-7.73 (2H, m, ArH), 7.39-7.35 (3H, m, ArH), 6.45 (2H, s, NCH_2); ^{13}C NMR (101 MHz, CDCl_3) δ 145.2 (CH), 144.0 (CH), 143.9 (CH), 135.9 (C), 132.6 (C), 130.4 (CH), 130.1 (2 \times CH), 129.8 (2 \times CH), 129.0 (CH), 64.4 (CH_2); HRMS (ESI) Exact mass calculated for $[\text{C}_{12}\text{H}_{11}\text{ClN}]^+$: 204.0575, found 204.0577.



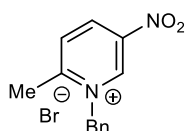
1-Benzyl-3-bromopyridin-1-ium bromide (433i). The title compound was

prepared according to General Procedure A, using 3-bromopyridine (963

μL , 10.0 mmol), benzyl bromide (1.78 mL, 15.0 mmol) and MeCN (20 mL)

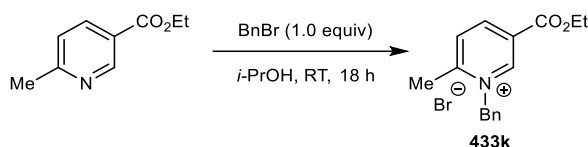
to give an off-white solid (3.29 g, 100%). ^1H NMR (400 MHz, $\text{DMSO}-d_6$) δ 9.74 (1H, s, ArH), 9.25 (1H, d, $J = 6.2$ Hz, ArH), 8.91 (1H, ddd, $J = 8.7, 1.9, 1.1$ Hz, ArH), 8.13 (1H, dd, $J = 8.4, 6.2$ Hz, ArH), 7.62-7.58 (2H, m, ArH), 7.48-7.41 (3H, m, ArH), 5.87 (2H, s, NCH_2); ^{13}C NMR (101 MHz, $\text{DMSO}-d_6$) δ 148.4 (CH), 146.0 (CH), 143.8 (CH),

133.8 (C), 129.5 (CH), 129.3 (CH), 129.2 (2 × CH), 129.0 (2 × CH), 122.4 (C), 63.4 (CH₂). Data consistent with previously reported literature.²⁰⁹



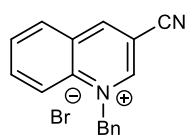
1-Benzyl-2-methyl-5-nitropyridin-1-ium bromide (433j). The title compound was prepared according to General Procedure A, using 2-methyl-5-nitropyridine (1.38 g, 10.0 mmol), benzyl bromide (1.78 mL, 15.0 mmol) and MeCN (20 mL) to give a black solid (359 mg, 12%). m.p. 149-151 °C (Et₂O); IR 2961, 1640, 1582, 1536 (NO₂), 1356 (NO₂), 1293, 812, 740, 732, 553 cm⁻¹; ¹H NMR (400 MHz, DMSO-*d*₆) δ 10.25 (1H, s, ArH), 9.33 (1H, d, *J* = 8.7 Hz, ArH), 8.37 (1H, d, *J* = 8.7 Hz, ArH), 7.48-7.34 (5H, m, ArH), 6.13 (2H, s, NCH₂), 2.84 (3H, s, CH₃); ¹³C NMR (101 MHz, DMSO-*d*₆) δ 161.4 (C), 145.1 (C), 143.7 (CH), 139.5 (CH), 132.3 (C), 131.0 (CH), 129.1 (2 × CH), 129.0 (CH), 127.7 (2 × CH), 61.4 (CH₂), 20.4 (CH₃); HRMS (ESI) Exact mass calculated for [C₁₃H₁₃N₂O₂]⁺: 229.0972, found 229.0980.

Preparation of substrate 433k



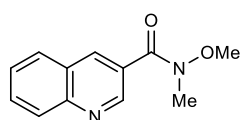
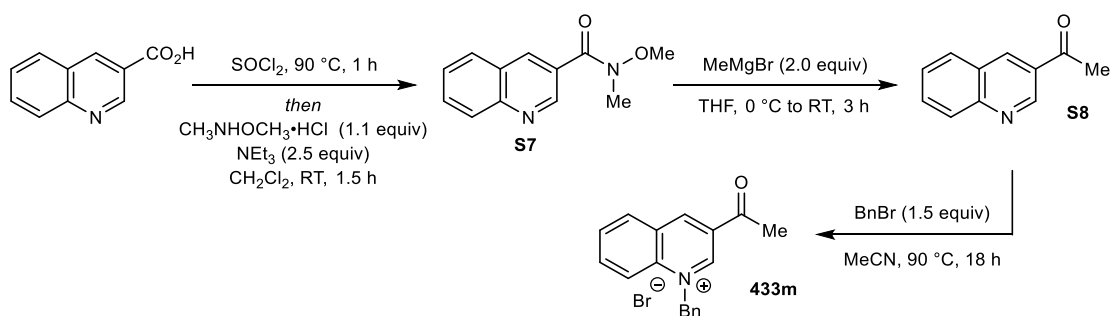
Following a modification of a reported procedure,²⁰⁶ a flask was charged with ethyl 6-methylnicotinate (1.65 g, 10.0 mmol) and *i*-PrOH (5 mL). Benzyl bromide (1.19 mL, 10.0 mmol) was added dropwise, and the resulting mixture was stirred at room temperature for 18 h. The mixture was added dropwise to Et₂O (200 mL) at 0 °C and stirred vigorously for 5 mins, at which point the product precipitated. The precipitated product was removed by vacuum filtration and washed with ice-cold Et₂O (3 × 50 mL) to give the title compound **433k** as an off-white solid (733 mg, 22%). m.p. 175-176 °C (Et₂O); IR 2980, 1747, 1731 (C=O), 1637, 1449, 1298, 1173, 1144, 740, 700 cm⁻¹; ¹H NMR (400 MHz, CDCl₃) δ 9.42 (1H, s, ArH), 8.76-8.73 (1H, m, ArH), 8.29 (1H, d, *J* = 8.2 Hz, ArH), 7.39-7.35 (5H, m, ArH), 6.32 (2H, s, NCH₂), 4.39 (2H, q, *J* = 7.1 Hz, OCH₂), 3.14 (3H, s, CCH₃), 1.37 (3H, t, *J* = 7.1 Hz, CH₂CH₃); ¹³C NMR (101 MHz, CDCl₃) δ 161.3 (C), 160.6 (C), 146.3 (CH), 144.7 (CH), 131.3 (CH), 131.0 (C), 129.9

(CH), 129.8 (2 × CH), 128.9 (2 × CH), 128.6 (C), 63.3 (CH₂), 62.7 (CH₂), 22.5 (CH₃), 14.2 (CH₃). HRMS (ESI) Exact mass calculated for [C₁₆H₁₈NO₂]⁺: 256.1332, found 256.1344.



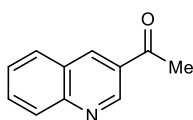
1-Benzyl-3-cyanoquinolin-1-ium bromide (433I). The title compound was prepared according to General Procedure A, using 3-quinolinecarbonitrile (771 mg, 5.00 mmol), benzyl bromide (892 μL, 7.50 mmol) and MeCN (10 mL) to give a light green solid (988 mg, 61%). m.p. 181-182 °C (Et₂O); IR 2947, 2246 (C≡N), 1627, 1381, 1249, 1163, 1051, 752, 731, 698 cm⁻¹; ¹H NMR (400 MHz, DMSO-*d*₆) δ 10.44 (1H, d, *J* = 1.7 Hz, ArH), 10.03 (1H, d, *J* = 1.7 Hz, ArH), 8.57-8.53 (2H, m, ArH), 8.37 (1H, ddd, *J* = 8.8, 7.0, 1.5 Hz, ArH), 8.14 (1H, t, *J* = 7.6, ArH), 7.53-7.50 (2H, m, ArH), 7.42-7.34 (3H, m, ArH), 6.42 (2H, s, NCH₂); ¹³C NMR (101 MHz, DMSO-*d*₆) δ 152.6 (2 × CH), 138.7 (CH), 137.9 (C), 133.2 (C), 131.9 (CH), 131.3 (CH), 129.0 (2 × CH), 128.9 (CH), 128.8 (C), 127.5 (2 × CH), 119.8 (CH), 114.6 (C), 107.2 (C), 60.8 (CH₂); HRMS (ESI) Exact mass calculated for [C₁₇H₁₃N₂]⁺: 245.1073, found 245.1072.

Preparation of substrate 433m

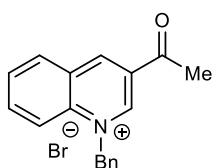


***N*-Methoxy-*N*-methylquinoline-3-carboxamide (S7).** A flask was charged with 3-quinolinecarboxylic acid (3.46 g, 20.0 mmol). Thionyl chloride (20.0 mL) was added in one portion and the reaction was stirred at 90 °C for 1 h. The reaction was cooled to room temperature and concentrated *in vacuo* to leave a residue, which was dissolved in anhydrous CH₂Cl₂ (20 mL). *N,O*-Dimethylhydroxylamine hydrochloride (2.15 g, 22.0 mmol) was added, followed by the dropwise addition of triethylamine (6.97 mL, 50.0 mmol) at 0 °C. The

reaction mixture was stirred at room temperature for 1.5 h. H₂O (50 mL) was added and the resulting mixture was extracted with CH₂Cl₂ (3 × 100 mL), and the combined organic layers were dried (MgSO₄), filtered, and concentrated *in vacuo*. Purification of the residue by column chromatography (100% EtOAc) gave the title compound **S7** as a brown solid (2.99 g, 69%). ¹H NMR (400 MHz, CDCl₃) δ 9.21 (1H, d, *J* = 2.1 Hz, ArH), 8.56 (1H, d, *J* = 2.1 Hz, ArH), 8.13 (1H, dd, *J* = 8.5, 1.2 Hz, ArH), 7.88 (1H, dd, *J* = 8.2, 1.5 Hz, ArH), 7.78 (1H, ddd, *J* = 8.5, 6.9, 1.5 Hz, ArH), 7.59 (1H, ddd, *J* = 8.2, 6.9, 1.2 Hz, ArH), 3.56 (3H, s, CH₃), 3.43 (3H, s, CH₃); ¹³C NMR (101 MHz, CDCl₃) δ 167.5 (C), 149.5 (CH), 148.7 (C), 137.1 (CH), 131.1 (CH), 129.4 (CH), 128.8 (CH), 127.3 (CH), 127.1 (C), 127.0 (C), 61.5 (CH₃), 33.4 (CH₃). Data consistent with previously reported literature.²¹⁰



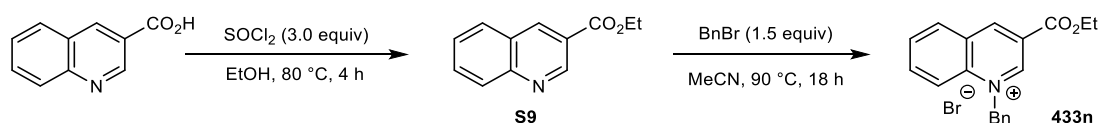
1-(Quinolin-3-yl)ethan-1-one (S8). A flask was charged with Weinreb amide **S7** (1.08 g, 5.00 mmol), purged with argon for 30 min, followed by the addition of THF (5 mL) at 0 °C. MeMgBr (3.0 M in Et₂O, 3.33 mL, 10.0 mmol) was added dropwise, and the resulting solution was warmed to room temperature and stirred for 3 h. The reaction was quenched with saturated aqueous NH₄Cl solution (10 mL) at 0 °C and extracted with EtOAc (3 × 15 mL). The combined organic layers were washed with H₂O (10 mL), brine (10 mL), dried (MgSO₄), filtered, and concentrated *in vacuo* to give the title compound **S8** as a brown solid (790 mg, 92%). ¹H NMR (400 MHz, CDCl₃) δ 9.41 (1H, d, *J* = 2.2 Hz, ArH), 8.69 (1H, d, *J* = 2.2 Hz, ArH), 8.14 (1H, dd, *J* = 8.5, 1.2 Hz, ArH), 7.93 (1H, dd, *J* = 8.2, 1.5 Hz, ArH), 7.82 (1H, ddd, *J* = 8.5, 6.9, 1.5 Hz, ArH), 7.61 (1H, ddd, *J* = 8.2, 6.9, 1.2 Hz, ArH), 2.73 (3H, s, CH₃); ¹³C NMR (101 MHz, CDCl₃) δ 196.8 (C), 149.9 (C), 149.3 (CH), 137.4 (CH), 132.1 (CH), 129.6 (CH), 129.5 (CH), 129.4 (C), 127.7 (CH), 126.9 (C), 26.9 (CH₃). Data consistent with previously reported literature.²¹¹



3-Acetyl-1-benzylquinolin-1-ium bromide (433m). The title compound was prepared according to General Procedure A, using **S8** (514 mg, 3.00 mmol), benzyl bromide (535 μL, 4.50 mmol) and MeCN (6 mL) to give a brown solid (844 mg, 82%). m.p. 232-233 °C (Et₂O); IR 2958, 1688 (C=O), 1626, 1361, 1236, 1200, 1019, 776, 742, 699 cm⁻¹; ¹H

NMR (400 MHz, DMSO-*d*₆) δ 10.26 (1H, d, J = 1.7 Hz, ArH), 10.01 (1H, d, J = 1.7 Hz, ArH), 8.69 (1H, dd, J = 8.3, 1.4 Hz, ArH), 8.53 (1H, d, J = 8.9 Hz, ArH), 8.31 (1H, ddd, J = 8.9, 7.0, 1.4 Hz, ArH), 8.10 (1H, t, J = 7.6 Hz, ArH), 7.45-7.33 (5H, m, ArH), 6.54 (2H, s, NCH₂), 2.89 (3H, s, CH₃); ¹³C NMR (101 MHz, DMSO-*d*₆) δ 194.3 (C), 150.2 (CH), 147.7 (CH), 138.1 (C), 137.6 (CH), 133.8 (C), 132.5 (CH), 130.7 (CH), 130.2 (C), 129.2 (C), 129.0 (2 \times CH), 128.8 (CH), 127.3 (2 \times CH), 119.6 (CH), 60.3 (CH₂), 27.3 (CH₃); HRMS (ESI) Exact mass calculated for [C₁₈H₁₆NO]⁺: 262.1226, found 262.1227.

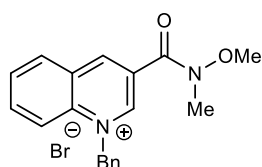
Preparation of substrate 433n



Ethyl 3-quinolinecarboxylate (S9). To a stirred solution of 3-quinolinecarboxylic acid (1.73 g, 10.0 mmol) in EtOH (40 mL) was added SOCl₂ (2.19 mL, 30.0 mmol) dropwise at room temperature. The mixture was stirred at 80 °C for 4 h. The reaction was cooled to room temperature and concentrated *in vacuo*. The residue was dissolved in EtOAc (40 mL), washed with saturated aqueous NaHCO₃ (40 mL), brine (40 mL), dried (Na₂SO₄) and concentrated *in vacuo* to afford the title compound **S9** as a brown solid (1.76 g, 88%). ¹H NMR (400 MHz, CDCl₃) δ 9.45 (1H, d, J = 2.1 Hz, ArH), 8.83 (1H, d, J = 2.1 Hz, ArH), 8.16 (1H, dd, J = 8.5, 1.0 Hz, ArH), 7.93 (1H, dd, J = 8.2, 1.5 Hz, ArH), 7.82 (1H, ddd, J = 8.5, 6.9, 1.5 Hz, ArH), 7.61 (1H, ddd, J = 8.2, 6.9, 1.2 Hz, ArH), 4.47 (2H, q, J = 7.1 Hz, CH₂CH₃), 1.46 (3H, t, J = 7.1 Hz, CH₃); ¹³C NMR (101 MHz, CDCl₃) δ 165.5 (C), 150.2 (CH), 149.9 (C), 138.8 (CH), 131.9 (CH), 129.6 (CH), 129.2 (CH), 127.5 (CH), 127.0 (C), 123.4 (C), 61.6 (CH₂), 14.5 (CH₃). Data consistent with previously reported literature.²¹²

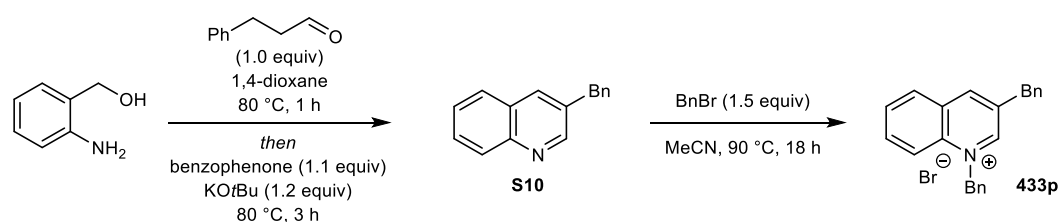
1-Benzyl-3-(ethoxycarbonyl)quinolin-1-ium bromide (433n). The title compound was prepared according to General Procedure A, using **S9** (1.01 g, 5.00 mmol), benzyl bromide (892 μ L, 7.50 mmol) and MeCN (10 mL) to give a light brown solid (1.45 g, 78%). ¹H NMR (400 MHz, CDCl₃) δ 10.51 (1H, s, ArH), 9.54 (1H, s, ArH), 8.81 (1H, d, J = 8.9 Hz, ArH), 8.40-8.36 (1H, m, ArH), 8.25 (1H, ddd, J = 8.8, 7.0, 1.4 Hz, ArH), 7.97 (1H, t, J = 7.6 Hz, ArH), 7.49-7.45

(2H, m, ArH), 7.36-7.30 (3H, m, ArH), 6.91 (2H, s, NCH₂), 4.54 (2H, q, *J* = 7.1 Hz, CH₂CH₃), 1.51 (3H, t, *J* = 7.1 Hz, CH₂CH₃); ¹³C NMR (101 MHz, CDCl₃) δ 161.6 (C), 150.0 (CH), 148.1 (CH), 139.7 (C), 138.5 (CH), 132.5 (C), 132.0 (CH), 131.3 (CH), 129.64 (2 × CH), 129.59 (CH), 129.3 (C), 128.2 (2 × CH), 125.0 (C), 120.7 (CH), 63.7 (CH₂), 62.1 (CH₂), 14.5 (CH₃). Data consistent with previously reported literature.²¹³



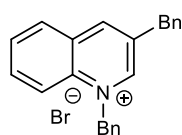
1-Benzyl-3-[methoxy(methyl)carbamoyl]quinolin-1-ium bromide (433o). The title compound was prepared according to General Procedure A, using **S7** (1.08 g, 5.0 mmol), benzyl bromide (892 μL, 7.5 mmol) and MeCN (10 mL) to give an off-white solid (1.53 g, 79%). m.p. 193-194 °C (Et₂O); IR 3036, 2879, 1668 (C=O), 1383, 1363, 1163, 1034, 753, 731, 699 cm⁻¹; ¹H NMR (400 MHz, CDCl₃) δ 10.19 (1H, s, ArH), 9.37 (1H, s, ArH), 8.71 (1H, d, *J* = 9.0 Hz, ArH), 8.37 (1H, dd, *J* = 8.3, 1.4 Hz, ArH), 8.16 (1H, ddd, *J* = 8.8, 7.0, 1.4 Hz, ArH), 7.90 (1H, t, *J* = 7.6, ArH), 7.49-7.45 (2H, m, ArH), 7.31-7.26 (3H, m, ArH), 6.77 (2H, s, NCH₂), 3.75 (3H, s, CH₃), 3.39 (3H, s, CH₃); ¹³C NMR (101 MHz, CDCl₃) δ 162.2 (C), 149.7 (CH), 147.2 (CH), 138.4 (C), 137.6 (CH), 132.4 (C), 131.8 (CH), 130.8 (CH), 129.51 (2 × CH), 129.50 (CH), 129.2 (C), 128.3 (2 × CH), 127.8 (C), 120.0 (CH), 62.8 (CH₂), 61.6 (CH₃), 33.3 (CH₃); HRMS (ESI) Exact mass calculated for [C₁₉H₁₉N₂O₂]⁺: 307.1441, found 307.1448.

Preparation of substrate 433p



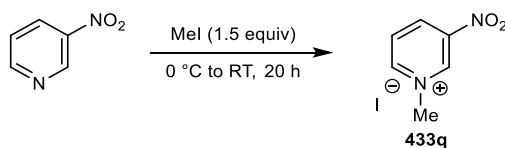
3-Benzylquinoline (S10). The title compound was prepared according to a previously reported procedure,²¹⁴ using 2-aminobenzyl alcohol (315 mg, 2.50 mmol), 3-phenylpropanal (332 μL, 2.50 mmol) and 1,4-dioxane (7.5 mL) to give the title compound **S10** as a brown oil (369 mg, 67%). ¹H NMR (400 MHz, CDCl₃) δ 8.82 (1H, d, *J* = 2.2 Hz, ArH), 8.08 (1H, d, *J* = 8.5 Hz, ArH), 7.88 (1H, dd, *J* = 2.2, 1.0 Hz, ArH), 7.74 (1H, dd, *J* = 8.0, 1.5 Hz, ArH), 7.66 (1H, ddd, *J* = 8.5, 6.9, 1.5 Hz, ArH),

7.54-7.49 (1H, m, ArH), 7.35-7.30 (3H, m, ArH), 7.25-7.22 (2H, m, ArH), 4.18 (2H, s, CH₂); ¹³C NMR (101 MHz, CDCl₃) δ 152.3 (CH), 147.0 (C), 139.8 (C), 135.0 (CH), 134.0 (C), 129.3 (CH), 129.1 (2 × CH), 129.0 (CH), 128.9 (2 × CH), 128.6 (C), 127.6 (CH), 126.8 (CH), 126.7 (CH), 39.4 (CH₂). Data consistent with previously reported literature.²¹⁴



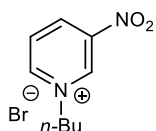
1,3-Dibenzylquinolin-1-ium bromide (433p). The title compound was prepared according to General Procedure A, using **S10** (329 mg, 1.50 mmol), benzyl bromide (268 μL, 2.25 mmol) and MeCN (5 mL) to give a beige solid (292 mg, 50%). m.p. 214-215 °C (Et₂O); IR 2949, 1585, 1528, 1492, 1370, 1217, 1027, 914, 743, 702 cm⁻¹; ¹H NMR (400 MHz, CDCl₃) δ 10.80 (1H, s, ArH), 8.61 (1H, s, ArH), 8.41 (1H, d, *J* = 8.9 Hz, ArH), 8.07 (1H, d, *J* = 8.2 Hz, ArH), 7.98 (1H, t, *J* = 8.0 Hz, ArH), 7.78 (1H, t, *J* = 7.6 Hz, ArH), 7.43-7.31 (6H, m, ArH), 7.28-7.23 (4H, m, ArH), 6.64 (2H, s, NCH₂), 4.53 (2H, s, CCH₂C); ¹³C NMR (101 MHz, CDCl₃) δ 151.7 (CH), 145.7 (CH), 137.5 (C), 137.3 (C), 136.8 (C), 135.2 (CH), 132.9 (C), 130.3 (CH), 130.1 (CH), 130.0 (C), 129.6 (2 × CH), 129.5 (2 × CH), 129.4 (2 × CH), 129.3 (CH), 127.7 (2 × CH), 127.5 (CH), 119.2 (CH), 60.9 (CH₂), 38.4 (CH₂); HRMS (ESI) Exact mass calculated for [C₂₃H₂₀N]⁺: 310.1590, found 310.1593.

1-Methyl-3-nitropyridin-1-ium iodide (433q)

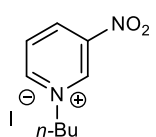


A flask was charged with 3-nitropyridine (745 mg, 6.00 mmol) and purged with argon for 30 min. Methyl iodide (560 μL, 9.00 mmol) was added dropwise at 0 °C and the reaction was stirred at room temperature for 20 h. The mixture was transferred to a beaker that was cooled to 0 °C and stirred vigorously for 5 min. Et₂O (200 mL) was added portionwise, and the mixture was stirred vigorously at 0 °C for 15 min, at which point the product precipitated. The precipitated product was removed by vacuum filtration and washed with ice-cold Et₂O (2 × 30 mL) and dried under vacuum to give the title compound **433q** as a yellow solid (494 mg, 31%). m.p. 223 °C (Et₂O); IR 3013, 1547

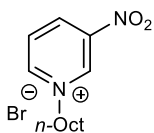
(NO₂), 1403, 1355 (NO₂), 1207, 1180, 1138, 803, 743, 652 cm⁻¹; ¹H NMR (400 MHz, DMSO-*d*₆) δ 10.11 (1H, s, ArH), 9.37-9.30 (2H, m, ArH), 8.42 (1H, dd, *J* = 8.6, 6.1 Hz, ArH), 4.50 (3H, s, CH₃); ¹³C NMR (101 MHz, DMSO-*d*₆) δ 150.3 (CH), 145.9 (C), 143.0 (CH), 139.5 (CH), 128.2 (CH), 48.7 (CH₃); HRMS (ESI) Exact mass calculated for [C₆H₇N₂O₂]⁺: 139.0502, found 139.0508.



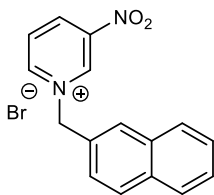
1-Butyl-3-nitropyridin-1-ium bromide (433r). The title compound was prepared according to General Procedure A, using 3-nitropyridine (621 mg, 5.00 mmol), *n*-butyl bromide (805 μL, 7.50 mmol) and MeCN (10 mL) to give a brown solid (163 mg, 12%). m.p. 181-182 °C (Et₂O); IR 3099, 2930, 1650, 1590, 1542 (NO₂), 1361 (NO₂), 1210, 1183, 809, 656 cm⁻¹; ¹H NMR (400 MHz, DMSO-*d*₆) δ 10.20 (1H, s, ArH), 9.50 (1H, d, *J* = 5.9 Hz, ArH), 9.34 (1H, ddd, *J* = 8.7, 2.3, 1.1 Hz, ArH), 8.44 (1H, dd, *J* = 8.6, 6.0 Hz, ArH), 4.80 (2H, t, *J* = 7.5 Hz, NCH₂), 1.98-1.90 (2H, m, CH₂CH₂CH₃), 1.38-1.28 (2H, m, CH₂CH₂CH₃), 0.92 (3H, t, *J* = 7.4 Hz, CH₃); ¹³C NMR (101 MHz, DMSO-*d*₆) δ 149.3 (CH), 146.6 (C), 142.5 (CH), 139.7 (CH), 128.7 (CH), 61.4 (CH₂), 32.7 (CH₂), 18.7 (CH₂), 13.3 (CH₃); HRMS (ESI) Exact mass calculated for [C₉H₁₃N₂O₂]⁺: 181.0972, found 181.0968.



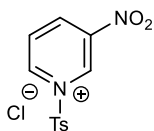
1-Butyl-3-nitropyridin-1-ium iodide (433s). The title compound was prepared according to General Procedure A, using 3-nitropyridine (621 mg, 5.00 mmol), *n*-butyl iodide (854 μL, 7.50 mmol) and MeCN (10 mL) to give an orange solid (616 mg, 40%). m.p. 181-182 °C (Et₂O); IR 3103, 2988, 2934, 1648, 1542 (NO₂), 1359 (NO₂), 1182, 1131, 731, 694 cm⁻¹; ¹H NMR (400 MHz, DMSO-*d*₆) δ 10.18 (1H, s, ArH), 9.44 (1H, dt, *J* = 6.2, 1.2 Hz, ArH), 9.36-9.32 (1H, m, ArH), 8.43 (1H, dd, *J* = 8.6, 6.2 Hz, ArH), 4.77 (2H, t, *J* = 7.5 Hz, NCH₂), 1.98-1.90 (2H, m, CH₂CH₂CH₃), 1.38-1.28 (2H, m, CH₂CH₂CH₃), 0.93 (3H, t, *J* = 7.4 Hz, CH₃); ¹³C NMR (101 MHz, DMSO-*d*₆) δ 149.3 (CH), 146.6 (C), 142.5 (CH), 139.7 (CH), 128.7 (CH), 61.5 (CH₂), 32.7 (CH₂), 18.7 (CH₂), 13.3 (CH₃); HRMS (ESI) Exact mass calculated for [C₉H₁₃N₂O₂]⁺: 181.0972, found 181.0977.



3-Nitro-1-octylpyridin-1-ium bromide (433t). The title compound was prepared according to General Procedure A, using 3-nitropyridine (621 mg, 5.00 mmol), *n*-octyl bromide (1.30 mL, 7.50 mmol) and MeCN (10 mL) to give a brown solid (169 mg, 11%). m.p. 110-111 °C (Et₂O); IR 3094, 2991, 2854, 1650, 1590, 1543 (NO₂), 1465, 1357 (NO₂), 731, 693 cm⁻¹; ¹H NMR (400 MHz, DMSO-*d*₆) δ 10.19 (1H, s, ArH), 9.49 (1H, d, *J* = 6.1 Hz, ArH), 9.35-9.32 (1H, m, ArH), 8.43 (1H, dd, *J* = 8.6, 6.0 Hz, ArH), 4.78 (2H, t, *J* = 7.6 Hz, NCH₂), 1.99-1.91 (2H, m, NCH₂CH₂), 1.34-1.21 (10H, m, (CH₂)₅CH₃), 0.88-0.83 (3H, m, CH₃); ¹³C NMR (101 MHz, DMSO-*d*₆) δ 149.3 (CH), 146.6 (C), 142.4 (CH), 139.7 (CH), 128.7 (CH), 61.6 (CH₂), 31.1 (CH₂), 30.8 (CH₂), 28.42 (CH₂), 28.37 (CH₂), 25.3 (CH₂), 22.0 (CH₂), 13.9 (CH₃); HRMS (ESI) Exact mass calculated for [C₁₃H₂₁N₂O₂]⁺: 237.1598, found 237.1600.

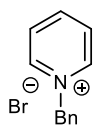


1-(Naphthalen-2-ylmethyl)-3-nitropyridin-1-ium bromide (433u). The title compound was prepared according to General Procedure A, using 3-nitropyridine (1.24 g, 10.0 mmol), 2-(bromomethyl)naphthalene (3.32 g, 15.0 mmol) and MeCN (20 mL) to give a yellow solid (2.72 g, 79%). ¹H NMR (400 MHz, DMSO-*d*₆) δ 10.45 (1H, s, ArH), 9.64 (1H, d, *J* = 6.2 Hz, ArH), 9.40-9.36 (1H, m, ArH), 8.45 (1H, dd, *J* = 8.6, 6.2 Hz, ArH), 8.20 (1H, s, ArH), 8.01 (1H, d, *J* = 8.5 Hz, ArH), 7.98-7.92 (2H, m, ArH), 7.72 (1H, dd, *J* = 8.5, 1.8 Hz, ArH), 7.61-7.56 (2H, m, ArH), 6.29 (2H, s, NCH₂); HRMS (ESI) Exact mass calculated for [C₁₆H₁₃N₂O₂]⁺: 265.0972, found 265.0974. Data consistent with previously reported literature.¹³⁶

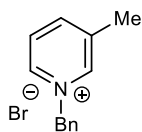


3-Nitro-1-tosylpyridin-1-ium chloride (433v). The title compound was prepared according to General Procedure A, using 3-nitropyridine (620 mg, 5.0 mmol), *p*-toluenesulfonyl chloride (1.43 g, 7.5 mmol) and MeCN (10 mL) to give an off-white solid (100 mg, 6%). m.p. 161-162 °C (Et₂O); IR 3066, 1630, 1545, 1361, 1219, 1162, 998, 724, 700, 617 cm⁻¹; ¹H NMR (400 MHz, DMSO-*d*₆) δ 9.38 (1H, d, *J* = 2.7 Hz, ArH), 8.98 (1H, dd, *J* = 4.8, 1.5 Hz, ArH), 8.61 (1H, ddd, *J* = 8.5, 2.7, 1.5 Hz, ArH), 7.74 (1H, dd, *J* = 8.5, 4.8 Hz, ArH), 7.49 (2H, d, *J* = 8.0 Hz, ArH), 7.12 (2H, d, *J* = 8.0 Hz, ArH), 2.29 (3H, s, CH₃); ¹³C NMR (101 MHz, DMSO-*d*₆) δ

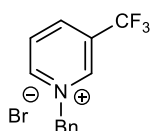
155.1 (CH), 145.4 (C), 144.5 (CH), 144.4 (C), 137.8 (C), 131.6 (CH), 128.1 (2 × CH), 125.5 (2 × CH), 124.6 (CH), 20.8 (CH₃). HRMS (ESI) Exact mass calculated for [C₁₂H₁₁N₂O₄S]⁺: 279.0434, found 279.0436.



1-Benzylpyridin-1-ium bromide (433w). The title compound was prepared according to General Procedure A, using pyridine (809 μL, 10.0 mmol), benzyl bromide (1.78 mL, 15.0 mmol) and MeCN (20 mL) to give an off-white solid (2.17 g, 87%). ¹H NMR (400 MHz, CDCl₃) δ 9.61 (2H, d, *J* = 5.9 Hz, ArH), 8.43 (1H, t, *J* = 7.7 Hz, ArH), 8.00 (2H, t, *J* = 7.0 Hz, ArH), 7.68-7.64 (2H, m, ArH), 7.28-7.25 (3H, m, ArH), 6.26 (2H, s, NCH₂); ¹³C NMR (101 MHz, CDCl₃) δ 145.4 (CH), 145.0 (2 × CH), 133.0 (C), 129.9 (CH), 129.53 (2 × CH), 129.50 (2 × CH), 128.3 (2 × CH), 63.8 (CH₂). Data consistent with previously reported literature.²¹⁵

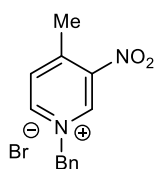


1-Benzyl-3-methylpyridin-1-ium bromide (433x). The title compound was prepared according to General Procedure A, using 3-methylpyridine (973 μL, 10.0 mmol), benzyl bromide (1.78 mL, 15.0 mmol) and MeCN (20 mL) to give an off-white solid (1.88 g, 71%). m.p. 104-105 °C (Et₂O); IR 3450, 3388, 3016, 1625, 1499, 1205, 1146, 775, 730, 707 cm⁻¹; ¹H NMR (400 MHz, CDCl₃) δ 9.55 (1H, s, ArH), 9.40 (1H, d, *J* = 6.1 Hz, ArH), 8.16 (1H, d, *J* = 7.9 Hz, ArH), 7.88 (1H, dd, *J* = 7.9, 6.1 Hz, ArH), 7.72-7.67 (2H, m, ArH), 7.32-7.28 (3H, m, ArH), 6.21 (2H, s, NCH₂), 2.53 (3H, s, CH₃); ¹³C NMR (101 MHz, CDCl₃) δ 145.8 (CH), 144.6 (CH), 142.2 (CH), 139.7 (C), 133.2 (C), 129.9 (CH), 129.7 (2 × CH), 129.6 (2 × CH), 127.7 (CH), 63.7 (CH₂), 18.8 (CH₃); HRMS (ESI) Exact mass calculated for [C₁₃H₁₄N]⁺: 184.1121, found 184.1128.



1-Benzyl-3-(trifluoromethyl)pyridin-1-ium bromide (433y). The title compound was prepared according to General Procedure A, using 3-(trifluoromethyl)pyridine (441 mg, 3.0 mmol), benzyl bromide (535 μL, 4.5 mmol) and MeCN (8 mL) to give an off-white white solid (949 mg, 99%). ¹H NMR (500 MHz, CDCl₃) δ 10.13 (1H, dd, *J* = 6.2, 1.3 Hz, ArH), 9.95 (1H, s, ArH), 8.64-8.61 (1H, m, ArH), 8.39 (1H, dd, *J* = 8.1, 6.2, ArH), 7.80-7.73 (2H, m, ArH), 7.40-7.35 (3H,

m, ArH), 6.57 (2H, s, NCH₂); ¹³C NMR (126 MHz, CDCl₃) δ 149.2 (CH), 142.5 (CH), 142.2 (CH), 132.3 (C), 130.9 (q, J_{C-F} = 36.9 Hz, C), 130.5 (CH), 130.1 (2 × CH), 129.9 (2 × CH), 129.4 (CH), 121.1 (q, J_{C-F} = 274.4 Hz, C), 64.9 (CH₂). ¹⁹F NMR (376 MHz, CDCl₃) δ -62.3 (s, 3 × F). Data consistent with previously reported literature.²¹⁶

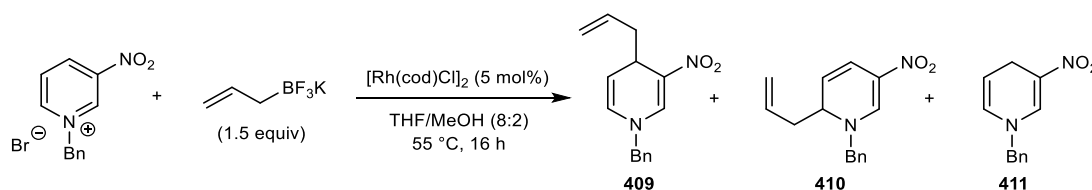


1-Benzyl-4-methyl-3-nitropyridin-1-ium bromide (433z). The title compound was prepared according to General Procedure A, using 4-methyl-3-nitropyridine (562 μL, 5.00 mmol), benzyl bromide (892 μL, 7.50 mmol) and MeCN (10 mL) to give an olive green solid (1.14 g, 74%).

m.p. 157-158 °C (Et₂O); IR 2974, 1644, 1565, 1536 (NO₂), 1453, 1349 (NO₂), 1114, 1053, 743, 704 cm⁻¹; ¹H NMR (400 MHz, DMSO-*d*₆) δ 10.17 (1H, s, ArH), 9.38 (1H, dd, *J* = 6.4, 1.3 Hz, ArH), 8.37 (1H, d, *J* = 6.4 Hz, ArH), 7.63-7.60 (2H, m, ArH), 7.48-7.42 (3H, m, ArH), 6.00 (2H, s, NCH₂), 2.85 (3H, s, CH₃); ¹³C NMR (101 MHz, DMSO-*d*₆) δ 154.4 (C), 146.8 (C), 146.4 (CH), 142.7 (CH), 133.7 (C), 131.9 (CH), 129.5 (CH), 129.14 (2 × CH), 129.05 (2 × CH), 63.0 (CH₂), 20.7 (CH₃); HRMS (ESI) Exact mass calculated for [C₁₃H₁₃N₂O₂]⁺: 229.0972, found 229.0977.

3.4 Gold-Catalysed Nucleophilic Allylation of Azinium Ions

4-Allyl-1-benzyl-3-nitro-1,4-dihydropyridine (409), 2-allyl-1-benzyl-5-nitro-1,2-dihydropyridine (410) and 1-benzyl-3-nitro-1,4-dihydropyridine (411)



An oven-dried microwave vial was fitted with a stirrer bar and charged with 1-benzyl-3-nitropyridin-1-ium bromide (88.5 mg, 0.30 mmol), potassium allyltrifluoroborate (66.6 mg, 0.45 mmol) and [Rh(cod)Cl]₂ (7.4 mg, 0.015 mmol). The vial was sealed with a septum-lined cap and purged with argon for 30 mins. Anhydrous THF (2.4 mL) and MeOH (0.6 mL) both of which were freshly deoxygenated separately (purging with argon for 30 min) were added. The mixture was stirred at 55 °C for 16 h. The reaction was

cooled to room temperature, diluted with Et₂O (5 mL), passed through a plug of silica gel (8 cm in height and 2 cm wide) using Et₂O as the eluent (20 mL) and concentrated *in vacuo*. Purification by column chromatography (10% EtOAc/*n*-pentane) gave 4-allylated product **409** (18.9 mg, 25%) as a red oil, followed by 6-allylated product **410** (17.0 mg, 22%) as a yellow oil, followed by reduced product **411** (10.6 mg, 14%) as an orange oil.

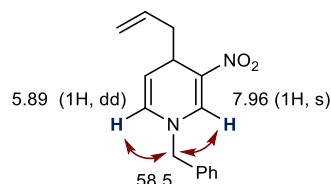
Data of major regioisomer 409: R_f = 0.56 (30% EtOAc/petroleum ether); IR 2918, 1672, 1593 (NO₂), 1475, 1361 (NO₂), 1271, 1211, 1171, 1028, 698 cm⁻¹; ¹H NMR (400 MHz, CDCl₃) δ 7.96 (1H, s, NCH=C), 7.42-7.35 (3H, m, ArH), 7.23-7.21 (2H, m, ArH), 5.89 (1H, dd, *J* = 7.9, 1.2 Hz, NCH=CH), 5.73 (1H, dddd, *J* = 16.8, 10.3, 8.3, 6.5 Hz, CH₂=CH), 5.13 (1H, dd, *J* = 7.9, 5.1 Hz, NCH=CH), 5.07-4.99 (2H, m, CH₂=CH), 4.47 (2H, s, NCH₂), 3.99-3.95 (1H, m, CHCN), 2.49-2.42 (1H, m, CH_aH_bCH), 2.29-2.23 (1H, m, CH_aH_bCH); ¹³C NMR (101 MHz, CDCl₃) δ 140.7 (CH), 135.3 (C), 134.4 (CH), 129.3 (2 × CH), 128.7 (CH), 127.5 (2 × CH), 127.1 (CH), 124.9 (C), 118.2 (CH₂), 112.8 (CH), 58.5 (CH₂), 39.3 (CH₂), 33.7 (CH). HRMS (ESI) Exact mass calculated for [C₁₅H₁₆N₂NaO₂]⁺ [M+Na]⁺ : 279.1104, found 279.1106.

Data of minor regioisomer 410: R_f = 0.48 (30% EtOAc/petroleum ether); IR 3063, 1633, 1575 (NO₂), 1492, 1420, 1288, 1172, 916, 728, 698 cm⁻¹; ¹H NMR (400 MHz, CDCl₃) δ 8.14 (1H, s, NCH=C), 7.45-7.37 (3H, m, ArH), 7.29-7.25 (2H, m, ArH), 6.84 (1H, dd, *J* = 10.3, 1.7 Hz, CHCH=CH), 5.82 (1H, dddd, *J* = 16.8, 10.4, 8.0, 6.5 Hz, CH₂=CH), 5.20-5.14 (2H, m, CH₂=CH), 5.07 (1H, dd, *J* = 10.3, 4.8 Hz, CHCH=CH), 4.56 (1H, d, *J* = 14.9 Hz, NCH_aH_b), 4.50 (1H, d, *J* = 14.9 Hz, NCH_aH_b), 4.21-4.17 (1H, m, CHN), 2.51-2.43 (1H, m, CH_aH_bCH), 2.32-2.24 (1H, m, CH_aH_bCH); ¹³C NMR (101 MHz, CDCl₃) δ 146.8 (CH), 133.8 (C), 131.6 (CH), 129.5 (2 × CH), 129.1 (CH), 128.0 (2 × CH), 123.4 (C), 120.0 (CH₂), 119.3 (CH), 113.8 (CH), 59.0 (CH₂), 57.6 (CH), 39.1 (CH₂). HRMS (ESI) Exact mass calculated for [C₁₅H₁₆N₂NaO₂]⁺ [M+Na]⁺ : 279.1104, found 279.1106.

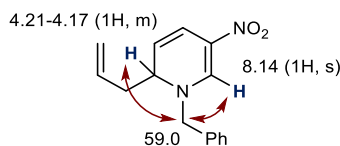
Data of reduced product 411: R_f = 0.35 (30% EtOAc/petroleum ether); IR 2917, 2849, 1672, 1593 (NO₂), 1475, 1271, 1211, 1171, 1083, 698 cm⁻¹; ¹H NMR (400 MHz, CDCl₃) δ 7.90 (1H, d, *J* = 1.6 Hz, NCH=C), 7.43-7.34 (3H, m, ArH), 7.26-7.23 (2H, m, ArH), 5.81-5.77 (1H, m, NCH=CH), 5.23-5.18 (1H, m, NCH=CH), 4.44 (2H, s, NCH₂), 3.48 (2H, dd, *J* = 3.7, 1.7 Hz, CHCH₂); ¹³C NMR (101 MHz, CDCl₃) δ 140.6 (CH), 135.2 (C), 129.5 (C), 129.4 (2 × CH), 128.8 (CH), 127.5 (2 × CH), 127.3 (CH), 110.4 (CH), 58.5

(CH₂), 24.0 (CH₂). HRMS (ESI) Exact mass calculated for [C₁₂H₁₂N₂NaO₂]⁺ [M+Na]⁺ : 239.0791, found 239.0797.

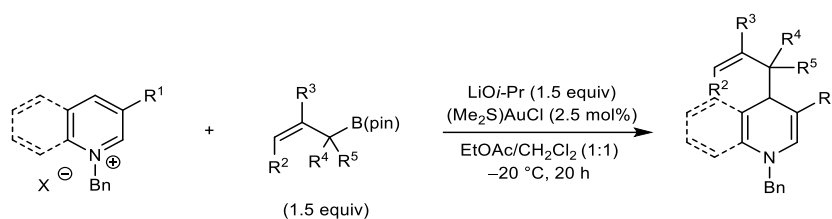
Due to the structural similarity of products **409** and **410**, the exact configuration of the two compounds was assigned based on their HMBC 2D NMR spectra. In the HMBC 2D NMR of product **409**, the benzyl methylene group at 58.5 ppm correlates with the signals at 7.96 ppm and 5.89 ppm. Only structure **409** is compatible with this experimental data.



In the HMBC 2D NMR of product **410**, the benzyl methylene group at 59.0 ppm correlates with the signals at 8.14 ppm and 4.21-4.17 ppm. Only structure **410** is compatible with this experimental data.

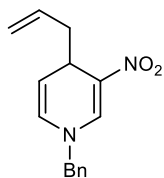


General Procedure B: Gold-Catalysed Allylation of Azinium Salts

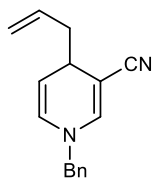


An oven-dried microwave vial fitted with a stirrer bar was charged with the appropriate azinium salt (0.50 mmol), (Me₂S)AuCl (3.7 mg, 0.0125 mmol) and LiO*i*-Pr (49.5 mg, 0.75 mmol). The vial was sealed with a septum-lined cap and EtOAc/CH₂Cl₂ (1:1) (4.0 mL) (both of which were undried, obtained from commercial vendors and used without further purification) was added. The mixture was stirred at -20 °C for 5 min and a solution of the appropriate allyl pinacolboronate (0.75 mmol) in 1.0 mL of EtOAc/CH₂Cl₂ (1:1) was added dropwise. The resulting solution was stirred at -20 °C for 20 h. The reaction was warmed to room temperature and then passed through a plug

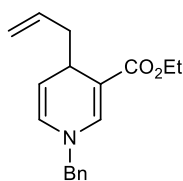
of silica (8 cm in height and 2 cm wide) using Et₂O (40 mL) as the eluent and the filtrate was concentrated *in vacuo*. The residue was purified by column chromatography (EtOAc/*n*-pentane) to give the allylated product.



4-Allyl-1-benzyl-3-nitro-1,4-dihydropyridine (409). The title compound was prepared according to a slight modification of General Procedure B (in that the reaction time was 1.5 h), using azinium salt **408** (148 mg, 0.50 mmol) and allyl pinacolboronate **414** (141 μ L, 0.75 mmol), and purified by column chromatography (5% EtOAc/*n*-pentane) to give a red oil (115 mg, 90%). Data for **409**: see above (page 147).

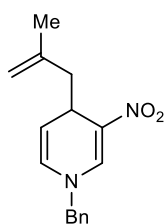


4-Allyl-1-benzyl-1,4-dihydropyridine-3-carbonitrile (423a). The title compound was prepared according to General Procedure B, using azinium salt **433a** (138 mg, 0.50 mmol) and allyl pinacolboronate **414** (141 μ L, 0.75 mmol), and purified by column chromatography (3% EtOAc/*n*-pentane) to give a green oil (77.4 mg, 65%). $R_f = 0.38$ (20% EtOAc/petroleum ether); IR 2922, 2190 (C \equiv N), 1672, 1592, 1409, 1179, 1077, 913, 732, 699 cm^{-1} ; ^1H NMR (400 MHz, CDCl_3) δ 7.40-7.30 (3H, m, ArH), 7.22-7.18 (2H, m, ArH), 6.62 (1H, d, $J = 1.6$ Hz, NCH=C), 5.87-5.76 (2H, m, CH₂=CH and NCH=CH), 5.15-5.08 (2H, m, CH₂=CH), 4.67 (1H, dd, $J = 8.1, 4.1$ Hz, NCH=CH), 4.28 (2H, s, NCH₂), 3.36-3.31 (1H, m, CH₂CH), 2.30 (2H, t, $J = 6.1$ Hz, CH₂CH); ^{13}C NMR (101 MHz, CDCl_3) δ 143.2 (CH), 136.5 (C), 134.4 (CH), 129.0 (2 \times CH), 128.3 (CH), 128.2 (CH), 127.2 (2 \times CH), 121.2 (C), 117.9 (CH₂), 105.7 (CH), 82.4 (C), 57.5 (CH₂), 42.4 (CH₂), 33.3 (CH); HRMS (ESI) Exact mass calculated for $[\text{C}_{16}\text{H}_{16}\text{N}_2\text{Na}]^+$ $[\text{M}+\text{Na}]^+$: 259.1206, found 259.1201.



Ethyl 4-allyl-1-benzyl-1,4-dihydropyridine-3-carboxylate (423b). The title compound was prepared according to General Procedure B, using azinium salt **433d** (161 mg, 0.50 mmol) and allyl pinacolboronate **414** (141 μ L, 0.75 mmol), and purified by column chromatography (5% EtOAc/*n*-pentane) to give a green oil (57.9 mg, 41%). $R_f = 0.62$ (20% EtOAc/petroleum ether); IR 2977, 1680 (C=O), 1587, 1397, 1276, 1203, 1160, 1027, 909, 730 cm^{-1} ; ^1H

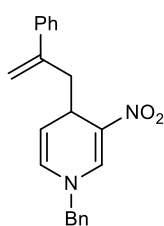
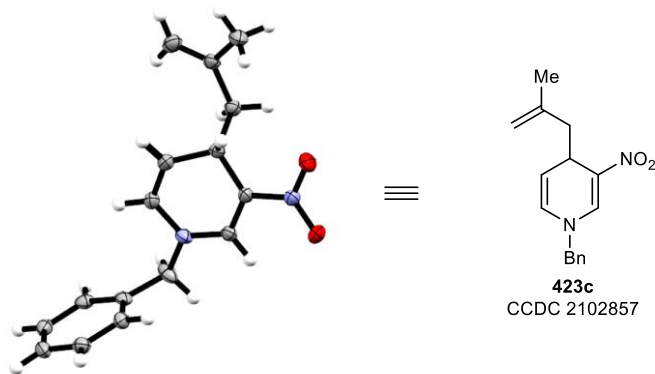
NMR (400 MHz, CDCl₃) δ 7.39-7.27 (3H, m, ArH), 7.25 (1H, d, *J* = 1.7 Hz, NCH=C), 7.24-7.20 (2H, m, ArH), 5.86-5.75 (2H, m, CH₂=CH and NCH=CH), 5.03-4.96 (2H, m, CH₂=CH), 4.80 (1H, dd, *J* = 7.9, 5.0 Hz, NCH=CH), 4.35 (2H, s, NCH₂), 4.22-4.09 (2H, m, OCH₂), 3.54-3.48 (1H, m, CH₂CH), 2.30-2.14 (2H, m, CH₂CH), 1.26 (3H, t, *J* = 7.1 Hz, CH₃); ¹³C NMR (101 MHz, CDCl₃) δ 168.3 (C), 141.7 (CH), 137.4 (C), 136.0 (CH), 128.9 (2 × CH), 128.2 (CH), 127.9 (CH), 127.1 (2 × CH), 116.6 (CH₂), 107.9 (CH), 101.2 (C), 59.5 (CH₂), 57.7 (CH₂), 42.7 (CH₂), 32.0 (CH), 14.6 (CH₃); HRMS (ESI) Exact mass calculated for [C₁₈H₂₁NNaO₂]⁺ [M+Na]⁺: 306.1464, found 306.1461.



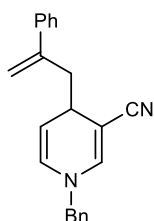
1-Benzyl-4-(2-methylallyl)-3-nitro-1,4-dihydropyridine (423c). The title compound was prepared according to a slight modification of General Procedure A (in that the reaction time was 4.5 h), using azinium salt **408** (148 mg, 0.50 mmol) and allyl pinacolboronate **418a** (137 mg, 0.75 mmol), and purified by column chromatography (5% EtOAc/*n*-

pentane) to give a red solid (133 mg, 98%). *R_f* = 0.40 (20% EtOAc/petroleum ether); m.p. 69-70 °C (Et₂O); IR 2922, 1667, 1583 (NO₂), 1471, 1396 (NO₂), 1173, 1156, 1048, 741, 697 cm⁻¹; ¹H NMR (400 MHz, CDCl₃) δ 7.95 (1H, s, NCH=C), 7.42-7.33 (3H, m, ArH), 7.24-7.20 (2H, m, ArH), 5.86 (1H, dt, *J* = 7.9, 1.2 Hz, NCH=CH), 5.19 (1H, dd, *J* = 7.9, 5.0 Hz, NCH=CH), 4.82-4.80 (1H, m, CH_aH_b=C), 4.65-4.63 (1H, m, CH_aH_b=C), 4.49 (2H, s, NCH₂), 3.99 (1H, ddd, *J* = 8.7, 5.0, 3.5 Hz, CH₂CH), 2.47-2.43 (1H, m, CH_aH_bCH), 2.20 (1H, dd, *J* = 13.1, 8.8 Hz, CH_aH_bCH), 1.76 (3H, s, =CCH₃); ¹³C NMR (101 MHz, CDCl₃) δ 141.8 (C), 140.3 (CH), 135.4 (C), 129.3 (2 × CH), 128.7 (CH), 127.4 (2 × CH), 126.4 (CH), 125.8 (C), 113.4 (CH₂), 113.1 (CH), 58.4 (CH₂), 44.3 (CH₂), 32.3 (CH), 22.8 (CH₃); HRMS (ESI) Exact mass calculated for [C₁₆H₁₈N₂NaO₂]⁺ [M+Na]⁺: 293.1260, found 293.1256.

Crystals suitable for X-ray analysis were prepared by slow diffusion of petroleum ether into a solution of **418a** in CH₂Cl₂.

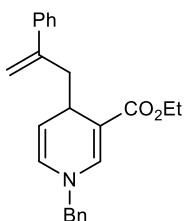


1-Benzyl-3-nitro-4-(2-phenylallyl)-1,4-dihydropyridine (423d). The title compound was prepared according to General Procedure B, using azinium salt **408** (148 mg, 0.50 mmol) and allyl pinacolboronate **418b** (183 mg, 0.75 mmol), and purified by column chromatography (5% EtOAc/*n*-pentane) to give a red oil (137 mg, 82%). $R_f = 0.32$ (20% EtOAc/petroleum ether); IR 2926, 1666, 1586 (NO₂), 1476, 1302 (NO₂), 1262, 1173, 905, 728, 696 cm⁻¹; ¹H NMR (400 MHz, CDCl₃) δ 7.84 (1H, t, $J = 1.1$ Hz, NCH=C), 7.49-7.46 (2H, m, ArH), 7.42-7.35 (3H, m, ArH), 7.35-7.26 (3H, m, ArH), 7.21-7.18 (2H, m, ArH), 5.77 (1H, dt, $J = 7.9, 1.2$ Hz, NCH=CH), 5.38 (1H, d, $J = 1.6$ Hz, CH_aH_b=C), 5.05 (1H, dd, $J = 7.9, 5.0$ Hz, NCH=CH), 5.01 (1H, d, $J = 1.6$ Hz, CH_aH_b=C), 4.42 (2H, s, NCH₂), 3.97 (1H, ddd, $J = 8.6, 4.9, 3.4$ Hz, CH₂CH), 3.19-3.14 (1H, m, CH_aH_bCH), 2.61 (1H, dd, $J = 13.5, 9.0$ Hz, CH_aH_bCH); ¹³C NMR (101 MHz, CDCl₃) δ 144.4 (C), 140.4 (C), 140.3 (CH), 135.2 (C), 129.3 (2 \times CH), 128.8 (CH), 128.4 (2 \times CH), 127.7 (CH), 127.5 (2 \times CH), 126.5 (2 \times CH), 126.3 (CH), 125.6 (C), 115.6 (CH₂), 112.8 (CH), 58.4 (CH₂), 41.4 (CH₂), 32.7 (CH); HRMS (ESI) Exact mass calculated for [C₂₁H₂₀N₂NaO₂]⁺ [M+Na]⁺: 355.1417, found 355.1417.



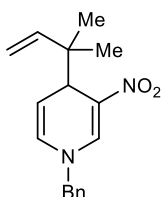
1-Benzyl-4-(2-phenylallyl)-1,4-dihydropyridine-3-carbonitrile (423e). The title compound was prepared according to General Procedure B, using azinium salt **433a** (138 mg, 0.50 mmol) and allyl pinacolboronate **418b** (183 mg, 0.75 mmol), and purified by column chromatography (2 to 5% EtOAc/*n*-pentane) to give a yellow oil (136 mg, 87%). $R_f = 0.56$ (20% EtOAc/petroleum ether); IR 2928, 2190 (C \equiv N), 1672, 1591, 1409, 1179, 1119, 1028,

902, 700 cm^{-1} ; ^1H NMR (400 MHz, CDCl_3) δ 7.43-7.24 (8H, m, ArH), 7.19-7.15 (2H, m, ArH), 6.59 (1H, d, $J = 1.6$ Hz, NCH=C), 5.71 (1H, dt, $J = 8.1, 1.3$ Hz, NCH=CH), 5.38-5.36 (1H, m, $\text{CH}_a\text{H}_b=\text{C}$), 5.11-5.09 (1H, m, $\text{CH}_a\text{H}_b=\text{C}$), 4.63 (1H, dd, $J = 8.1, 4.1$ Hz, NCH=CH), 4.27 (2H, s, NCH_2), 3.32-3.26 (1H, m, CH_2CH), 3.01 (1H, ddd, $J = 13.8, 4.1, 1.3$ Hz, $\text{CH}_a\text{H}_b\text{CH}$), 2.62 (1H, dd, $J = 13.8, 9.2$ Hz, $\text{CH}_a\text{H}_b\text{CH}$); ^{13}C NMR (101 MHz, CDCl_3) δ 144.3 (C), 142.9 (CH), 140.7 (C), 136.5 (C), 129.1 ($2 \times \text{CH}$), 128.5 ($2 \times \text{CH}$), 128.3 (CH), 127.7 (CH), 127.6 (CH), 127.3 ($2 \times \text{CH}$), 126.5 ($2 \times \text{CH}$), 121.3 (C), 115.7 (CH_2), 105.7 (CH), 82.9 (C), 57.5 (CH_2), 45.1 (CH_2), 32.0 (CH); HRMS (ESI) Exact mass calculated for $[\text{C}_{22}\text{H}_{20}\text{N}_2\text{Na}]^+$ $[\text{M}+\text{Na}]^+$: 335.1519, found 335.1517.



Ethyl 1-benzyl-4-(2-phenylallyl)-1,4-dihydropyridine-3-carboxylate

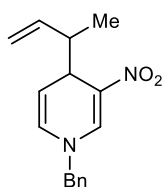
(423f). The title compound was prepared according to General Procedure B, using azinium salt **433d** (161 mg, 0.50 mmol) and allyl pinacolboronate **418b** (183 mg, 0.75 mmol), and purified by column chromatography (1 to 3% EtOAc/*n*-pentane) to give a yellow oil (134 mg, 75%). $R_f = 0.65$ (20% EtOAc/petroleum ether); IR 2979, 1678 (C=O), 1585, 1398, 1204, 1160, 1073, 907, 727, 695 cm^{-1} ; ^1H NMR (500 MHz, CDCl_3) δ 7.55-7.52 (2H, m, ArH), 7.39-7.28 (5H, m, ArH), 7.27-7.25 (1H, m, ArH), 7.24-7.22 (2H, m, ArH), 7.21 (1H, s, NCH=C), 5.77 (1H, dd, $J = 7.9, 1.6$ Hz, NCH=CH), 5.38-5.37 (1H, m, $\text{CH}_a\text{H}_b=\text{C}$), 5.01-5.00 (1H, m, $\text{CH}_a\text{H}_b=\text{C}$), 4.75 (1H, dd, $J = 7.9, 5.0$ Hz, NCH=CH), 4.37 (2H, s, NCH_2), 4.23-4.14 (2H, m, OCH_2), 3.52 (1H, ddd, $J = 10.2, 5.0, 3.6$ Hz, CH_2CH), 3.05 (1H, dd, $J = 13.3, 3.7$ Hz, $\text{CH}_a\text{H}_b\text{CH}$), 2.43 (1H, dd, $J = 13.3, 10.0$ Hz, $\text{CH}_a\text{H}_b\text{CH}$), 1.30 (3H, t, $J = 7.1$ Hz, CH_2CH_3); ^{13}C NMR (126 MHz, CDCl_3) δ 168.5 (C), 144.7 (C), 141.5 (CH), 140.8 (C), 137.4 (C), 129.0 ($2 \times \text{CH}$), 128.3 ($2 \times \text{CH}$), 127.9 (CH), 127.5 (CH), 127.4 (CH), 127.1 ($2 \times \text{CH}$), 126.5 ($2 \times \text{CH}$), 114.5 (CH_2), 107.9 (CH), 101.9 (C), 59.6 (CH_2), 57.7 (CH_2), 44.9 (CH_2), 30.8 (CH), 14.7 (CH_3); HRMS (ESI) Exact mass calculated for $[\text{C}_{24}\text{H}_{25}\text{NNaO}_2]^+$ $[\text{M}+\text{Na}]^+$: 382.1777, found 382.1776.



1-Benzyl-4-(2-methylbut-3-en-2-yl)-3-nitro-1,4-dihydropyridine

(423g). The title compound was prepared according to General Procedure B, using azinium salt **408** (148 mg, 0.50 mmol) and allyl pinacolboronate **418c** (147 mg, 0.75 mmol), and purified by column chromatography (5%

EtOAc/*n*-pentane) to give a red oil (77.3 mg, 54%). $R_f = 0.45$ (20% EtOAc/petroleum ether); IR 2965, 1660, 1581 (NO₂), 1350 (NO₂), 1265, 1176, 1073, 909, 732, 699 cm⁻¹; ¹H NMR (400 MHz, CDCl₃) δ 8.08 (1H, t, $J = 1.5$ Hz, NCH=C), 7.42-7.35 (3H, m, ArH), 7.24-7.21 (2H, m, ArH), 6.07 (1H, dd, $J = 7.6, 1.4$ Hz, NCH=CH), 5.77 (1H, dd, $J = 17.4, 10.8$ Hz, CH₂=CH), 5.15 (1H, dd, $J = 7.6, 6.3$ Hz, NCH=CH), 4.89-4.83 (2H, m, CH₂=CH), 4.50 (2H, s, NCH₂), 3.91 (1H, dd, $J = 6.3, 1.6$ Hz, CCHC), 0.91 (3H, s, CH₃), 0.89 (3H, s, CH₃); ¹³C NMR (101 MHz, CDCl₃) δ 145.1 (CH), 140.6 (CH), 135.3 (C), 129.3 (2 \times CH), 128.8 (CH), 128.4 (CH), 127.8 (2 \times CH), 123.2 (C), 112.3 (CH₂), 109.4 (CH), 58.8 (CH₂), 45.1 (C), 41.9 (CH), 22.9 (2 \times CH₃); HRMS (ESI) Exact mass calculated for [C₁₇H₂₀N₂NaO₂]⁺ [M+Na]⁺: 307.1417, found 307.1414.



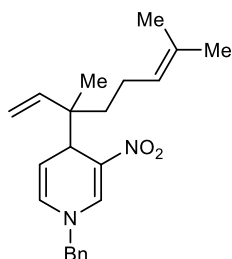
1-Benzyl-4-(but-3-en-2-yl)-3-nitro-1,4-dihydropyridine (423h). The title compound was prepared according to General Procedure B, using azinium salt **408** (148 mg, 0.50 mmol) and allyl pinacolboronate *rac*-**418d** (137 mg, 0.75 mmol), and purified by column chromatography (5%

EtOAc/*n*-pentane) to give a 2:1 mixture of inseparable diastereomers as a red solid (76.5 mg, 57%). $R_f = 0.44$ (20% EtOAc/petroleum ether); m.p. 79-80 °C (Et₂O); IR 3069, 2963, 1666, 1576 (NO₂), 1314 (NO₂), 1263, 1172, 913, 737, 696 cm⁻¹; HRMS (ESI) Exact mass calculated for [C₁₆H₁₈N₂NaO₂]⁺ [M+Na]⁺: 293.1260, found 293.1266.

NMR data of major diastereomer: ¹H NMR (400 MHz, CDCl₃) δ 7.99 (1H, t, $J = 1.3$ Hz, NCH=C), 7.42-7.32 (3H, m, ArH), 7.24-7.20 (2H, m, ArH), 5.96-5.93 (1H, m, NCH=CH), 5.64 (1H, ddd, $J = 17.0, 10.4, 8.3$ Hz, CH₂=CH), 5.15 (1H, dd, $J = 7.9, 5.4$ Hz, NCH=CH), 4.97-4.90 (2H, m, CH₂=CH), 4.46 (2H, s, NCH₂), 3.89-3.86 (1H, m, CHCHC), 2.73-2.64 (1H, m, CHCH₃), 1.01 (3H, d, $J = 7.1$ Hz, CH₃); ¹³C NMR (101 MHz, CDCl₃) δ 140.75 (CH), 140.5 (CH), 135.30 (C), 129.2 (2 \times CH), 128.69 (CH), 128.2 (CH), 127.6 (2 \times CH), 124.9 (C), 116.1 (CH₂), 109.1 (CH), 58.58 (CH₂), 40.5 (CH), 39.4 (CH₂), 15.9 (CH₃).

Characteristic NMR data of minor diastereomer: ¹H NMR (400 MHz, CDCl₃) δ 8.04 (1H, t, $J = 1.2$ Hz, NCH=C), 5.99-5.96 (1H, m, NCH=CH), 5.81 (1H, ddd, $J = 16.9, 10.6, 6.2$ Hz, CH₂=CH), 5.07-5.01 (3H, m, NCH=CH and CH₂=CH), 4.48 (2H, s, NCH₂), 4.01-3.98 (1H, m, CHCHC), 2.81-2.74 (1H, m, CHCH₃), 0.93 (3H, d, $J = 7.1$ Hz, CH₃); ¹³C NMR (101 MHz, CDCl₃) δ 140.83 (CH), 140.4 (CH), 135.27 (C), 129.3 (2 \times CH),

128.74 (CH), 127.6 (2 × CH), 124.4 (C), 114.1 (CH₂), 109.8 (CH), 58.55 (CH₂), 38.94 (CH), 38.86 (CH₂), 13.4 (CH₃).

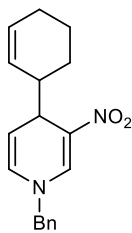


1-Benzyl-4-(3,7-dimethylocta-1,6-dien-3-yl)-3-nitro-1,4-dihydropyridine (423i). The title compound was prepared according to General Procedure B, using azinium salt **408** (148 mg, 0.50 mmol) and allyl pinacolboronate *rac*-**418e** (198 mg, 0.75 mmol), and purified by column chromatography (5% EtOAc/*n*-pentane) to give a 2.1:1 mixture of inseparable diastereomers as a red oil (44.0 mg, 25%).

$R_f = 0.52$ (20% EtOAc/petroleum ether); IR 2922, 1661, 1581 (NO₂), 1375 (NO₂), 1268, 1176, 1072, 909, 730, 698 cm⁻¹; HRMS (ESI) Exact mass calculated for [C₂₂H₂₈N₂NaO₂]⁺ [M+Na]⁺: 375.2043, found 375.2042.

NMR data of major diastereomer: ¹H NMR (400 MHz, CDCl₃) δ 8.07 (1H, t, $J = 1.5$ Hz, NCH=C), 7.41-7.33 (3H, m, ArH), 7.24-7.21 (2H, m, ArH), 6.09 (1H, dd, $J = 7.6, 1.4$ Hz, NCH=CH), 5.76 (1H, dd, $J = 17.4, 10.8$ Hz, CH₂=CH), 5.14 (1H, dd, $J = 7.6, 6.3$ Hz, NCH=CH), 5.06-5.01 (1H, m, CH₂CH=C), 4.90 (1H, dd, $J = 10.8, 1.5$ Hz, CH_aH_b=CH), 4.85 (1H, dd, $J = 17.4, 1.5$ Hz, CH_aH_b=CH), 4.50 (2H, s, NCH₂), 3.99-3.95 (1H, m, CCHC), 1.85-1.77 (2H, m, CCH₂CH₂), 1.66 (3H, s, =C(CH₃)), 1.56 (3H, s, =C(CH₃)), 1.42-1.27 (2H, m, CCH₂CH₂), 0.85 (3H, s, CHCCH₃); ¹³C NMR (101 MHz, CDCl₃) δ 143.5 (CH), 140.5 (CH), 135.4 (C), 131.4 (C), 129.27 (2 × CH), 128.78 (CH), 128.7 (CH), 127.8 (2 × CH), 124.9 (CH), 123.1 (C), 113.6 (CH₂), 108.7 (CH), 58.8 (CH₂), 48.7 (C), 42.0 (CH), 36.5 (CH₂), 25.9 (CH₃), 22.9 (CH₂), 17.8 (CH₃), 16.9 (CH₃).

Characteristic NMR data of minor diastereomer: ¹H NMR (400 MHz, CDCl₃) 8.09 (1H, t, $J = 1.5$ Hz, NCH=C), 5.59 (1H, dd, $J = 17.4, 10.8$ Hz, CH₂=CH), 5.44-5.40 (1H, m, CH₂CH=C), 4.95 (1H, dd, $J = 10.8, 1.5$ Hz, CH_aH_b=CH), 4.16 (1H, d, $J = 7.0$ Hz, CCHC), 1.68 (3H, s, =C(CH₃)); ¹³C NMR (101 MHz, CDCl₃) δ 143.1 (CH), 140.9 (CH), 135.2 (C), 129.25 (2 × CH), 128.77 (CH), 128.4 (CH), 127.9 (2 × CH), 125.0 (CH), 123.5 (C), 114.3 (CH₂), 109.4 (CH), 58.9 (CH₂), 48.4 (C), 41.7 (CH), 36.4 (CH₂), 25.8 (CH₃), 23.0 (CH₂), 17.9 (CH₃), 16.4 (CH₃).

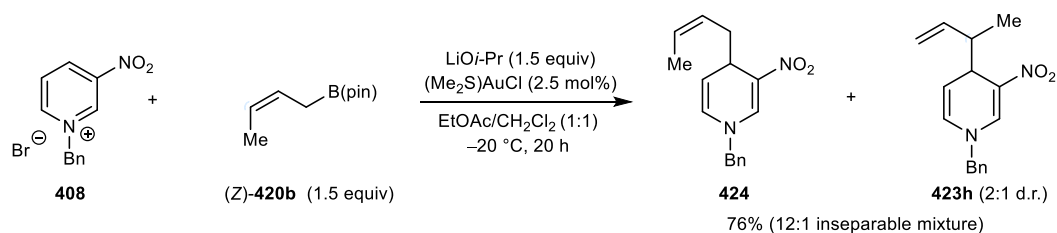


1-Benzyl-4-(cyclohex-2-en-1-yl)-3-nitro-1,4-dihydropyridine (423j). The title compound was prepared according to General Procedure B, using azinium salt **408** (148 mg, 0.50 mmol) and allyl pinacolboronate *rac*-**420a** (156 mg, 0.75 mmol), and purified by column chromatography (5% EtOAc/*n*-pentane) to give a 2.2:1 mixture of inseparable diastereomers as a red solid (103 mg, 70%). $R_f = 0.48$ (20% EtOAc/petroleum ether); m.p. 76-77 °C (Et₂O); IR 3066, 2931, 1661, 1579 (NO₂), 1345 (NO₂), 1253, 1165, 931, 702, 586 cm⁻¹; HRMS (ESI) Exact mass calculated for [C₁₈H₂₀N₂NaO₂]⁺ [M+Na]⁺: 319.1417, found 319.1418.

NMR data of major diastereomer: ¹H NMR (400 MHz, CDCl₃) δ 8.06 (1H, t, $J = 1.3$ Hz, NCH=C), 7.42-7.32 (3H, m, ArH), 7.25-7.21 (2H, m, ArH), 5.96-5.93 (1H, m, NCH=CH), 5.70 (1H, dt, $J = 10.1, 3.3$ Hz, CH=CHCH₂), 5.53-5.49 (1H, m, CH=CHCH₂), 5.12 (1H, dd, $J = 7.9, 5.4$ Hz, NCH=CH), 4.49 (2H, s, NCH₂), 3.90-3.87 (1H, m, CHCHC), 2.59-2.52 (1H, m, =CHCHCH₂), 1.96-1.90 (2H, m, =CHCH₂), 1.81-1.68 (2H, m, =CHCH₂CH₂CH₂), 1.62-1.19 (2H, m, =CHCH₂CH₂CH₂); ¹³C NMR (101 MHz, CDCl₃) δ 140.9 (CH), 135.34 (C), 129.3 (2 × CH), 129.2 (CH), 128.7 (CH), 128.3 (CH), 127.9 (CH), 127.6 (2 × CH), 124.4 (C), 110.5 (CH), 58.6 (CH₂), 39.8 (CH), 37.9 (CH), 25.7 (CH₂), 25.32 (CH₂), 22.4 (CH₂).

Characteristic NMR data of minor diastereomer: ¹H NMR (400 MHz, CDCl₃) δ 8.04-8.01 (1H, m, NCH=C), 5.82-5.76 (1H, m, CH=CHCH₂), 5.45 (1H, dt, $J = 10.1, 1.9$ Hz, CH=CHCH₂), 5.05 (1H, dd, $J = 7.9, 5.0$ Hz, NCH=CH), 4.47 (2H, s, NCH₂), 4.03-3.99 (1H, m, CHCHC), 2.82-2.75 (1H, m, =CHCHCH₂); ¹³C NMR (101 MHz, CDCl₃) δ 135.30 (C), 129.7 (CH), 128.8 (CH), 127.8 (CH), 127.5 (2 × CH), 124.3 (C), 111.2 (CH), 58.5 (CH₂), 38.6 (CH), 37.8 (CH), 25.30 (CH₂), 24.6 (CH₂), 21.8 (CH₂).

(Z)-1-Benzyl-4-(but-2-en-1-yl)-3-nitro-1,4-dihydropyridine (424) and 1-benzyl-4-(but-3-en-2-yl)-3-nitro-1,4-dihydropyridine (423h)

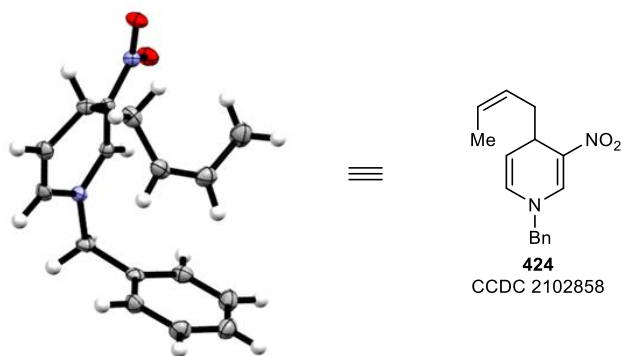


The title compounds were prepared according to General Procedure B, using azinium salt **408** (148 mg, 0.50 mmol) and allyl pinacolboronate (*Z*)-**420b** (137 mg, 0.75 mmol), and purified by column chromatography (5% EtOAc/*n*-pentane) to give a 12:1 mixture of inseparable regioisomers as a red solid (102 mg, 76%). $R_f = 0.44$ (20% EtOAc/petroleum ether); m.p. 84-85 °C (Et₂O); IR 3064, 3020, 1655, 1570 (NO₂), 1496, 1365 (NO₂), 1255, 1172, 908, 696 cm⁻¹; HRMS (ESI) Exact mass calculated for [C₁₆H₁₈N₂NaO₂]⁺ [M+Na]⁺: 293.1260, found 293.1251.

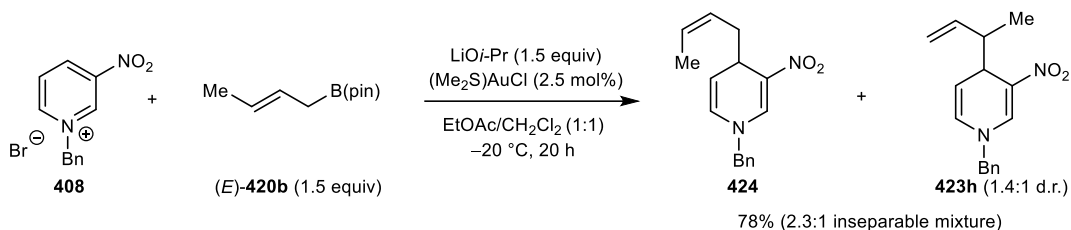
NMR data of major regioisomer 424: ¹H NMR (400 MHz, CDCl₃) δ 7.96 (1H, s, NCH=C), 7.42-7.32 (3H, m, ArH), 7.25-7.21 (2H, m, ArH), 5.87 (1H, dt, *J* = 7.9, 1.3 Hz, NCH=CH), 5.62-5.54 (1H, m, CH₃CH=CH), 5.43-4.34 (1H, m, CH₃CH=CH), 5.14 (1H, dd, *J* = 7.9, 5.1 Hz, NCH=CH), 4.47 (2H, s, NCH₂), 3.99-3.95 (1H, m, CH₂CH), 2.59-2.51 (1H, m, CH_aH_bCH), 2.24-2.17 (1H, m, CH_aH_bCH), 1.58-1.54 (3H, m, CH₃); ¹³C NMR (101 MHz, CDCl₃) δ 140.7 (CH), 135.4 (C), 129.3 (2 × CH), 128.7 (CH), 127.4 (2 × CH), 127.3 (CH), 127.1 (CH), 125.9 (CH), 125.2 (C), 112.8 (CH), 58.5 (CH₂), 34.0 (CH), 32.2 (CH₂), 13.1 (CH₃).

Characteristic NMR data of minor regioisomer 423h as a 2:1 mixture of diastereoisomers; major diastereomer: ¹H NMR (400 MHz, CDCl₃) δ 7.99 (1H, t, *J* = 1.3 Hz, NCH=C), 4.97-4.90 (2H, m, CH₂=CH), 3.90-3.86 (1H, m, CHCHC), 2.72-2.64 (1H, m, CHCH₃), 1.01 (3H, d, *J* = 7.1 Hz, CH₃); ¹³C NMR (101 MHz, CDCl₃) δ 128.2 (CH), 127.6 (2 × CH), 116.1 (CH₂), 109.1 (CH), 40.5 (CH), 39.4 (CH₂), 15.9 (CH₃); *minor diastereomer*: ¹H NMR (400 MHz, CDCl₃) δ 8.04 (1H, t, *J* = 1.3 Hz, NCH=C), 5.07-5.01 (2H, m, CH₂=CH), 2.80-2.74 (1H, m, CHCH₃), 0.93 (3H, d, *J* = 7.1 Hz, CH₃).

Crystals suitable for X-ray analysis were prepared by slow diffusion of petroleum ether into a solution of **424** in CH₂Cl₂.



(Z)-1-Benzyl-4-(but-2-en-1-yl)-3-nitro-1,4-dihydropyridine (424) and 1-benzyl-4-(but-3-en-2-yl)-3-nitro-1,4-dihydropyridine (423h)



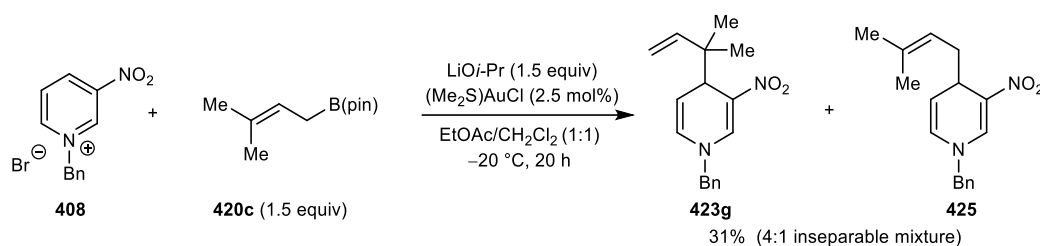
The title compounds were prepared according to General Procedure B, using azinium salt **408** (148 mg, 0.50 mmol) and allyl pinacolboronate (*E*)-**420b** (137 mg, 0.75 mmol), and purified by column chromatography (5% EtOAc/*n*-pentane) to give a 2.3:1 mixture of inseparable regioisomers as a red solid (105 mg, 78%). $R_f = 0.42$ (20% EtOAc/petroleum ether); m.p. 72-73 °C (Et₂O); IR 3065, 2964, 1656, 1574 (NO₂), 1364 (NO₂), 1260, 1204, 1171, 909, 696 cm⁻¹; HRMS (ESI) Exact mass calculated for [C₁₆H₁₈N₂NaO₂]⁺ [M+Na]⁺: 293.1260, found 293.1259.

NMR data of major regioisomer 424: ¹H NMR (400 MHz, CDCl₃) δ 7.96 (1H, s, NCH=C), 7.42-7.32 (3H, m, ArH), 7.25-7.20 (2H, m, ArH), 5.87 (1H, dt, *J* = 7.9, 1.3 Hz, NCH=CH), 5.62-5.53 (1H, m, CH₃CH=CH), 5.43-4.34 (1H, m, CH₃CH=CH), 5.14 (1H, dd, *J* = 7.9, 5.7 Hz, NCH=CH), 4.47 (2H, s, NCH₂), 3.99-3.95 (1H, m, CH₂CH), 2.60-2.51 (1H, m, CH_aH_bCH), 2.24-2.16 (1H, m, CH_aH_bCH), 1.58-1.53 (3H, m, CH₃); ¹³C NMR (101 MHz, CDCl₃) δ 140.7 (CH), 135.4 (C), 129.26 (2 × CH), 128.7 (CH), 127.42 (2 × CH), 127.36 (CH), 127.1 (CH), 125.9 (CH), 125.2 (C), 113.1 (CH), 58.5 (CH₂), 34.0 (CH), 32.2 (CH₂), 13.1 (CH₃).

Characteristic NMR data of minor regioisomer 423h as a 1.4:1 mixture of diastereoisomers; major diastereomer: ¹H NMR (400 MHz, CDCl₃) δ 7.99 (1H, t, *J* = 1.3 Hz, NCH=C), 5.96-5.93 (1H, m, NCH=CH), 4.97-4.90 (2H, m, CH₂=CH), 4.46 (2H, s, NCH₂), 3.90-3.86 (1H, m, CHCHC), 2.72-2.65 (1H, m, CHCH₃), 1.01 (3H, d, *J* = 7.1 Hz, CH₃); ¹³C NMR (101 MHz, CDCl₃) δ 140.75 (CH), 140.5 (CH), 135.31 (C), 129.2 (2 × CH), 128.2 (CH), 127.6 (2 × CH), 124.9 (C), 116.1 (CH₂), 109.2 (CH), 58.6 (CH₂), 40.5 (CH), 39.4 (CH₂), 15.9 (CH₃); *minor diastereomer*: ¹H NMR (400 MHz, CDCl₃) δ 8.04 (1H, t, *J* = 1.3 Hz, NCH=C), 5.99-5.96 (1H, m, NCH=CH), 5.07-5.01 (2H, m, CH₂=CH), 4.48 (2H, s, NCH₂), 2.79-2.74 (1H, m, CHCH₃), 0.93 (3H, d, *J* = 7.1 Hz,

CH₃); ¹³C NMR (101 MHz, CDCl₃) δ 140.83 (CH), 140.4 (CH), 135.27 (C), 129.32 (2 × CH), 127.5 (2 × CH), 114.8 (CH₂), 109.8 (CH), 39.0 (CH), 38.9 (CH₂), 13.4 (CH₃).

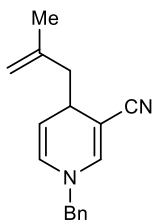
1-Benzyl-4-(2-methylbut-3-en-2-yl)-3-nitro-1,4-dihydropyridine (423g) and 1-benzyl-4-(3-methylbut-2-en-1-yl)-3-nitro-1,4-dihydropyridine (425).



The title compounds were prepared according to General Procedure B, using azinium salt **408** (148 mg, 0.50 mmol) and allyl pinacolboronate **420c** (166 μL, 0.75 mmol), and purified by column chromatography (5% EtOAc/*n*-pentane) to give a 4:1 mixture of inseparable regioisomers as a red oil (43.9 mg, 31%). R_f = 0.49 (20% EtOAc/petroleum ether); IR 2965, 1661, 1581 (NO₂), 1478, 1350 (NO₂), 1265, 1175, 1073, 909, 698 cm⁻¹; HRMS (ESI) Exact mass calculated for [C₁₇H₂₀N₂NaO₂]⁺ [M+Na]⁺: 307.1417, found 307.1418.

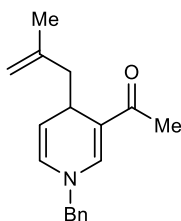
NMR data of major regioisomer 423g: ¹H NMR (400 MHz, CDCl₃) δ 8.08 (1H, t, *J* = 1.6 Hz, NCH=C), 7.41-7.33 (3H, m, ArH), 7.24-7.21 (2H, m, ArH), 6.08 (1H, dd, *J* = 7.6, 1.4 Hz, NCH=CH), 5.77 (1H, dd, *J* = 17.4, 10.8 Hz, CH₂=CH), 5.17-5.11 (1H, m, NCH=CH), 4.89-4.83 (2H, m, CH₂=CH), 4.50 (2H, s, NCH₂), 3.90 (1H, dd, *J* = 6.3, 1.6 Hz, CCHC), 0.91 (3H, s, CH₃), 0.89 (3H, s, CH₃); ¹³C NMR (101 MHz, CDCl₃) δ 145.0 (CH), 140.6 (CH), 135.3 (C), 129.2 (2 × CH), 128.7 (CH), 128.4 (CH), 127.8 (2 × CH), 123.1 (C), 112.2 (CH₂), 109.4 (CH), 58.8 (CH₂), 45.1 (C), 41.9 (CH), 22.9 (2 × CH₃).

Characteristic NMR data of minor regioisomer 425: ¹H NMR (400 MHz, CDCl₃) δ 7.95 (1H, t, *J* = 1.2 Hz, NCH=C), 5.86 (1H, dt, *J* = 7.9, 1.3 Hz, NCH=CH), 4.47 (2H, s, NCH₂), 2.53-2.43 (1H, m, CH_aH_bCH), 2.19-2.12 (1H, m, CH_aH_bCH), 1.69 (3H, s, CH₃), 1.56 (3H, s, CH₃); ¹³C NMR (101 MHz, CDCl₃) δ 140.7 (CH), 129.3 (2 × CH), 128.6 (CH), 127.3 (2 × CH), 127.0 (CH), 119.9 (CH), 113.4 (CH), 110.1 (C), 58.5 (CH₂), 34.2 (CH), 33.3 (CH₂), 26.1 (CH₃), 18.0 (CH₃).



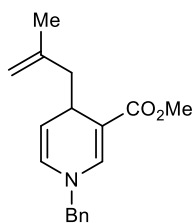
1-Benzyl-4-(2-methylallyl)-1,4-dihydropyridine-3-carbonitrile (435a).

The title compound was prepared according to General Procedure B, using azinium salt **433a** (138 mg, 0.50 mmol) and allyl pinacolboronate **418a** (137 mg, 0.75 mmol), and purified by column chromatography (3 to 5% EtOAc/*n*-pentane) to give a green oil (114 mg, 91%). $R_f = 0.51$ (20% EtOAc/petroleum ether); IR 3066, 2926, 2191 (C≡N), 1672, 1591, 1409, 1179, 1077, 889, 729 cm^{-1} ; ^1H NMR (400 MHz, CDCl_3) δ 7.41-7.30 (3H, m, ArH), 7.21-7.18 (2H, m, ArH), 6.62 (1H, d, $J = 1.7$ Hz, NCH=C), 5.77 (1H, dt, $J = 8.1, 1.3$ Hz, NCH=CH), 4.86-4.84 (1H, m, $\text{CH}_a\text{H}_b=\text{C}$), 4.74-4.69 (2H, m, $\text{CH}_a\text{H}_b=\text{C}$ and NCH=CH), 4.30 (2H, s, NCH₂), 3.40-3.35 (1H, m, CH₂CH), 2.37 (1H, ddd, $J = 13.5, 4.5, 1.1$ Hz, $\text{CH}_a\text{H}_b\text{CH}$), 2.23 (1H, ddd, $J = 13.4, 9.0, 0.8$ Hz, $\text{CH}_a\text{H}_b\text{CH}$), 1.74 (3H, s, =CCH₃); ^{13}C NMR (101 MHz, CDCl_3) δ 143.0 (CH), 141.4 (C), 136.5 (C), 129.1 (2 × CH), 128.3 (CH), 127.7 (CH), 127.2 (2 × CH), 121.4 (C), 113.6 (CH₂), 105.9 (CH), 83.1 (C), 57.5 (CH₂), 47.4 (CH₂), 31.7 (CH), 22.7 (CH₃); HRMS (ESI) Exact mass calculated for $[\text{C}_{17}\text{H}_{18}\text{N}_2\text{Na}]^+$ $[\text{M}+\text{Na}]^+$: 273.1362, found 273.1359.



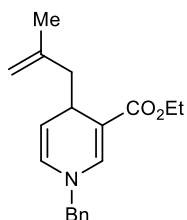
1-(1-Benzyl-4-(2-methylallyl)-1,4-dihydropyridin-3-yl)ethan-1-one (435b).

The title compound was prepared according to General Procedure B, using azinium salt **433b** (146 mg, 0.50 mmol) and allyl pinacolboronate **418a** (137 mg, 0.75 mmol), and purified by column chromatography (5 to 15% EtOAc/*n*-pentane) to give an orange oil (111 mg, 83%). $R_f = 0.22$ (20% EtOAc/petroleum ether); IR 3065, 2914, 1668 (C=O), 1614, 1570, 1384, 1208, 1177, 881, 729 cm^{-1} ; ^1H NMR (400 MHz, CDCl_3) δ 7.41-7.36 (2H, m, ArH), 7.34-7.29 (1H, m, ArH), 7.24-7.21 (2H, m, ArH), 7.11 (1H, d, $J = 1.4$ Hz, NCH=C), 5.85 (1H, dd, $J = 7.8, 1.4$ Hz, NCH=CH), 4.96 (1H, dd, $J = 7.8, 5.1$ Hz, NCH=CH), 4.76-4.73 (1H, m, $\text{CH}_a\text{H}_b=\text{C}$), 4.61-4.59 (1H, m, $\text{CH}_a\text{H}_b=\text{C}$), 4.43 (2H, s, NCH₂), 3.69 (1H, dt, $J = 9.1, 4.5$ Hz, CH₂CH), 2.24-2.19 (1H, m, $\text{CH}_a\text{H}_b\text{CH}$), 2.18 (3H, s, O=CCH₃), 2.02 (1H, dd, $J = 12.7, 9.3$ Hz, $\text{CH}_a\text{H}_b\text{CH}$), 1.77 (3H, s, =CCH₃); ^{13}C NMR (101 MHz, CDCl_3) δ 195.1 (C), 143.0 (C), 142.7 (CH), 137.1 (C), 129.1 (2 × CH), 128.1 (CH), 127.3 (CH), 127.0 (2 × CH), 113.9 (C), 112.2 (CH₂), 109.8 (CH), 57.9 (CH₂), 46.9 (CH₂), 29.6 (CH), 24.7 (CH₃), 22.8 (CH₃); HRMS (ESI) Exact mass calculated for $[\text{C}_{18}\text{H}_{22}\text{NO}]^+$ $[\text{M}+\text{H}]^+$: 268.1696, found 268.1693.



Methyl 1-benzyl-4-(2-methylallyl)-1,4-dihydropyridine-3-carboxylate (435c).

The title compound was prepared according to General Procedure B, using azinium salt **433c** (154 mg, 0.50 mmol) and allyl pinacolboronate **418a** (137 mg, 0.75 mmol), and purified by column chromatography (3% EtOAc/*n*-pentane) to give a pale-yellow oil (106 mg, 75%). $R_f = 0.48$ (20% EtOAc/petroleum ether); IR 2945, 1685 (C=O), 1588, 1408, 1271, 1161, 1082, 884, 764, 729 cm^{-1} ; ^1H NMR (400 MHz, CDCl_3) δ 7.38-7.33 (2H, m, ArH), 7.32-7.27 (1H, m, ArH), 7.24 (1H, d, $J = 1.6$ Hz, NCH=C), 7.23-7.19 (2H, m, ArH), 5.81 (1H, dd, $J = 7.8, 1.6$ Hz, NCH=CH), 4.86 (1H, dd, $J = 7.8, 5.0$ Hz, NCH=CH), 4.77-4.75 (1H, m, $\text{CH}_a\text{H}_b=\text{C}$), 4.64-4.61 (1H, m, $\text{CH}_a\text{H}_b=\text{C}$), 4.37 (2H, s, NCH₂), 3.68 (3H, s, OCH₃), 3.54 (1H, dt, $J = 9.0, 4.4$ Hz, CH₂CH), 2.27 (1H, dd, $J = 12.8, 3.8$ Hz, $\text{CH}_a\text{H}_b\text{CH}$), 2.08 (1H, dd, $J = 12.8, 9.1$ Hz, $\text{CH}_a\text{H}_b\text{CH}$), 1.76 (3H, s, =CCH₃); ^{13}C NMR (101 MHz, CDCl_3) δ 168.8 (C), 142.8 (C), 141.5 (CH), 137.4 (C), 129.0 (2 \times CH), 127.9 (CH), 127.6 (CH), 127.1 (2 \times CH), 112.3 (CH₂), 108.2 (CH), 101.9 (C), 57.7 (CH₂), 51.0 (CH₃), 47.9 (CH₂), 30.4 (CH), 22.7 (CH₃); HRMS (ESI) Exact mass calculated for $[\text{C}_{18}\text{H}_{21}\text{NNaO}_2]^+ [\text{M}+\text{Na}]^+$: 306.1464, found 306.1465.

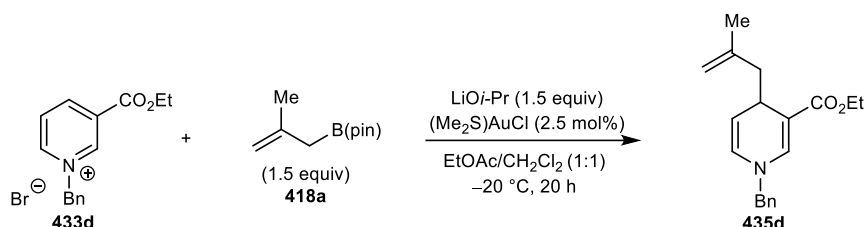


Ethyl 1-benzyl-4-(2-methylallyl)-1,4-dihydropyridine-3-carboxylate (435d).

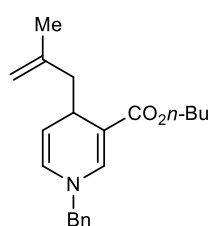
The title compound was prepared according to General Procedure B, using azinium salt **433d** (161 mg, 0.50 mmol) and allyl pinacolboronate **418a** (137 mg, 0.75 mmol), and purified by column chromatography (3% EtOAc/*n*-pentane) to give a pale-yellow oil (133 mg, 89%). $R_f = 0.55$ (20% EtOAc/petroleum ether); IR 2977, 1680 (C=O), 1587, 1397, 1203, 1160, 1074, 885, 729, 697 cm^{-1} ; ^1H NMR (500 MHz, CDCl_3) δ 7.38-7.34 (2H, m, ArH), 7.32-7.28 (1H, m, ArH), 7.25 (1H, d, $J = 1.6$ Hz, NCH=C), 7.23-7.20 (2H, m, ArH), 5.80 (1H, dd, $J = 7.8, 1.6$ Hz, NCH=CH), 4.86 (1H, dd, $J = 7.8, 5.0$ Hz, NCH=CH), 4.77-4.75 (1H, m, $\text{CH}_a\text{H}_b=\text{C}$), 4.64-4.62 (1H, m, $\text{CH}_a\text{H}_b=\text{C}$), 4.38 (2H, s, NCH₂), 4.21-4.12 (2H, m, OCH₂), 3.54 (1H, ddd, $J = 9.0, 5.0, 3.8$ Hz, CH₂CH), 2.28 (1H, ddd, $J = 12.9, 3.8, 1.2$ Hz, $\text{CH}_a\text{H}_b\text{CH}$), 2.09 (1H, ddd, $J = 12.8, 9.2, 0.7$ Hz, $\text{CH}_a\text{H}_b\text{CH}$), 1.76 (3H, s, =CCH₃), 1.27 (3H, t, $J = 7.1$ Hz, CH₂CH₃); ^{13}C NMR (126 MHz, CDCl_3) δ 168.5 (C), 142.8 (C), 141.3 (CH), 137.5 (C), 129.0 (2 \times CH), 127.9 (CH), 127.5 (CH), 127.1 (2 \times CH), 112.3 (CH₂), 108.2 (CH), 102.1 (C), 59.5 (CH₂), 57.7 (CH₂),

48.0 (CH₂), 30.5 (CH), 22.7 (CH₃), 14.6 (CH₃); HRMS (ESI) Exact mass calculated for [C₁₉H₂₃NNaO₂]⁺ [M+Na]⁺: 320.1621, found 320.1616.

Gram-Scale Reaction:



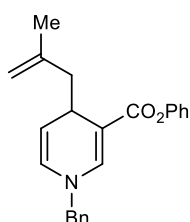
An oven-dried flask equipped with a stirrer bar was charged with azinium salt **433d** (1.29 g, 4.00 mmol), (Me₂S)AuCl (29.5 mg, 0.10 mmol) and LiO-*i*Pr (396 mg, 6.00 mmol). The vial was sealed and EtOAc/CH₂Cl₂ (1:1) (20 mL) (both of which were undried, obtained from commercial vendors and used without further purification) was added. The mixture was stirred at -20 °C for 5 min and a solution of allyl pinacolboronate **418a** (1.09 g, 6.00 mmol) in 10 mL of EtOAc/CH₂Cl₂ (1:1) was added dropwise. The resulting solution was stirred at -20 °C for 20 h. The reaction was warmed to room temperature and then passed through a plug of silica (8 cm in height and 2 cm wide) using Et₂O (100 mL) as the eluent and the filtrate was concentrated *in vacuo*. The residue was purified by column chromatography using EtOAc/*n*-pentane (1 to 3% EtOAc/*n*-pentane) to give the title compound **435d** as an orange oil (1.01 g, 85%).



Butyl 1-benzyl-4-(2-methylallyl)-1,4-dihydropyridine-3-carboxylate (435e). The title compound was prepared according to General Procedure B, using azinium salt **433e** (175 mg, 0.50 mmol) and allyl pinacolboronate **418a** (137 mg, 0.75 mmol), and purified by column chromatography (1 to 2% EtOAc/*n*-pentane) to give a brown

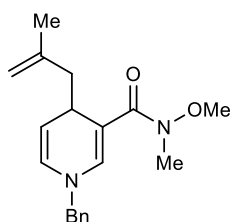
oil (96.0 mg, 59%). R_f = 0.59 (20% EtOAc/petroleum ether); IR 2959, 1684 (C=O), 1588, 1455, 1271, 1162, 1044, 884, 730, 697 cm⁻¹; ¹H NMR (400 MHz, CDCl₃) δ 7.38-7.33 (2H, m, ArH), 7.32-7.27 (1H, m, ArH), 7.24 (1H, d, *J* = 1.6 Hz, NCH=C), 7.23-7.20 (2H, m, ArH), 5.81 (1H, dd, *J* = 7.9, 1.6 Hz, NCH=CH), 4.86 (1H, dd, *J* = 7.8, 5.0 Hz, NCH=CH), 4.77-4.75 (1H, m, CH_aH_b=C), 4.64-4.62 (1H, m, CH_aH_b=C), 4.37 (2H, s, NCH₂), 4.16-4.05 (2H, m, OCH₂), 3.53 (1H, ddd, *J* = 9.0, 5.0, 3.8 Hz, CH₂CH), 2.29

(1H, dd, $J = 12.8, 3.7$ Hz, $\text{CH}_a\text{H}_b\text{CH}$), 2.09 (1H, dd, $J = 12.8, 9.3$ Hz, $\text{CH}_a\text{H}_b\text{CH}$), 1.75 (3H, s, $=\text{CCH}_3$), 1.66-1.59 (2H, m, $\text{CH}_2\text{CH}_2\text{CH}_3$), 1.44-1.35 (2H, m, CH_2CH_3), 0.93 (3H, t, $J = 7.4$ Hz, CH_2CH_3); ^{13}C NMR (101 MHz, CDCl_3) δ 168.6 (C), 142.8 (C), 141.3 (CH), 137.5 (C), 129.0 (2 \times CH), 127.9 (CH), 127.5 (CH), 127.1 (2 \times CH), 112.3 (CH_2), 108.2 (CH), 102.1 (C), 63.5 (CH_2), 57.7 (CH_2), 47.9 (CH_2), 31.1 (CH_2), 30.5 (CH), 22.7 (CH_3), 19.5 (CH_2), 13.9 (CH_3); HRMS (ESI) Exact mass calculated for $[\text{C}_{21}\text{H}_{27}\text{NNaO}_2]^+$ $[\text{M}+\text{Na}]^+$: 348.1934, found 348.1929.



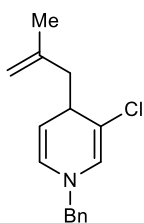
Phenyl 1-benzyl-4-(2-methylallyl)-1,4-dihydropyridine-3-carboxylate (435f). The title compound was prepared according to General Procedure B, using azinium salt **433f** (185 mg, 0.50 mmol) and allyl pinacolboronate **418a** (137 mg, 0.75 mmol), and purified by column chromatography (1 to 3% EtOAc/*n*-pentane) to give a brown oil

(144 mg, 83%). $R_f = 0.65$ (20% EtOAc/petroleum ether); IR 2929, 1699 (C=O), 1582, 1415, 1195, 1148, 1026, 907, 726, 690 cm^{-1} ; ^1H NMR (400 MHz, CDCl_3) δ 7.48 (1H, d, $J = 1.5$ Hz, $\text{NCH}=\text{C}$), 7.42-7.30 (5H, m, ArH), 7.27-7.24 (2H, m, ArH), 7.21-7.16 (1H, m, ArH), 7.12-7.09 (2H, m, ArH), 5.86 (1H, dd, $J = 7.9, 1.5$ Hz, $\text{NCH}=\text{CH}$), 4.96 (1H, dd, $J = 7.9, 5.0$ Hz, $\text{NCH}=\text{CH}$), 4.81-4.78 (1H, m, $\text{CH}_a\text{H}_b=\text{C}$), 4.69-4.67 (1H, m, $\text{CH}_a\text{H}_b=\text{C}$), 4.44 (2H, s, NCH_2), 3.65 (1H, dt, $J = 9.0, 4.5$ Hz, CH_2CH), 2.38 (1H, dd, $J = 12.8, 4.1$ Hz, $\text{CH}_a\text{H}_b\text{CH}$), 2.19 (1H, dd, $J = 12.8, 9.0$ Hz, $\text{CH}_a\text{H}_b\text{CH}$), 1.77 (3H, s, $=\text{CCH}_3$); ^{13}C NMR (101 MHz, CDCl_3) δ 166.8 (C), 151.5 (C), 142.9 (CH), 142.7 (C), 137.1 (C), 129.4 (2 \times CH), 129.1 (2 \times CH), 128.1 (CH), 127.4 (CH), 127.2 (2 \times CH), 125.2 (CH), 122.1 (2 \times CH), 112.6 (CH_2), 109.1 (CH), 100.9 (C), 57.9 (CH_2), 47.9 (CH_2), 30.6 (CH), 22.7 (CH_3); HRMS (ESI) Exact mass calculated for $[\text{C}_{23}\text{H}_{23}\text{NNaO}_2]^+$ $[\text{M}+\text{Na}]^+$: 368.1621, found 368.1620.

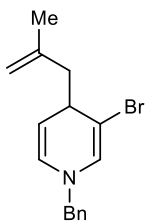


1-Benzyl-N-methoxy-N-methyl-4-(2-methylallyl)-1,4-dihydropyridine-3-carboxamide (435g). The title compound was prepared according to General Procedure B, using azinium salt **433g** (169 mg, 0.50 mmol) and allyl pinacolboronate **418a** (137 mg, 0.75 mmol), and purified by column chromatography (15% EtOAc/*n*-pentane) to give a brown oil (49.3 mg, 32%). $R_f = 0.32$ (40% EtOAc/petroleum ether);

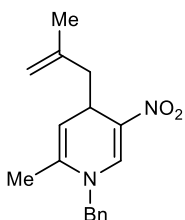
IR 2929, 1672 (C=O), 1591, 1397, 1349, 1170, 1134, 885, 728, 700 cm^{-1} ; ^1H NMR (400 MHz, CDCl_3) δ 7.37-7.32 (2H, m, ArH), 7.30-7.27 (1H, m, ArH), 7.24-7.20 (2H, m, ArH), 7.08 (1H, d, $J = 1.6$ Hz, NCH=C), 5.84 (1H, dd, $J = 7.8, 1.6$ Hz, NCH=CH), 4.79 (1H, dd, $J = 7.8, 4.9$ Hz, NCH=CH), 4.76-4.74 (1H, m, $\text{CH}_a\text{H}_b=\text{C}$), 4.66-4.63 (1H, m, $\text{CH}_a\text{H}_b=\text{C}$), 4.34 (2H, s, NCH_2), 3.75 (1H, dt, $J = 9.3, 4.7$ Hz, CH_2CH), 3.57 (3H, s, CH_3), 3.20 (3H, s, CH_3), 2.19 (1H, dd, $J = 13.0, 4.5$ Hz, $\text{CH}_a\text{H}_b\text{C}$), 2.07 (1H, ddd, $J = 13.0, 9.2, 0.8$ Hz, $\text{CH}_a\text{H}_b\text{C}$), 1.74 (3H, s, $=\text{CCH}_3$); ^{13}C NMR (101 MHz, CDCl_3) δ 170.7 (C), 142.8 (C), 139.0 (CH), 137.9 (C), 128.9 (2 \times CH), 127.8 (2 \times CH), 127.2 (2 \times CH), 112.3 (CH_2), 106.9 (CH), 104.8 (C), 60.4 (CH_3), 57.6 (CH_2), 48.3 (CH_2), 34.6 (CH_3), 31.2 (CH), 22.5 (CH_3); HRMS (ESI) Exact mass calculated for $[\text{C}_{19}\text{H}_{24}\text{N}_2\text{NaO}_2]^+$ $[\text{M}+\text{Na}]^+$: 335.1730, found 335.1730.



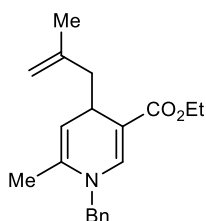
1-Benzyl-3-chloro-4-(2-methylallyl)-1,4-dihydropyridine (435h). The title compound was prepared according to General Procedure B, using azinium salt **433h** (142 mg, 0.50 mmol) and allyl pinacolboronate **418a** (137 mg, 0.75 mmol), and purified by passing through a plug of neutralised silica (8 cm in height and 2 cm wide) using 89:10:1 *n*-pentane:EtOAc:Et₃N (60 mL) as the eluent to give a brown oil (122 mg, 94%). $R_f = 0.50$ (10% EtOAc/petroleum ether); IR 2928, 1674, 1615, 1392, 1214, 1168, 1024, 887, 729, 697 cm^{-1} ; ^1H NMR (400 MHz, CDCl_3) δ 7.38-7.32 (2H, m, ArH), 7.31-7.27 (1H, m, ArH), 7.24-7.20 (2H, m, ArH), 6.08 (1H, d, $J = 1.6$ Hz, NCH=C), 5.82 (1H, dt, $J = 7.9, 1.2$ Hz, NCH=CH), 4.84-4.81 (1H, m, $\text{CH}_a\text{H}_b=\text{C}$), 4.71-4.69 (1H, m, $\text{CH}_a\text{H}_b=\text{C}$), 4.47 (1H, dd, $J = 7.8, 3.9$ Hz, NCH=CH), 4.20 (2H, s, NCH_2), 3.44 (1H, dt, $J = 8.5, 3.8$ Hz, CH_2CH), 2.51 (1H, dd, $J = 13.4, 3.7$ Hz, $\text{CH}_a\text{H}_b\text{CH}$), 2.18 (1H, dd, $J = 13.4, 9.0$ Hz, $\text{CH}_a\text{H}_b\text{CH}$), 1.74 (3H, s, $=\text{CCH}_3$); ^{13}C NMR (101 MHz, CDCl_3) δ 142.6 (C), 138.2 (C), 129.1 (CH), 128.85 (CH), 128.83 (2 \times CH), 127.7 (CH), 127.3 (2 \times CH), 112.7 (CH_2), 111.2 (C), 101.0 (CH), 56.9 (CH_2), 45.3 (CH_2), 38.7 (CH), 22.9 (CH_3); HRMS (ESI) Exact mass calculated for $[\text{C}_{16}\text{H}_{19}\text{ClN}]^+$ $[\text{M}+\text{H}]^+$: 262.1176, found 262.1173.



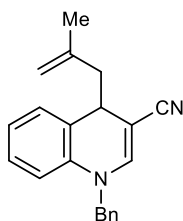
1-Benzyl-3-bromo-4-(2-methylallyl)-1,4-dihydropyridine (435i). The title compound was prepared according to General Procedure B, using azinium salt **433i** (165 mg, 0.50 mmol) and allyl pinacolboronate **418a** (137 mg, 0.75 mmol), and purified by passing through a plug of neutralised silica (8 cm in height and 2 cm wide) using 89:10:1 *n*-pentane:EtOAc:Et₃N (60 mL) as the eluent to give a brown oil (124 mg, 82%). *R_f* = 0.54 (10% EtOAc/petroleum ether); IR 2928, 1671, 1610, 1389, 1213, 1166, 1010, 887, 728, 696 cm⁻¹; ¹H NMR (400 MHz, CDCl₃) δ 7.38-7.33 (2H, m, ArH), 7.31-7.27 (1H, m, ArH), 7.24-7.20 (2H, m, ArH), 6.22 (1H, d, *J* = 1.6 Hz, NCH=C), 5.84 (1H, dt, *J* = 7.9, 1.1 Hz, NCH=CH), 4.84-4.81 (1H, m, CH_aH_b=C), 4.72-4.69 (1H, m, CH_aH_b=C), 4.43 (1H, dd, *J* = 7.9, 4.1 Hz, NCH=CH), 4.20 (2H, s, NCH₂), 3.48 (1H, dt, *J* = 9.5, 3.8 Hz, CH₂CH), 2.52 (1H, dd, *J* = 13.2, 3.4 Hz, CH_aH_bCH), 2.19 (1H, dd, *J* = 13.2, 9.2 Hz, CH_aH_bCH), 1.73 (3H, s, =CCH₃); ¹³C NMR (101 MHz, CDCl₃) δ 142.5 (C), 138.2 (C), 131.7 (CH), 129.0 (CH), 128.8 (2 × CH), 127.7 (CH), 127.3 (2 × CH), 112.8 (CH₂), 101.6 (C), 100.9 (CH), 56.9 (CH₂), 46.0 (CH₂), 39.8 (CH), 22.9 (CH₃); HRMS (ESI) Exact mass calculated for [C₁₆H₁₉BrN]⁺ [M+H]⁺: 306.0680, found 306.0675.



1-Benzyl-2-methyl-4-(2-methylallyl)-5-nitro-1,4-dihydropyridine (435j). The title compound was prepared according to General Procedure B, using azinium salt **433j** (155 mg, 0.50 mmol) and allyl pinacolboronate **418a** (137 mg, 0.75 mmol), and purified by column chromatography (5% EtOAc/*n*-pentane) to give a red oil (40.3 mg, 28%). *R_f* = 0.34 (20% EtOAc/petroleum ether); IR 2914, 1676, 1600 (NO₂), 1386 (NO₂), 1271, 1210, 1075, 891, 726, 695 cm⁻¹; ¹H NMR (400 MHz, CDCl₃) δ 7.96 (1H, s, NCH=C), 7.42-7.36 (2H, m, ArH), 7.35-7.30 (1H, m, ArH), 7.21-7.17 (2H, m, ArH), 4.98 (1H, dd, *J* = 5.3, 1.3 Hz, NC=CH), 4.83-4.81 (1H, m, CH_aH_b=C), 4.69 (1H, d, *J* = 16.5 Hz, NCH_aH_b), 4.66-4.64 (1H, m, CH_aH_b=C), 4.57 (1H, d, *J* = 16.5 Hz, NCH_aH_b), 3.99-3.93 (1H, m, CH₂CH), 2.44 (1H, dd, *J* = 13.2, 3.5 Hz, CH_aH_bCH), 2.21 (1H, dd, *J* = 13.2, 8.6 Hz, CH_aH_bCH), 1.81 (3H, s, NCCH₃), 1.77 (3H, s, =CCH₃); ¹³C NMR (101 MHz, CDCl₃) δ 142.1 (C), 142.0 (CH), 136.9 (C), 132.6 (C), 129.3 (2 × CH), 128.3 (CH), 126.3 (C), 126.1 (2 × CH), 113.3 (CH₂), 110.8 (CH), 55.3 (CH₂), 44.3 (CH₂), 33.1 (CH), 23.0 (CH₃), 18.2 (CH₃); HRMS (ESI) Exact mass calculated for [C₁₇H₂₀N₂NaO₂]⁺ [M+Na]⁺: 307.1417, found 307.1416.

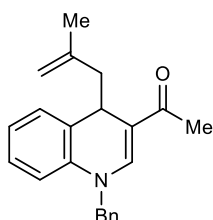


Ethyl 1-benzyl-6-methyl-4-(2-methylallyl)-1,4-dihydropyridine-3-carboxylate (435k). The title compound was prepared according to General Procedure B, using azinium salt **433k** (168 mg, 0.50 mmol) and allyl pinacolboronate **418a** (136 mg, 0.75 mmol), and purified by column chromatography (1 to 3% EtOAc/*n*-pentane) to give a yellow oil (111 mg, 71%). $R_f = 0.59$ (20% EtOAc/petroleum ether); IR 2978, 1683, 1603 (C=O), 1403, 1367, 1203, 1168, 1064, 726, 695 cm^{-1} ; $^1\text{H NMR}$ (400 MHz, CDCl_3) δ 7.38-7.32 (2H, m, ArH), 7.29-7.27 (1H, m, ArH), 7.25 (1H, s, NCH=C), 7.21-7.18 (2H, m, ArH), 4.76-4.75 (1H, m, $\text{CH}_a\text{H}_b=\text{C}$), 4.69-4.66 (1H, m, NC=CH), 4.64-4.57 (2H, m, $\text{CH}_a\text{H}_b=\text{C}$ and NH_aH_b), 4.47 (1H, d, $J = 16.9$ Hz, NH_aH_b), 4.19-4.11 (2H, m, OCH_2), 3.51 (1H, dt, $J = 8.9, 4.4$ Hz, CHCC), 2.28 (1H, dd, $J = 12.8, 3.8$ Hz, $\text{CH}_a\text{H}_b\text{CH}$), 2.09 (1H, dd, $J = 12.8, 9.0$ Hz, $\text{CH}_a\text{H}_b\text{CH}$), 1.76 (3H, s, =CCH₃), 1.75 (3H, s, NCCH₃), 1.26 (3H, t, $J = 7.1$ Hz, CH_2CH_3); $^{13}\text{C NMR}$ (101 MHz, CDCl_3) δ 168.5 (C), 143.1 (C), 143.0 (CH), 138.9 (C), 133.1 (C), 128.9 (2 \times CH), 127.5 (CH), 126.0 (2 \times CH), 112.1 (CH_2), 106.3 (CH), 102.6 (C), 59.5 (CH_2), 54.3 (CH_2), 47.9 (CH_2), 31.5 (CH), 22.8 (CH_3), 18.5 (CH_3), 14.6 (CH_3). HRMS (ESI) Exact mass calculated for $[\text{C}_{20}\text{H}_{26}\text{NO}_2]^+$ $[\text{M}+\text{H}]^+$: 312.1958, found 312.1958.



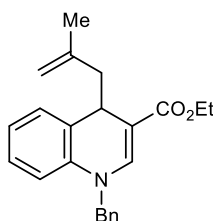
1-Benzyl-4-(2-methylallyl)-1,4-dihydroquinoline-3-carbonitrile (435l). The title compound was prepared according to General Procedure B, using azinium salt **433l** (163 mg, 0.50 mmol) and allyl pinacolboronate **418a** (137 mg, 0.75 mmol), and purified by column chromatography (2 to 20% EtOAc/*n*-pentane) to give a brown solid (126 mg, 84%). $R_f = 0.49$ (20% EtOAc/petroleum ether); m.p. 82-83 $^\circ\text{C}$ (Et_2O); IR 2977, 2183 (C \equiv N), 1601, 1471, 1394, 1218, 1161, 1106, 791, 751 cm^{-1} ; $^1\text{H NMR}$ (500 MHz, CDCl_3) δ 7.38-7.33 (2H, m, ArH), 7.32-7.28 (1H, m, ArH), 7.24-7.21 (2H, m, ArH), 7.09-7.04 (2H, m, ArH), 6.99 (1H, td, $J = 7.4, 1.2$ Hz, ArH), 6.95 (1H, s, NCH=C), 6.72 (1H, dd, $J = 8.1, 1.1$ Hz, ArH), 4.88-4.83 (2H, m, NCH_aH_b and $\text{CH}_a\text{H}_b=\text{C}$), 4.72 (1H, d, $J = 16.6$ Hz, NCH_aH_b), 4.65-4.63 (1H, m, $\text{CH}_a\text{H}_b=\text{C}$), 3.90 (1H, t, $J = 6.2$ Hz, CH_2CH), 2.38 (2H, qdd, $J = 13.2, 6.3, 0.9$ Hz, CH_2CH), 1.69 (3H, s, =CCH₃); $^{13}\text{C NMR}$ (126 MHz, CDCl_3) δ 144.3 (CH), 141.4 (C), 137.1 (C), 136.1 (C), 129.5 (CH), 129.1 (2 \times CH), 128.0 (CH),

127.6 (CH), 126.4 (2 × CH), 124.6 (C), 123.7 (CH), 121.1 (C), 115.2 (CH₂), 113.6 (CH), 82.5 (C), 54.9 (CH₂), 47.9 (CH₂), 37.2 (CH), 23.0 (CH₃); HRMS (ESI) Exact mass calculated for [C₂₁H₂₁N₂]⁺ [M+H]⁺: 301.1699, found 301.1696.



1-[1-Benzyl-4-(2-methylallyl)-1,4-dihydroquinolin-3-yl]ethan-1-one (435m). The title compound was prepared according to General Procedure B, using azinium salt **433m** (171 mg, 0.50 mmol) and allyl pinacolboronate **418a** (137 mg, 0.75 mmol), and purified by column chromatography (5 to 15% EtOAc/*n*-pentane) to give a brown solid

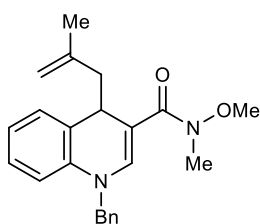
(149 mg, 94%). *R_f* = 0.22 (20% EtOAc/petroleum ether); m.p. 83-84 °C (Et₂O); IR 2956, 1643 (C=O), 1594, 1567, 1358, 1222, 968, 887, 752, 693 cm⁻¹; ¹H NMR (500 MHz, CDCl₃) δ 7.39 (1H, s, NCH=C), 7.38-7.34 (2H, m, ArH), 7.32-7.25 (3H, m, ArH), 7.13 (1H, dd, *J* = 7.5, 1.6 Hz, ArH), 7.04 (1H, td, *J* = 7.4, 1.2 Hz, ArH), 6.97 (1H, td, *J* = 7.4, 1.1 Hz, ArH), 6.75 (1H, dd, *J* = 8.2, 1.1 Hz, ArH), 4.99 (1H, d, *J* = 16.6 Hz, NCH_aH_b), 4.84 (1H, d, *J* = 16.6 Hz, NCH_aH_b), 4.68-4.66 (1H, m, CH_aH_b=C), 4.34-4.29 (2H, m, CH_aH_b=C and CH₂CH), 2.26 (3H, s, O=CCH₃), 2.18 (2H, d, *J* = 6.3 Hz, CH₂CH), 1.69 (3H, s, =CCH₃); ¹³C NMR (126 MHz, CDCl₃) δ 194.2 (C), 144.1 (CH), 143.1 (C), 137.5 (C), 136.4 (C), 130.0 (CH), 129.1 (2 × CH), 127.9 (CH), 127.5 (C), 126.8 (CH), 126.4 (2 × CH), 123.4 (CH), 114.4 (C), 113.6 (CH₂), 113.2 (CH), 55.3 (CH₂), 47.2 (CH₂), 34.8 (CH), 24.6 (CH₃), 22.9 (CH₃); HRMS (ESI) Exact mass calculated for [C₂₂H₂₄NO]⁺ [M+H]⁺: 318.1852, found 318.1853.



Ethyl 1-benzyl-4-(2-methylallyl)-1,4-dihydroquinoline-3-carboxylate (435n). The title compound was prepared according to General Procedure B, using azinium salt **433n** (186 mg, 0.50 mmol) and allyl pinacolboronate **418a** (137 mg, 0.75 mmol), and purified by column chromatography (3% EtOAc/*n*-pentane) to give an off-white solid

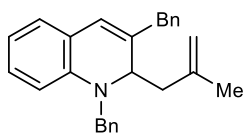
(161 mg, 93%). *R_f* = 0.35 (20% EtOAc/petroleum ether); m.p. 70-71 °C (Et₂O); IR 2902, 1687 (C=O), 1623, 1572, 1468, 1180, 1139, 1076, 850, 769 cm⁻¹; ¹H NMR (400 MHz, CDCl₃) δ 7.52 (1H, s, NCH=C), 7.37-7.31 (2H, m, ArH), 7.29-7.23 (3H, m, ArH), 7.10 (1H, dd, *J* = 7.4, 1.6 Hz, ArH), 7.04-6.99 (1H, m, ArH), 6.97-6.92 (1H, m, ArH), 6.70 (1H, dd, *J* = 8.2, 1.1 Hz, ArH), 4.92 (1H, d, *J* = 16.8 Hz, NCH_aH_b), 4.80 (1H, d, *J*

= 16.8 Hz, NCH_aH_b), 4.71-4.69 (1H, m, CH_aH_b=C), 4.39-4.37 (1H, m, CH_aH_b=C), 4.25-4.18 (2H, m, OCH₂), 4.13 (1H, dd, *J* = 7.1, 5.4 Hz, CH₂CH), 2.29-2.19 (2H, m, CH₂CH), 1.71 (3H, s, =CCH₃), 1.31 (3H, t, *J* = 7.1 Hz, CH₂CH₃); ¹³C NMR (101 MHz, CDCl₃) δ 167.7 (C), 142.8 (C), 142.6 (CH), 137.8 (C), 136.9 (C), 129.9 (CH), 129.0 (2 × CH), 127.7 (CH), 127.0 (C), 126.9 (CH), 126.4 (2 × CH), 123.0 (CH), 113.7 (CH₂), 113.2 (CH), 102.5 (C), 59.7 (CH₂), 55.1 (CH₂), 48.0 (CH₂), 35.9 (CH), 22.9 (CH₃), 14.7 (CH₃); HRMS (ESI) Exact mass calculated for [C₂₃H₂₆NNaO₂]⁺ [M+H]⁺: 348.1958, found 348.1955.



1-Benzyl-N-methoxy-N-methyl-4-(2-methylallyl)-1,4-dihydroquinoline-3-carboxamide (435o). The title compound was prepared according to General Procedure B, using azinium salt **433o** (194 mg, 0.50 mmol) and allyl pinacolboronate **418a** (137 mg, 0.75 mmol), and purified by column chromatography

(10 to 15% EtOAc/*n*-pentane) to give an off-white solid (152 mg, 84%). *R*_f = 0.48 (40% EtOAc/petroleum ether); m.p. 127-128 °C (Et₂O); IR 2971, 1630 (C=O), 1602, 1389, 1218, 1184, 971, 756, 729, 695 cm⁻¹; ¹H NMR (500 MHz, CDCl₃) δ 7.52 (1H, s, NCH=C), 7.36-7.32 (2H, m, ArH), 7.29-7.24 (3H, m, ArH), 7.10 (1H, dd, *J* = 7.5, 1.6 Hz, ArH), 7.04 (1H, ddd, *J* = 8.1, 7.3, 1.6 Hz, ArH), 6.94 (1H, td, *J* = 7.4, 1.1 Hz, ArH), 6.74 (1H, dd, *J* = 8.2, 1.1 Hz, ArH), 4.91 (1H, d, *J* = 16.5 Hz, NCH_aH_b), 4.78 (1H, d, *J* = 16.5 Hz, NCH_aH_b), 4.70-4.68 (1H, m, CH_aH_b=C), 4.41-4.39 (1H, m, CH_aH_b=C), 4.29 (1H, dd, *J* = 7.6, 5.8 Hz, CH₂CH), 3.58 (3H, s, CH₃), 3.25 (3H, s, CH₃), 2.31 (1H, ddd, *J* = 12.8, 5.8, 1.0 Hz, CH_aH_bCH), 2.16 (1H, ddd, *J* = 12.8, 7.6, 0.8 Hz, CH_aH_bCH), 1.74 (3H, s, =CCH₃); ¹³C NMR (126 MHz, CDCl₃) δ 169.4 (C), 143.1 (C), 140.8 (CH), 138.1 (C), 137.1 (C), 129.7 (CH), 129.0 (2 × CH), 127.7 (CH), 126.9 (C), 126.7 (CH), 126.6 (2 × CH), 122.5 (CH), 113.5 (CH₂), 112.6 (CH), 105.1 (C), 60.3 (CH₃), 54.7 (CH₂), 47.9 (CH₂), 36.9 (CH), 34.7 (CH₃), 22.7 (CH₃); HRMS (ESI) Exact mass calculated for [C₂₃H₂₇N₂O₂]⁺ [M+H]⁺: 363.2067, found 363.2064.

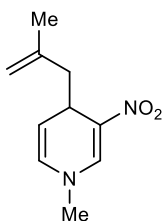
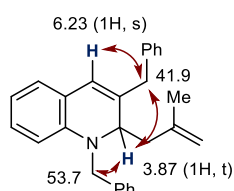


1,3-Dibenzyl-2-(2-methylallyl)-1,2-dihydroquinoline (435p).

The title compound was prepared according to General Procedure B, using azinium salt **433p** (195 mg, 0.50 mmol) and allyl

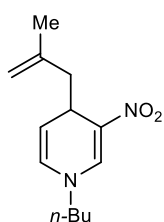
pinacolboronate **418a** (137 mg, 0.75 mmol), and purified by column chromatography (0.5 to 1% EtOAc/*n*-pentane) to give a yellow oil (73.6 mg, 40%). $R_f = 0.69$ (10% EtOAc/petroleum ether); IR 3026, 2912, 1644, 1597, 1493, 1451, 1273, 907, 728, 696 cm^{-1} ; $^1\text{H NMR}$ (400 MHz, CDCl_3) δ 7.30-7.16 (8H, m, ArH), 7.13-7.08 (2H, m, ArH), 7.04-6.96 (2H, m, ArH), 6.66 (1H, td, $J = 7.4, 1.0$ Hz, ArH), 6.55 (1H, d, $J = 8.1$ Hz, ArH), 6.23 (1H, s, $\text{CH}=\text{CCH}_2$), 4.82-4.79 (1H, m, $\text{CH}_a\text{H}_b=\text{C}$), 4.76-4.73 (1H, m, $\text{CH}_a\text{H}_b=\text{C}$), 4.64 (1H, d, $J = 15.7$ Hz, NCH_aH_b), 4.23 (1H, d, $J = 15.7$ Hz, NCH_aH_b), 3.87 (1H, t, $J = 6.5$ Hz, CHCH_2), 3.55 (1H, d, $J = 15.3$ Hz, $\text{CCH}_a\text{H}_b\text{C}$), 3.35 (1H, dd, $J = 15.3, 1.7$ Hz, $\text{CCH}_a\text{H}_b\text{C}$), 2.34 (1H, dd, $J = 13.0, 6.8$ Hz, CHCH_aH_b), 2.13 (1H, dd, $J = 13.0, 6.2$ Hz, CHCH_aH_b), 1.69 (3H, s, $=\text{CCH}_3$); $^{13}\text{C NMR}$ (101 MHz, CDCl_3) δ 142.9 (C), 142.6 (C), 139.1 (C), 138.2 (C), 137.4 (C), 129.2 (2 \times CH), 128.5 (4 \times CH), 128.2 (CH), 127.4 (2 \times CH), 127.0 (CH), 126.7 (CH), 126.5 (CH), 123.8 (C), 122.4 (CH), 117.2 (CH), 114.1 (CH_2), 112.6 (CH), 58.9 (CH), 53.7 (CH_2), 41.9 (CH_2), 40.7 (CH_2), 22.7 (CH_3); HRMS (ESI) Exact mass calculated for $[\text{C}_{27}\text{H}_{28}\text{N}]^+$ $[\text{M}+\text{H}]^+$: 366.2216, found 366.2218.

The regioisomeric structure of product **435p** was assigned based on its HMBC 2D NMR spectra. In the HMBC 2D NMR of product **435p**, the benzyl methylene group at 53.7 ppm correlates with the signal at 3.87 ppm, while the benzyl methylene group at 41.9 ppm correlates with the signals at 3.87 ppm and 6.23 ppm. Only structure **435p** is compatible with this experimental data.



1-Methyl-4-(2-methylallyl)-3-nitro-1,4-dihydropyridine (437a). The title compound was prepared according to a slight modification of General Procedure B (in that the reaction time was 40 h), using azinium salt **433q** (133 mg, 0.50 mmol) and allyl pinacolboronate **418a** (137 mg, 0.75 mmol), and purified by column chromatography (5% EtOAc/*n*-pentane) to give a red solid (56.3 mg, 58%). $R_f = 0.29$ (20% EtOAc/petroleum ether); m.p. 71-72 $^\circ\text{C}$ (Et_2O); IR 3070, 2918, 1668, 1579 (NO_2), 1364 (NO_2), 1248, 1192, 1076, 880, 739 cm^{-1} ; $^1\text{H NMR}$ (400 MHz, CDCl_3) δ 7.82 (1H, t, $J = 1.2$ Hz, $\text{NCH}=\text{C}$), 5.81

(1H, dt, $J = 7.9, 1.2$ Hz, NCH=CH), 5.19 (1H, dd, $J = 7.9, 5.1$ Hz, NCH=CH), 4.81-4.79 (1H, m, CH_aH_b=C), 4.66-4.63 (1H, m, CH_aH_b=C), 3.97-3.91 (1H, m, CH₂CH), 3.16 (3H, s, NCH₃), 2.50-2.44 (1H, m, CH_aH_bCH), 2.13 (1H, dd, $J = 13.1, 9.2$ Hz, CH_aH_bCH), 1.76 (3H, s, =CCH₃); ¹³C NMR (101 MHz, CDCl₃) δ 141.8 (C), 140.8 (CH), 127.1 (CH), 125.2 (C), 113.2 (CH₂), 113.0 (CH), 44.5 (CH₂), 41.7 (CH₃), 31.9 (CH), 22.6 (CH₃); HRMS (ESI) Exact mass calculated for [C₁₀H₁₄N₂NaO₂]⁺ [M+Na]⁺: 217.0947, found 217.0948.

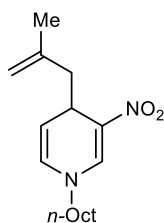


1-Butyl-4-(2-methylallyl)-3-nitro-1,4-dihydropyridine (437b).

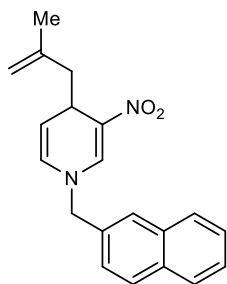
Using azinium salt 433r: The title compound was prepared according to a slight modification of General Procedure B (in that the reaction time was 40 h), using azinium salt **433r** (131 mg, 0.50 mmol) and allyl pinacolboronate **418a** (137 mg, 0.75 mmol), and purified by column chromatography (4% EtOAc/*n*-pentane) to give a red oil (98.7 mg, 84%).

Using azinium salt 433s: The title compound was prepared according to a slight modification of General Procedure B (in that the reaction time was 40 h), using azinium salt **433s** (154 mg, 0.50 mmol) and allyl pinacolboronate **418a** (137 mg, 0.75 mmol), and purified by column chromatography (5% EtOAc/*n*-pentane) to give an orange oil (44.1 mg, 37%).

$R_f = 0.46$ (20% EtOAc/petroleum ether); IR 3072, 2930, 1667, 1584 (NO₂), 1371 (NO₂), 1259, 1183, 1017, 888, 734 cm⁻¹; ¹H NMR (400 MHz, CDCl₃) δ 7.85 (1H, t, $J = 1.2$ Hz, NCH=C), 5.85 (1H, dt, $J = 7.9, 1.2$ Hz, NCH=CH), 5.19 (1H, dd, $J = 7.9, 5.1$ Hz, NCH=CH), 4.82-4.80 (1H, m, CH_aH_b=C), 4.66-4.64 (1H, m, CH_aH_b=C), 3.97 (1H, ddd, $J = 8.7, 5.0, 3.5$ Hz, CH₂CH), 3.30 (2H, td, $J = 7.0, 3.4$ Hz, NCH₂), 2.45 (1H, dd, $J = 13.1, 8.9$ Hz, CH_aH_bCH), 2.17 (1H, dd, $J = 13.1, 3.4$ Hz, CH_aH_bCH), 1.77 (3H, s, =CCH₃), 1.65-1.57 (2H, m, CH₂CH₂CH₃), 1.40-1.30 (2H, m, CH₂CH₃), 0.96 (3H, t, $J = 7.3$ Hz, CH₂CH₃); ¹³C NMR (101 MHz, CDCl₃) δ 141.9 (C), 140.3 (CH), 126.3 (CH), 125.0 (C), 113.3 (CH₂), 113.1 (CH), 54.9 (CH₂), 44.3 (CH₂), 32.3 (CH), 32.0 (CH₂), 22.7 (CH₃), 19.6 (CH₂), 13.7 (CH₃); HRMS (ESI) Exact mass calculated for [C₁₃H₂₀N₂NaO₂]⁺ [M+Na]⁺: 259.1417, found 259.1416.



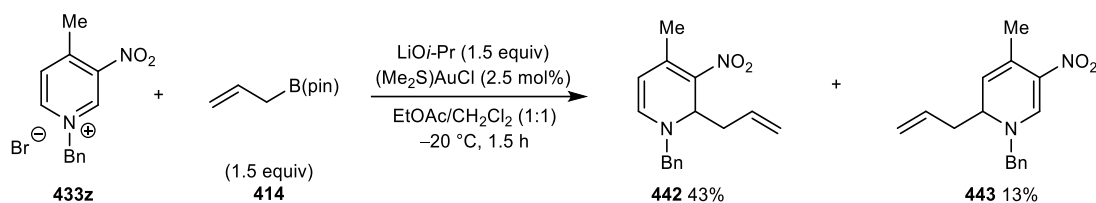
4-(2-Methylallyl)-3-nitro-1-octyl-1,4-dihydropyridine (437c). The title compound was prepared according to a slight modification of General Procedure B (in that the reaction time was 40 h), using azinium salt **433t** (159 mg, 0.50 mmol) and allyl pinacolboronate **418a** (137 mg, 0.75 mmol), and purified by column chromatography (2 to 3% EtOAc/*n*-pentane) to give a red oil (118 mg, 81%). $R_f = 0.55$ (20% EtOAc/petroleum ether); IR 3073, 2925, 2855, 1667, 1585 (NO₂), 1373 (NO₂), 1259, 1189, 888, 730 cm⁻¹; ¹H NMR (400 MHz, CDCl₃) δ 7.84 (1H, t, $J = 1.1$ Hz, NCH=C), 5.84 (1H, dt, $J = 8.0, 1.0$ Hz, NCH=CH), 5.19 (1H, dd, $J = 7.8, 5.1$ Hz, NCH=CH), 4.82-4.80 (1H, m, CH_aH_b=C), 4.66-4.64 (1H, m, CH_aH_b=C), 3.97 (1H, ddd, $J = 8.7, 5.0, 3.6$ Hz, CH₂CH), 3.35-3.23 (2H, m, NCH₂), 2.45 (1H, dd, $J = 13.0, 3.4$ Hz, CH_aH_bCH), 2.16 (1H, dd, $J = 13.0, 8.9$ Hz, CH_aH_bCH), 1.76 (3H, s, =CCH₃), 1.65-1.58 (2H, m, NCH₂CH₂), 1.34-1.22 (10H, m, (CH₂)₅CH₃), 0.90-0.86 (3H, m, CH₂CH₃); ¹³C NMR (126 MHz, CDCl₃) δ 141.9 (C), 140.3 (CH), 126.3 (CH), 125.0 (C), 113.3 (CH₂), 113.1 (CH), 55.2 (CH₂), 44.3 (CH₂), 32.3 (CH), 31.8 (CH₂), 29.9 (CH₂), 29.23 (CH₂), 29.21 (CH₂), 26.3 (CH₂), 22.7 (CH₂ and CH₃), 14.2 (CH₃); HRMS (ESI) Exact mass calculated for [C₁₇H₂₉N₂O₂]⁺ [M+H]⁺: 293.2224, found 293.2221.



4-(2-Methylallyl)-1-(naphthalen-2-ylmethyl)-3-nitro-1,4-dihydropyridine (437d). The title compound was prepared according to a slight modification of General Procedure B (in that the reaction time was 40 h), using azinium salt **433u** (173 mg, 0.50 mmol) and allyl pinacolboronate **418a** (137 mg, 0.75 mmol), and purified by column chromatography (5% EtOAc/*n*-pentane) to give a red oil (139 mg, 87%). $R_f = 0.36$ (20% EtOAc/petroleum ether); IR 3066, 2916, 1999, 1765, 1509 (NO₂), 1369 (NO₂), 1176, 1079, 889, 730 cm⁻¹; ¹H NMR (400 MHz, CDCl₃) δ 8.03 (1H, t, $J = 1.1$ Hz, NCH=C), 7.90-7.82 (3H, m, ArH), 7.67 (1H, s, ArH), 7.56-7.50 (2H, m, ArH), 7.31 (1H, dd, $J = 8.4, 1.8$ Hz, ArH), 5.91 (1H, dt, $J = 7.9, 1.2$ Hz, NCH=CH), 5.19 (1H, dd, $J = 7.9, 5.1$ Hz, NCH=CH), 4.83-4.81 (1H, m, CH_aH_b=C), 4.67-4.65 (1H, m, CH_aH_b=C), 4.64 (2H, s, NCH₂), 4.02 (1H, ddd, $J = 8.7, 5.0, 3.5$ Hz, CH₂CH), 2.47 (1H, dd, $J = 13.1, 3.4$ Hz, CH_aH_bCH), 2.23 (1H, dd, $J = 13.1, 8.8$ Hz, CH_aH_bCH), 1.77 (3H, s, =CCH₃); ¹³C NMR (101 MHz, CDCl₃) δ 141.8 (C), 140.4 (CH), 133.4 (C), 133.3 (C), 132.7 (C), 129.4 (CH), 127.98 (CH), 127.96 (CH), 127.0 (CH),

126.8 (CH), 126.7 (CH), 126.4 (CH), 125.9 (C), 124.7 (CH), 113.5 (CH₂), 113.2 (CH), 58.7 (CH₂), 44.4 (CH₂), 32.4 (CH), 22.8 (CH₃); HRMS (ESI) Exact mass calculated for [C₂₀H₂₁N₂O₂]⁺ [M+H]⁺: 321.1598, found 321.1595.

2-Allyl-1-benzyl-4-methyl-3-nitro-1,2-dihydropyridine (442) and 2-allyl-1-benzyl-4-methyl-5-nitro-1,2-dihydropyridine (443)



The title compounds were prepared according to a slight modification of General Procedure B (in that the reaction was left to stir for 1.5 h), using azinium salt **433z** (155 mg, 0.50 mmol), and allyl pinacolboronate **418a** (141 μL, 0.75 mmol), and purified by column chromatography (5% to 15% EtOAc/*n*-pentane) to give *allylated product* **442** as a red oil (57.9 mg, 43%), followed by *allylated product* **443** as a yellow oil (17.6 mg, 13%).

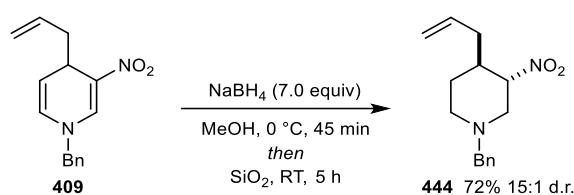
Data of major regioisomer 442: R_f = 0.51 (20% EtOAc/petroleum ether); IR 2924, 1600 (NO₂), 1480, 1398, 1333 (NO₂), 1258, 1160, 994, 917, 728 cm⁻¹; ¹H NMR (400 MHz, CDCl₃) δ 7.39-7.30 (3H, m, ArH), 7.23-7.19 (2H, m, ArH), 6.64 (1H, d, *J* = 6.3 Hz, NCH=CH), 5.96-5.85 (1H, m, CH=CH₂), 5.24 (1H, ddd, *J* = 6.6, 5.2, 1.3 Hz, NCHCH₂), 5.13-5.06 (2H, m, CH=CH₂), 4.90 (1H, d, *J* = 6.3 Hz, NCH=CH), 4.57 (1H, d, *J* = 15.0 Hz, NCH_aH_b), 4.50 (1H, d, *J* = 15.0 Hz, NCH_aH_b), 2.52-2.45 (1H, m, CHCH_aH_b), 2.44 (3H, s, CH₃), 2.33-2.25 (1H, m, CHCH_aH_b); ¹³C NMR (101 MHz, CDCl₃) δ 148.1 (C), 145.0 (CH), 135.4 (C), 133.7 (CH), 129.3 (2 × CH), 128.7 (CH), 127.8 (2 × CH), 123.1 (C), 118.8 (CH₂), 101.0 (CH), 59.5 (CH₂), 57.4 (CH), 35.6 (CH₂), 22.6 (CH₃); HRMS (ESI) Exact mass calculated for [C₁₆H₁₈N₂NaO₂]⁺ [M+Na]⁺: 293.1260, found 293.1256.

Data of minor regioisomer 443: R_f = 0.45 (20% EtOAc/petroleum ether); IR 2967, 1643, 1575 (NO₂), 1390, 1346 (NO₂), 1274, 1168, 993, 816, 699 cm⁻¹; ¹H NMR (400 MHz, CDCl₃) δ 8.28 (1H, s, NCH=C), 7.44-7.36 (3H, m, ArH), 7.29-7.25 (2H, m, ArH), 5.86-5.76 (1H, m, CH₂=CH), 5.19-5.12 (2H, m, CH₂=CH), 4.78 (1H, d, *J* = 4.9 Hz, NCHCH), 4.57-4.49 (2H, m, NCH₂), 4.12-4.07 (1H, m, CH₂CH), 2.46-2.37 (1H, m, CH_aH_bCH),

2.29-2.23 (1H, m, CH_aH_bCH), 2.21 (3H, s, CH₃); ¹³C NMR (101 MHz, CDCl₃) δ 148.5 (CH), 134.0 (C), 132.2 (CH), 129.4 (2 × CH), 129.0 (CH and C), 128.0 (2 × CH), 124.8 (C), 119.6 (CH₂), 112.2 (CH), 58.8 (CH₂), 57.9 (CH), 39.1 (CH₂), 21.4 (CH₃); HRMS (ESI) Exact mass calculated for [C₁₆H₁₈N₂NaO₂]⁺ [M+Na]⁺: 293.1260, found 293.1257.

3.5 Product Manipulations

(±)-(3*S*,4*R*)-4-Allyl-1-benzyl-3-nitropiperidine (**444**)



To a solution of 1,4-dihydropyridine **409** (128 mg, 0.50 mmol) in MeOH (3 mL) at 0 °C was added NaBH₄ (132 mg, 3.50 mmol) portionwise. The resulting reaction mixture was stirred at 0 °C for 45 min. The reaction was quenched with saturated aqueous NH₄Cl solution (10 mL) and extracted with CH₂Cl₂ (15 mL). The organic layer was washed with saturated aqueous NH₄Cl solution (10 mL), dried (MgSO₄), filtered, and concentrated *in vacuo*. The residue was dissolved in CH₂Cl₂ (10 mL) and SiO₂ (10.0 g) was added. The resulting suspension was concentrated *in vacuo* and left standing absorbed on SiO₂ at room temperature for 5 h. CHCl₃ (75 mL) was added, and the slurry was stirred for an additional 30 min. The slurry was filtered using EtOAc (50 mL) as the eluent and the filtrate was concentrated *in vacuo* to give the title compound **444** as a 15:1 mixture of inseparable diastereomers as a pale-yellow oil (93.2 mg, 72%). R_f = 0.31 (10% EtOAc/petroleum ether); IR 2921, 2812, 1552 (NO₂), 1453, 1357 (NO₂), 1163, 983, 916, 735, 698 cm⁻¹; HRMS (ESI) Exact mass calculated for [C₁₅H₂₁N₂O₂]⁺ [M+H]⁺: 261.1598, found 261.1602.

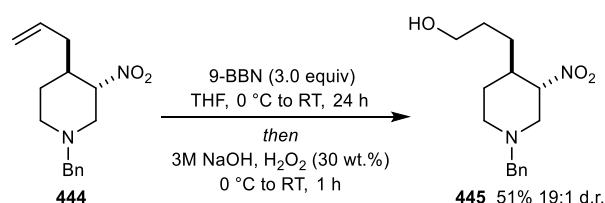
NMR data of major diastereomer: ¹H NMR (400 MHz, CDCl₃) δ 7.34-7.24 (5H, m, ArH), 5.71 (1H, ddt, *J* = 17.0, 10.5, 7.1 Hz, CH₂=CH), 5.09-5.03 (2H, m, CH₂=), 4.41 (1H, td, *J* = 10.4, 4.1 Hz, CHNO₂), 3.59 (1H, d, *J* = 13.1 Hz, CH_aH_bPh), 3.51 (1H, d, *J* = 13.1 Hz, CH_aH_bPh), 3.24 (1H, ddd, *J* = 10.4, 4.1, 1.7 Hz, NCH_aH_bCH), 2.89-2.84 (1H, m, NCH_aH_bCH₂), 2.43 (1H, t, *J* = 10.4 Hz, NCH_aH_bCH), 2.23-2.16 (1H, m,

CH₂=CHCH_aH_b), 2.12-2.03 (2H, m, NCH_aH_bCH₂ and CHCHN), 2.02-1.94 (1H, m, CH₂=CHCH_aH_b), 1.84 (1H, dq, *J* = 13.8, 3.2 Hz, NCH₂CH_aCH_b), 1.42-1.32 (1H, m, NCH₂CH_aCH_b); ¹³C NMR (101 MHz, CDCl₃) δ 137.5 (C), 134.0 (CH), 129.1 (2 × CH), 128.53 (2 × CH), 127.5 (CH), 118.3 (CH₂), 87.8 (CH), 62.5 (CH₂), 56.6 (CH₂), 52.6 (CH₂), 39.1 (CH), 36.6 (CH₂), 28.8 (CH₂).

Characteristic NMR data of minor diastereomer: ¹H NMR (400 MHz, CDCl₃) δ 4.61-4.57 (1H, m, CHN), 2.77-2.70 (1H, m, NCH_aH_bCH), 2.60-2.54 (1H, m, NCH_aH_bCH₂), 1.63 (1H, dq, *J* = 13.8, 4.6 Hz, NCH₂CH_aH_b); ¹³C NMR (101 MHz, CDCl₃) δ 137.8 (C), 135.3 (CH), 128.8 (2 × CH), 128.47 (2 × CH), 127.4 (CH), 117.8 (CH₂), 83.7 (CH), 26.8 (CH₂).

The relative configuration of **444** was determined by ¹H NMR spectroscopy, on the basis of the coupling constant of the α-proton adjacent to the nitro substituent at 4.41 ppm (²*J* = 10.4 Hz). This coupling constant indicates a *trans*-diaxial relationship, allowing the two bulky substituents to occupy the more favourable equatorial positions.

(±)-3-[(3*S*,4*R*)-1-Benzyl-3-nitropiperidin-4-yl]propan-1-ol (**445**)



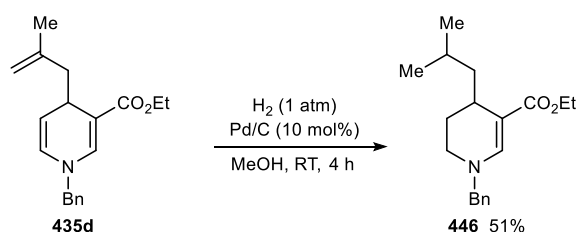
To a solution of alkene **444** (26.0 mg, 0.10 mmol) in THF (0.5 mL) at 0 °C was added 9-BBN (0.5 M in THF, 600 μL, 0.30 mmol). The resulting solution was warmed to room temperature and stirred for 24 h. The reaction was cooled to 0 °C and 3 M aqueous NaOH (0.3 mL) and H₂O₂ (30 wt.% in H₂O, 0.5 mL) were added. The mixture was warmed to room temperature and stirred for 1 h. The reaction was diluted with H₂O (5 mL), extracted with EtOAc (3 × 10 mL), and the combined organic layers were dried (MgSO₄), filtered, and concentrated *in vacuo*. Purification of the residue by column chromatography (10 to 30% EtOAc/*n*-pentane) gave the title compound **445** as a 19:1 mixture of inseparable diastereomers as a colourless oil (14.3 mg, 51%). *R_f* = 0.21 (40% EtOAc/petroleum ether); IR 3364 (OH), 2924, 2815, 1558 (NO₂), 1344 (NO₂), 1173, 1055, 910, 734, 698

cm⁻¹; HRMS (ESI) Exact mass calculated for [C₁₅H₂₃N₂O₃]⁺ [M+H]⁺: 279.1703, found 279.1701.

NMR data of major diastereomer: ¹H NMR (400 MHz, CDCl₃) δ 7.34-7.25 (5H, m, ArH), 4.40 (1H, td, *J* = 10.5, 4.0 Hz, CHNO₂), 3.66-3.57 (3H, m, HOCH₂ and CH_aH_bPh), 3.52 (1H, d, *J* = 13.1 Hz, CH_aH_bPh), 3.24 (1H, ddd, *J* = 10.5, 4.0, 1.7 Hz, NCH_aH_bCH), 2.91-2.87 (1H, m, NCH_aH_bCH₂), 2.43 (1H, t, *J* = 10.5 Hz, NCH_aH_bCH), 2.10 (1H, td, *J* = 11.8, 2.8 Hz, NCH_aH_bCH₂), 2.05-1.96 (1H, m, CHCHN), 1.93-1.87 (1H, m, NCH₂CH_aH_b), 1.70-1.58 (2H, m, HOCH₂CH_aH_b and HOCH₂), 1.52-1.43 (2H, m, HOCH₂CH_aH_b and HOCH₂CH₂CH_aH_b), 1.38-1.28 (2H, m, HOCH₂CH₂CH_aH_b and NCH₂CH_aH_b); ¹³C NMR (101 MHz, CDCl₃) δ 137.5 (C), 129.1 (2 × CH), 128.6 (2 × CH), 127.6 (CH), 88.6 (CH), 62.8 (CH₂), 62.5 (CH₂), 56.6 (CH₂), 52.7 (CH₂), 39.5 (CH), 29.1 (CH₂), 29.0 (CH₂), 28.5 (CH₂).

Characteristic NMR data of minor diastereomer: ¹H NMR (400 MHz, CDCl₃) δ 4.64-4.59 (1H, m, CHN), 2.74-2.67 (1H, m, NCH_aH_bCH), 2.65-2.59 (1H, m, NCH_aH_bCH₂).

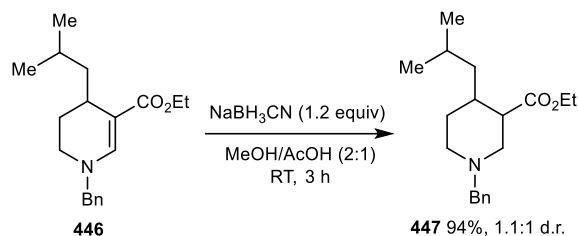
Ethyl 1-benzyl-4-isobutyl-1,4,5,6-tetrahydropyridine-3-carboxylate (**446**)



To a solution of 1,4-dihydropyridine **435d** (297 mg, 1.00 mmol) in MeOH (10 mL) was added 10% Pd/C (106 mg, 0.10 mmol). The flask was sealed, evacuated, and backfilled with hydrogen (3 cycles) and the solution was stirred at room temperature for 4 h. The reaction was filtered and concentrated *in vacuo*. Purification of the residue by column chromatography (1 to 3% EtOAc/*n*-pentane) gave the title compound **446** as a yellow oil (154 mg, 51%). *R_f* = 0.34 (10% EtOAc/petroleum ether); IR 2952, 2867, 1674 (C=O), 1599, 1361, 1263, 1193, 1148, 729, 697 cm⁻¹; ¹H NMR (500 MHz, CDCl₃) δ 7.54 (1H, s, NCH=C), 7.37-7.33 (2H, m, ArH), 7.31-7.28 (1H, m, ArH), 7.22-7.19 (2H, m, ArH), 4.33 (1H, d, *J* = 15.3 Hz, CH_aH_bPh), 4.29 (1H, d, *J* = 15.3 Hz, CH_aH_bPh), 4.21-4.08 (2H, m, OCH₂), 3.01 (1H, td, *J* = 12.7, 3.7 Hz, NCH_aH_bCH₂), 2.92-2.88 (1H, m, NCH_aH_bCH₂), 2.71 (1H, dtt, *J* = 9.3, 4.6, 1.5 Hz, CHC=C), 1.73 (1H, ddt, *J* = 13.3, 3.9,

2.2 Hz, NCH₂CH_aH_b), 1.67-1.56 (2H, m, NCH₂CH_aH_b and (CH₃)₂CH), 1.34 (1H, dddd, *J* = 13.6, 9.4, 4.2, 0.9 Hz, (CH₃)₂CHCH_aH_b), 1.27 (3H, t, *J* = 7.1 Hz, CH₂CH₃), 1.06 (1H, dddd, *J* = 14.0, 9.7, 4.7, 0.9 Hz, (CH₃)₂CHCH_aH_b), 0.94 (3H, d, *J* = 6.5 Hz, (CH₃)₂CH), 0.89 (3H, d, *J* = 6.5 Hz, (CH₃)₂CH); ¹³C NMR (126 MHz, CDCl₃) δ 168.9 (C), 145.7 (CH), 137.3 (C), 128.9 (2 × CH), 127.9 (CH), 127.5 (2 × CH), 100.1 (C), 59.9 (CH₂), 59.0 (CH₂), 45.4 (CH₂), 41.4 (CH₂), 27.0 (CH), 25.1 (CH), 24.5 (CH₂), 24.1 (CH₃), 21.9 (CH₃), 14.8 (CH₃); HRMS (ESI) Exact mass calculated for [C₁₉H₂₇NNaO₂]⁺ [M+Na]⁺: 324.1934, found 324.1927.

Ethyl 1-benzyl-4-isobutylpiperidine-3-carboxylate (**447**)



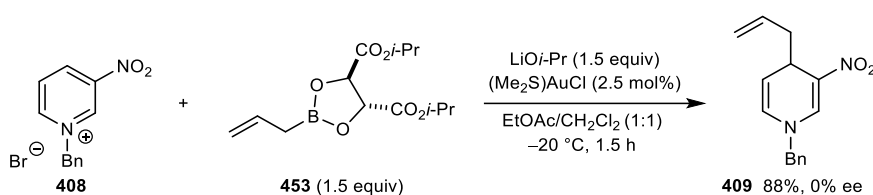
A flask was charged with tetrahydropyridine **446** (30.1 mg, 0.10 mmol), purged with argon for 30 min, followed by the addition of AcOH (0.5 mL). A solution of NaBH₃CN (7.5 mg, 0.12 mmol) in MeOH (1 mL) was added and the resulting solution was stirred at room temperature for 3 h. The reaction was diluted with Et₂O (5 mL) and extracted with 1 M aqueous HCl solution (3 × 5 mL). The combined aqueous layers were neutralised with saturated aqueous NaHCO₃ solution (20 mL), extracted with EtOAc (3 × 10 mL), dried (MgSO₄), filtered, and concentrated *in vacuo* to give the title compound **447** as a 1.1:1 mixture of inseparable diastereomers as a yellow oil (28.3 mg, 93%). IR 2953, 2928, 2804, 1642 (C=O), 1494, 1367, 1144, 1029, 733, 697 cm⁻¹; HRMS (ESI) Exact mass calculated for [C₁₉H₃₀NO₂]⁺ [M+H]⁺: 304.2271, found 304.2276.

NMR data of major diastereomer: ¹H NMR (400 MHz, CDCl₃) δ 7.32-7.21 (5H, m, ArH), 4.11 (2H, qd, *J* = 7.1, 2.1 Hz, OCH₂), 3.50 (2H, s, NCH₂C), 2.96 (1H, ddd, *J* = 10.9, 3.8, 1.8 Hz, NCH_aH_bCH), 2.86 (1H, dd, *J* = 12.2, 3.9 Hz, NCH_aH_bCH₂), 2.32 (1H, td, *J* = 10.7, 3.8 Hz, CHC=O), 2.12 (1H, t, *J* = 10.9 Hz, NCH_aH_bCH), 2.01 (1H, td, *J* = 11.7, 2.8 Hz, NCH_aH_bCH₂), 1.87-1.76 (1H, m, NCH₂CH_aH_b), 1.68-1.52 (2H, m, CHCHC=O and (CH₃)₂CH), 1.26-1.17 (4H, m, CH₂CH₃ and NCH₂CH_aH_b), 1.11-1.07 (2H, m, CH₂CHCHC=O), 0.89-0.81 (6H, m, (CH₃)₂CH). ¹³C NMR (101 MHz, CDCl₃) δ 174.5 (C), 138.4 (C), 129.3 (2 × CH), 128.33 (2 × CH), 127.1 (CH), 63.1 (CH₂), 60.3

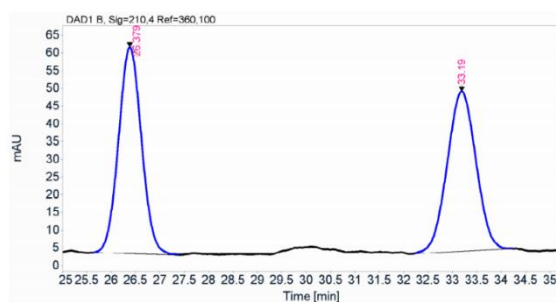
(CH₂), 56.1 (CH₂), 53.5 (CH₂), 49.8 (CH), 43.8 (CH₂), 35.6 (CH), 30.4 (CH₂), 24.8 (CH), 24.2 (CH₃), 21.5 (CH₃), 14.4 (CH₃).

Characteristic NMR data of minor diastereomer: ¹H NMR (400 MHz, CDCl₃) δ 3.58 (1H, d, *J* = 13.3 Hz, NCH_aH_bC), 3.42 (1H, d, *J* = 13.3 Hz, NCH_aH_bC), 2.53-2.44 (1H, m, NCH_aH_bCH₂), 1.91-1.83 (1H, m, NCH₂CH_aH_b); ¹³C NMR (101 MHz, CDCl₃) δ 173.5 (C), 138.8 (C), 129.1 (2 × CH), 128.25 (2 × CH), 127.0 (CH), 63.3 (CH₂), 60.0 (CH₂), 28.5 (CH₂), 25.5 (CH), 23.5 (CH₃), 22.3 (CH₃).

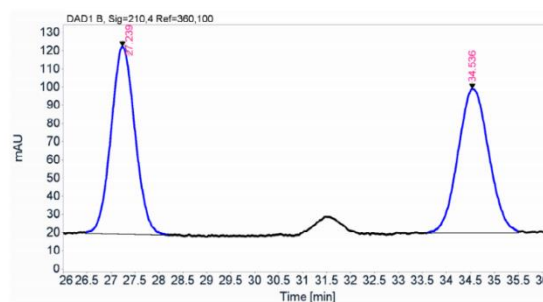
3.6 Alkylation using Enantiopure Allyl Pinacolboronate **453**



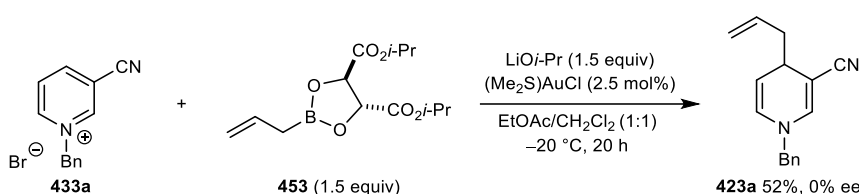
An oven-dried microwave vial fitted with a stirrer bar was charged with azinium salt **408** (29.5 mg, 0.10 mmol), (Me₂S)AuCl (0.74 mg, 0.0025 mmol) and Li*Oi*-Pr (9.9 mg, 0.15 mmol). The vial was sealed with a septum-lined cap and EtOAc/CH₂Cl₂ (1:1) (0.6 mL) (both of which were undried, obtained from commercial vendors and used without further purification) was added. The mixture was stirred at -20 °C for 5 min and a solution of allyl pinacolboronate **453** (contaminated with 32% (+)-diisopropyl L-tartrate, which is consistent with previously reported literature)²⁰¹ (56.2 mg, 0.15 mmol) in 0.4 mL of EtOAc/CH₂Cl₂ (1:1) was added dropwise. The resulting solution was stirred at -20 °C for 1.5 h. The reaction was warmed to room temperature and then passed through a plug of silica (4 cm in height and 1 cm wide) using Et₂O (20 mL) as the eluent and the filtrate was concentrated *in vacuo*. 1,3,5-Trimethoxybenzene was added as an internal standard, and the crude material was analyzed by ¹H NMR spectroscopy (88% yield). Enantiomeric excess was determined by HPLC using a Chiralcel IC column (80:20 *iso*-hexane:*i*-PrOH, 1.0 mL/min, 210 nm, 25 °C): *t*_r = 27.2 and 34.5 min, 0% ee.

HPLC trace using **414**

Signal:	DAD1 B, Sig=210,4 Ref=360,100				
RT [min]	Type	Width [min]	Area	Height	Area%
26.379	BB	0.4948	1912.465	58.2828	50.77
33.190	BB	0.5953	1854.317	45.1389	49.23

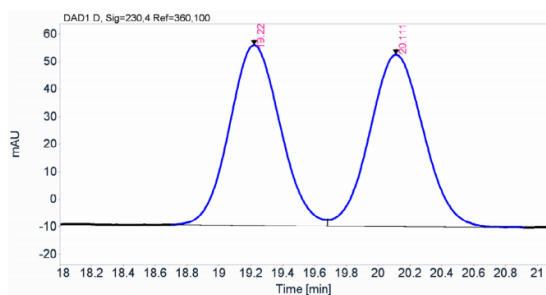
HPLC trace using **453**

Signal:	DAD1 B, Sig=210,4 Ref=360,100				
RT [min]	Type	Width [min]	Area	Height	Area%
27.239	VB	0.4640	3567.040	103.0003	50.28
34.536	VV	0.5381	3527.187	79.1174	49.72



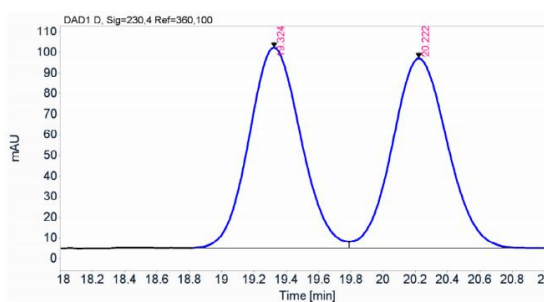
An oven-dried microwave vial fitted with a stirrer bar was charged with azinium salt **433a** (29.5 mg, 0.10 mmol), (Me₂S)AuCl (0.74 mg, 0.0025 mmol) and LiO*i*-Pr (9.9 mg, 0.15 mmol). The vial was sealed with a septum-lined cap and EtOAc/CH₂Cl₂ (1:1) (0.6 mL) (both of which were undried, obtained from commercial vendors and used without further purification) was added. The mixture was stirred at –20 °C for 5 min and a solution of allyl pinacolboronate **453** (contaminated with 32% (+)-diisopropyl L-tartrate, which is consistent with previously reported literature)²⁰¹ (56.2 mg, 0.15 mmol) in 0.4 mL of EtOAc/CH₂Cl₂ (1:1) was added dropwise. The resulting solution was stirred at –20 °C for 20 h. The reaction was warmed to room temperature and then passed through a plug of silica (4 cm in height and 1 cm wide) using Et₂O (20 mL) as the eluent and the filtrate was concentrated *in vacuo*. 1,3,5-Trimethoxybenzene was added as an internal standard, and the crude material was analyzed by ¹H NMR spectroscopy (52% yield). Enantiomeric excess was determined by HPLC using a Chiralcel IC column (90:10 *iso*-hexane:*i*-PrOH, 1.0 mL/min, 230 nm, 25 °C): *t*_r = 19.3 and 20.2 min, 0% ee.

HPLC trace using 414



Signal: DAD1 D, Sig=230,4 Ref=360,100					
RT [min]	Type	Width [min]	Area	Height	Area%
19.220	BV	0.3444	1451.283	65.5285	49.74
20.111	VB	0.3539	1466.676	62.4817	50.26

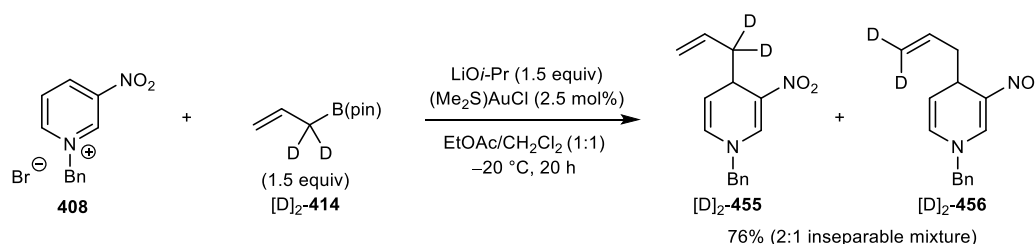
HPLC trace using 453



Signal: DAD1 D, Sig=230,4 Ref=360,100					
RT [min]	Type	Width [min]	Area	Height	Area%
19.324	BV	0.3475	2160.957	97.1660	49.83
20.222	VB	0.3595	2175.803	92.1442	50.17

3.7 Deuterium Labelling Studies

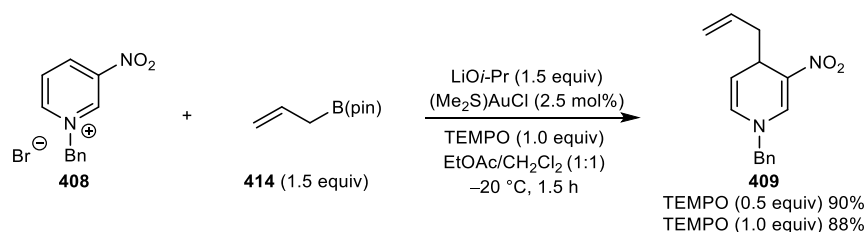
4-(Allyl-1,1-d₂)-1-benzyl-3-nitro-1,4-dihydropyridine ([D]₂-455) and 4-(allyl-3,3-d₂)-1-benzyl-3-nitro-1,4-dihydropyridine ([D]₂-456).



An oven-dried microwave vial fitted with a stirrer bar was charged with azinium salt **408** (29.5 mg, 0.10 mmol), (Me₂S)AuCl (0.74 mg, 0.0025 mmol) and Li*o*-Pr (9.9 mg, 0.15 mmol). The vial was sealed with a septum-lined cap and EtOAc/CH₂Cl₂ (1:1) (0.6 mL) (both of which were undried, obtained from commercial vendors and used without further purification) was added. The mixture was stirred at –20 °C for 5 min and a solution of dideuterated allyl pinacolboronate [D]₂-**414** (contaminated with 15% vinylboronic acid pinacol ester, which is consistent with previously reported literature)^{202,217,218} (29.3 mg, 0.15 mmol) in 0.4 mL of EtOAc/CH₂Cl₂ (1:1) was added dropwise. The resulting solution was stirred at –20 °C for 20 h. The reaction was warmed to room temperature and then passed through a plug of silica (4 cm in height and 1 cm wide) using Et₂O (20 mL) as the eluent and the filtrate was concentrated *in vacuo*. Purification of the residue by column chromatography (5% EtOAc/*n*-pentane) gave a 2:1 mixture of *allylated products* [D]₂-**455** and [D]₂-**456** as a red oil (19.6 mg, 76%). R_f = 0.40 (20% EtOAc/petroleum ether);

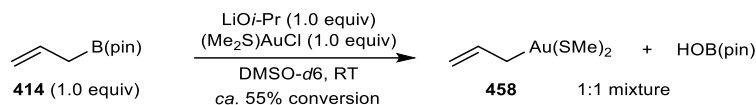
IR 2925, 1667, 1585 (NO₂), 1356 (NO₂), 1264, 1173, 1076, 915, 730, 698 cm⁻¹; ¹H NMR (400 MHz, CDCl₃) δ 7.96 (1H, t, *J* = 1.1 Hz, NCH=C), 7.42-7.33 (3H, m, ArH), 7.24-7.20 (2H, m, ArH), 5.89 (1H, dt, *J* = 7.9, 1.2 Hz, NCH=CH), 5.73 (1H, dd, *J* = 16.9, 10.2 Hz, CH₂=CH of [D]₂-**455** and CD₂=CH of [D]₂-**456**), 5.13 (1H, dd, *J* = 7.9, 5.1 Hz, NCH=CH), 5.07-5.00 (1.33H, m, CH₂=CH of [D]₂-**455**), 4.47 (2H, s, NCH₂), 3.99-3.95 (1H, m, CHCHC), 2.45 (0.33H, ddd, *J* = 13.7, 8.3, 6.6 Hz, CH_aH_bCH of [D]₂-**456**), 2.26 (0.33H, ddd, *J* = 13.7, 6.6, 3.4 Hz, CH_aH_bCH of [D]₂-**456**); ²H NMR (77 MHz, CHCl₃) δ 5.13-5.01 (2D, m, CD₂=C of [D]₂-**456**), 2.44 (1D, s, CD_aD_bCH of [D]₂-**455**), 2.25 (1D, s, CD_aD_bCH of [D]₂-**455**); ¹³C NMR (101 MHz, CDCl₃) δ 140.7 (CH), 135.3 (C), 134.3 (CH), 134.2 (CH), 129.3 (2 × CH), 128.7 (CH), 127.5 (2 × CH), 127.1 (CH), 125.0 (C), 118.2 (CH₂), 112.8 (CH), 58.5 (CH₂), 39.3 (CH₂) 33.7 (CH), 33.6 (CH); HRMS (ESI) Exact mass calculated for [C₁₅H₁₅D₂N₂O₂]⁺ [M+H]⁺: 259.1410, found 259.1409.

3.8 TEMPO Studies



An oven-dried flask equipped with a stirrer bar was charged with azinium salt **408** (29.5 mg, 0.10 mmol), (Me₂S)AuCl (0.74 mg, 0.0025 mmol), TEMPO [7.8 mg, 0.05 mmol (0.5 equiv) or 15.6 mg, 0.10 mmol (1.0 equiv)] and LiO-*i*Pr (9.9 mg, 0.15 mmol). The vial was sealed and EtOAc/CH₂Cl₂ (1:1) (0.6 mL) (both of which were undried, obtained from commercial vendors and used without further purification) was added. The mixture was stirred at -20 °C for 5 min and a solution of the allyl pinacolboronate **414** (28.1 μL, 0.15 mmol) in 0.4 mL of EtOAc/CH₂Cl₂ (1:1) was added dropwise. The resulting solution was stirred at -20 °C for 1.5 h. The reaction was warmed to room temperature and then passed through a plug of silica (4 cm in height and 1 cm wide) using Et₂O (20 mL) as the eluent and the filtrate was concentrated *in vacuo*. 1,3,5-Trimethoxybenzene was added as an internal standard, and the crude material was analysed by ¹H NMR spectroscopy [90% yield using TEMPO (0.5 equiv) and 88% using TEMPO (1.0 equiv)].

3.9 ^1H NMR and ^{11}B NMR Studies



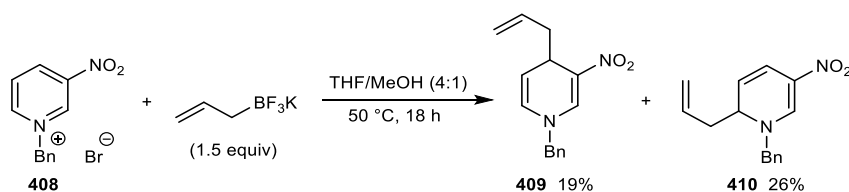
To an NMR tube was added a solution of $(\text{Me}_2\text{S})\text{AuCl}$ (29.5 mg, 0.10 mmol) and LiOi-Pr (6.6 mg, 0.10 mmol) in $\text{DMSO-}d_6$ (0.5 mL). Allyl pinacolboronate **414** (18.8 μL , 0.10 mmol) was added and the mixture was analysed by ^1H and ^{11}B NMR spectroscopy.

NMR data for 458: ^1H NMR (400 MHz, $\text{DMSO-}d_6$) δ 5.81-5.71 (1H, m, =CH), 5.04-4.98 (1H, m, $\text{CH}_a\text{H}_b=$), 4.97-4.92 (1H, m, $\text{CH}_a\text{H}_b=$), 2.11-2.08 (2H, m, CH_2Au), 2.03 (6H, s, $\text{S}(\text{CH}_3)_2$).

NMR data for HOB(pin): ^1H NMR (400 MHz, $\text{DMSO-}d_6$) δ 7.99 (1H, s, OH), 1.14 (12H, s, $2 \times \text{C}(\text{CH}_3)_2$); ^{11}B NMR ($\text{DMSO-}d_6$, 128 MHz) δ 22.2. Data consistent with previously reported literature.²¹⁹

3.10 Uncatalysed Nucleophilic Allylation of Azinium Ions

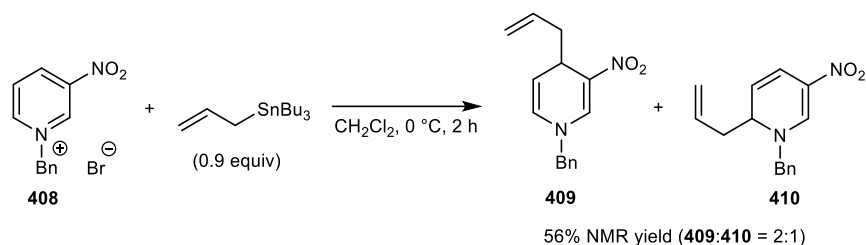
Using potassium allyltrifluoroborate:



An oven-dried microwave vial fitted with a stirrer bar was charged with azinium salt **408** (148 mg, 0.50 mmol) and potassium allyltrifluoroborate (111 mg, 0.75 mmol). The vial was sealed with a septum-lined cap and purged with argon for 30 min. THF (4.0 mL) and MeOH (1.0 mL), both of which were freshly degassed separately (purging with argon for 30 min) were added. The mixture was stirred at 50 °C for 18 h. The reaction was cooled to room temperature and then passed through a plug of silica (8 cm in height and 2 cm wide) using Et_2O (40 mL) as the eluent and the filtrate was concentrated *in vacuo*. The residue was purified by column chromatography (5% to 20% EtOAc/n -pentane) to give

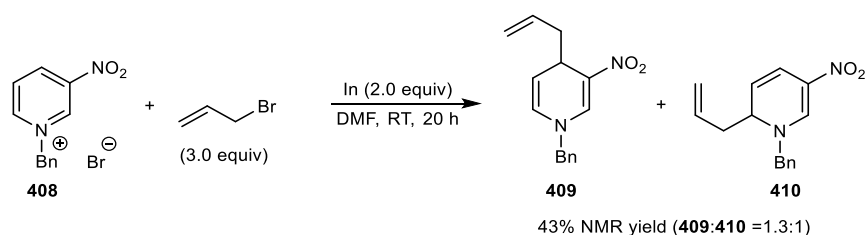
allylated product **409** as a red oil (23.9 mg, 19%) followed by allylated product **410** (32.9 mg, 26%) as a yellow oil. Data for **409** and **410**: see above (page 147).

Using allyltributylstannane:



An oven-dried microwave vial fitted with a stirrer bar was charged with azinium salt **408** (32.5 mg, 0.11 mmol). The vial was sealed with a septum-lined cap and purged with argon for 30 min. Freshly degassed (purging with argon for 30 min) CH_2Cl_2 (1.0 mL) was added, followed by the dropwise addition of allyltributylstannane (31.0 μL , 0.10 mmol) at 0°C . The mixture was stirred at room temperature for 3 h. The reaction was passed through a plug of silica (4 cm in height and 1 cm wide) using Et_2O (20 mL) as the eluent and the filtrate was concentrated *in vacuo*. 1,3,5-Trimethoxybenzene was added as an internal standard, and the crude material was analysed by ^1H NMR spectroscopy (56% yield as a 2:1 mixture of **409**:**410**).

Using allylindium bromide:

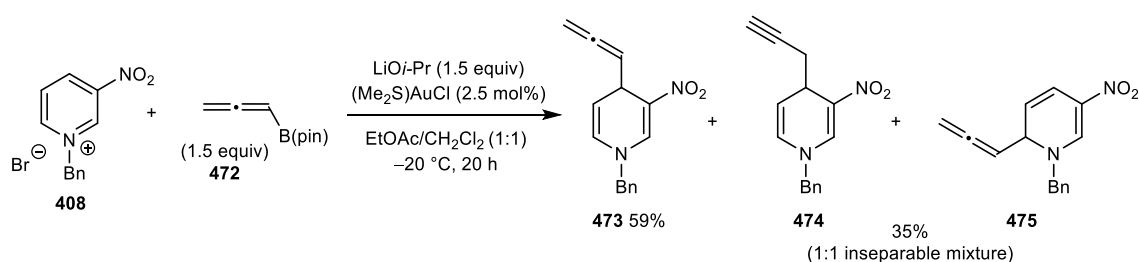


An oven-dried microwave vial fitted with a stirrer bar was charged with indium (23.0 mg, 0.20 mmol). The vial was sealed with a septum-lined cap and purged with argon for 30 min. A solution of allyl bromide (26.0 μL , 0.30 mmol) in freshly degassed (purging with argon for 30 min) DMF (0.5 mL) was added dropwise. The mixture was stirred at room temperature for 4 h. To a separate oven-dried microwave vial fitted with a stirrer bar was added azinium salt **408** (29.5 mg, 0.10 mmol). The vial was sealed with a septum-

lined cap and purged with argon for 30 min. Freshly degassed (purging with argon for 30 min) DMF (0.5 mL) was added, followed by the dropwise addition of the allyl indium solution (see above). The mixture was stirred at room temperature for 16 h. The reaction was passed through a plug of silica (4 cm in height and 1 cm wide) using Et₂O (20 mL) as the eluent and the filtrate was concentrated *in vacuo*. 1,3,5-Trimethoxybenzene was added as an internal standard, and the crude material was analysed by ¹H NMR spectroscopy (43% yield as a 1.3:1 mixture of **409:410**).

3.11 Other Gold-Catalysed Nucleophilic Additions to Azinium Ions

1-Benzyl-3-nitro-4-(propa-1,2-dien-1-yl)-1,4-dihydropyridine (473), **1-benzyl-3-nitro-4-(prop-2-yn-1-yl)-1,4-dihydropyridine (474)** and **1-benzyl-5-nitro-2-(propa-1,2-dien-1-yl)-1,2-dihydropyridine (475)**



The title compounds were prepared according to General Procedure B using azinium salt **408** (148 mg, 0.50 mmol), and allenyl pinacolboronate **472** (135 μL, 0.75 mmol), and purified by column chromatography (5% to 10% EtOAc/*n*-pentane) to give *allenylated product* **473** as a red oil (74.9 mg, 59%), followed by *propargylated product* **474** and *allenylated product* **475** as an orange oil as a 1:1 inseparable mixture (45.1 mg, 35%).

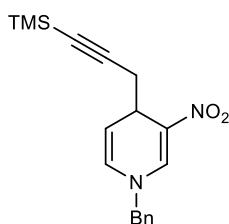
Data of major regioisomer 473: R_f = 0.34 (20% EtOAc/petroleum ether); IR 3064, 2923, 1666, 1584 (NO₂), 1476, 1396 (NO₂), 1265, 1173, 1079, 840, 728 cm⁻¹; ¹H NMR (500 MHz, CDCl₃) δ 7.93 (1H, d, *J* = 1.6 Hz, NCH=C), 7.41-7.33 (3H, m, ArH), 7.23-7.20 (2H, m, ArH), 5.93 (1H, dt, *J* = 7.8, 1.3 Hz, NCH=CH), 5.47-5.43 (1H, m, CHCH=C), 5.18 (1H, dd, *J* = 7.8, 5.0 Hz, NCH=CH), 4.80 (2H, qdd, *J* = 10.6, 6.6, 2.2 Hz, CH₂=), 4.51 (2H, s, NCH₂), 4.44-4.40 (1H, m, CHCH=C); ¹³C NMR (126 MHz, CDCl₃) δ 209.5 (C), 139.3 (CH), 135.3 (C), 129.3 (2 × CH), 128.7 (CH), 127.3 (2 × CH), 126.7 (CH),

125.1 (C), 111.4 (CH), 93.8 (CH), 78.4 (CH₂), 58.5 (CH₂), 32.9 (CH); HRMS (ESI) Exact mass calculated for [C₁₅H₁₄N₂NaO₂]⁺ [M+Na]⁺: 277.0947, found 277.0947.

Data of minor regioisomers 474 and 475 as a 1:1 inseparable mixture: R_f = 0.29 (20% EtOAc/petroleum ether); IR 3063, 2922, 1670, 1575 (NO₂), 1454, 1396 (NO₂), 1270, 1173, 1083, 853, 726 cm⁻¹; HRMS (ESI) Exact mass calculated for [C₁₅H₁₄N₂NaO₂]⁺ [M+Na]⁺: 277.0947, found 277.0948.

NMR data of regioisomer 474: ¹H NMR (500 MHz, CDCl₃) δ 8.02 (1H, d, *J* = 1.2 Hz, NCH=C), 7.43-7.33 (3H, m, ArH), 7.29-7.24 (2H, m, ArH), 6.00 (1H, dt, *J* = 7.8, 1.3 Hz, NCH=CH), 5.24 (1H, dd, *J* = 7.8, 4.9 Hz, NCH=CH), 4.50 (2H, s, NCH₂), 4.07-4.04 (1H, m, CH₂CH), 2.68 (1H, ddd, *J* = 16.8, 6.3, 2.7 Hz, CH_aH_bCH), 2.39 (1H, dt, *J* = 16.8, 3.0 Hz, CH_aH_bCH), 1.83 (1H, t, *J* = 2.7 Hz, CH≡); ¹³C NMR (126 MHz, CDCl₃) δ 141.0 (CH), 135.0 (C), 129.2 (2 × CH), 129.1 (CH), 127.9 (CH), 127.6 (2 × CH), 123.0 (C), 111.7 (CH), 81.4 (C), 70.2 (CH), 58.6 (CH₂), 33.4 (CH), 25.2 (CH₂).

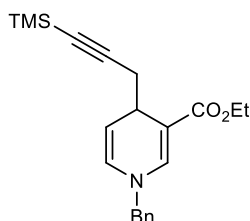
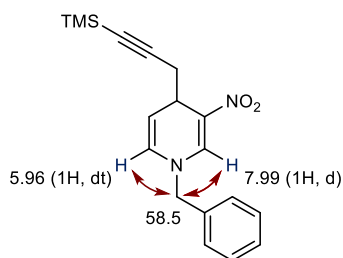
Characteristic NMR data of regioisomer 475: ¹H NMR (500 MHz, CDCl₃) δ 8.13 (1H, d, *J* = 1.7 Hz, NCH=C), 6.79 (1H, dd, *J* = 10.1, 2.0 Hz, CHCH=CH), 5.19 (1H, dt, *J* = 8.0, 6.5 Hz, C=CHCH), 5.09 (1H, dd, *J* = 10.2, 4.7 Hz, CHCH=CH), 4.96-4.92 (2H, m, CH₂=), 4.65-4.61 (1H, m, CHCHN); 4.59 (1H, d, *J* = 14.7 Hz, NCH_aH_b), 4.48 (1H, d, *J* = 14.8 Hz, NCH_aH_b); ¹³C NMR (126 MHz, CDCl₃) δ 208.0 (C), 145.8 (CH), 133.5 (C), 129.4 (2 × CH), 128.7 (CH), 128.4 (2 × CH), 123.9 (C), 118.5 (CH), 113.3 (CH), 89.4 (CH), 78.0 (CH₂), 58.5 (CH₂), 58.0 (CH).



1-Benzyl-3-nitro-4-[3-(trimethylsilyl)prop-2-yn-1-yl]-1,4-dihydropyridine (484). The title compound was prepared according to General Procedure B, using azinium salt **408** (148 mg, 0.50 mmol) and propargyl pinacolboronate **477** (179 mg, 0.75 mmol), and purified by column chromatography (5% EtOAc/*n*-pentane) to give a red solid (155 mg, 95%). R_f = 0.46 (20% EtOAc/petroleum ether); m.p. 93-94 °C (Et₂O); IR 2962, 1688, 1584 (NO₂), 1447, 1339 (NO₂), 1269, 1174, 1083, 837, 677 cm⁻¹; ¹H NMR (400 MHz, CDCl₃) δ 7.99 (1H, d, *J* = 0.9 Hz, NCH=C), 7.42-7.34 (3H, m, ArH), 7.24-7.21 (2H, m, ArH), 5.96 (1H, dt, *J* = 8.0, 1.3 Hz, NCH=CH), 5.32 (1H, dd, *J* = 8.0, 4.9 Hz, NCH=CH), 4.51 (1H, d, *J* = 15.3 Hz, NCH_aH_b), 4.46 (1H, d, *J* = 15.3 Hz, NCH_aH_b), 4.07-4.02 (1H, m, CH₂CH), 2.60-2.57 (2H, m, CH₂CH), 0.14 (9H, s,

Si(CH₃)₃); ¹³C NMR (101 MHz, CDCl₃) δ 140.7 (CH), 135.0 (C), 129.4 (2 × CH), 128.8 (CH), 127.6 (2 × CH), 127.4 (CH), 124.5 (C), 112.1 (CH), 103.9 (C), 87.0 (C), 58.5 (CH₂), 33.8 (CH), 26.8 (CH₂), 0.3 (3 × CH₃); HRMS (ESI) Exact mass calculated for [C₁₈H₂₃N₂O₂Si]⁺ [M+H]⁺: 327.1523, found 327.1525.

The regioisomeric configuration of **484** was determined by HMBC NMR spectroscopy. In the HMBC NMR spectra of product **484**, the benzyl methylene group at 58.5 ppm correlates with the signals at 7.99 ppm and 5.96 ppm. Only structure **484** is compatible with this experimental data.

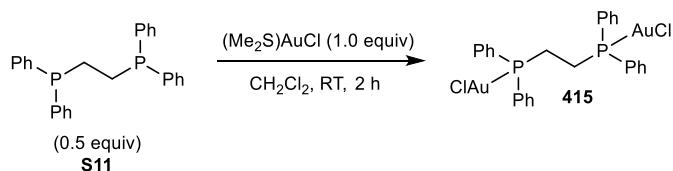


Ethyl 1-benzyl-4-[3-(trimethylsilyl)prop-2-yn-1-yl]-1,4-dihydropyridine-3-carboxylate (488a). The title compound was prepared according to General Procedure B, using azinium salt **433d** (161 mg, 0.50 mmol) and propargyl pinacolboronate **477** (179 mg, 0.75 mmol), and purified by column chromatography (1

to 3% EtOAc/*n*-pentane) to give a brown oil (153 mg, 87%). *R*_f = 0.69 (20% EtOAc/petroleum ether); IR 2958, 1679 (C=O), 1589, 1400, 1282, 1204, 1162, 1075, 838, 729 cm⁻¹; ¹H NMR (500 MHz, CDCl₃) δ 7.38-7.34 (2H, m, ArH), 7.32-7.28 (1H, m, ArH), 7.27 (1H, d, *J* = 1.7 Hz, NCH=C), 7.22-7.19 (2H, m, ArH), 5.90-5.87 (1H, m, NCH=CH), 5.03 (1H, dd, *J* = 7.9, 4.8 Hz, NCH=CH), 4.37 (2H, s, NCH₂), 4.16 (2H, qd, *J* = 7.1, 2.4 Hz, OCH₂), 3.61 (1H, dt, *J* = 8.4, 4.2 Hz, CH₂CH), 2.48 (1H, dd, *J* = 16.5, 3.8 Hz, CH_aH_bCH), 2.33 (1H, dd, *J* = 16.5, 8.4 Hz, CH_aH_bCH), 1.26 (3H, t, *J* = 7.1 Hz, CH₃), 0.15 (9H, s, Si(CH₃)₃); ¹³C NMR (126 MHz, CDCl₃) δ 168.1 (C), 141.9 (CH), 137.1 (C), 129.0 (2 × CH), 128.4 (CH), 128.0 (CH), 127.2 (2 × CH), 107.2 (CH), 105.6 (C), 100.7 (C), 86.0 (C), 59.6 (CH₂), 57.7 (CH₂), 32.2 (CH), 29.5 (CH₂), 14.7 (CH₃), 0.4 (3 × CH₃); HRMS (ESI) Exact mass calculated for [C₂₁H₂₈NO₂Si]⁺ [M+H]⁺: 354.1884, found 354.1885.

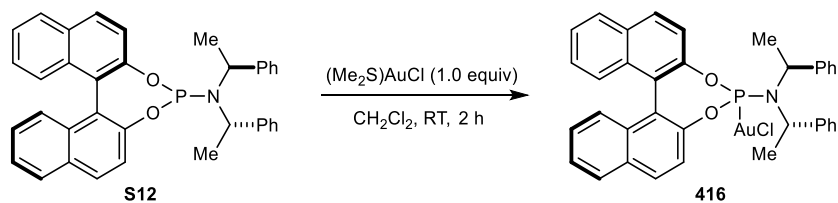
3.12 Synthesis of Gold Complexes

1,2-Bis(diphenylphosphaneyl)ethane-(AuCl)₂ (**415**)



An oven-dried microwave vial fitted with a stirrer bar was charged with $(\text{Me}_2\text{S})\text{AuCl}$ (20.0 mg, 0.068 mmol) and bis-phosphine ligand **S11** (13.5 mg, 0.034 mmol). CH_2Cl_2 (2 mL) was added, and the resulting mixture was stirred at room temperature for 2 h. The mixture was concentrated *in vacuo* and dried under a vacuum for 1 h to give the titled compound **415** (58.2 mg, 99%) as an off-white solid. ^1H NMR (500 MHz, CDCl_3) δ 7.66-7.63 (8H, m, ArH), 7.57-7.54 (4H, m, ArH), 7.51-7.48 (8H, m, ArH), 2.64 (4H, s, $2 \times \text{CH}_2$); ^{31}P NMR (202 MHz, CDCl_3) δ 31.9; HRMS (ESI) Exact mass calculated for $[\text{C}_{26}\text{H}_{24}\text{Au}_2\text{Cl}_2\text{NaP}_2]^+$ $[\text{M}+\text{Na}]^+$: 884.9954, found 884.9986. Data consistent with previously reported literature.²²⁰

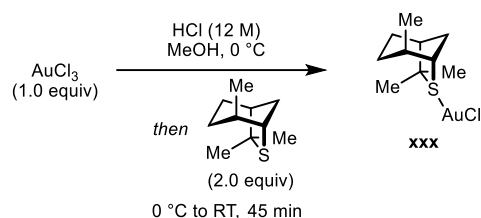
N,N-Bis[(*S*)-1-phenylethyl]dinaphtho[2,1-d:1',2'-f][1,3,2]dioxaphosphepin-4-amine-AuCl (**416**)



An oven-dried microwave vial fitted with a stirrer bar was charged with $(\text{Me}_2\text{S})\text{AuCl}$ (20.0 mg, 0.068 mmol) and phosphoramidite ligand **S12** (36.6 mg, 0.068 mmol). CH_2Cl_2 (2 mL) was added, and the resulting mixture was stirred at room temperature for 2 h. The mixture was concentrated *in vacuo* and dried under a vacuum for 1 h to give the titled compound **416** (52.2 mg, 99%) as an off-white solid. ^1H NMR (500 MHz, CDCl_3) δ 8.02 (2H, dd, $J = 16.1, 8.9$ Hz, ArH), 7.97-7.92 (2H, m, ArH), 7.52-7.44 (3H, m, ArH), 7.40-7.35 (2H, m, ArH), 7.30 (1H, ddd, $J = 8.4, 6.6, 1.3$ Hz, ArH), 7.28-7.23 (7H, m, ArH), 7.22-7.18 (5H, m, ArH), 4.98-4.89 (2H, m, $2 \times \text{NCHCH}_3$), 1.70 (6H, d, $J = 7.1$ Hz, $2 \times$

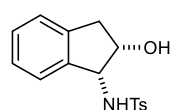
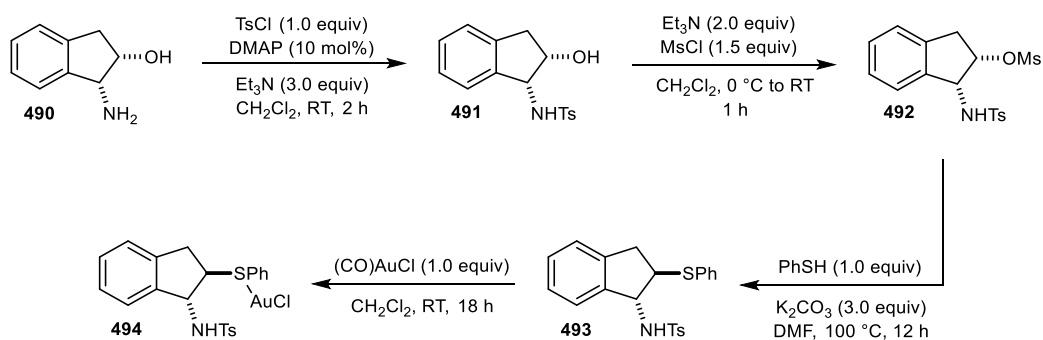
CH_3); ^{31}P NMR (202 MHz, CDCl_3) δ 129.5; HRMS (ESI) Exact mass calculated for $[\text{C}_{36}\text{H}_{30}\text{AuClINNaO}_2\text{P}]^+ [\text{M}+\text{Na}]^+$: 794.1266, found 794.1248. Data consistent with previously reported literature.²²¹

(1*S*,4*S*,5*S*)-4,7,7-Trimethyl-6-thiabicyclo[3.2.1]octane-AuCl (462)



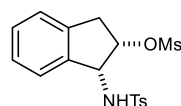
An oven-dried microwave vial equipped with a stirrer bar was charged with AuCl_3 (0.30 mmol, 91.0 mg). MeOH (3 mL) was added, followed by the dropwise addition of aqueous HCl (12 M) at 0°C until the reaction was homogeneous. (1*S*,4*S*,5*S*)-4,7,7-Trimethyl-6-thiabicyclo[3.2.1]octane (0.60 mmol, 102 mg) was added dropwise, and the resulting mixture was stirred vigorously at 0°C for 15 min. The reaction mixture was warmed to room temperature and stirred vigorously for an additional 30 min, diluted with CH_2Cl_2 (5 mL), filtered and slowly concentrated *in vacuo* at 0°C until no further product precipitation was observed. The precipitated product was removed by vacuum filtration, washed with ice-cold *n*-pentane (3×10 mL) and dried under vacuum to give the title compound **462** as a yellow solid (85.8 mg, 86%). m.p. decomposes *ca* 139°C (Et_2O); IR 3074, 2964, 2925, 1459, 1387, 1347, 1273, 1196, 983, 867, 738 cm^{-1} ; $[\alpha]_{\text{D}}^{25} -120.0$ (*c* 1.00, CHCl_3); ^1H NMR (500 MHz, CDCl_3) δ 4.49-4.46 (1H, m, CHS), 2.56-2.50 (1H, m, $\text{CH}_a\text{H}_b\text{CHS}$), 2.41-2.33 (2H, m, $\text{CH}_a\text{H}_b\text{CHS}$ and CHCS), 2.28-2.21 (1H, m, CHCHS), 1.97-1.89 (4H, m, $\text{CH}_a\text{H}_b\text{CHCH}_3$ and CH_3CS), 1.86 (3H, s, CH_3CS), 1.77-1.73 (2H, m, $\text{CH}_2\text{CH}_2\text{CHCS}$), 1.55-1.52 (1H, m, $\text{CH}_a\text{H}_b\text{CHCH}_3$), 1.22 (3H, d, $J = 7.1$ Hz, CHCH_3); ^{13}C NMR (126 MHz, CDCl_3) δ 77.3 (C), 60.8 (CH), 49.2 (CH), 35.6 (CH_3), 34.4 (CH_2), 33.6 (CH), 25.0 (CH_2), 24.9 (CH_3), 22.7 (CH_2), 18.6 (CH_3); HRMS (ESI) Exact mass calculated for $[\text{C}_{10}\text{H}_{22}\text{NAuClS}]^+ [\text{M}+\text{NH}_4]^+$: 420.0822, found 420.0811.

Preparation of gold complex **494**



***N*-[(1*R*,2*S*)-2-Hydroxy-2,3-dihydro-1*H*-inden-1-yl]-4-methylbenzenesulfonamide (**491**).**

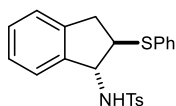
A flask was charged with (*1R,2S*)-1-amino-2,3-dihydro-1*H*-inden-2-ol (**490**) (1.49 g, 10.0 mmol), *p*-toluenesulfonyl chloride (1.91 g, 10.0 mmol) and DMAP (122 mg, 1.00 mmol). CH₂Cl₂ (30 mL) was added, followed by the dropwise addition of triethylamine (4.18 mL, 30.0 mmol). The resulting solution was stirred at room temperature for 2 h. The mixture was washed with H₂O (50 mL), saturated aqueous NaHCO₃ (50 mL), brine (50 mL), dried (MgSO₄), filtered, and concentrated *in vacuo*. The residue was recrystallised from CHCl₃/petroleum ether to give the title compound **491** as an off-white solid (2.14 g, 71%). ¹H NMR (500 MHz, CDCl₃) δ 7.86 (2H, d, *J* = 8.4 Hz, ArH), 7.34 (2H, d, *J* = 8.0 Hz, ArH), 7.23-7.13 (3H, m, ArH), 7.06 (1H, d, *J* = 7.5 Hz, ArH), 5.43 (1H, br s, NH), 4.66 (1H, d, *J* = 4.8 Hz, CHNH), 4.28 (1H, td, *J* = 5.0, 1.6 Hz, CHOH), 3.02 (1H, dd, *J* = 16.7, 5.0 Hz, CCH_aH_b), 2.87 (1H, dd, *J* = 16.7, 1.5 Hz, CCH_aH_b), 2.45 (3H, s, CH₃), 2.34 (1H, br s, OH); ¹³C NMR (126 MHz, CDCl₃) δ 143.9 (C), 139.6 (C), 139.5 (C), 137.7 (C), 130.0 (2 × CH), 128.6 (CH), 127.4 (2 × CH), 127.3 (CH), 125.5 (CH), 124.7 (CH), 72.9 (CH), 61.4 (CH), 39.4 (CH₂), 21.7 (CH₃). Data consistent with previously reported literature.²²²



(1*R*,2*S*)-1-[(4-Methylphenyl)sulfonylamino]-2,3-dihydro-1*H*-inden-2-yl methanesulfonate (492**).**

A solution of methanesulfonyl chloride (580 μL, 7.50 mmol) in CH₂Cl₂ (5 mL) was added to a solution of *N*-[(*1R,2S*)-2-hydroxy-2,3-dihydro-1*H*-inden-1-yl]-4-methylbenzenesulfonamide (**491**) (1.52 g, 5.00 mmol) and triethylamine (1.39 mL, 10.0 mmol) in CH₂Cl₂ (20 mL) dropwise at 0 °C. The resulting solution was stirred at room temperature for 1 h. H₂O (30 mL) was added, and the resulting mixture was extracted with CH₂Cl₂ (3 × 20 mL), dried (MgSO₄), filtered, and

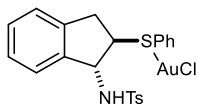
concentrated *in vacuo* to give the title compound **492** as an off-white solid (1.90 g, 99%). m.p. 162-163 °C (Et₂O); IR 3012, 2933, 1417, 1351, 1216, 1177, 1092, 942, 748, 667 cm⁻¹; [α]_D²⁵ +20.0 (*c* 1.00, CHCl₃); ¹H NMR (500 MHz, CDCl₃) δ 7.87 (2H, d, *J* = 8.3 Hz, ArH), 7.36 (2H, d, *J* = 8.0 Hz, ArH), 7.27-7.17 (3H, m, ArH), 7.03 (1H, d, *J* = 7.5 Hz, ArH), 5.34 (1H, d, *J* = 10.0 Hz, NH), 5.28 (1H, t, *J* = 4.6 Hz, CHO), 4.94 (1H, dd, *J* = 10.0, 4.8 Hz, CHNH), 3.32 (1H, d, *J* = 17.6 Hz, CCH_aH_b), 3.18 (1H, dd, *J* = 17.6, 4.5 Hz, CCH_aH_b), 3.07 (3H, s, CH₃), 2.45 (3H, s, CH₃); ¹³C NMR (126 MHz, CDCl₃) δ 144.2 (C), 138.4 (C), 137.9 (C), 137.5 (C), 130.1 (2 \times CH), 129.1 (CH), 127.8 (CH), 127.3 (2 \times CH), 125.4 (CH), 123.8 (CH), 83.6 (CH), 60.1 (CH), 38.7 (CH₃), 38.4 (CH₂), 21.7 (CH₃). HRMS (ESI) Exact mass calculated for [C₁₇H₁₉NNaO₅S₂]⁺ [M+Na]⁺: 404.0597, found 404.0591.



4-Methyl-N-[(1R,2R)-2-(phenylthio)-2,3-dihydro-1H-inden-1-yl]benzenesulfonamide (493).

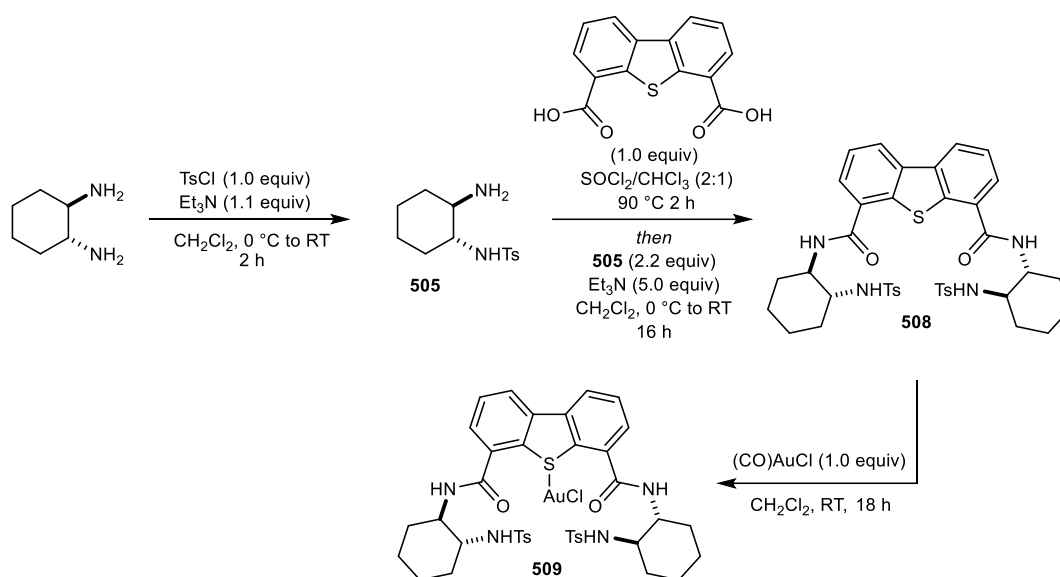
An oven-dried flask was charged with (1R,2S)-1-[(4-methylphenyl)sulfonamido]-2,3-dihydro-1H-inden-2-yl methanesulfonate (**492**) (1.00 mmol, 381 mg), K₂CO₃ (3.00 mmol, 415 mg) and purged with argon for 30 min. Anhydrous DMF (10 mL) was added, and the reaction mixture was stirred at room temperature for 10 min. Thiophenol (1.00 mmol, 103 μ L) was added dropwise and the resulting mixture was stirred at 100 °C for 12 h. The reaction was cooled to room temperature and then passed through a plug of Celite (8 cm in height and 2 cm wide) using EtOAc (30 mL) as the eluent and the filtrate was concentrated *in vacuo*. The residue was purified by column chromatography (0 to 15% EtOAc/*n*-pentane), followed by trituration (*n*-pentane) to give the title compound **493** as an off-white solid (260 mg, 66%). R_f = 0.42 (40% EtOAc/petroleum ether); m.p. 167-168 °C (Et₂O); IR 3023, 2921, 1494, 1478, 1438, 1108, 1075, 770, 666, 545 cm⁻¹; [α]_D²⁵ +16.0 (*c* 1.00, CHCl₃); ¹H NMR (500 MHz, CDCl₃) δ 7.70 (2H, d, *J* = 8.3 Hz, ArH), 7.37-7.34 (2H, m, ArH), 7.32-7.27 (5H, m, ArH), 7.25-7.21 (1H, m, ArH), 7.18-7.13 (2H, m, ArH), 7.01 (1H, d, *J* = 7.5 Hz, ArH), 4.72 (1H, d, *J* = 7.6 Hz, NH), 4.65 (1H, dd, *J* = 7.6, 4.8 Hz, CHNH), 3.82 (1H, dt, *J* = 7.2, 5.1 Hz, CHS), 3.41 (1H, dd, *J* = 16.5, 7.2 Hz, CCH_aH_b), 2.86 (1H, dd, *J* = 16.5, 5.3 Hz, CCH_aH_b), 2.44 (3H, s, CH₃); ¹³C NMR (126 MHz, CDCl₃) δ 143.7 (C), 141.3 (C), 140.5 (C), 137.6 (C), 134.1 (C), 132.5 (2 \times CH), 129.8 (2 \times CH), 129.1 (3 \times CH), 127.7 (CH), 127.54 (2 \times CH), 127.45 (CH), 125.1 (CH), 125.0 (CH), 63.7 (CH), 53.2

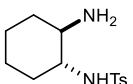
(CH), 37.8 (CH₂), 21.7 (CH₃). HRMS (ESI) Exact mass calculated for [C₂₂H₂₁NNaO₂S₂]⁺ [M+Na]⁺: 418.0906, found 418.0909.



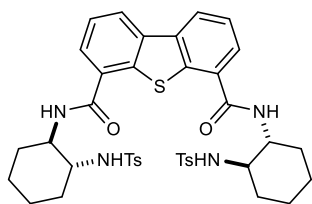
4-Methyl-N-[(1R,2R)-2-(phenylthio)-2,3-dihydro-1H-inden-1-yl]benzenesulfonamide-AuCl (494). An oven-dried microwave vial equipped with a stirrer bar was charged with (CO)AuCl (0.10 mmol, 26.0 mg). A solution of 4-methyl-N-[(1R,2R)-2-(phenylthio)-2,3-dihydro-1H-inden-1-yl]benzenesulfonamide (**493**) (0.10 mmol, 39.6 mg) in anhydrous CH₂Cl₂ (3 mL) was added dropwise and the resulting mixture was stirred at room temperature for 18 h. The reaction mixture was filtered and added dropwise to rapidly stirring *n*-pentane at 0 °C, at which point the product precipitated. The precipitated product was removed by vacuum filtration, washed with ice-cold *n*-pentane (2 × 5 mL) and dried under vacuum to give the title compound **494** as an off-white solid (48.1 mg, 77%). m.p. decomposes *ca* 142 °C (Et₂O); IR 3023, 2869, 1494, 1477, 1440, 1158, 1077, 746, 664, 546 cm⁻¹; [α]_D²⁵ +8.0 (*c* 1.00, CHCl₃); ¹H NMR (500 MHz, CDCl₃) δ 7.78 (2H, d, *J* = 7.6 Hz, ArH), 7.69-7.49 (5H, m, ArH), 7.36 (2H, d, *J* = 7.9 Hz, ArH), 7.31 (1H, t, *J* = 7.5 Hz, ArH), 7.23-7.18 (2H, m, ArH), 6.89 (1H, d, *J* = 7.6 Hz, ArH), 4.79 (1H, s, NH), 4.71-4.66 (1H, m, CHNH), 4.31-4.20 (1H, m, CHS), 3.50-3.40 (1H, m, CCH_aH_b), 3.06 (1H, d, *J* = 16.1, CCH_aH_b), 2.49 (3H, s, CH₃); ¹³C NMR (126 MHz, CDCl₃) δ 144.6 (C), 139.6 (C), 138.3 (C), 136.4 (C), 134.7 (CH and C), 131.9 (CH), 130.4 (2 × CH), 130.3 (CH), 130.2 (2 × CH), 128.7 (CH), 127.6 (3 × CH), 125.6 (CH), 125.0 (CH), 62.5 (CH), 53.2 (CH), 37.8 (CH₂), 21.8 (CH₃). HRMS (ESI) Exact mass calculated for [C₂₂H₂₁AuNNaO₂S₂]⁺: 592.0674, found 592.0682.

Preparation of gold complex 509



 ***N*-[(1R,2R)-2-Aminocyclohexyl]-4-methylbenzenesulfonamide (505).**

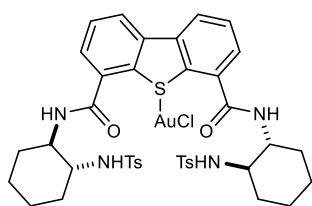
To a solution of (1R,2R)-(-)-1,2-diaminocyclohexane (571 mg, 5.00 mmol) in anhydrous CH₂Cl₂ (10 mL) was added triethylamine (767 μL, 5.50 mmol) at 0 °C and the reaction was stirred at 0 °C for 15 min. *p*-Toluenesulfonyl chloride (953 mg, 5.00 mmol) was added and the reaction was stirred at room temperature for 2 h. The mixture was washed with H₂O (10 mL), extracted with CHCl₃ (3 × 15 mL), dried (MgSO₄), filtered, and concentrated *in vacuo* to give the title compound **505** (1.09 g, 78%) as a 1.7:1 mixture of rotamers as an orange oil. ¹H NMR (500 MHz, CDCl₃) *major rotamer*: δ 7.76 (2H, d, *J* = 8.4 Hz, ArH), 7.29 (2H, d, *J* = 8.0 Hz, ArH), 3.21 (3H, br s, NH₂ and NH), 2.69-2.62 (1H, m, CHNH), 2.44-2.34 (4H, m, CHNH₂ and CH₃), 1.86-1.74 (2H, m, NHCHCH₂), 1.64-1.49 (2H, m, NH₂CHCH₂), 1.24-1.00 (4H, m, NH₂CHCH₂CH₂ and NHCHCH₂CH₂); *observable signals of minor rotamer*: δ 2.79-2.73 (1H, m, CHNH), 1.95-1.89 (2H, m, NHCHCH₂); ¹³C NMR (126 MHz, CDCl₃) *major rotamer*: δ 143.4 (C), 138.0 (C), 129.8 (2 × CH), 127.2 (2 × CH), 60.3 (CH), 54.9 (CH), 32.7 (2 × CH₂), 25.0 (2 × CH₂), 21.66 (CH₃), *observable signals of minor rotamer*: δ 143.6 (C), 137.3 (C), 129.9 (2 × CH), 127.3 (2 × CH), 56.7 (CH), 35.5 (2 × CH₂), 24.9 (2 × CH₂), 21.69 (CH₃). Data consistent with previously reported literature.²²³



***N*4,*N*6-Bis-((1*R*,2*R*)-2-[(4-methylphenyl)sulfonamido]cyclohexyl)dibenzo[*b*,*d*]thiophene-4,6-**

dicarboxamide (508). A flask was charged with dibenzo[*b*,*d*]thiophene-4,6-dicarboxylic acid (163 mg, 0.60

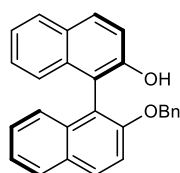
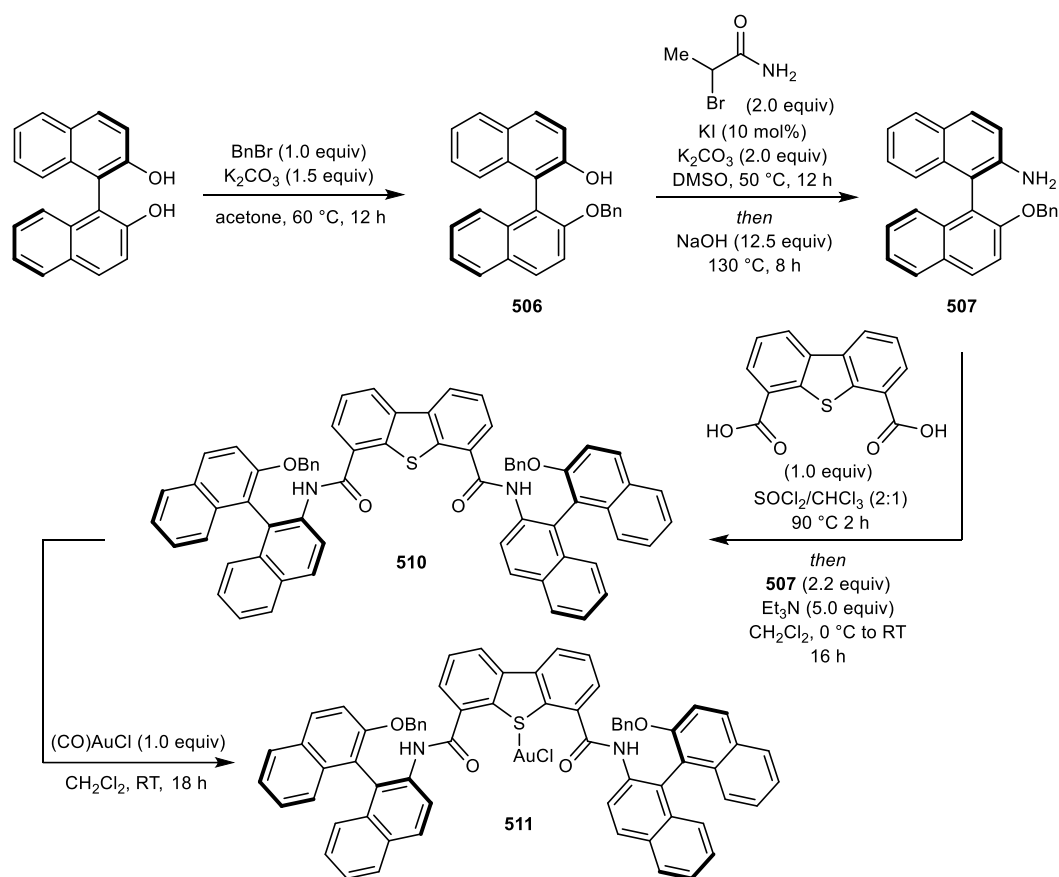
mmol). Thionyl chloride (6 mL) and CHCl₃ (3 mL) were added in one portion and the reaction was stirred at 90 °C for 2 h. The reaction was cooled to room temperature and concentrated *in vacuo* to leave a residue, which was dissolved in anhydrous CH₂Cl₂ (6 mL). *N*-[(1*R*,2*R*)-2-Aminocyclohexyl]-4-methylbenzenesulfonamide (505) (354 mg, 1.32 mmol) was added, followed by the dropwise addition of triethylamine (419 μL, 3.00 mmol) at 0 °C. The reaction mixture was stirred at room temperature for 16 h. H₂O (20 mL) was added, and the resulting mixture was extracted with CH₂Cl₂ (3 × 20 mL), and the combined organic layers were dried (MgSO₄), filtered, and concentrated *in vacuo*. The residue was purified by column chromatography (70 to 90% EtOAc/petroleum ether), to give the title compound 508 as an off-white solid (192 mg, 41%). R_f = 0.36 (90% EtOAc/petroleum ether); m.p. 280-281 °C (Et₂O); IR 2929, 2856, 1631 (C=O), 1567, 1304, 1156, 1089, 838, 662, 547 cm⁻¹; [α]_D²⁵ +36.0 (*c* 1.00, CHCl₃); ¹H NMR (500 MHz, CDCl₃) δ 8.00 (2H, d, *J* = 7.9 Hz, ArH), 7.63 (4H, d, *J* = 8.3 Hz, ArH), 7.51 (2H, d, *J* = 6.7 Hz, ArH), 7.21 (2H, t, *J* = 7.6 Hz, ArH), 7.08 (2H, d, *J* = 7.6 Hz, 2 × NH(C=O)), 6.87 (4H, d, *J* = 8.0 Hz, ArH), 5.83 (2H, d, *J* = 7.2 Hz, 2 × NHS), 3.95 (2H, tdd, *J* = 11.4, 7.5, 4.2 Hz, 2 × CHNHC=O), 3.27 (2H, tdd, *J* = 11.2, 7.1, 4.2 Hz, 2 × CHNHS), 2.28-2.23 (2H, m, 2 × CH_aH_bCHNHC=O), 2.13 (6H, s, 2 × CH₃), 1.98-1.92 (2H, m, 2 × CH_aH_bCHNHS), 1.78-1.68 (4H, m, 2 × CH_aH_bCHNHC=O and 2 × CH_aH_bCHNHS), 1.51-1.41 (4H, m, 2 × CH_aH_bCH₂CHNHC=O) and 2 × CH_aH_bCH₂CHNHS), 1.37-1.23 (4H, m, 2 × CH_aH_bCH₂CHNHC=O and 2 × CH_aH_bCH₂CHNHS); ¹³C NMR (126 MHz, CDCl₃) δ 167.8 (2 × C), 142.8 (2 × C), 141.2 (2 × C), 138.5 (2 × C), 135.6 (2 × C), 129.9 (4 × CH), 128.2 (2 × C), 126.7 (4 × CH), 125.2 (2 × CH), 124.0 (2 × CH), 123.6 (2 × CH), 58.4 (2 × CH), 53.7 (2 × CH), 34.2 (2 × CH₂), 32.6 (2 × CH₂), 25.1 (2 × CH₂), 24.8 (2 × CH₂), 21.4 (2 × CH₃). HRMS (ESI) Exact mass calculated for [C₄₀H₄₄N₄NaO₆S₃]⁺ [M+Na]⁺: 795.2315, found 795.2291.



***N4,N6*-Bis{(1*R*,2*R*)-2-[(4-methylphenyl)sulfonamido]cyclohexyl}dibenzo[*b,d*]thiophene-4,6-dicarboxamide-AuCl (509).**

An oven-dried microwave vial equipped with a stirrer bar was charged with (CO)AuCl (0.10 mmol, 26.0 mg). A solution of *N4,N6*-bis{(1*R*,2*R*)-2-[(4-methylphenyl)sulfonamido]cyclohexyl}dibenzo[*b,d*]thiophene-4,6-dicarboxamide (508) (0.10 mmol, 77.3 mg) in anhydrous CH₂Cl₂ (3 mL) was added dropwise and the resulting mixture was stirred at room temperature for 18 h. The reaction mixture was filtered and added dropwise to rapidly stirring *n*-pentane at 0 °C, at which point the product precipitated. The precipitated product was removed by vacuum filtration, washed with ice-cold *n*-pentane (2 × 5 mL) and dried under vacuum to give the title compound 509 as an off-white solid (43.1 mg, 43%). m.p. decomposes *ca* 169 °C (Et₂O); IR 2931, 2858, 1632 (C=O), 1567, 1305, 1157, 1090, 839, 664, 548 cm⁻¹; [α]_D²⁵ +36.0 (*c* 1.00, CHCl₃); ¹H NMR (500 MHz, CDCl₃) δ 7.97 (2H, s, ArH), 7.66 (4H, d, *J* = 7.8 Hz, ArH), 7.60 (2H, d, *J* = 7.5 Hz, ArH), 7.30 (2H, t, *J* = 7.8 Hz, ArH), 7.25 (2H, br s, 2 × NH(C=O)), 6.97 (4H, d, *J* = 8.0 Hz, ArH), 5.86 (2H, br s, 2 × NHS), 4.03-3.93 (2H, m, 2 × CHNHC=O), 3.27-3.17 (2H, m, 2 × CHNHS), 2.26-2.16 (8H, m, 2 × CH_aH_bCHNHC=O and 2 × CH₃), 1.89-1.81 (2H, m, 2 × CH_aH_bCHNHS), 1.75-1.62 (4H, m, 2 × CH_aH_bCHNHC=O and 2 × CH_aH_bCHNHS), 1.48-1.36 (4H, m, 2 × CH_aH_bCH₂CHNHC=O and 2 × CH_aH_bCH₂CHNHS), 1.33-1.18 (4H, m, 2 × CH_aH_bCH₂CHNHC=O and 2 × CH_aH_bCH₂CHNHS); ¹³C NMR (126 MHz, CDCl₃) δ 168.1 (2 × C), 143.1 (2 × C), 140.8 (2 × C), 138.3 (2 × C), 135.6 (2 × C), 129.7 (4 × CH), 127.6 (2 × C), 126.7 (4 × CH), 125.6 (2 × CH), 124.5 (2 × CH), 124.0 (2 × CH), 58.2 (2 × CH), 54.0 (2 × CH), 33.8 (2 × CH₂), 32.6 (2 × CH₂), 25.0 (2 × CH₂), 24.6 (2 × CH₂), 21.5 (2 × CH₃). HRMS (ESI) Exact mass calculated for [C₄₀H₄₅N₄AuClO₆S₃]⁺: 1005.1855, found 1005.1839.

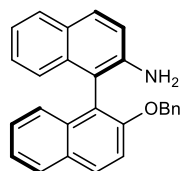
Preparation of gold complex 511



(R)-2'-(Benzyloxy)-[1,1'-binaphthalen]-2-ol (506). To a solution of (R)-(+)-1,1'-bi(2-naphthol) (1.00 g, 3.50 mmol) in acetone (25 mL) was added K_2CO_3 (726 mg, 5.25 mmol) and benzyl bromide (416 μL , 3.50 mmol) and the resulting solution was stirred at 60 °C for 12 h. The

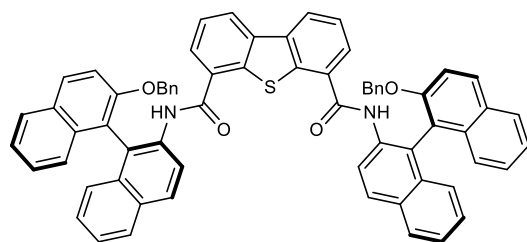
reaction was cooled to room temperature and then passed through a plug of Celite (8 cm in height and 2 cm wide) using CH_2Cl_2 (50 mL) as the eluent, extracted with CH_2Cl_2 (3 x 25 mL) and the combined organic layers washed with brine (50 mL), dried (MgSO_4), filtered, and concentrated *in vacuo*. The residue was purified by column chromatography (5 to 10% EtOAc/petroleum ether), to give the title compound **506** as a yellow oil (1.02 g, 77%). ^1H NMR (500 MHz, CDCl_3) δ 7.98 (1H, d, $J = 9.0$ Hz, ArH), 7.94 (1H, d, $J = 8.9$ Hz, ArH), 7.89 (2H, d, $J = 8.3$ Hz, ArH), 7.47 (1H, d, $J = 9.0$ Hz, ArH), 7.40-7.37 (2H, m, ArH), 7.33 (1H, ddd, $J = 8.1, 6.7, 1.3$ Hz, ArH), 7.30 (1H, ddd, $J = 8.1, 6.7, 1.3$ Hz, ArH), 7.26-7.22 (2H, m, ArH), 7.20-7.17 (3H, m, ArH), 7.10 (1H, dd, $J = 8.5, 1.1$ Hz, ArH), 7.07-7.03 (2H, m, ArH), 5.12 (1H, d, $J = 12.6$ Hz, OCH_aH_b), 5.08 (1H, d, $J = 12.6$ Hz, OCH_aH_b), 4.95 (1H, s, OH); ^{13}C NMR (126 MHz, CDCl_3) δ 155.1 (C), 151.4

(C), 137.1 (C), 134.2 (C), 134.0 (C), 131.0 (CH), 130.0 (CH), 129.8 (C), 129.3 (C), 128.5 (2 × CH), 128.3 (CH), 128.2 (CH), 127.8 (CH), 127.4 (CH), 127.0 (2 × CH), 126.5 (CH), 125.2 (CH), 125.1 (CH), 124.6 (CH), 123.4 (CH), 117.6 (CH), 116.9 (C), 116.1 (CH), 115.2 (C), 71.3 (CH₂). Data consistent with previously reported literature.²²⁴



(R)-2'-(Benzyloxy)-[1,1'-binaphthalen]-2-amine (507). A flask was charged with (R)-2'-(benzyloxy)-[1,1'-binaphthalen]-2-ol (**506**) (941 mg, 2.50 mmol), 2-bromopropanamide (760 mg, 5.00 mmol), K₂CO₃ (692 mg, 5.00 mmol) and KI (41.5 mg, 0.25 mmol). DMSO (20 mL) was

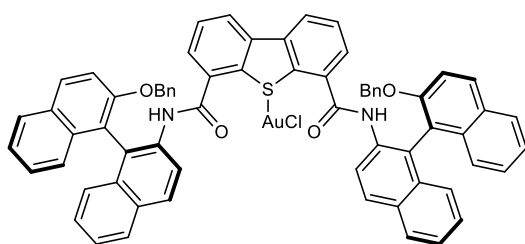
added, and the resulting solution was stirred at 50 °C for 12 h. The reaction was cooled to room temperature and NaOH (1.25 g, 31.3 mmol) was added. The reaction mixture was stirred at 130 °C for 8 h. The reaction was cooled to room temperature and quenched with H₂O (50 mL), extracted with EtOAc (2 x 30 mL), dried (Na₂SO₄), filtered, and concentrated *in vacuo*. The residue was purified by column chromatography (10 to 20% EtOAc/petroleum ether), to give the title compound **507** as an orange oil (646 mg, 69%).
¹H NMR (500 MHz, CDCl₃) δ 7.94 (1H, d, *J* = 9.0 Hz, ArH), 7.88 (1H, d, *J* = 8.2 Hz, ArH), 7.82 (2H, ddd, *J* = 8.1, 5.3, 1.1 Hz, ArH), 7.46 (1H, d, *J* = 9.0 Hz, ArH), 7.37 (1H, ddd, *J* = 8.1, 5.4, 2.6 Hz, ArH), 7.30-7.27 (2H, m, ArH), 7.23 (1H, ddd, *J* = 8.1, 6.7, 1.3 Hz, ArH), 7.19-7.16 (4H, m, ArH), 7.14 (1H, d, *J* = 8.7 Hz, ArH), 7.05-7.01 (3H, m, ArH), 5.09 (1H, d, *J* = 12.6 Hz, OCH_aH_b), 5.04 (1H, d, *J* = 12.6 Hz, OCH_aH_b), 3.57 (2H, s, NH₂); ¹³C NMR (126 MHz, CDCl₃) δ 154.6 (C), 142.3 (C), 137.5 (C), 134.4 (C), 133.8 (C), 130.0 (C), 129.9 (CH), 129.2 (CH), 128.3 (2 × CH and C), 128.2 (CH), 128.1 (CH), 127.6 (CH), 127.2 (2 × CH), 127.0 (CH), 126.4 (CH), 125.3 (CH), 124.6 (CH), 124.3 (CH), 122.2 (CH), 120.6 (C), 118.3 (CH), 116.8 (CH), 113.9 (C), 71.5 (CH₂). Data consistent with previously reported literature.²²⁵



N4-[(S)-2'-(Benzyloxy)-[1,1'-binaphthalen]-2-yl]-N6-[2'-(benzyloxy)-[1,1'-binaphthalen]-2-yl] dibenzo[*b,d*]thiophene-4,6-dicarboxamide (510). A

flask was charged with dibenzo[*b,d*]thiophene-4,6-dicarboxylic acid (81.7 mg, 0.30 mmol). Thionyl chloride

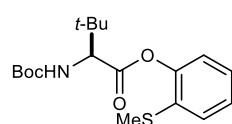
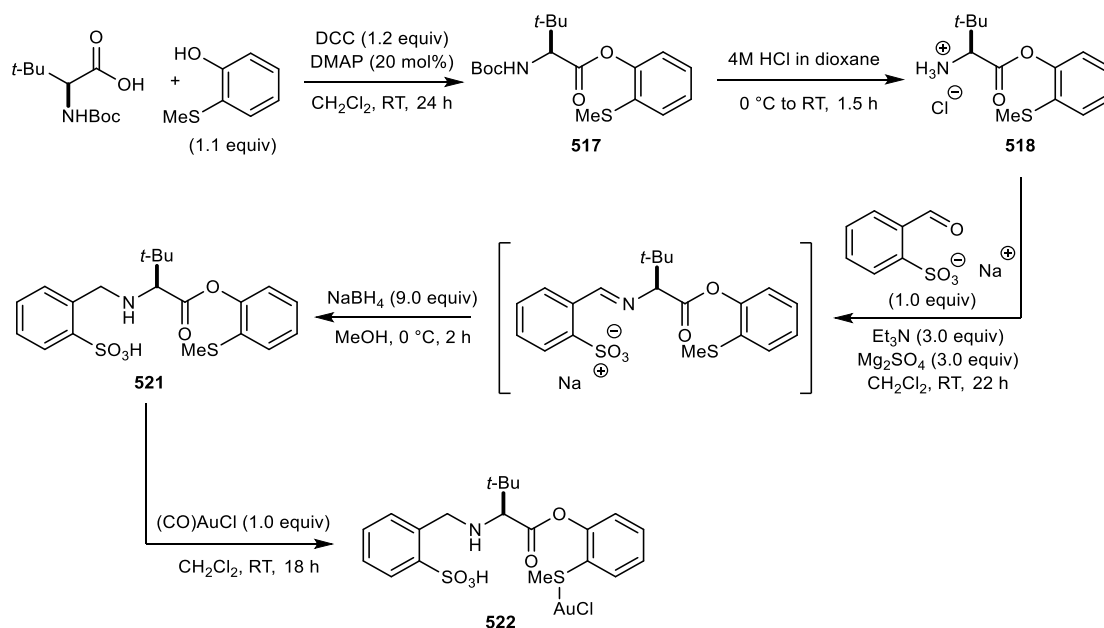
(3.0 mL) and CHCl_3 (1.5 mL) were added in one portion and the reaction was stirred at 90 °C for 2 h. The reaction was cooled to room temperature and concentrated *in vacuo* to leave a residue, which was dissolved in anhydrous CH_2Cl_2 (3 mL). (*R*)-2'-(Benzyloxy)-[1,1'-binaphthalen]-2-amine (**507**) (248 mg, 0.66 mmol) was added, followed by the dropwise addition of triethylamine (210 μL , 1.50 mmol) at 0 °C. The reaction mixture was stirred at room temperature for 16 h. H_2O (10 mL) was added, and the resulting mixture was extracted with CH_2Cl_2 (3×10 mL), and the combined organic layers were dried (MgSO_4), filtered, and concentrated *in vacuo*. The residue was purified by column chromatography (20:79:1 to 50:49:1 EtOAc/*n*-pentane/ Et_3N), to give the title compound **510** as a brown solid (190 mg, 64%). $R_f = 0.29$ (50% EtOAc/petroleum ether); m.p. 213–214 °C (Et_2O); IR 3054, 1665 (C=O), 1620, 1590, 1494, 1426, 1276, 1016, 808, 738 cm^{-1} ; $[\alpha]_{\text{D}}^{25} -24.0$ (*c* 1.00, CHCl_3); ^1H NMR (500 MHz, CDCl_3) δ 8.99 (2H, d, $J = 9.0$ Hz, ArH), 8.10 (2H, d, $J = 9.0$ Hz, ArH), 8.06 (2H, dd, $J = 7.9, 1.0$ Hz, ArH), 7.98 (1H, d, $J = 8.2$ Hz, ArH), 7.95 (2H, d, $J = 9.0$ Hz, ArH), 7.90 (2H, s, $2 \times \text{NH}$), 7.85 (2H, dt, $J = 8.2, 0.9$ Hz, ArH), 7.51 (2H, d, $J = 9.0$ Hz, ArH), 7.44 (2H, ddd, $J = 8.0, 6.6, 1.2$ Hz, ArH), 7.33 (2H, ddd, $J = 8.0, 6.4, 1.5$ Hz, ArH), 7.30–7.26 (2H, m, ArH), 7.25–7.18 (6H, m, ArH), 7.09 (2H, t, $J = 7.7$ Hz, ArH), 7.00–6.93 (12H, m, ArH), 6.57 (1H, d, $J = 6.8$ Hz, ArH), 5.15 (2H, d, $J = 12.8$ Hz, $2 \times \text{OCH}_a\text{H}_b$), 5.08 (2H, d, $J = 12.8$ Hz, $2 \times \text{OCH}_a\text{H}_b$); ^{13}C NMR (126 MHz, CDCl_3) δ 164.2 ($2 \times \text{C}$), 154.3 ($2 \times \text{C}$), 142.0 ($2 \times \text{C}$), 136.8 ($2 \times \text{C}$), 136.1 ($2 \times \text{C}$), 134.7 ($2 \times \text{C}$), 133.7 ($2 \times \text{C}$), 133.2 ($2 \times \text{C}$), 131.2 ($2 \times \text{C}$), 130.9 ($2 \times \text{CH}$), 129.7 ($2 \times \text{C}$), 129.09 ($2 \times \text{CH}$), 129.06 ($2 \times \text{C}$), 128.4 ($4 \times \text{CH}$), 128.3 ($2 \times \text{CH}$), 128.2 ($2 \times \text{CH}$), 127.8 ($2 \times \text{CH}$), 127.7 ($2 \times \text{CH}$), 127.2 ($4 \times \text{CH}$), 126.5 ($2 \times \text{CH}$), 126.1 ($2 \times \text{CH}$), 125.2 ($2 \times \text{CH}$), 124.9 ($2 \times \text{CH}$), 124.7 ($2 \times \text{CH}$), 124.3 ($2 \times \text{CH}$), 124.14 ($2 \times \text{CH}$), 124.08 ($2 \times \text{CH}$), 121.7 ($2 \times \text{C}$), 120.7 ($2 \times \text{CH}$), 118.7 ($2 \times \text{C}$), 116.1 ($2 \times \text{CH}$), 71.4 ($2 \times \text{CH}_2$). HRMS (ESI) Exact mass calculated for $[\text{C}_{68}\text{H}_{46}\text{N}_2\text{NaO}_4\text{S}]^+$ $[\text{M}+\text{Na}]^+$: 1009.3076, found 1009.3092.



***N*4-[(*S*)-2'-(Benzyloxy)-[1,1'-binaphthalen]-2-yl]-*N*6-[2'-(benzyloxy)-[1,1'-binaphthalen]-2-yl]dibenzo[*b,d*]thiophene-4,6-dicarboxamide-AuCl (**511**).**
An oven-dried microwave vial equipped

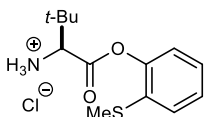
with a stirrer bar was charged with (CO)AuCl (0.10 mmol, 26.0 mg). A solution of *N*4-[(*S*)-2'-(benzyloxy)-[1,1'-binaphthalen]-2-yl]-*N*6-[2'-(benzyloxy)-[1,1'-binaphthalen]-2-yl]dibenzo[*b,d*]thiophene-4,6-dicarboxamide (**510**) (0.10 mmol, 98.7 mg) in anhydrous CH₂Cl₂ (3 mL) was added dropwise and the resulting mixture was stirred at room temperature for 18 h. The reaction mixture was filtered and added dropwise to rapidly stirring *n*-pentane at 0 °C, at which point the product precipitated. The precipitated product was removed by vacuum filtration, washed with ice-cold *n*-pentane (2 × 5 mL) and dried under vacuum to give the title compound **511** as an olive green solid (60.5 mg, 50%). m.p. decomposes *ca* 151 °C (Et₂O); IR 3057, 1666 (C=O), 1620, 1591, 1497, 1427, 1282, 1017, 809, 740 cm⁻¹; [α]_D²⁵ -8.0 (*c* 1.00, CHCl₃); ¹H NMR (500 MHz, CDCl₃) δ 8.85 (2H, d, *J* = 8.5 Hz, ArH), 8.07-8.00 (4H, m, ArH), 7.97-7.92 (5H, m, ArH and 2 × NH), 7.84 (2H, d, *J* = 8.2 Hz, ArH), 7.51 (2H, d, *J* = 9.1 Hz, ArH), 7.44 (2H, t, *J* = 7.5 Hz, ArH), 7.33-7.27 (4H, m, ArH), 7.22-7.15 (6H, m, ArH), 7.09-7.02 (2H, m, ArH), 7.00-6.93 (12H, m, ArH), 6.55-6.51 (1H, m, ArH), 5.13 (2H, d, *J* = 12.7 Hz, OCH_aH_b), 5.08 (2H, d, *J* = 12.7 Hz, OCH_aH_b); ¹³C NMR (126 MHz, CDCl₃) δ 164.5 (2 × C), 154.2 (2 × C), 141.7 (2 × C), 136.7 (2 × C), 136.0 (2 × C), 134.3 (2 × C), 133.6 (2 × C), 133.2 (2 × C), 131.3 (2 × C), 131.0 (2 × CH), 129.7 (2 × C), 129.1 (2 × CH), 128.6 (2 × C), 128.4 (4 × CH), 128.3 (4 × CH), 127.9 (2 × CH), 127.7 (2 × CH), 127.2 (4 × CH), 126.6 (2 × CH), 126.1 (2 × CH), 125.13 (2 × CH), 125.10 (2 × CH), 124.7 (2 × CH), 124.5 (2 × CH), 124.34 (2 × CH), 124.30 (2 × CH), 122.4 (2 × C), 120.8 (2 × CH), 118.6 (2 × C), 116.1 (2 × CH), 71.4 (2 × CH₂). HRMS (ESI) Exact mass calculated for [C₆₈H₄₆AuN₂O₄S]⁺: 1184.1526, found 1184.1520.

Preparation of gold complex 522



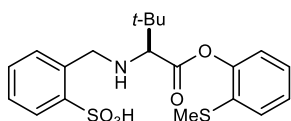
2-(Methylthio)phenyl (S)-2-[(*tert*-butoxycarbonyl)amino]-3,3-dimethylbutanoate (517**).** An oven-dried flask was charged with *Boc*-Tle-OH (1.73 g, 7.50 mmol) and purged with argon for 30 min.

Anhydrous CH_2Cl_2 (20 mL) was added, followed by DCC (1.86 g, 9.00 mmol), DMAP (183 mg, 1.50 mmol) and 2-(methylthio)phenol (962 μL , 8.25 mmol). The reaction was stirred at room temperature for 24 h and concentrated *in vacuo*. EtOAc (30 mL) was added and the resulting suspension was filtered under vacuum. The filtrate was concentrated *in vacuo* and the residue was purified by column chromatography (0 to 5% EtOAc/petroleum ether), to give the title compound **517** as a colourless oil (2.64 g, 99%). $R_f = 0.49$ (20% EtOAc/petroleum ether); IR 3369 (NH), 2968, 1760 (C=O), 1705 (C=O), 1497, 1242, 1191, 1067, 953, 742 cm^{-1} ; $[\alpha]_D^{25} -16.0$ (c 1.00, CHCl_3); ^1H NMR (400 MHz, CDCl_3) δ 7.30-7.26 (1H, m, ArH), 7.23 (1H, td, $J = 7.5, 1.6$ Hz, ArH), 7.18 (1H, td, $J = 7.5, 1.9$ Hz, ArH), 7.06 (1H, dd, $J = 7.8, 1.6$ Hz, ArH), 5.18 (1H, d, $J = 9.8$ Hz, NH), 4.39 (1H, d, $J = 9.8$ Hz, NHCH), 2.42 (3H, s, SCH_3), 1.47 (9H, s, $\text{C}(\text{CH}_3)_3$), 1.14 (9H, s, $\text{C}(\text{CH}_3)_3$); ^{13}C NMR (101 MHz, CDCl_3) δ 170.2 (C), 155.7 (C), 147.8 (C), 131.5 (C), 127.7 (CH), 126.9 (CH), 126.2 (CH), 122.4 (CH), 80.0 (C), 62.3 (CH), 34.9 (C), 28.5 (3 \times CH_3), 26.8 (3 \times CH_3), 15.6 (CH_3); HRMS (ESI) Exact mass calculated for $[\text{C}_{18}\text{H}_{27}\text{NNaO}_4\text{S}]^+ [\text{M}+\text{Na}]^+$: 376.1553, found 376.1543.



(S)-3,3-Dimethyl-1-[2-(methylthio)phenoxy]-1-oxobutan-2-aminium chloride (518). An oven-dried flask was charged with 2-(methylthio)phenyl

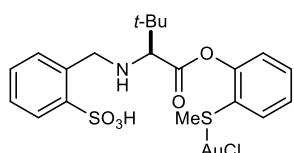
(*S*)-2-[(*tert*-butoxycarbonyl)amino]-3,3-dimethylbutanoate (**517**) (2.12 g, 6.00 mmol). HCl (4.0 M in dioxane, 9.00 mL, 36.0 mmol) was added dropwise at 0 °C and the reaction was stirred at room temperature for 1.5 h. The reaction mixture was degassed under a stream of argon for 30 min and concentrated *in vacuo* to give the title compound **518** as an off-white solid (1.54 g, 89%). m.p. 213-214 °C (Et₂O); IR 2871 (NH₃), 1754 (C=O), 1612, 1503, 1472, 1370, 1232, 1069, 825, 748 cm⁻¹; [α]_D²⁵ -20.0 (*c* 1.00, CHCl₃); ¹H NMR (500 MHz, CDCl₃) δ 8.99 (3H, s, NH₃), 7.43 (1H, d, *J* = 6.1 Hz, ArH), 7.26-7.17 (2H, m, ArH), 7.13-7.08 (1H, m, ArH), 3.96-3.89 (1H, m, NH₃CH), 2.40 (3H, s, SCH₃), 1.26 (9H, s, C(CH₃)₃); ¹³C NMR (126 MHz, CDCl₃) δ 166.8 (C), 148.0 (C), 130.8 (C), 127.8 (CH), 127.3 (CH), 126.7 (CH), 123.1 (CH), 62.7 (CH), 34.0 (C), 27.1 (3 × CH₃), 16.2 (CH₃); HRMS (ESI) Exact mass calculated for [C₁₃H₂₀NO₂S]⁺: 254.1209, found 254.1205.



(S)-2-[[[3,3-Dimethyl-1-[2-(methylthio)phenoxy]-1-oxobutan-2-yl]amino]methyl]benzenesulfonic acid (521).

To a stirred solution of (*S*)-3,3-dimethyl-1-[2-(methylthio)phenoxy]-1-oxobutan-2-aminium chloride (**518**) (1.16 g, 4.00 mmol), 2-formylbenzenesulfonic acid sodium salt (833 mg, 4.00 mmol) and MgSO₄ (1.44 g, 12.0 mmol) in CH₂Cl₂ (70 mL) under argon at 0 °C was added triethylamine (1.67 mL, 12.0 mmol) dropwise. The reaction was stirred at room temperature for 22 h and then passed through a plug of silica (8 cm in height and 2 cm wide) using EtOAc (100 mL) as the eluent and the filtrate was concentrated *in vacuo*. To this residue was added MeOH (50 mL), followed by NaBH₄ (1.36 g, 36.0 mmol) portionwise at 0 °C and the reaction was stirred at 0 °C for 2 h. The reaction was slowly quenched with saturated aqueous NaHCO₃ (30 mL) and extracted with CH₂Cl₂ (3 x 50 mL). The combined organic layers were dried (Na₂SO₄), filtered and concentrated *in vacuo*. The residue was purified by column chromatography (0 to 2% CH₂Cl₂/MeOH), to give the title compound **521** as a white solid (545 mg, 32%). R_f = 0.19 (5% CH₂Cl₂/MeOH); m.p. 150-151 °C (Et₂O); IR 2968, 1758 (C=O), 1470, 1436, 1142, 1086, 1068, 822, 700, 618 cm⁻¹; [α]_D²⁵ -84.0 (*c* 1.00, CHCl₃); ¹H NMR (500 MHz, CDCl₃) δ 10.09 (1H, br s, OH), 9.47 (1H, br s, NH), 8.19

(1H, dd, $J = 7.7, 1.5$ Hz, ArH), 7.55-7.50 (2H, m, ArH), 7.46 (1H, td, $J = 7.4, 1.5$ Hz, ArH), 7.37 (1H, dd, $J = 7.8, 1.6$ Hz, ArH), 7.30 (1H, td, $J = 7.6, 1.4$ Hz, ArH), 7.24 (1H, td, $J = 7.7, 1.7$ Hz, ArH), 7.09 (1H, dd, $J = 8.0, 1.4$ Hz, ArH), 5.33 (1H, d, $J = 13.5$ Hz, CCH_aH_b), 4.56 (1H, d, $J = 13.5$ Hz, CCH_aH_b), 3.59 (1H, s, NHCH), 2.50 (3H, s, SCH₃), 1.29 (9H, s, C(CH₃)₃); ¹³C NMR (126 MHz, CDCl₃) δ 165.4 (C), 147.8 (C), 145.5 (C), 133.7 (CH), 131.1 (CH), 130.9 (C), 130.7 (CH), 129.5 (CH), 128.9 (CH), 127.8 (CH), 127.0 (CH), 126.1 (C), 122.0 (CH), 67.3 (CH), 50.1 (CH₂), 35.1 (C), 27.2 (3 × CH₃), 16.4 (CH₃); HRMS (ESI) Exact mass calculated for [C₂₀H₂₅NNaO₅S₂]⁺ [M+Na]⁺: 446.1066, found 446.1057.



(S)-2-{{{3,3-Dimethyl-1-[2-(methylthio)phenoxy]-1-oxobutan-2-yl}amino}methyl}benzenesulfonic acid-AuCl (**522**). An oven-dried microwave vial equipped with a stirrer bar

was charged with (CO)AuCl (0.10 mmol, 26.0 mg). A solution of (S)-2-{{{3,3-dimethyl-1-[2-(methylthio)phenoxy]-1-oxobutan-2-yl}amino}methyl}benzenesulfonic acid (**521**) (0.10 mmol, 42.5 mg) in anhydrous CH₂Cl₂ (3 mL) was added dropwise and the resulting mixture was stirred at room temperature for 18 h. The reaction mixture was filtered and added dropwise to rapidly stirring *n*-pentane at 0 °C, at which point the product precipitated. The precipitated product was removed by vacuum filtration, washed with ice-cold *n*-pentane (2 × 5 mL) and dried under vacuum to give the title compound **522** as a yellow solid (34.9 mg, 53%). m.p. 228-229 °C (Et₂O); IR 2960, 1760 (C=O), 1470, 1440, 1144, 1087, 1015, 796, 701, 618 cm⁻¹; [α]_D²⁵ -52.0 (*c* 1.00, CHCl₃); ¹H NMR (500 MHz, CDCl₃) δ 9.80 (1H, br s, OH), 9.35 (1H, br s, NH), 8.15-8.07 (1H, m, ArH), 7.62-7.28 (6H, m, ArH), 7.09 (1H, d, $J = 7.9$ Hz, ArH), 5.40-5.27 (1H, m, CCH_aH_b), 4.62-4.41 (1H, m, CCH_aH_b), 3.61 (1H, s, NHCH), 2.55 (3H, br s, SCH₃), 1.20 (9H, s, C(CH₃)₃); ¹³C NMR (126 MHz, CDCl₃) δ 165.5 (C), 147.7 (C), 145.0 (C), 134.0 (CH), 131.5 (CH), 130.9 (CH and C), 129.3 (CH), 129.2 (CH), 128.1 (CH), 127.1 (CH), 125.9 (C), 122.0 (CH), 67.1 (CH), 50.2 (CH₂), 35.0 (C), 27.0 (3 × CH₃), 16.5 (CH₃); HRMS (ESI) Exact mass calculated for [C₂₀H₂₆AuClNO₅S₂]⁺ [M+H]⁺: 656.0601, found 656.0598

4.0 References

1. G. Brahmachari, *RSC Adv.* **2016**, *6*, 64676–64725.
2. H. M. Huang, P. Bellotti, F. Glorius, *Chem. Soc. Rev.* **2020**, *49*, 6186–6197.
3. K. J. Szabó, *Chem. Eur. J.* **2004**, *10*, 5268–5275.
4. B. M. Trost, M. L. Crawley, *Chem. Rev.* **2003**, *103*, 2921–2943.
5. Y. Yamamoto, N. Asao, *Chem. Rev.* **1993**, *93*, 2207–2293.
6. M. Yus, J. C. González-Gómez, F. Foubelo, *Chem. Rev.* **2011**, *111*, 7774–7854.
7. L. Chabaud, P. James, Y. Landais, *Eur. J. Org. Chem.* **2004**, 3173–3199.
8. J. A. Marshall, *Chem. Rev.* **1996**, *96*, 31–47.
9. N. D. Bartolo, J. A. Read, E. M. Valentín, K. A. Woerpel, *Chem. Rev.* **2020**, *120*, 1513–1619.
10. H. X. Huo, J. R. Duvall, M. Y. Huang, R. Hong, *Org. Chem. Front.* **2014**, *1*, 303–320.
11. S. E. Denmark, E. J. Weber, *Helv. Chim. Acta* **1983**, *66*, 1655–1660.
12. R. W. Hoffmann, H. -J Zeiss, *Angew. Chem. Int. Ed.* **1979**, *18*, 306–307.
13. Y. Yamamoto, H. Yatagai, Y. Naruta, K. Maruyama, *J. Am. Chem. Soc.* **1980**, *102*, 7107–7109.
14. R. A. Fernandes, J. L. Nallasivam, *Org. Biomol. Chem.* **2019**, *17*, 8647–8672.
15. Y. Luo, H. B. Hepburn, N. Chotsaeng, H. W. Lam, *Angew. Chem. Int. Ed.* **2012**, *51*, 8309–8313.
16. J. F. Han, P. Guo, X. G. Zhang, J. Bin Liao, K. Y. Ye, *Org. Biomol. Chem.* **2020**, *18*, 7740–7750.
17. R. Wada, K. Oisaki, M. Kanai, M. Shibasaki, *J. Am. Chem. Soc.* **2004**, *126*, 8910–8911.
18. A. Quintavalla, M. Bandini, *ChemCatChem* **2016**, *8*, 1437–1453.
19. A. S. K. Hashmi, G. J. Hutchings, *Angew. Chem. Int. Ed.* **2006**, *45*, 7896–7936.
20. R. A. Widenhoefer, *Chem. Eur. J.* **2008**, *14*, 5382–5391.
21. S. A. Shahzad, M. A. Sajid, Z. A. Khan, D. Canseco-Gonzalez, *Synth. Commun.* **2017**, *47*, 735–755.
22. V. W. Bhoyare, A. G. Tathe, A. Das, C. C. Chintawar, N. T. Patil, *Chem. Soc. Rev.* **2021**, *50*, 10422–10450.
23. D. Pflästerer, A. S. K. Hashmi, *Chem. Soc. Rev.* **2016**, *45*, 1331–1367.
24. M. Jia, M. Bandini, *ACS Catal.* **2015**, *5*, 1638–1652.
25. N. Krause, C. Winter, *Chem. Rev.* **2011**, *111*, 1994–2009.
26. R. Dorel, A. M. Echavarren, *Chem. Rev.* **2015**, *115*, 9028–9072.
27. S. G. Bratsch, *J. Phys. Chem. Ref. Data* **1989**, *18*, 1–21.

28. G. Zhang, Y. Peng, L. Cui, L. Zhang, *Angew. Chem. Int. Ed.* **2009**, *48*, 3112–3115.
29. Z. Zheng, X. Ma, X. Cheng, K. Zhao, K. Gutman, T. Li, L. Zhang, *Chem. Rev.* **2021**, *121*, 8979–9038.
30. A. Leyva-Pérez, A. Doménech, S. I. Al-Resayes, A. Corma, *ACS Catal.* **2012**, *2*, 121–126.
31. Z. Zheng, Z. Wang, Y. Wang, L. Zhang, *Chem. Soc. Rev.* **2016**, *45*, 4448–4458.
32. J. Miró, C. Del Pozo, *Chem. Rev.* **2016**, *116*, 11924–11966.
33. B. Huang, M. Hu, F. D. Toste, *Trends Chem.* **2020**, *2*, 707–720.
34. M. Bandini, A. Eichholzer, *Angew. Chem. Int. Ed.* **2009**, *48*, 9533–9537.
35. M. Bandini, A. Bottoni, M. Chiarucci, G. Cera, G. Pietro Miscione, *J. Am. Chem. Soc.* **2012**, *134*, 20690–20700.
36. M. Chiarucci, M. Di Lillo, A. Romaniello, P. G. Cozzi, G. Cera, M. Bandini, *Chem. Sci.* **2012**, *3*, 2859–2863.
37. P. Kothandaraman, W. Rao, X. Zhang, P. W. H. Chan, *Tetrahedron* **2009**, *65*, 1833–1838.
38. D. L. Usanov, H. Yamamoto, *Org. Lett.* **2012**, *14*, 414–417.
39. M. M. Mastandrea, N. Mellonie, P. Giacinto, A. Collado, S. P. Nolan, G. Pietro Miscione, A. Bottoni, M. Bandini, *Angew. Chem. Int. Ed.* **2015**, *54*, 14885–14889.
40. A. Preinfalk, A. Misale, N. Maulide, *Chem. Eur. J.* **2016**, *22*, 14471–14474.
41. A. Aponick, C. Y. Li, B. Biannic, *Org. Lett.* **2008**, *10*, 669–671.
42. T. Ghebreghiorgis, B. Biannic, B. H. Kirk, D. H. Ess, A. Aponick, *J. Am. Chem. Soc.* **2012**, *134*, 16307–16318.
43. A. Aponick, B. Biannic, *Org. Lett.* **2011**, *13*, 1330–1333.
44. M. Bandini, M. Monari, A. Romaniello, M. Tragni, *Chem. Eur. J.* **2010**, *16*, 14272–14277.
45. U. Uria, C. Vila, M. Y. Lin, M. Rueping, *Chem. Eur. J.* **2014**, *20*, 13913–13917.
46. M. L. Lanier, H. Park, P. Mukherjee, J. C. Timmerman, A. A. Ribeiro, R. A. Widenhoefer, J. Hong, *Chem. Eur. J.* **2017**, *23*, 7180–7184.
47. M. Chiarucci, R. Mocchi, L. D. Syntrivanis, G. Cera, A. Mazzanti, M. Bandini, *Angew. Chem. Int. Ed.* **2013**, *52*, 10850–10853.
48. P. C. Young, N. A. Schopf, A. L. Lee, *Chem. Commun.* **2013**, *49*, 4262–4264.
49. P. Tosatti, A. Nelson, S. P. Marsden, *Org. Biomol. Chem.* **2012**, *10*, 3147–3163.
50. L. Herkert, S. L. J. Green, G. Barker, D. G. Johnson, P. C. Young, S. A. Macgregor, A. L. Lee, *Chem. Eur. J.* **2014**, *20*, 11540–11548.
51. S. Guo, F. Song, Y. Liu, *Synlett* **2007**, *2007*, 964–968.
52. P. Kothandaraman, J. F. Shi, P. W. H. Chan, *J. Org. Chem.* **2009**, *74*, 5947–5952.
53. P. Mukherjee, R. A. Widenhoefer, *Org. Lett.* **2011**, *13*, 1334–1337.
54. P. Mukherjee, R. A. Widenhoefer, *Angew. Chem. Int. Ed.* **2012**, *51*, 1405–1407.
55. Y. Park, J. S. Lee, J. S. Ryu, *Adv. Synth. Catal.* **2021**, *363*, 2183–2188.

56. S. Porcel, V. López-Carrillo, C. García-Yebra, A. M. Echavarren, *Angew. Chem. Int. Ed.* **2008**, *47*, 1883–1886.
57. Z. Chen, Y. X. Zhang, Y. H. Wang, L. L. Zhu, H. Liu, X. X. Li, L. Guo, *Org. Lett.* **2010**, *12*, 3468–3471.
58. Y. H. Wang, L. L. Zhu, Y. X. Zhang, Z. Chen, *Chem. Commun.* **2010**, *46*, 577–579.
59. L. L. Zhu, Y. H. Wang, Y. X. Zhang, X. X. Li, H. Liu, Z. Chen, *J. Org. Chem.* **2011**, *76*, 441–449.
60. M. S. M. Holmsen, A. Nova, S. Øien-Ødegaard, R. H. Heyn, M. Tilset, *Angew. Chem. Int. Ed.* **2020**, *59*, 1516–1520.
61. J. Rodriguez, G. Szalóki, E. D. Sosa Carrizo, N. Saffon-Merceron, K. Miqueu, D. Bourissou, *Angew. Chem. Int. Ed.* **2020**, *132*, 1527–1531.
62. S. Komiya, S. Ozaki, *Chem. Lett.* **1988**, *17*, 1431–1432.
63. M. D. Levin, T. Q. Chen, M. E. Neubig, C. M. Hong, C. A. Theulier, I. J. Kobylanski, M. Janabi, J. P. O’Neil, F. D. Toste, *Science* **2017**, *356*, 1272–1275.
64. J. Rodriguez, M. S. M. Holmsen, Y. García-Rodeja, E. D. Sosa Carrizo, P. Lavedan, S. Mallet-Ladeira, K. Miqueu, D. Bourissou, *J. Am. Chem. Soc.* **2021**, *143*, 11568–11581.
65. C. Obradors, A. M. Echavarren, *Acc. Chem. Res.* **2014**, *47*, 902–912.
66. C. Silva, O. N. Faza, M. M. Luna, *Front. Chem.* **2019**, *7*, 296.
67. J. Y. Cheong, D. Im, M. Lee, W. Lim, Y. H. Rhee, *J. Org. Chem.* **2011**, *76*, 324–327.
68. F. M. Istrate, F. Gagosz, *Beilstein J. Org. Chem.* **2011**, *7*, 878–885.
69. M. Ackermann, J. Bucher, M. Rappold, K. Graf, F. Rominger, A. S. K. Hashmi, *Chem. Asian J.* **2013**, *8*, 1786–1794.
70. J. Renault, Z. Qian, P. Uriac, N. Gouault, *Tetrahedron Lett.* **2011**, *52*, 2476–2479.
71. M. C. B. Jaimes, A. Ahrens, D. Pflästerer, M. Rudolph, A. S. K. Hashmi, *Chem. Eur. J.* **2015**, *21*, 427–433.
72. H. Wang, T. Li, Z. Zheng, L. Zhang, *ACS Catal.* **2019**, *9*, 10339–10342.
73. T. Li, S. Dong, C. Tang, M. Zhu, N. Wang, W. Kong, W. Gao, J. Zhu, L. Zhang, *Org. Lett.* **2022**, *24*, 4427–4432.
74. J. Fu, H. Shang, Z. Wang, L. Chang, W. Shao, Z. Yang, Y. Tang, *Angew. Chem. Int. Ed.* **2013**, *52*, 4198–4202.
75. J. M. Ketcham, B. Biannic, A. Aponick, *Chem. Commun.* **2013**, *49*, 4157–4159.
76. A. Gómez-Suárez, D. Gasperini, S. V. C. Vummaleti, A. Poater, L. Cavallo, S. P. Nolan, *ACS Catal.* **2014**, *4*, 2701–2705.
77. S. R. Park, C. Kim, D. G. Kim, N. Thrimurtulu, H. S. Yeom, J. Jun, S. Shin, Y. H. Rhee, *Org. Lett.* **2013**, *15*, 1166–1169.
78. A. Wetzel, F. Gagosz, *Angew. Chem. Int. Ed.* **2011**, *123*, 7492–7496.
79. B. Lu, Y. Luo, L. Liu, L. Ye, Y. Wang, L. Zhang, *Angew. Chem. Int. Ed.* **2011**, *50*, 8358–8362.
80. I. Nakamura, T. Sato, Y. Yamamoto, *Angew. Chem. Int. Ed.* **2006**, *118*, 4585–4587.

81. T. S. A. Heugebaert, L. P. D. Vervaecke, C. V. Stevens, *Org. Biomol. Chem.* **2011**, *9*, 4791–4794.
82. J. Li, K. Ji, R. Zheng, J. Nelson, L. Zhang, *Chem. Commun.* **2014**, *50*, 4130–4133.
83. M. Dos Santos, P. W. Davies, *Chem. Commun.* **2014**, *50*, 6001–6004.
84. W. Kirmse, M. Kapps, *Chem. Ber.* **1968**, *101*, 994–1003.
85. H. Kim, J. Jang, S. Shin, *J. Am. Chem. Soc.* **2020**, *142*, 20788–20795.
86. W. Debrouwer, R. A. J. Seigneur, T. S. A. Heugebaert, C. V. Stevens, *Chem. Commun.* **2015**, *51*, 729–732.
87. T. S. A. Heugebaert, C. V. Stevens, *Org. Lett.* **2009**, *11*, 5018–5021.
88. K. C. Majumdar, S. Hazra, B. Roy, *Tetrahedron Lett.* **2011**, *52*, 6697–6701.
89. V. Gobé, M. Dousset, P. Retailleau, V. Gandon, X. Guinchard, *J. Org. Chem.* **2018**, *83*, 898–912.
90. Y. Horino, M. R. Luzung, F. D. Toste, *J. Am. Chem. Soc.* **2006**, *128*, 11364–11365.
91. S. Park, D. Lee, *J. Am. Chem. Soc.* **2006**, *128*, 10664–10665.
92. T. Matsuda, S. Kadowaki, Y. Yamaguchi, M. Murakami, *Chem. Commun.* **2008**, 2744–2746.
93. G. Kovács, A. Lledós, G. Ujaque, *Organometallics* **2010**, *29*, 3252–3260.
94. Y. Horino, Y. Takahashi, Y. Nakashima, H. Abe, *RSC Adv.* **2014**, *4*, 6215–6218.
95. J. Li, X. Liu, D. Lee, *Org. Lett.* **2012**, *14*, 410–413.
96. D. J. Gorin, B. D. Sherry, F. D. Toste, *Chem. Rev.* **2008**, *108*, 3351–3378.
97. P. W. Davies, S. J. C. Albrecht, *Chem. Commun.* **2008**, 238–240.
98. P. W. Davies, S. J. C. Albrecht, *Angew. Chem. Int. Ed.* **2009**, *48*, 8372–8375.
99. M. Uemura, I. D. G. Watson, M. Katsukawa, F. Dean Toste, *J. Am. Chem. Soc.* **2009**, *131*, 3464–3465.
100. Y. Shi, K. E. Roth, S. D. Ramgren, S. A. Blum, *J. Am. Chem. Soc.* **2009**, *131*, 18022–18023.
101. A. S. K. Hashmi, C. Lothschütz, R. Döpp, M. Ackermann, J. De Buck Becker, M. Rudolph, C. Scholz, F. Rominger, *Adv. Synth. Catal.* **2012**, *354*, 133–147.
102. H. Wu, Y. P. He, L. Z. Gong, *Adv. Synth. Catal.* **2012**, *354*, 975–980.
103. D. Xing, D. Yang, *Beilstein J. Org. Chem.* **2011**, *7*, 781–785.
104. D. Xing, D. Yang, *Org. Lett.* **2010**, *12*, 1068–1071.
105. N. Marion, R. Gealageas, S. P. Nolan, *Org. Lett.* **2007**, *9*, 2653–2656.
106. M. Georgy, V. Boucard, J. M. Campagne, *J. Am. Chem. Soc.* **2005**, *127*, 14180–14181.
107. S. Bhunia, S. M. Abu Sohel, C. C. Yang, S. F. Lush, F. M. Shen, R. S. Liu, *J. Organomet. Chem.* **2009**, *694*, 566–570.
108. C. Y. Yang, C. D. Wang, S. F. Tian, R. S. Liu, *Adv. Synth. Catal.* **2010**, *352*, 1605–1609.
109. C. C. Lin, T. M. Teng, A. Odedra, R. S. Liu, *J. Am. Chem. Soc.* **2007**, *129*, 3798–3799.

110. C. C. Lin, T. M. Teng, C. C. Tsai, H. Y. Liao, R. S. Liu, *J. Am. Chem. Soc.* **2008**, *130*, 16417–16423.
111. Y. C. Hsu, S. Datta, C. M. Ting, R. S. Liu, *Org. Lett.* **2008**, *10*, 521–524.
112. Y. Sawama, Y. Sawama, N. Krause, *Org. Lett.* **2009**, *11*, 5034–5037.
113. T. Sone, S. Ozaki, N. C. Kasuga, A. Fukuoka, S. Komiya, *Bull. Chem. Soc. Jpn.* **1995**, *68*, 1523–1533.
114. M. Kojima, K. Mikami, *Chem. Eur. J.* **2011**, *17*, 13950–13953.
115. R. K. R. Singh, R. S. Liu, *Adv. Synth. Catal.* **2016**, *358*, 1421–1427.
116. G. Dong, M. Bao, X. Xie, S. Jia, W. Hu, X. Xu, *Angew. Chem. Int. Ed.* **2021**, *133*, 2020–2027.
117. J. T. Bauer, M. S. Hadfield, A. L. Lee, *Chem. Commun.* **2008**, 6405–6407.
118. R. J. Mudd, P. C. Young, J. A. Jordan-Hore, G. M. Rosair, A. L. Lee, *J. Org. Chem.* **2012**, *77*, 7633–7639.
119. J. Barluenga, G. Lonzi, M. Tomás, L. A. López, *Chem. Eur. J.* **2013**, *19*, 1573–1576.
120. E. López, G. Lonzi, L. A. López, *Organometallics* **2014**, *33*, 5924–5927.
121. D. Huang, G. Xu, S. Peng, J. Sun, *Chem. Commun.* **2017**, *53*, 3197–3200.
122. P. Garcia, M. Malacria, C. Aubert, V. Gandon, L. Fensterbank, *ChemCatChem* **2010**, *2*, 493–497.
123. M. N. Hopkinson, A. D. Gee, V. Gouverneur, *Chem. Eur. J.* **2011**, *17*, 8248–8262.
124. M. D. Levin, F. D. Toste, *Angew. Chem. Int. Ed.* **2014**, *126*, 6325–6329.
125. K. Liu, T. Li, D. Y. Liu, W. Li, J. Han, C. Zhu, J. Xie, *Sci. China Chem.* **2021**, *64*, 1958–1963.
126. J. Rodriguez, D. Vesseur, A. Tabey, S. Mallet-Ladeira, K. Miqueu, D. Bourissou, *ACS Catal.* **2022**, *12*, 993–1003.
127. M. O. Akram, P. S. Mali, N. T. Patil, *Org. Lett.* **2017**, *19*, 3075–3078.
128. J. Wang, S. Zhang, C. Xu, L. Wojtas, N. G. Akhmedov, H. Chen, X. Shi, *Angew. Chem. Int. Ed.* **2018**, *57*, 6915–6920.
129. E. Vitaku, D. T. Smith, J. T. Njardarson, *J. Med. Chem.* **2014**, *57*, 10257–10274.
130. M. Mąkosza, *Chem. Eur. J.* **2020**, *26*, 15346–15353.
131. S. Rohrbach, A. J. Smith, J. H. Pang, D. L. Poole, T. Tuttle, S. Chiba, J. A. Murphy, *Angew. Chem. Int. Ed.* **2019**, *58*, 16368–16388.
132. A. R. Katritzky, W. Q. Fan, *Heterocycles* **1992**, *34*, 2179–2229.
133. J. A. Bull, J. J. Mousseau, G. Pelletier, A. B. Charette, *Chem. Rev.* **2012**, *112*, 2642–2713.
134. G. Bertuzzi, L. Bernardi, M. Fochi, *Catalysts* **2018**, *8*, 632.
135. V. K. Sharma, S. K. Singh, *RSC Adv.* **2017**, *7*, 2682–2732.
136. G. Bertuzzi, A. Sinisi, L. Caruana, A. Mazzanti, M. Fochi, L. Bernardi, *ACS Catal.* **2016**, *6*, 6473–6477.
137. D. L. Connors, J. D. Brown, *Tetrahedron Lett.* **1986**, *27*, 4549–4552.

138. D. L. Comins, H. Hong, J. M. Salvador, *J. Org. Chem.* **1991**, *56*, 7197–7199.
139. D. L. Comins, N. B. Mantlo, *J. Org. Chem.* **1985**, *50*, 4410–4411.
140. E. Ichikawa, M. Suzuki, K. Yabu, M. Albert, M. Kanai, M. Shibasaki, *J. Am. Chem. Soc.* **2004**, *126*, 11808–11809.
141. D. L. Comins, J. D. Brown, *Tetrahedron Lett.* **1986**, *27*, 2219–2222.
142. R. Yamaguchi, M. Moriyasu, M. Yoshioka, M. Kawanisi, *J. Org. Chem.* **1985**, *50*, 287–288.
143. R. Yamaguchi, M. Moriyasu, M. Yoshioka, M. Kawanisi, *J. Org. Chem.* **1988**, *53*, 3507–3512.
144. P. Magnus, J. Rodriguez-López, K. Mulholland, I. Matthews, *J. Am. Chem. Soc.* **1992**, *114*, 382–383.
145. R. Yamaguchi, K. Mochizuki, S. Kozima, H. Takaya, *J. Chem. Soc. Chem. Commun.* **1993**, 981–982.
146. S. Yamada, M. Ichikawa, *Tetrahedron Lett.* **1999**, *40*, 4231–4234.
147. S. Joseph, Q. N. Duong, L. Schifferer, O. García Mancheño, *Tetrahedron* **2022**, *114*, DOI 10.1016/j.tet.2022.132767.
148. R. Yamaguchi, B. Hatano, T. Nakayasu, S. Kozima, *Tetrahedron Lett.* **1997**, *38*, 403–406.
149. R. Yamaguchi, T. Nakayasu, B. Hatano, T. Nagura, S. Kozima, K. I. Fujita, *Tetrahedron* **2001**, *57*, 109–118.
150. R. Yamaguchi, M. Tanaka, T. Matsuda, T. Okano, T. Nagura, K. I. Fujita, *Tetrahedron Lett.* **2002**, *43*, 8871–8874.
151. T. P. Loh, P. L. Lye, R. Bin Wang, K. Y. Sim, *Tetrahedron Lett.* **2000**, *41*, 7779–7783.
152. J. H. Lee, J. S. Kweon, C. M. Yoon, *Tetrahedron Lett.* **2002**, *43*, 5771–5774.
153. S. H. Lee, Y. S. Park, M. H. Nam, C. M. Yoon, *Org. Biomol. Chem.* **2004**, *2*, 2170–2172.
154. S. Yamada, M. Inoue, *Org. Lett.* **2007**, *9*, 1477–1480.
155. P. Jochmann, T. S. Dols, T. P. Spaniol, L. Perrin, L. Maron, J. Okuda, *Angew. Chem. Int. Ed.* **2010**, *49*, 7795–7798.
156. Z. Liu, L. Chen, J. Li, K. Liu, J. Zhao, M. Xu, L. Feng, R. Z. Wan, W. Li, L. Liu, *Org. Biomol. Chem.* **2017**, *15*, 7600–7606.
157. B. J. Knight, Z. A. Tolchin, J. M. Smith, *Chem. Commun.* **2021**, *57*, 2693–2696.
158. B. G. Reed-Berendt, D. E. Latham, M. B. Dambatta, L. C. Morrill, *ACS Cent. Sci.* **2021**, *7*, 570–585.
159. G. Berionni, B. Maji, P. Knochel, H. Mayr, *Chem. Sci.* **2012**, *3*, 878–882.
160. R. Wada, T. Shibuguchi, S. Makino, K. Oisaki, M. Kanai, M. Shibasaki, *J. Am. Chem. Soc.* **2006**, *128*, 7687–7691.
161. S. L. Shi, L. W. Xu, K. Oisaki, M. Kanai, M. Shibasaki, *J. Am. Chem. Soc.* **2010**, *132*, 6638–6639.
162. D. Saulys, V. Joshkin, M. Khoudiakov, T. F. Kuech, A. B. Ellis, S. R. Oktyabrsky, L.

- McCaughan, *J. Cryst. Growth* **2000**, *217*, 287–301.
163. J. W. Clary, T. J. Rettenmaier, R. Snelling, W. Bryks, J. Banwell, W. T. Wipke, B. Singaram, *J. Org. Chem.* **2011**, *76*, 9602–9610.
164. G. Dutheuil, N. Selander, K. J. Szabó, V. K. Aggarwal, *Synthesis* **2008**, 2293–2297.
165. D. P. Hari, J. C. Abell, V. Fasano, V. K. Aggarwal, *J. Am. Chem. Soc.* **2020**, *142*, 5515–5520.
166. Y. Yasuda, H. Ohmiya, M. Sawamura, *Angew. Chem. Int. Ed.* **2016**, *55*, 10816–10820.
167. B. Qin, U. Schneider, *J. Am. Chem. Soc.* **2016**, *138*, 13119–13122.
168. S. Shimada, A. S. Batsanov, J. A. K. Howard, T. B. Marder, *Angew. Chem. Int. Ed.* **2001**, *40*, 2168–2171.
169. H. F. Bettinger, M. Filthaus, H. Bornemann, I. M. Oppel, *Angew. Chem. Int. Ed.* **2008**, *47*, 4744–4747.
170. C. Adamo, V. Barone, *J. Chem. Phys.* **1999**, *110*, 6158–6170.
171. F. Weigend, R. Ahlrichs, *Phys. Chem. Chem. Phys.* **2005**, *7*, 3297–3305.
172. F. Weigend, *Phys. Chem. Chem. Phys.* **2006**, *8*, 1057–1065.
173. A. V. Marenich, C. J. Cramer, D. G. Truhlar, *J. Phys. Chem. B* **2009**, *113*, 6378–6396.
174. G. Luchini, J. V Alegre-Requena, I. Funes-Ardoiz, R. S. Paton, *F1000Research* **2020**, *9*, 291.
175. A. S. K. Hashmi, A. M. Schuster, S. Litters, F. Rominger, M. Pernpointner, *Chem. Eur. J.* **2011**, *17*, 5661–5667.
176. D. R. Fandrick, K. R. Fandrick, J. T. Reeves, Z. Tan, W. Tang, A. G. Capacci, S. Rodriguez, J. J. Song, H. Lee, N. K. Yee, C. H. Senanayake, *J. Am. Chem. Soc.* **2010**, *132*, 7600–7601.
177. K. R. Fandrick, D. R. Fandrick, J. T. Reeves, J. Gao, S. Ma, W. Li, H. Lee, N. Grinberg, B. Lu, C. H. Senanayake, *J. Am. Chem. Soc.* **2011**, *133*, 10332–10335.
178. N. W. Mszar, F. Haeffner, A. H. Hoveyda, *J. Am. Chem. Soc.* **2014**, *136*, 3362–3365.
179. W. Zi, F. Dean Toste, *Chem. Soc. Rev.* **2016**, *45*, 4567–4589.
180. M. Mellah, A. Voituriez, E. Schulz, *Chem. Rev.* **2007**, *107*, 5133–5209.
181. B. M. Trost, M. Rao, *Angew. Chem. Int. Ed.* **2015**, *54*, 5026–5043.
182. S. Otocka, M. Kwiatkowska, L. Madalińska, P. Kielbasiński, *Chem. Rev.* **2017**, *117*, 4147–4181.
183. X. Liu, R. An, X. Zhang, J. Luo, X. Zhao, *Angew. Chem. Int. Ed.* **2016**, *55*, 5846–5850.
184. Q. Cao, J. Luo, X. Zhao, *Angew. Chem. Int. Ed.* **2019**, *58*, 1315–1319.
185. D. A. Kutateladze, E. N. Jacobsen, *J. Am. Chem. Soc.* **2021**, *143*, 20077–20083.
186. A. J. Bendel-Smith, S. C. Kim, M. Wasa, S. P. Roche, E. N. Jacobsen, *J. Am. Chem. Soc.* **2019**, *141*, 11414–11419.
187. A. E. Wendlandt, P. Vangal, E. N. Jacobsen, *Nature* **2018**, *556*, 447–451.
188. Y. Park, C. S. Schindler, E. N. Jacobsen, *J. Am. Chem. Soc.* **2016**, *138*, 14848–14851.

189. A. Voituriezh, J. C. Fiaud, E. Schulz, *Tetrahedron Lett.* **2002**, *43*, 4907–4909.
190. T. Hashimoto, K. Maruoka, *Chem. Rev.* **2007**, *107*, 5656–5682.
191. R. J. Phipps, G. L. Hamilton, F. D. Toste, *Nat. Chem.* **2012**, *4*, 603–614.
192. W. Guo, L. Zuo, M. Cui, B. Yan, S. Ni, *J. Am. Chem. Soc.* **2021**, *143*, 7629–7634.
193. G. Chen, J. Gui, L. Li, J. Liao, *Angew. Chem. Int. Ed.* **2011**, *50*, 7681–7685.
194. R. Mariz, X. Luan, M. Gatti, A. Linden, R. Dorta, *J. Am. Chem. Soc.* **2008**, *130*, 2172–2173.
195. M. Rachwalski, T. Leenders, S. Kaczmarczyk, P. Kiełbasiński, S. Leśniak, F. P. J. T. Rutjes, *Org. Biomol. Chem.* **2013**, *11*, 4207–4213.
196. H. Xu, S. J. Zuend, M. G. Woll, Y. Tao, E. N. Jacobsen, *Science* **2010**, *327*, 986–990.
197. W. Ma, J. Fang, J. Ren, Z. Wang, *Org. Lett.* **2015**, *17*, 4180–4183.
198. R. Corberán, N. W. Mszar, A. H. Hoveyda, *Angew. Chem. Int. Ed.* **2011**, *50*, 7079–7082.
199. H. B. Hepburn, H. W. Lam, *Angew. Chem. Int. Ed.* **2014**, *53*, 11605–11610.
200. N. Selander, K. J. Szabó, *J. Org. Chem.* **2009**, *74*, 5695–5698.
201. W. R. Roush, A. E. Walts, L. K. Hoong, *J. Am. Chem. Soc.* **1985**, *107*, 8186–8190.
202. C. García-Ruiz, J. L. Y. Chen, C. Sandford, K. Feeney, P. Lorenzo, G. Berionni, H. Mayr, V. K. Aggarwal, *J. Am. Chem. Soc.* **2017**, *139*, 15324–15327.
203. D. R. Fandrick, F. Roschangar, C. Kim, B. J. Hahm, M. H. Cha, H. Y. Kim, G. Yoo, T. Kim, J. T. Reeves, J. J. Song, Z. Tan, B. Qu, N. Haddad, S. Shen, N. Grinberg, H. Lee, N. Yee, C. H. Senanayake, *Org. Process Res. Dev.* **2012**, *16*, 1131–1140.
204. G. Bertuzzi, A. Sinisi, D. Pecorari, L. Caruana, A. Mazzanti, L. Bernardi, M. Fochi, *Org. Lett.* **2017**, *19*, 834–837.
205. C. E. Paul, S. Gargiulo, D. J. Opperman, I. Lavandera, V. Gotor-Fernández, V. Gotor, A. Taglieber, I. W. C. E. Arends, F. Hollmann, *Org. Lett.* **2013**, *15*, 180–183.
206. N. Christian, S. Aly, K. Belyk, *J. Am. Chem. Soc.* **2011**, *133*, 2878–2880.
207. C. Baumert, M. Günthel, S. Krawczyk, M. Hemmer, T. Wersig, A. Langner, J. Molnár, H. Lage, A. Hilgeroth, *Bioorganic Med. Chem.* **2013**, *21*, 166–177.
208. T. Thanh Dang, A. Chen, A. Majeed Seayad, *RSC Adv.* **2014**, *4*, 30019–30027.
209. J. Day, M. Uroos, R. A. Castledine, W. Lewis, B. McKeever-Abbas, J. Dowden, *Org. Biomol. Chem.* **2013**, *11*, 6502–6509.
210. R. Krishnamoorthy, S. Q. Lam, C. M. Manley, R. J. Herr, *J. Org. Chem.* **2010**, *75*, 1251–1258.
211. S. Khong, O. Kwon, *J. Org. Chem.* **2012**, *77*, 8257–8267.
212. A. Monrose, H. Salembier, T. Bousquet, S. Pellegrini, L. Pélineski, *Adv. Synth. Catal.* **2017**, *359*, 2699–2704.
213. A. Hilgeroth, C. Baumert, C. Coburger, M. Seifert, S. Krawczyk, C. Hempel, F. Neubauer, M. Krug, J. Molnar, H. Lage, *Med. Chem.* **2013**, *9*, 487–493.
214. H. Vander Mierde, P. Van Der Voort, F. Verpoort, *Tetrahedron Lett.* **2009**, *50*, 201–203.

215. A. W. Jensen, J. M. Moore, M. E. V. Kimble, A. P. Ausmus, W. L. Dilling, *Tetrahedron Lett.* **2016**, *57*, 5636–5638.
216. M. Renom-Carrasco, P. Gajewski, L. Pignataro, J. G. de Vries, U. Piarulli, C. Gennari, L. Lefort, *Chem. Eur. J.* **2016**, *22*, 9528–9532.
217. J. D. Sieber, J. P. Morken, *J. Am. Chem. Soc.* **2008**, *130*, 4978–4983.
218. D. L. Silverio, S. Torner, T. Pilyugina, E. M. Vieira, M. L. Snapper, F. Haeffner, A. H. Hoveyda, *Nature* **2013**, *494*, 216–221.
219. S. Cao, R. Christiansen, X. Peng, *Chem. Eur. J.* **2013**, *19*, 9050–9058.
220. J. Wang, X. Mi, J. Wang, Y. Yang, *Green Chem.* **2017**, *19*, 634–637.
221. I. Alonso, B. Trillo, F. López, S. Montserrat, G. Ujaque, L. Castedo, A. Lledós, J. L. Mascareñas, *J. Am. Chem. Soc.* **2009**, *131*, 13020–13030.
222. Z. Han, D. Krishnamurthy, P. Grover, Q. K. Fang, C. H. Senanayake, *J. Am. Chem. Soc.* **2002**, *124*, 7880–7881.
223. S. Saha, J. N. Moorthy, *J. Org. Chem.* **2011**, *76*, 396–402.
224. E. Fernández-Mateos, B. Maclá, D. J. Ramón, M. Yus, *Chem. Eur. J.* **2011**, *2011*, 6851–6855.
225. X. Chang, Q. Zhang, C. Guo, *Org. Lett.* **2019**, *21*, 4915–4918.

5.0 Appendix: Publication

This thesis contains results reported in the following publication:



Homogeneous Catalysis Hot Paper

 How to cite: *Angew. Chem. Int. Ed.* **2022**, *61*, e202202305

International Edition: doi.org/10.1002/anie.202202305

German Edition: doi.org/10.1002/ange.202202305

Gold(I)-Catalyzed Nucleophilic Allylation of Azinium Ions with Allylboronates

Luke O'Brien, Stephen P. Argent, Kristaps Ermanis,* and Hon Wai Lam*

Abstract: Gold(I)-catalyzed nucleophilic allylations of pyridinium and quinolinium ions with various allyl pinacolboronates are reported. The reactions are completely selective with respect to the site of the azinium ion that is attacked, to give various functionalized 1,4-dihydropyridines and 1,4-dihydroquinolines. Evidence suggests that the reactions proceed through nucleophilic allylgold(I) intermediates formed by transmetalation from allylboronates. Density functional theory (DFT) calculations provided mechanistic insight.

Introduction

Since the turn of the century, the application of homogeneous gold catalysis in organic synthesis has grown significantly.^[1,2] The ability of gold complexes to act as powerful carbophilic Lewis acids for carbon-carbon multiple bonds, as well as to achieve other modes of substrate activation, has led to the development of myriad new synthetic methods.^[1,2] Allylation reactions are important transformations that have been subject to gold catalysis.^[2] Gold-catalyzed allylic substitutions involving nucleophilic additions to electrophilic allylating agents have been developed extensively.^[2,3] Gold-catalyzed rearrangements that result in overall allylation are also well-known.^[2] In contrast, gold-mediated or gold-catalyzed allylations involving the addition of nucleophilic allylating agents to electrophiles are comparatively underdeveloped.^[2,4] Given the many unique features of gold catalysts, addressing this deficiency could provide valuable new synthetic methods.

Our research into gold-catalyzed nucleophilic allylations arose when we became interested in nucleophilic additions to azines or their corresponding azinium ions.^[5,6] These are powerful reactions to access partially saturated nitrogen heterocycles, which are valuable chemical building blocks.^[5,6] Nucleophilic allylations of in situ-generated *N*-acylazinium ions have also been explored,^[7] typically using allyltin,^[7a-c,g,j,m,n] allylindium,^[7h,j,l,m] allylmagnesium,^[7a,b,p,q] allylzinc,^[7m] or allylsilicon reagents.^[7i-k,o,p] However, these reactions are somewhat limited in scope and often lead to mixtures of regioisomeric products favoring those of addition to the 2- or 6-positions. (Scheme 1A). Therefore, there is a need for nucleophilic allylations of azinium ions that exhibit high selectivity for addition to the 4-position. It is known that catalytic enantioselective nucleophilic additions to azinium ions containing a strongly electron-withdrawing group at the 3-position often exhibit high selectivity for addition at C4,^[6i-k,p] and this class of substrate therefore seemed a logical choice to study. Furthermore, despite the broad utility of allylboron reagents in nucleophilic allylations,^[8,9] only limited examples of their use in additions to azines^[10] or azinium ions^[7k,m] have been reported. Herein, we describe the first gold-catalyzed nucleophilic allylations of azinium ions with allylboronates to provide dihydropyridines and dihydroquinolines with complete regioselectivity in favor of addition to the 4-position (Scheme 1B). The reactions proceed well without special precautions to exclude air or moisture. Nucleophilic allylgold(I) species^[11] are the likely intermediates in these reactions, which are formed by transmetalation from the allylboronates.

[*] L. O'Brien, Prof. H. W. Lam

The GlaxoSmithKline Carbon Neutral Laboratories for Sustainable Chemistry, University of Nottingham, Jubilee Campus, Triumph Road, Nottingham, NG7 2TU (UK)

E-mail: hon.lam@nottingham.ac.uk

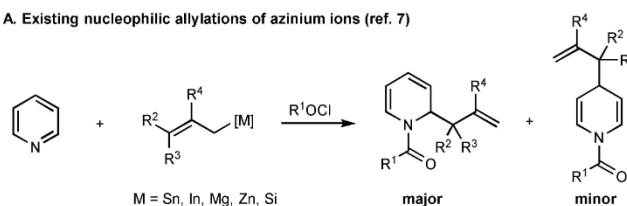
Homepage: http://www.nottingham.ac.uk/~pczh/

 L. O'Brien, Dr. S. P. Argent, Dr. K. Ermanis, Prof. H. W. Lam
 School of Chemistry, University of Nottingham, University Park, Nottingham, NG7 2RD (UK)

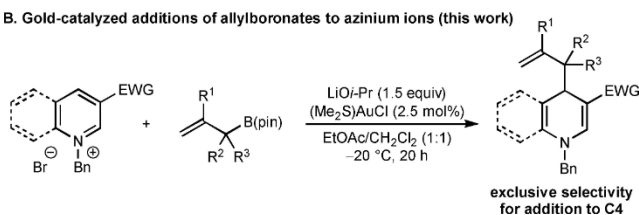
E-mail: Kristaps.Ermanis@nottingham.ac.uk

© 2022 The Authors. Angewandte Chemie International Edition published by Wiley-VCH GmbH. This is an open access article under the terms of the Creative Commons Attribution License, which permits use, distribution and reproduction in any medium, provided the original work is properly cited.

A. Existing nucleophilic allylations of azinium ions (ref. 7)



B. Gold-catalyzed additions of allylboronates to azinium ions (this work)



Scheme 1. Nucleophilic allylations of azinium ions. pin = pinacolato.

Results and Discussion

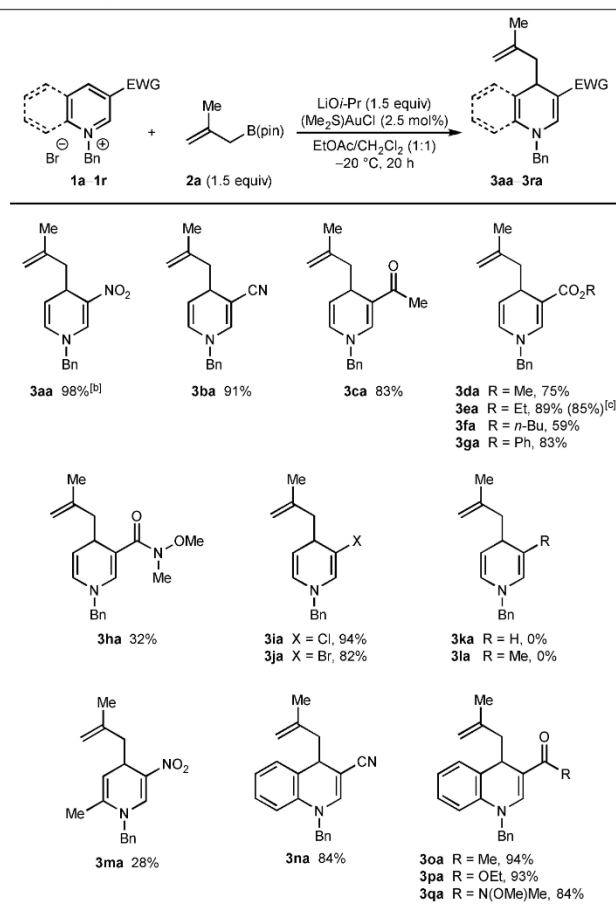
Our study began with the reaction of *N*-benzyl-3-nitropyridinium bromide (**1a**) with 2-methylallyl pinacolboronate (**2a**) (Table 1). Stirring a mixture of **1a** and **2a** (1.5 equiv) together with (Me₂S)AuCl (2.5 mol%) and Li*O**i*-Pr (1.5 equiv) in undried EtOAc/CH₂Cl₂ (1:1) at -20 °C under an air atmosphere for 1.5 h gave the allylated 1,4-dihydropyridine **3aa** in 98% yield as determined by ¹H NMR analysis using an internal standard (entry 1). Regioisomeric products resulting from allylation at either the 2- or 6-positions of **1a** were not detected. However, uncatalyzed additions of potassium allyltrifluoroborate, allyltributylstannane, or allylindium bromide to **1a** gave mixtures of products resulting from addition to both the 4- and 6-positions (see Supporting Information for details), which suggests that gold catalysis is important for high regioselectivity. A lower yield was obtained at room temperature (entry 2), and the mixed solvent system was important for reaction efficiency as shown by experiments using either EtOAc (entry 3) or CH₂Cl₂ (entry 4) alone. Although the reaction was successful using Na*O**t*-Bu (entry 5) or LiOH (entry 6), lower yields were obtained. Omitting either (Me₂S)AuCl (entry 7) or Li*O**i*-Pr (entry 8) was detrimental, and both (Me₃P)AuCl (entry 9) and (Ph₃P)AuCl (entry 10) were inferior precatalysts. Precatalysts based on other metals such as rhodium, iridium, palladium, cobalt, nickel, or copper showed little to no reactivity.

With effective reaction conditions (Table 1, entry 1) in hand, the scope of the process with respect to the *N*-benzylazinium bromide **1** was evaluated in reactions with 2-methylallyl pinacolboronate (**2a**) (Table 2). In all cases, complete regioselectivity for allylation at the 4-position of the azinium ion was observed and alternative regioisomers were not detected. As well as the high-yielding reaction to

Table 1: Evaluation of reaction conditions.^[a]

Entry	Deviation from Standard Conditions	Yield of 3aa ^[b]
1	None	98
2	At room temperature	64
3	EtOAc as solvent	56
4	CH ₂ Cl ₂ as solvent	36
5	Na <i>O</i> <i>t</i> -Bu instead of Li <i>O</i> <i>i</i> -Pr	30
6	LiOH instead of Li <i>O</i> <i>i</i> -Pr	71
7	No (Me ₂ S)AuCl	4
8	No Li <i>O</i> <i>i</i> -Pr	NR
9	(Me ₃ P)AuCl instead of (Me ₂ S)AuCl	21
10	(Ph ₃ P)AuCl instead of (Me ₂ S)AuCl	17

[a] Reactions were conducted with 0.10 mmol of **1a** in 1 mL of solvent. [b] Determined by ¹H NMR analysis using 1,3,5-trimethoxybenzene as an internal standard. NR=no reaction.

Table 2: Scope of azinium salts.^[a]

[a] Reactions were conducted with 0.50 mmol of **1** in 5 mL of EtOAc/CH₂Cl₂ (1:1). Yields are of isolated products. [b] The reaction time was 4.5 h. [c] Yield in parentheses is of a reaction conducted using 4.0 mmol of **1e**.

form **3aa**, the reaction was successful with *N*-benzylpyridinium bromides containing various electron-withdrawing groups at the 3-position, such as cyano (**3ba**), acetyl (**3ca**), a range of esters (**3da–3ga**), or a Weinreb amide (**3ha**). Good yields were generally observed but the yields were lower in the case of substrates containing an *n*-butyl ester (**3fa**) or Weinreb amide (**3ha**). Notably, substrates containing chloro or bromo groups at 3-position also reacted successfully to give 1,4-dihydropyridines **3ia** and **3ja** in 94% and 82% yield, respectively. However, a 3-unsubstituted substrate and a substrate with a methyl group at the 3-position were unreactive, and none of the desired products **3ka** or **3la** were observed. *N*-Benzyl-2-methyl-5-nitropyridinium bromide provided 1,4-dihydropyridine **3ma** in 28% yield. Pleasingly, a range of *N*-benzylquinolinium bromides also reacted efficiently with **2a** to give 1,4-dihydroquinolines **3na–3qa** in 84–94% yield; these substrates had cyano (**3na**), acetyl (**3oa**), ester (**3pa**), or Weinreb amide (**3qa**) groups at the 3-position. A gram-scale reaction using 4.00 mmol of substrate **1e** also proceeded well to give **3ea** in 85% yield.

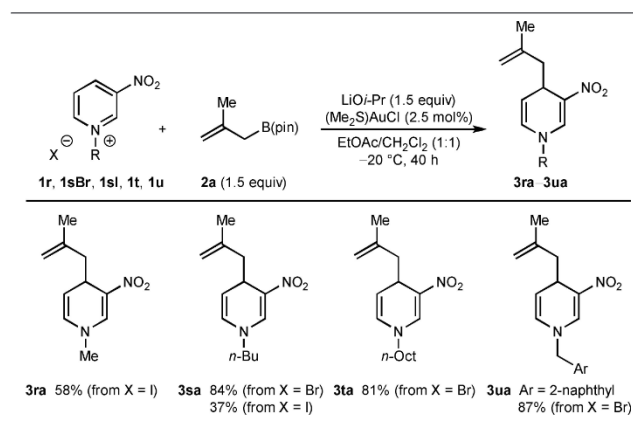
Next, variation of the nitrogen substituent and counterion was briefly investigated using 2-methylallyl pinacolboronate

nate (**2a**) as the allylating agent (Table 3). *N*-Methyl-3-nitropyridinium iodide (**1r**) provided 1,4-dihydropyridine **3ra** in 58 % yield. Changing the *N*-substituent to an *n*-butyl group was also tolerated (**3sa**) but a much higher yield was obtained using the bromide salt (84 %) as opposed to the iodide salt (37 %), possibly because of increased solubility. *N*-Octyl-3-nitropyridinium bromide (**1t**) gave **3ta** in 81 % yield. Finally, *N*-(2-naphthylmethyl)-3-nitropyridinium bromide gave **3ua** in 87 % yield.

The scope of this method with respect to the allylboronate was then investigated using azinium salts **1a**, **1b**, and **1e** (Table 4). Allyl pinacolboronate (**2b**) reacted successfully with various 3-substituted *N*-benzylpyridinium bromides to give **3ab**, **3bb**, and **3eb** in 41–90 % yield. These yields are lower than those of the corresponding reactions with 2-methylallyl pinacolboronate (Table 2, **3aa**, **3ba**, and **3ea**) and this may be attributed to the lower nucleophilicity of allyl pinacolboronate. 2-Phenylallyl pinacolboronate (**2c**) is an effective allylating agent and provided **3ac**, **3bc**, and **3ec** in good yields. Interestingly, the reaction of α,α -dimethylallyl pinacolboronate (**2d**) with **1a** occurred with high α -regioselectivity (with respect to the allylating agent) to give the reverse-prenylated 1,4-dihydropyridine **3ad** in 58 % yield, and none of the alternative prenylation product resulting from γ -allylation was observed. High α -regioselectivities were also observed in the reactions of **1a** with α -methyl-substituted allylboronate *rac*-**2e** and the geranyl-bromide-derived α,α -disubstituted allylboronate *rac*-**2f** to give 1,4-dihydropyridines **3ae** and **3af** in 57 % and 25 % yield, respectively, as mixtures of inseparable diastereomers. 2-Cyclohexenyl pinacolboronate (*rac*-**2g**) reacted with **1a** to give 1,4-dihydropyridine **3ag** in 70 % yield as a 2.2:1 mixture of inseparable diastereomers.

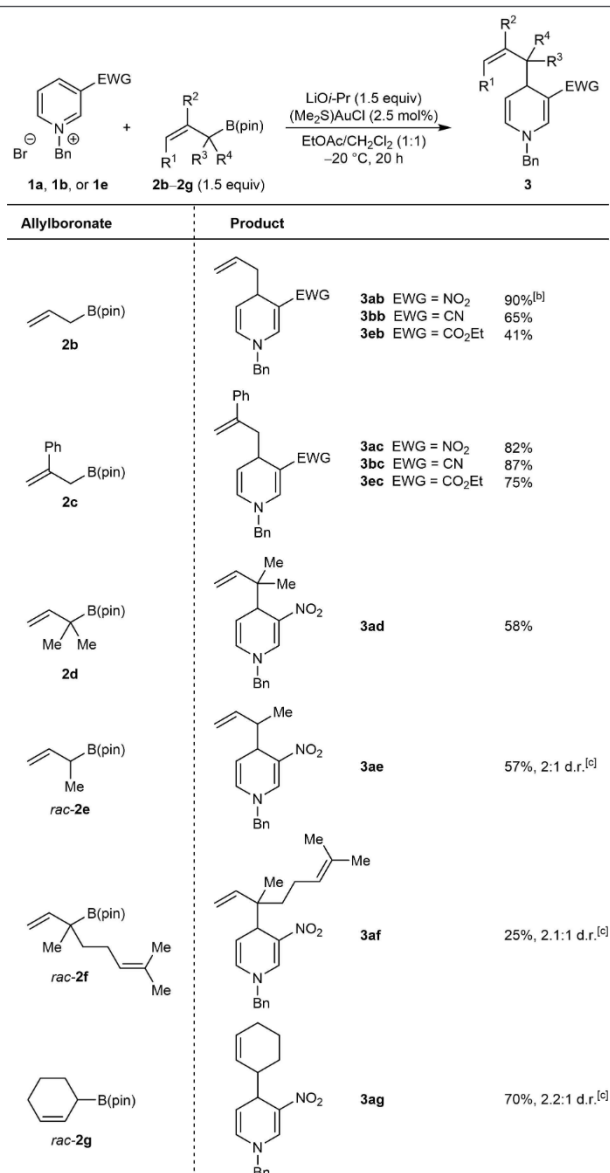
The reactions described thus far are completely regioselective with respect to addition to the 4-position of the azinium ion to give 1,4-dihydropyridines and 1,4-dihydroquinolines. Therefore, it was of interest to examine the reaction of pyridinium bromide **1v**, which contains a methyl group at the 4-position that could block allylation at this site

Table 3: Variation of *N*-substituent and counterion in the azinium salt.^[a]



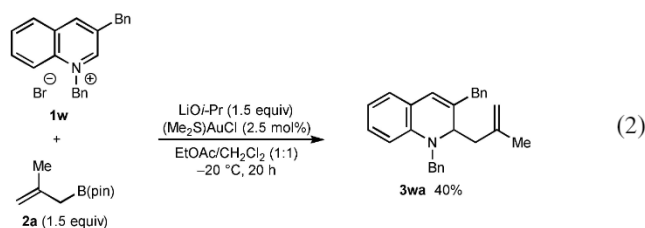
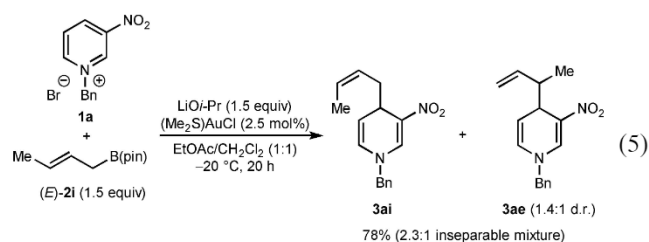
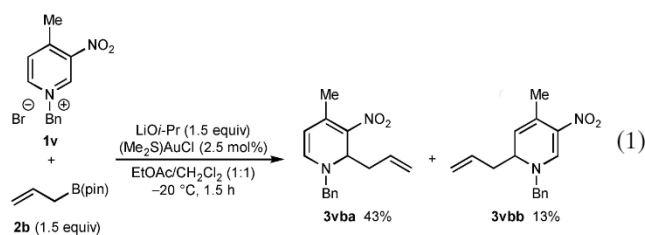
[a] Reactions were conducted with 0.50 mmol of **1** in 5 mL of $\text{EtOAc}/\text{CH}_2\text{Cl}_2$ (1:1).

Table 4: Scope of allylboronate.^[a]

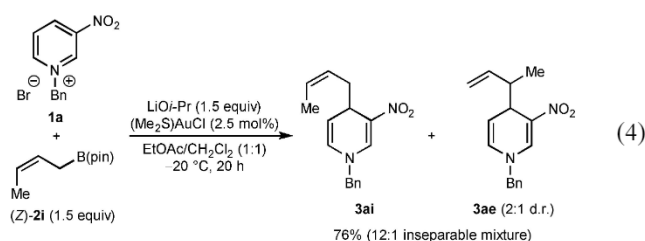
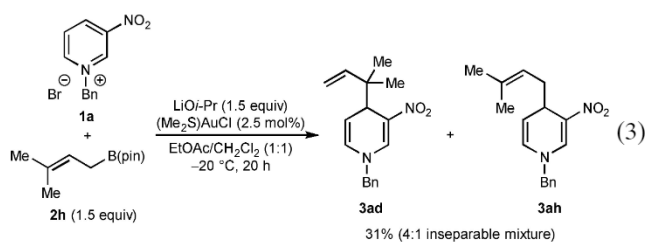


[a] Reactions were conducted with 0.50 mmol of **1a**, **1b**, or **1e** in 5 mL of $\text{EtOAc}/\text{CH}_2\text{Cl}_2$ (1:1). [b] The reaction time was 1.5 h. [c] Isolated as a mixture of inseparable diastereomers.

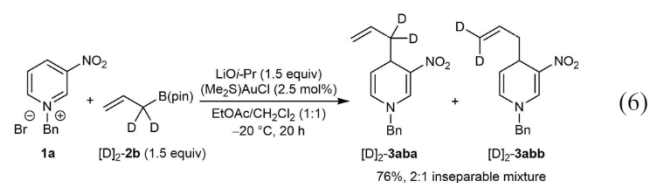
[Eq. (1)]. Indeed, reaction of **1v** with allyl pinacolboronate (**2b**) gave the 2-allylated product **3vba** in 43 % yield and the 6-allylated product **3vbb** in 13 % yield. The importance of a strong electron-withdrawing group at the 3-position in promoting allylation at the 4-position is shown by the reaction of allylboronate **2a** with substrate **1w**, which contains a benzyl group at C3. This reaction gave the 2-allylated product **3wa** in 40 % yield and none of the 4-allylated product was observed [Eq. (2)].



Additional experiments revealed examples where lower $\alpha:\gamma$ selectivity with respect to the allylboronate was observed [Eqs. (3)–(5)]. First, reaction of prenyl pinacolboronate **2h** with **1a** gave a 31 % yield of a 4:1 mixture of the inseparable regioisomers **3ad** and **3ah** favoring the reverse prenylated product **3ad**. This result should be contrasted with the corresponding reaction using α,α -dimethylallyl pinacolboronate shown in Table 2, which gave only the reverse prenylation product **3ad**. Furthermore, regioisomeric mixtures were also obtained in the reactions of pyridinium salt **1a** with crotyl pinacolboronates [Eqs. (4) and (5)]. With (*Z*)-crotyl boronate (*Z*)-**2i**, a 12:1 mixture of regioisomers was obtained, favoring the α -allylation product **3ai**^[12] over the γ -allylation product **3ae**, the latter of which was formed in 2:1 d.r. [Eq. (4)]. In contrast, with (*E*)-crotylboronate (*E*)-**2i**, the $\alpha:\gamma$ selectivity decreased to 2.3:1 [Eq. (5)]. Interestingly, the α -addition product **3ai** was obtained as the *Z*-isomer^[13] and **3ae** was formed as 1.4:1 mixture of inseparable diastereomers.

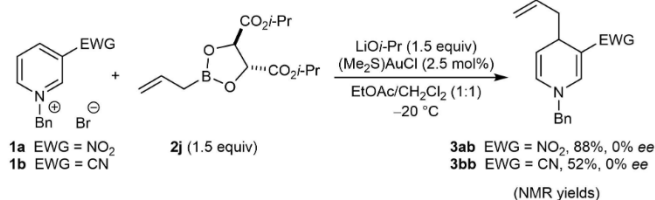


The experiments shown in Equations (3)–(5) employ allylboronates containing unsymmetrical allyl moieties and therefore it was of interest to examine the reaction of **1a** with the α,α -dideuterated allylboronate [D]₂-**2b**, which has a pseudosymmetrical allyl fragment [Eq. (6)]. This experiment gave a 2:1 mixture of regioisomers [D]₂-**3aba** and [D]₂-**3abb** in 76 % yield in favor of the α -allylation product [D]₂-**3aba**. The production of regioisomers in Equations (3)–(6) suggest that these reactions proceed through nucleophilic allylgold(I) intermediates that can exist in one of two σ -isomeric forms. Allylgold(I)^[11] or allylgold(III) species^[3,4a,b,i,j,14] have been described as intermediates or products in various gold-catalyzed or gold-mediated reactions.

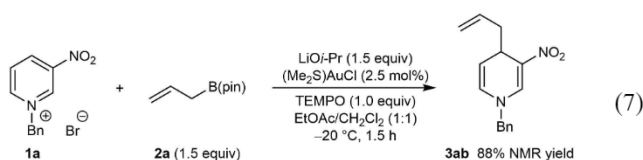


The reaction of the chiral allylboronate **2j**^[15] with pyridinium salts **1a** or **1b** under the standard conditions gave products **3ab** and **3bb** but in 0 % *ee* (Scheme 2). The complete lack of asymmetric induction may indicate that boron is not involved in the carbon-carbon bond-forming step, and further suggests that allylgold(I) species are likely intermediates.

To rule out the participation of allylic radicals in these reactions, which in principle could also explain the production of regioisomeric products in Equation (3)–(6), the reaction of **1a** with **2a** was conducted in the presence of TEMPO (1.0 equiv) [Eq. (7)]. TEMPO did not have a detrimental effect on the yield of **2a**, which suggests allylic radicals are not involved.

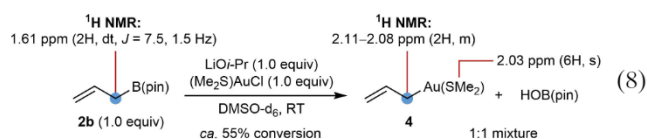


Scheme 2. Alkylation reactions using a chiral allylboronate.

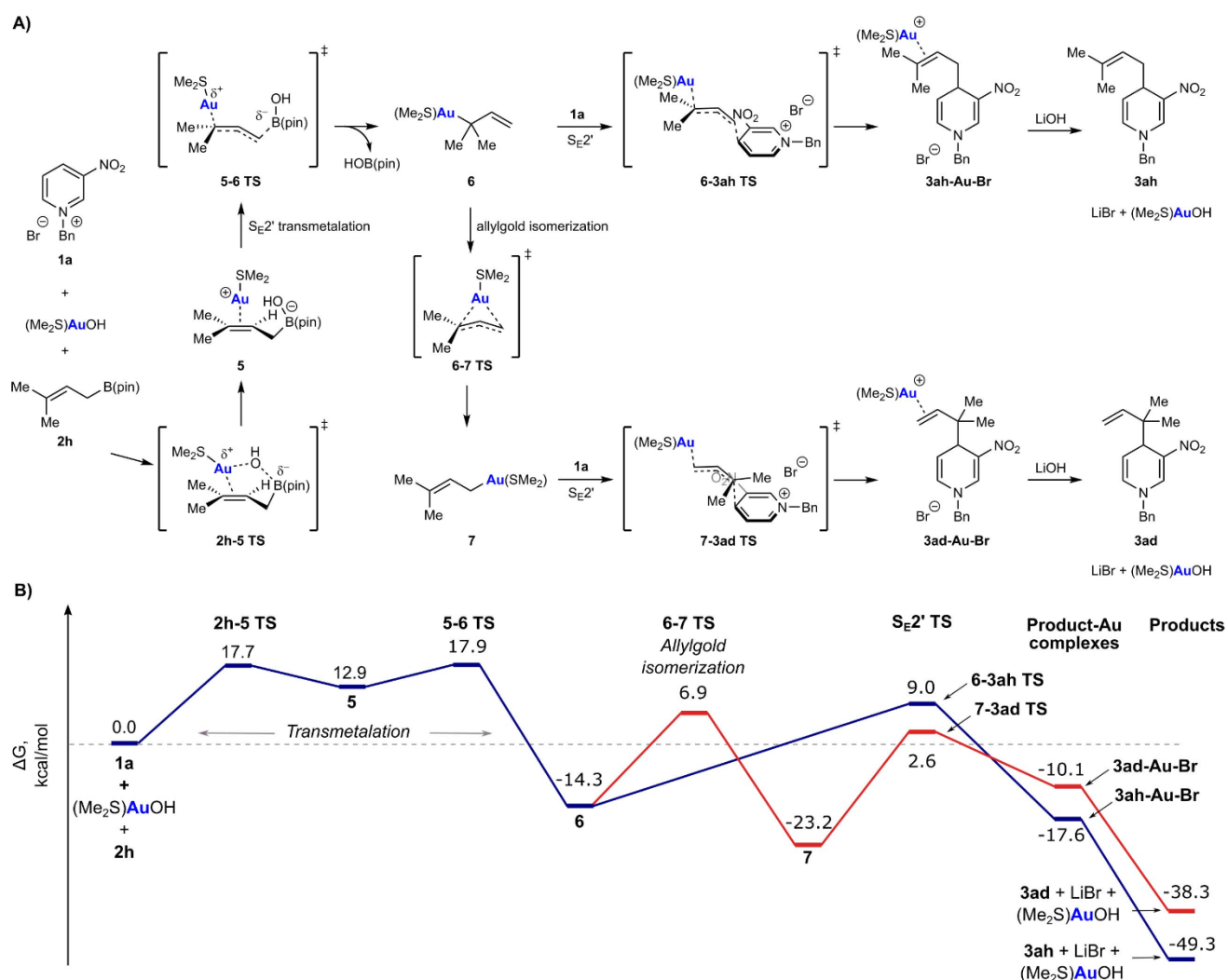


Finally, to provide more direct evidence for allylgold(I) species, equimolar quantities of allyl pinacolboronate **2b**, LiOi-Pr, and (Me₂S)AuCl were combined in DMSO-d₆^[16] and the mixture was analyzed by ¹H NMR spectroscopy [Eq. (8)]. Although full consumption of **2b** was not observed, new signals consistent with the formation of a 1:1 mixture of the σ-allylgold species **4** and HOB(pin) appeared, the latter of which was further confirmed by ¹¹B NMR spectroscopy. The hydroxyl group of HOB(pin) likely results from the presence of H₂O in DMSO-d₆. Essentially identical results were observed when a 1:1 mixture of (Me₂S)AuCl and LiOi-Pr were mixed in DMSO-d₆ for 30 min prior to the addition of allyl pinacolboronate. To our

knowledge, the reactions described herein are the first examples of the formation of allylgold(I) species from allylboron reagents.^[17,18]



To gain further mechanistic insight, computational studies were performed at the PBE0^[19]/def2-TZVP^[20]/SMD-(CH₂Cl₂)^[21] level. First, the nature of the active catalytic species was investigated. LiOi-Pr is used as the base in the reactions, but because undried solvents were used and no precautions were taken to exclude air or moisture, it is likely that LiOH is also present, formed by reaction of LiOi-Pr with H₂O. Reaction of (Me₂S)AuCl with LiOi-Pr or LiOH likely produces a gold(I) isopropoxide or hydroxide by ligand exchange.^[22] The relative computational free energies

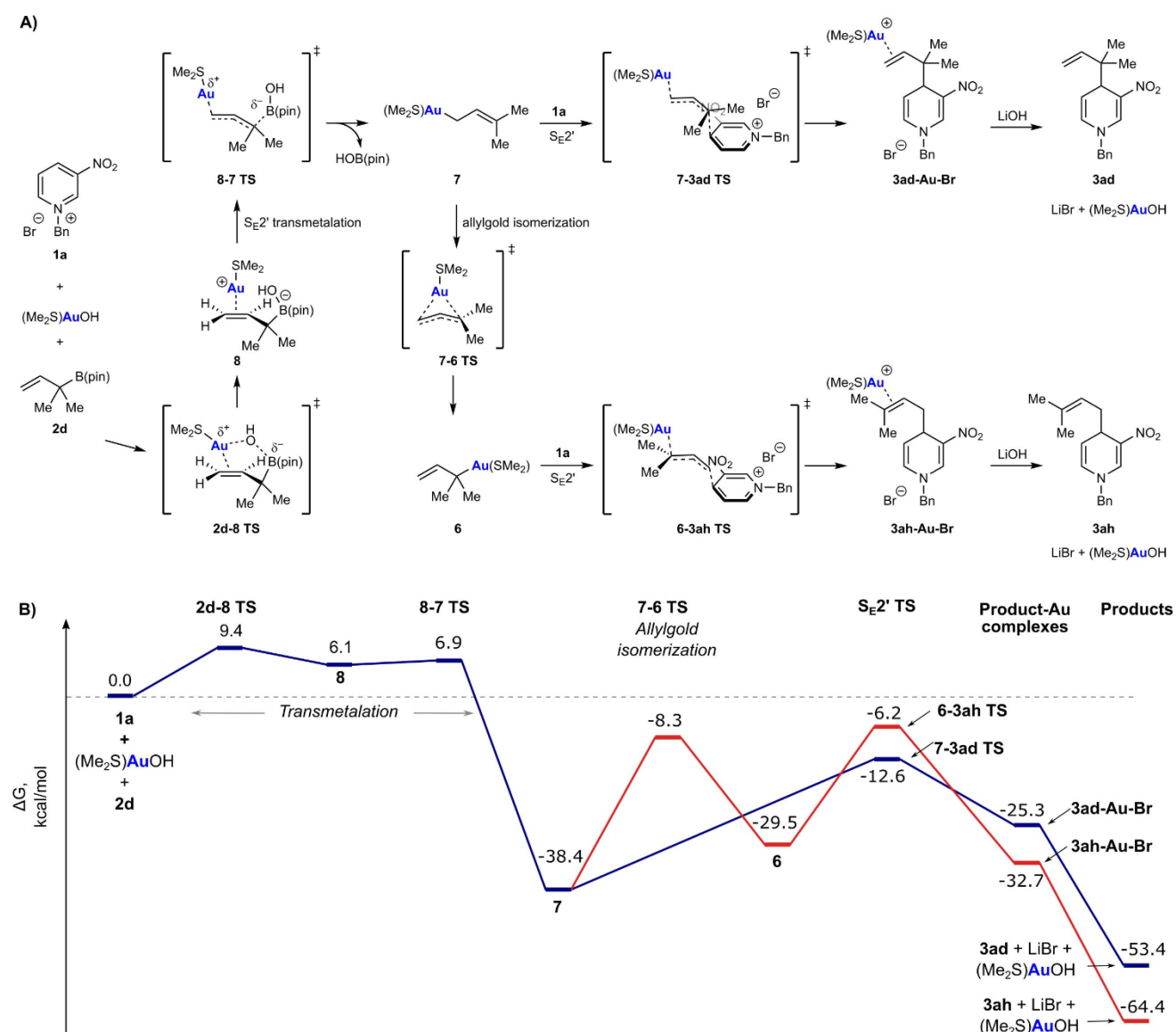


Scheme 3. Computational exploration of reaction pathways arising from **1a** and **2h**. Mechanistic pathways explored (A) and the corresponding starting material, intermediate, product and transition state energy diagram (B). Free energies shown are relative to the starting materials and calculated at PBE0/def2-TZVP/SMD(CH₂Cl₂).

of $(\text{Me}_2\text{S})\text{AuCl}$, $(\text{Me}_2\text{S})\text{AuOH}$ and $(\text{Me}_2\text{S})\text{AuOi-Pr}$ were calculated to be $0.0 \text{ kcal mol}^{-1}$, $1.8 \text{ kcal mol}^{-1}$, and $5.8 \text{ kcal mol}^{-1}$, respectively, which suggests $(\text{Me}_2\text{S})\text{AuOi-Pr}$ is unlikely to be the active catalyst. Because $(\text{Me}_2\text{S})\text{AuCl}$ is unable to catalyze the reaction on its own (Table 1, entry 8), $(\text{Me}_2\text{S})\text{AuOH}$ was assumed to be the active catalyst in the following calculations.

With the likely catalytic species identified, reactions between the pyridinium bromide **1a** with either the primary allylboronate **2h** [Eq. (3)] or the tertiary allylboronate **2d** (Table 4, product **3ad**) were investigated computationally. Allylboronates **2h** and **2d** were selected to compare their transmetalation to gold, investigate possible interconversion between isomeric σ -allylgold species, and gain insight into the $\alpha:\gamma$ allylation regioselectivity.

With the primary allylboronate **2h**, transmetalation with $(\text{Me}_2\text{S})\text{AuOH}$ was calculated to be most favorable through an $\text{S}_{\text{E}}2'$ mechanism^[23] involving the boron-ate complex **5**, with the alkene coordinated to a cationic $[(\text{Me}_2\text{S})\text{Au}]^+$ fragment (Scheme 3A). The formation of **5** occurs by a *syn* pathway through transition state **2h-5-TS**, which allows facile transfer of the hydroxide ligand from gold to boron, with minimal ion separation. From **5**, $\text{S}_{\text{E}}2'$ transmetalation is completed by formation of the carbon-gold bond and loss of $\text{HOB}(\text{pin})$ through transition state **5-6-TS** to give the tertiary allylgold species **6**. The formation of **5** and **6** have relatively low barriers of $17.7 \text{ kcal mol}^{-1}$ and $17.9 \text{ kcal mol}^{-1}$, respectively, relative to the starting materials, and overall, transmetalation is thermodynamically very favorable (Scheme 3B).

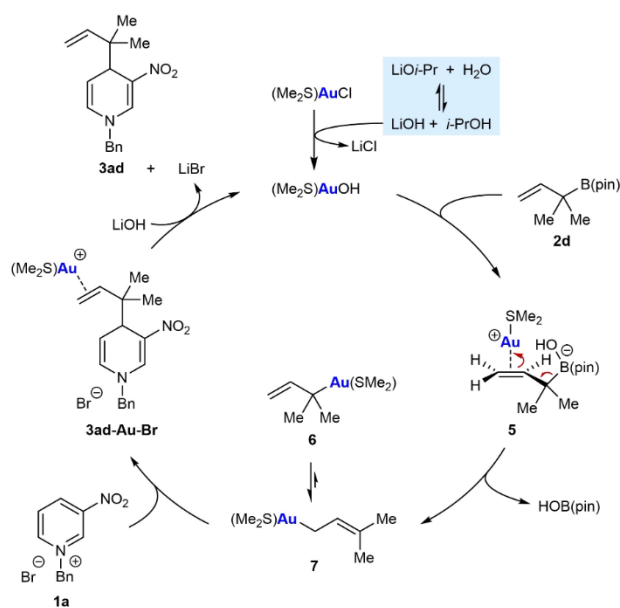


Scheme 4. Computational exploration of reaction pathways arising from **1a** and **2d**. Mechanistic pathways explored (A) and the corresponding starting material, intermediate, product and transition state energy diagram (B). Free energies shown are relative to the starting materials and calculated at PBE0/def2-TZVP/SMD(CH_2Cl_2).

The tertiary allylgold species **6** can then react directly with pyridinium bromide **1a** in an S_E2' allylation to give the prenylated product **3ah** through transition state **6-3ah-TS**, with a barrier of 23.3 kcal mol⁻¹. Experimentally, however, **3ah** was the minor product, with the major product being the reverse-prenylated isomer **3ad** [Eq. (3)]. Product **3ad** most likely arises from the isomerization of the tertiary allylgold species **6** into the primary allylgold species **7** through a π -allylgold transition state **6-7-TS**,^[11d] which then engages in S_E2' allylation of **1a** with a barrier of 25.8 kcal mol⁻¹. The isomerization of **6** to **7** was found to be thermodynamically very favorable, with a barrier of 21.2 kcal mol⁻¹, which is 2.1 kcal mol⁻¹ lower than the competing nucleophilic allylation of **1a** with **6**. Therefore, the DFT calculations suggest that the production of **3ad** should be favored over **3ah**, which matches the experimental results (4:1 ratio of **3ad**:**3ah**). Our findings of the relative energies of primary vs tertiary allylgold(I) species and their interconversion through a high-energy π -allylgold transition state are consistent with a previous study by Hashmi and co-workers.^[11d] Alternative pathways for producing **3ad** involving transmetalation and/or nucleophilic allylation proceeding through S_E2 rather than S_E2' mechanisms were also calculated and discounted because of high barriers (see the Supporting Information for details).

Next, the reaction of the isomeric tertiary allylboronate **2d** with pyridinium bromide **1a**, which gave only the reverse-prenylated product **3ad** (Table 4), was investigated computationally (Scheme 4). Transmetalation (via **8**) was once again found to be very facile and compared with the primary allylboronate **2h** (Scheme 3), is even more thermodynamically favorable ($\Delta G = -38.4$ kcal mol⁻¹ vs. -14.3 kcal mol⁻¹) because it produces a more stable primary allylgold species **7** (relative to the tertiary allylgold species **6**) from a higher energy tertiary allylboronate. As described previously (Scheme 3), the nucleophilic allylation of **1a** with **7** to give **3ad** has a barrier of 25.8 kcal mol⁻¹. However, the competing allylgold isomerization of **7** to give **6** has a barrier of 30.1 kcal mol⁻¹, which is 4.3 kcal mol⁻¹ higher than nucleophilic allylation, thus making the production of the tertiary allylgold species **6** and the corresponding allylation product **3ah** much less feasible. This is a good match for the experiment, where no **3ah** was observed (Table 4). The different outcomes of the crotylation reactions using allylboronates (*Z*)-**2i** or (*E*)-**2i** Equations (4) and (5) are more difficult to explain at the present time and are likely to require more detailed computational studies in future.

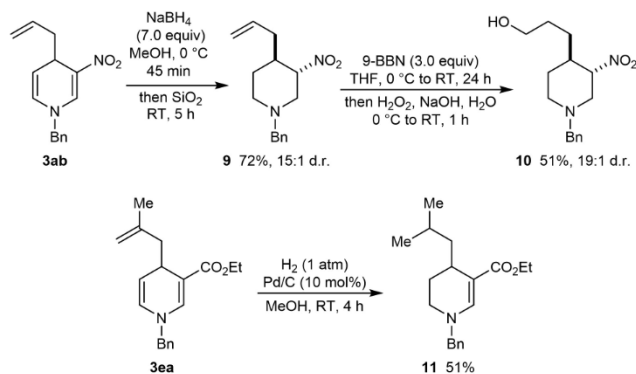
Based on our experimental results and computational studies, a proposed catalytic cycle for these reactions using representative substrates **1a** and **2d** is illustrated in Scheme 5. The reaction of LiOi-Pr with trace H₂O present in the reactions produces LiOH, which then reacts with (Me₂S)AuCl to give (Me₂S)AuOH. Transmetalation of (Me₂S)AuOH with allylboronate **2d** through the gold-bound, boron-ate complex **5** gives primary allylgold species **7**. As described above, the isomerization of **7** into the tertiary allylgold species **6** is unfavorable compared to the reaction of **7** with the pyridinium salt **1a**. The S_E2' nucleophilic allylation of **1a** with **7** gives the gold-bound product **3ad**-



Scheme 5. Proposed catalytic cycle.

Au-Br, which can react with LiOH to release the product **3ad**, LiBr, and (Me₂S)AuOH.

To demonstrate the synthetic utility of the products, further transformations were conducted on representative allylation products **3ab** and **3ea** (Scheme 6). Reduction of the enamines of **3ab** was accomplished using NaBH₄ in MeOH,^[60,d] and after treatment with SiO₂ to epimerize the stereocenter bearing the nitro group,^[61] piperidine **9** was obtained in 72 % yield as a 15:1 mixture of diastereomers. Hydroboration/oxidation of the alkene of **9** then gave primary alcohol **10**, which was isolated in 51 % yield as a 19:1 mixture of diastereomers. In another example, Pd-catalyzed hydrogenation of **3ea** led to selective reduction of the 1,1-disubstituted alkene and the less substituted enamine to give tetrahydropyridine **11** in 51 % yield (Scheme 6).



Scheme 6. Further transformations of representative products **3ab** and **3ea**.

Conclusion

Herein, we have described gold(I)-catalyzed nucleophilic allylations of diverse azinium ions with allyl pinacolboronates to give functionalized 1,4-dihydropyridines and 1,4-dihydroquinolines. The reactions exhibit exclusive regioselectivity for attack at the 4-position of the substrates and require no special precautions to exclude air or moisture. The likely reactive species are nucleophilic σ -allylgold(I) species formed by transmetalation from the allylboronate, and this assertion was supported by NMR spectroscopy, the results of reactions using unsymmetrical allylboronates, and computational studies. To our knowledge, these reactions are the first demonstrations of accessing allylgold(I) species from allylboron reagents. Future work is aimed at enantioselective variants of this process^[24] along with gold(I)-catalyzed nucleophilic allylations of other electrophiles.

Acknowledgements

This work was supported by the Engineering and Physical Sciences Research Council (EPSRC) Centre for Doctoral Training in Sustainable Chemistry (grant number EP/L015633/1), the University of Nottingham, and GlaxoSmithKline.

Conflict of Interest

The authors declare no conflict of interest.

Data Availability Statement

The data that support the findings of this study are available in the supplementary material of this article and at: <https://doi.org/10.17639/nott.7173>.

Keywords: Allylation · Allylboron · Azinium Ions · Catalysis · Gold

- [1] For selected reviews on gold-catalyzed reactions in organic synthesis, see: a) A. S. K. Hashmi, *Chem. Rev.* **2021**, *121*, 8309–8310; b) B. R. Huang, M. Y. Hu, F. D. Toste, *Trends Chem.* **2020**, *2*, 707–720; c) W. Zi, F. Dean Toste, *Chem. Soc. Rev.* **2016**, *45*, 4567–4589; d) Y.-M. Wang, A. D. Lackner, F. D. Toste, *Acc. Chem. Res.* **2014**, *47*, 889–901; e) N. D. Shapiro, F. D. Toste, *Synlett* **2010**, 675–691; f) D. J. Gorin, B. D. Sherry, F. D. Toste, *Chem. Rev.* **2008**, *108*, 3351–3378; g) E. Jiménez-Núñez, A. M. Echavarren, *Chem. Rev.* **2008**, *108*, 3326–3350; h) N. Marion, S. P. Nolan, *Chem. Soc. Rev.* **2008**, *37*, 1776–1782; i) A. S. K. Hashmi, M. Rudolph, *Chem. Soc. Rev.* **2008**, *37*, 1766–1775.
- [2] For a review of gold-catalyzed allylation reactions, see: A. Quintavalla, M. Bandini, *ChemCatChem* **2016**, *8*, 1437–1453.
- [3] For the addition of nucleophiles to π -allylgold(III) complexes, see: a) J. Rodríguez, G. Szalóki, E. D. Sosa Carrizo, N. Saffon-Merceron, K. Miqueu, D. Bourissou, *Angew. Chem. Int. Ed.* **2020**, *59*, 1511–1515; *Angew. Chem.* **2020**, *132*, 1527–1531; b) J. Rodríguez, M. S. M. Holmsen, Y. García-Rodeja, E. D. Sosa Carrizo, P. Lavedan, S. Mallet-Ladeira, K. Miqueu, D. Bourissou, *J. Am. Chem. Soc.* **2021**, *143*, 11568–11581; c) J. Rodríguez, D. Vasseur, A. Tabey, S. Mallet-Ladeira, K. Miqueu, D. Bourissou, *ACS Catal.* **2022**, *12*, 993–1003.
- [4] For gold-mediated or gold-catalyzed allylations involving the reaction of nucleophilic allylating agents with electrophiles, see: a) K. Sanshiro, O. Satoshi, *Chem. Lett.* **1988**, *17*, 1431–1432; b) S. Takuo, O. Satoshi, K. N. C., F. Atsushi, K. Sanshiro, *Bull. Chem. Soc. Jpn.* **1995**, *68*, 1523–1533; c) M. Georgy, V. Boucard, J.-M. Campagne, *J. Am. Chem. Soc.* **2005**, *127*, 14180–14181; d) Y.-C. Hsu, S. Datta, C.-M. Ting, R.-S. Liu, *Org. Lett.* **2008**, *10*, 521–524; e) S. Porcel, V. López-Carrillo, C. García-Yebra, A. M. Echavarren, *Angew. Chem. Int. Ed.* **2008**, *47*, 1883–1886; *Angew. Chem.* **2008**, *120*, 1909–1912; f) C.-C. Lin, T.-M. Teng, C.-C. Tsai, H.-Y. Liao, R.-S. Liu, *J. Am. Chem. Soc.* **2008**, *130*, 16417–16423; g) Y. Sawama, Y. Sawama, N. Krause, *Org. Lett.* **2009**, *11*, 5034–5037; h) M. Kojima, K. Mikami, *Chem. Eur. J.* **2011**, *17*, 13950–13953; i) R. R. Singh, R.-S. Liu, *Adv. Synth. Catal.* **2016**, *358*, 1421–1427; j) G. Dong, M. Bao, X. Xie, S. Jia, W. Hu, X. Xu, *Angew. Chem. Int. Ed.* **2021**, *60*, 1992–1999; *Angew. Chem.* **2021**, *133*, 2020–2027.
- [5] For reviews, see: a) M. Ahamed, M. H. Todd, *Eur. J. Org. Chem.* **2010**, 5935–5942; b) G. Bertuzzi, L. Bernardi, M. Fochi, *Catalysts* **2018**, *8*, 632; c) J. A. Bull, J. J. Mousseau, G. Pelletier, A. B. Charette, *Chem. Rev.* **2012**, *112*, 2642–2713.
- [6] For selected examples of catalytic enantioselective nucleophilic additions to azinium ions or their parent azines, see: a) E. Ichikawa, M. Suzuki, K. Yabu, M. Albert, M. Kanai, M. Shibasaki, *J. Am. Chem. Soc.* **2004**, *126*, 11808–11809; b) M. S. Taylor, N. Tokunaga, E. N. Jacobsen, *Angew. Chem. Int. Ed.* **2005**, *44*, 6700–6704; *Angew. Chem.* **2005**, *117*, 6858–6862; c) Y. Yamaoka, H. Miyabe, Y. Takemoto, *J. Am. Chem. Soc.* **2007**, *129*, 6686–6687; d) M. Á. Fernández-Ibáñez, B. Maciá, M. G. Pizzuti, A. J. Minnaard, B. L. Feringa, *Angew. Chem. Int. Ed.* **2009**, *48*, 9339–9341; *Angew. Chem.* **2009**, *121*, 9503–9505; e) C. Nadeau, S. Aly, K. Belyk, *J. Am. Chem. Soc.* **2011**, *133*, 2878–2880; f) S. T. Chau, J. P. Lutz, K. Wu, A. G. Doyle, *Angew. Chem. Int. Ed.* **2013**, *52*, 9153–9156; *Angew. Chem.* **2013**, *125*, 9323–9326; g) O. García Mancheño, S. Asmus, M. Zurro, T. Fischer, *Angew. Chem. Int. Ed.* **2015**, *54*, 8823–8827; *Angew. Chem.* **2015**, *127*, 8947–8951; h) M. Pappoppula, F. S. P. Cardoso, B. O. Garrett, A. Aponick, *Angew. Chem. Int. Ed.* **2015**, *54*, 15202–15206; *Angew. Chem.* **2015**, *127*, 15417–15421; i) J. P. Lutz, S. T. Chau, A. G. Doyle, *Chem. Sci.* **2016**, *7*, 4105–4109; j) G. Bertuzzi, A. Sinisi, L. Caruana, A. Mazzanti, M. Fochi, L. Bernardi, *ACS Catal.* **2016**, *6*, 6473–6477; k) G. Bertuzzi, A. Sinisi, D. Pecorari, L. Caruana, A. Mazzanti, L. Bernardi, M. Fochi, *Org. Lett.* **2017**, *19*, 834–837; l) Darrin M. Flanigan, T. Rovis, *Chem. Sci.* **2017**, *8*, 6566–6569; m) M. W. Gribble, S. Guo, S. L. Buchwald, *J. Am. Chem. Soc.* **2018**, *140*, 5057–5060; n) D. J. Robinson, S. P. Spurlin, J. D. Gorden, R. R. Karimov, *ACS Catal.* **2020**, *10*, 51–55; o) X. Yan, L. Ge, M. Castiñeira Reis, S. R. Harutyunyan, *J. Am. Chem. Soc.* **2020**, *142*, 20247–20256; p) M. Gómez-Martínez, M. del Carmen Pérez-Aguilar, D. G. Piekarski, C. G. Daniliuc, O. García Mancheño, *Angew. Chem. Int. Ed.* **2021**, *60*, 5102–5107; *Angew. Chem.* **2021**, *133*, 5162–5167; q) Y. Guo, M. Castiñeira Reis, J. Kootstra, S. R. Harutyunyan, *ACS Catal.* **2021**, *11*, 8476–8483; r) C. McLaughlin, J. Bitai, L. J. Barber, Alexandra M. Z. Slawin, A. D. Smith, *Chem. Sci.* **2021**, *12*, 12001–12011.
- [7] For representative examples of nucleophilic allylation of azinium ions, see: a) R. Yamaguchi, M. Moriyasu, M. Yoshio-ka, M. Kawanisi, *J. Org. Chem.* **1985**, *50*, 287–288; b) R. Yamaguchi, M. Moriyasu, M. Yoshio-ka, M. Kawanisi, *J. Org. Chem.* **1988**, *53*, 3507–3512; c) P. Magnus, J. Rodríguez-Lopez,

- K. Mulholland, I. Matthews, *J. Am. Chem. Soc.* **1992**, *114*, 382–383; d) R. Yamaguchi, K. Mochizuki, S. Kozima, H. Takaya, *J. Chem. Soc. Chem. Commun.* **1993**, 981–982; e) P. Magnus, J. Rodríguez-López, K. Mulholland, I. Matthews, *Tetrahedron* **1993**, *49*, 8059–8072; f) R. Yamaguchi, B. Hatano, T. Nakayasu, S. Kozima, *Tetrahedron Lett.* **1997**, *38*, 403–406; g) S. Yamada, M. Ichikawa, *Tetrahedron Lett.* **1999**, *40*, 4231–4234; h) T.-P. Loh, P.-L. Lye, R.-B. Wang, K.-Y. Sim, *Tetrahedron Lett.* **2000**, *41*, 7779–7783; i) R. Yamaguchi, T. Nakayasu, B. Hatano, T. Nagura, S. Kozima, K.-i. Fujita, *Tetrahedron* **2001**, *57*, 109–118; j) J. H. Lee, J. S. Kweon, C. M. Yoon, *Tetrahedron Lett.* **2002**, *43*, 5771–5774; k) R. Yamaguchi, M. Tanaka, T. Matsuda, T. Okano, T. Nagura, K.-i. Fujita, *Tetrahedron Lett.* **2002**, *43*, 8871–8874; l) S. H. Lee, Y. S. Park, M. H. Nam, C. M. Yoon, *Org. Biomol. Chem.* **2004**, *2*, 2170–2172; m) S. Yamada, M. Inoue, *Org. Lett.* **2007**, *9*, 1477–1480; n) Z. Liu, L. Chen, J. Li, K. Liu, J. Zhao, M. Xu, L. Feng, R.-z. Wan, W. Li, L. Liu, *Org. Biomol. Chem.* **2017**, *15*, 7600–7606; o) D. Yoshie, I. Atsuto, JP2018/104361, **2018**, A; p) Q.-N. Duong, L. Schifferer, O. García Mancheño, *Eur. J. Org. Chem.* **2019**, 5452–5461; q) B. J. Knight, Z. A. Tolchin, J. M. Smith, *Chem. Commun.* **2021**, 57, 2693–2696.
- [8] a) C. Diner, K. J. Szabo, *J. Am. Chem. Soc.* **2017**, *139*, 2–14; b) H.-X. Huo, J. R. Duvall, M.-Y. Huang, R. Hong, *Org. Chem. Front.* **2014**, *1*, 303–320.
- [9] For the catalytic enantioselective nucleophilic allylation of indoles with allylboron reagents, see: a) R. Alam, C. Diner, S. Jonker, L. Eriksson, K. J. Szabó, *Angew. Chem. Int. Ed.* **2016**, *55*, 14417–14421; *Angew. Chem.* **2016**, *128*, 14629–14633; b) G. Huang, C. Diner, K. J. Szabó, F. Himo, *Org. Lett.* **2017**, *19*, 5904–5907.
- [10] a) Y. N. Bubnov, S. V. Evchenko, A. V. Ignatenko, *Russ. Chem. Bull.* **1992**, *41*, 2239–2240; b) Y. N. Bubnov, *Pure Appl. Chem.* **1994**, *66*, 235–244; c) Y. N. Bubnov, *Russ. Chem. Bull.* **1995**, *44*, 1156–1170.
- [11] For examples of allylgold(I) species, see ref. [4i], [4j], and: a) M. Uemura, I. D. G. Watson, M. Katsukawa, F. D. Toste, *J. Am. Chem. Soc.* **2009**, *131*, 3464–3465; b) E. Jiménez-Núñez, M. Raducan, T. Lauterbach, K. Molawi, C. R. Solorio, A. M. Echavarren, *Angew. Chem. Int. Ed.* **2009**, *48*, 6152–6155; *Angew. Chem.* **2009**, *121*, 6268–6271; c) M.-C. P. Yeh, H.-F. Pai, Z.-J. Lin, B.-R. Lee, *Tetrahedron* **2009**, *65*, 4789–4794; d) A. S. K. Hashmi, A. M. Schuster, S. Littler, F. Rominger, M. Pernpointner, *Chem. Eur. J.* **2011**, *17*, 5661–5667; e) S. Dupuy, A. M. Z. Slawin, S. P. Nolan, *Chem. Eur. J.* **2012**, *18*, 14923–14928; f) F. F. Mulks, P. W. Antoni, F. Rominger, A. S. K. Hashmi, *Adv. Synth. Catal.* **2018**, *360*, 1810–1821; g) C.-N. Chen, R.-S. Liu, *Angew. Chem. Int. Ed.* **2019**, *58*, 9831–9835; *Angew. Chem.* **2019**, *131*, 9936–9940.
- [12] The structures of **3ab** and **3ai** were further confirmed by X-ray crystallography. Deposition numbers 2102857 and 2102858 contain the supplementary crystallographic data for this paper. These data are provided free of charge by the joint Cambridge Crystallographic Data Centre and Fachinformationszentrum Karlsruhe Access Structures service.
- [13] V. Fargeas, F. Zammattio, J.-M. Chrétien, M.-J. Bertrand, M. Paris, J.-P. Quintard, *Eur. J. Org. Chem.* **2008**, 1681–1688.
- [14] For examples of allylgold(III) species, see ref. [4a], [4b], and: a) N. D. Shapiro, F. D. Toste, *J. Am. Chem. Soc.* **2008**, *130*, 9244–9245; b) M. D. Levin, F. D. Toste, *Angew. Chem. Int. Ed.* **2014**, *53*, 6211–6215; *Angew. Chem.* **2014**, *126*, 6325–6329; c) M. D. Levin, T. Q. Chen, M. E. Neubig, C. M. Hong, C. A. Theulier, I. J. Kobylanski, M. Janabi, J. P. O’Neil, F. D. Toste, *Science* **2017**, *356*, 1272; d) M. S. M. Holmsen, A. Nova, S. Øien-Ødegaard, R. H. Heyn, M. Tilst, *Angew. Chem. Int. Ed.* **2020**, *59*, 1516–1520; *Angew. Chem.* **2020**, *132*, 1532–1536.
- [15] a) W. R. Roush, A. E. Walts, L. K. Hoong, *J. Am. Chem. Soc.* **1985**, *107*, 8186–8190; b) W. R. Roush, L. K. Hoong, M. A. J. Palmer, J. C. Park, *J. Org. Chem.* **1990**, *55*, 4109–4117.
- [16] DMSO- d_6 was superior to CD_2Cl_2 in solubilizing the reaction mixture, although $LiOi-Pr$ did not fully dissolve.
- [17] For examples of the formation of organogold(I) species by transmetalation from organoboron reagents, see: a) D. V. Partyka, M. Zeller, A. D. Hunter, T. G. Gray, *Angew. Chem. Int. Ed.* **2006**, *45*, 8188–8191; *Angew. Chem.* **2006**, *118*, 8368–8371; b) S. Gaillard, A. M. Z. Slawin, S. P. Nolan, *Chem. Commun.* **2010**, *46*, 2742–2744; c) D. V. Partyka, M. Zeller, A. D. Hunter, T. G. Gray, *Inorg. Chem.* **2012**, *51*, 8394–8401; d) N. V. Tzouras, M. Saab, W. Janssens, T. Cauwenbergh, K. Van Hecke, F. Nahra, S. P. Nolan, *Chem. Eur. J.* **2020**, *26*, 5541–5551; e) F. J. L. Ingner, Z. X. Giustra, S. Novosedlik, A. Orthaber, P. J. Gates, C. Dyrager, L. T. Pilarski, *Green Chem.* **2020**, *22*, 5648–5655.
- [18] For the formation of an allylgold(I) species by transmetalation from an allylsilane, see ref. [11e].
- [19] C. Adamo, V. Barone, *J. Chem. Phys.* **1999**, *110*, 6158–6170.
- [20] a) F. Weigend, R. Ahlrichs, *Phys. Chem. Chem. Phys.* **2005**, *7*, 3297–3305; b) F. Weigend, *Phys. Chem. Chem. Phys.* **2006**, *8*, 1057–1065.
- [21] A. V. Marenich, C. J. Cramer, D. G. Truhlar, *J. Phys. Chem. B* **2009**, *113*, 6378–6396.
- [22] For reactions that describe the preparation of gold(I) *tert*-butoxides by the reaction of gold(I) halides with alkali metal *tert*-butoxides, see: a) B. R. Sutherland, K. Folting, W. E. Streib, D. M. Ho, J. C. Huffman, K. G. Caulton, *J. Am. Chem. Soc.* **1987**, *109*, 3489–3490; b) D. S. Laitar, P. Müller, T. G. Gray, J. P. Sadighi, *Organometallics* **2005**, *24*, 4503–4505; c) E. Y. Tsui, P. Müller, J. P. Sadighi, *Angew. Chem. Int. Ed.* **2008**, *47*, 8937–8940; *Angew. Chem.* **2008**, *120*, 9069–9072; d) R. Corberán, S. Marrot, N. Dellus, N. Merceron-Saffon, T. Kato, E. Peris, A. Baceiredo, *Organometallics* **2009**, *28*, 326–330; e) A. S. Romanov, M. Bochmann, *Organometallics* **2015**, *34*, 2439–2454.
- [23] For examples of S_E2' transmetalations of allylboron or allylsilicon reagents to palladium, see: a) Y. Yamamoto, S. Takada, N. Miyaoura, T. Iyama, H. Tachikawa, *Organometallics* **2009**, *28*, 152–160; b) S. E. Denmark, N. S. Werner, *J. Am. Chem. Soc.* **2010**, *132*, 3612–3620; c) M. J. Ardolino, J. P. Morken, *J. Am. Chem. Soc.* **2014**, *136*, 7092–7100.
- [24] A preliminary evaluation of various chiral ligands for gold, such as phosphines and phosphoramidites, led to poor conversions and little to no enantioselectivity.

Manuscript received: February 11, 2022

Accepted manuscript online: March 3, 2022

Version of record online: March 25, 2022